UNIVERSITÉ DU QUÉBEC EN ABITIBI-TÉMISCAMINGUE

PRÉDICTION DU COMPORTEMENT GÉOCHIMIQUE DE REJETS MINIERS SÉQUESTREURS DE CARBONE : CAS DU PROJET DUMONT

THÈSE

PRÉSENTÉE

COMME EXIGENCE PARTIELLE

DU DOCTORAT EN SCIENCES DE L'ENVIRONNEMENT

PAR
EL HADJI BABACAR KANDJI

MARS 2017

À la mémoire de mon père Samba Kandji
À ma maman Aminata
À ma grand-mère Anna diallo,
À ma douce moitié Khady
À ma fille Aminata

REMERCIEMENTS

Mes premiers remerciements vont à l'endroit de Benoît Plante, mon directeur de thèse, pour son soutien constant, sa sollicitude et aussi pour ses conseils. Je remercie aussi Bruno Bussière et Georges Beaudoin, mes co-directeurs pour leur soutien tout le long de mon cheminement. Merci de m'avoir donné du courage.

Je remercie aussi les partenaires financiers dont le CRSNG pour avoir financé une partie du projet dans le cadre d'une subvention de Recherche et Développement Coopératif (RDC). Je remercie aussi Royal Nickel Corporation, et plus particulièrement Pierre-Philippe Dupont, Stanislas Kételers et Michelle Sciortino, pour leur apport durant tout le projet. Je tiens à remercier les membres de mon comité de thèse, Isabelle Demers et Carmen Neculita. Je remercie aussi les autres étudiants qui ont travaillé sur ce projet, il s'agit de Amiirah Saïb, Antoine Gras et Ali Entzari.

Je remercie chaleureusement ma maman, sans elle, je ne serai pas rendu si loin dans les études. Je remercie aussi ma douce moitié, Khady pour son aide, ses encouragements constants et surtout pour avoir supporté mes absences. Merci aussi Amina, mon soleil, pour être dans ma vie. Je remercie aussi mon frère Pape et mes amis de toujours : Abou, Khadim, Samba, Thierno, Omar et Assane.

Je tiens à adresser mes remerciements à des personnes qui m'ont beaucoup aidé durant ma thèse : Il s'agit d'Aicha Hamani et son mari Ibrahim, pour leur soutien à tous les niveaux, Akué Sylvette pour ses encouragements et ses conseils précieux. Un grand Merci aussi à mon ami et frère Ibrahima Hane et sa femme pour les bons moments passés ensemble.

Je remercie toute l'équipe de l'URSTM de l'UQAT, en commençant par Denis Bois, les agents administratifs, Louise Labbé, Danièle Laporte, les techniciens Alain Perreault, Yvan, Mélanie, Melinda, Marc, Mathieu, Janie, Bruno, Patrick, pour leur disponibilité et leur aide précieuse.

A mes collègues et amis étudiants, je dis merci pour les bons moments passés ensemble. Mention spéciale à Mohamed Bini, Sékou Diaby, Patrick, Alex Kalonji, Mohamed, Abdel, Bissé, Richard Bassolé, Aurèlie C, Christelle, Cherif, Vincent, Marie-Pier, Koly, Drissa, Ousseynou, Yassine, Nathalie, Raphael etc.

Merci aussi à la communauté sénégalaise de Rouyn-Noranda.

Enfin, je tiens à remercier Dr. Ann Lamontagne et Dr. Josée Duchesne, évaluateurs externes, pour leur évaluation de ma thèse, et Vincent Cloutier, pour présider le jury.

AVANT-PROPOS

Le présent projet de doctorat s'inscrit dans le cadre d'un grand projet RDC (Recherche et Développement Coopérative), impliquant un partenaire industriel (*RNC Minerals*) et deux institutions universitaires qui sont l'Université du Québec en Abitibi-Témiscamingue (UQAT) et l'université Laval. Au total, cinq étudiants ont été impliqués dans ce vaste projet de recherche. Les travaux de cette thèse contribuent à améliorer les connaissances de le domaine de la prédiction du comportement géochimique de rejets miniers et pour le cas particulier de rejets miniers capables de séquestrer du carbone par voie chimique.

Cette thèse a été rédigée sous forme de trois articles dont deux ont été acceptés pour publication dans les revues scientifiques internationales «*Applied Geochemistry*» et «*Environmental Science and Pollution Research*». Le troisième article est en préparation pour être soumis à la revue «*Journal of Geochemical Exploration*».

Je suis le principal auteur de l'ensemble des chapitres de cette thèse. Mon Directeur de recherche Benoît Plante a révisé tous les chapitres et a contribué à les rendre plus concis et structurés. Il m'a aussi orienté lors de l'interprétation des résultats. J'ai aussi bénéficié des commentaires de mes co-directeurs de recherche Bruno Bussière et Georges Beaudoin qui ont permis d'améliorer la qualité de la thèse. Pierre-Philippe Dupont de *RNC Minerals* a aussi révisé tous les articles. Enfin, Les interprétations des résultats ont été aussi bonifiées grâce aux échanges entre les autres étudiants impliqués dans le projet global, les encadreurs et les représentants de *RNC Minerals* lors de nos rencontres annuelles de suivi du projet.

TABLE DES MATIÈRES

LISTE DES FIGURES

LISTE DES TABLEAUX

LISTE DES ABBRÉVIATIONS, SIGLES ET ACRONYMES

ABA : Acid-Base Accounting

AMD : Acid-mine drainage

An : Année

AP : Acid-potential

ASTM : American Society for Testing and Materials, : American Society for Testing and Materials

BCR : British Columbia Research

C_{Mi} : Concentration du minéral i (% massique)

CND : Contaminated neutral drainage

Cu : Coefficient d'uniformité (-)

D_{90} : Diamètre correspondant à 90 % cumulé de la distribution granulométrique (µm)

DESS : Diplôme d'Études Supérieures Spécialisées

DMA : Drainage minier acide

DNC : Drainage neutre contaminé

DRIFT : Diffuse Reflectance Infrared Fourier Transform

EDS : Energy dispersive spectroscopy

GIEC : Groupe d'experts intergouvernemental sur l'évolution du climat

H : Henry coefficient

ICP-AES : Inductively Coupled Plasma Atomic Emission Spectroscopy

IPCC : Intergovernmental Panel on Climate Change

Ks : Produit de solubilité

ksat : Conductivité hydraulique saturée

L : Litre

M_{CaCO3} : Masse molaire de la calcite (g/mol)

MEND : Mine Environment Neutral Drainage

MSS : Monosulfide solid solution

n_{Mi} : nombre de moles du minéral i pour neutraliser 1 mole d'acide sulfurique

NNP : Net Neutralization potential

NP : Neutralization potential

NPR : Neutralization potential ratio

PA : Potentiel d'acidification

PN : Potentiel de neutralisation

PNC : Pouvoir de Neutralisation des Carbonates

PNN : Pouvoir net de neutralisation

QC : Quebec

R.F.I : Radio France Internationale

REMM. : Règlement sur les effluents des mines de métaux

RIME Research institute of mining and environment

RLS : Rapport liquide-solide

RNC : Royal Nickel Corporation

SDD : Silicon Drift Detector

SEM : Scanning electron microscope

SI : Saturation indice

SSA : Specific surface area

ULAVAL : Université Laval

UQAT : Université du Québec en Abitibi-Témiscamingue

US EPA : United States Environmental Protection Agency

Xi : Pourcentage massique du minéral i

XRD : X-ray diffraction

XRF : X-ray fluorescence

$\Delta_f H°$: Enthalpie standard de formation

ν_1 : C-O Symmetric Stretching mode

ν_2 : Out-of-plane CO32- bending modes

ω_a : Masse molaire de H2S04 (g/mol)

ω_i : Masse molaire et du minéral i (g/mol)

RÉSUMÉ

Certains minéraux et métaux de base sont souvent associés à des roches mafiques et ultramafiques. L'exploitation de ces métaux et minéraux peut conduire à la production d'importants volumes de rejets miniers riches en minéraux capables de réagir avec le CO2 pour former des carbonates stables. Cependant, les processus impliqués dans la carbonatation des rejets ultramafiques peuvent avoir un impact sur la qualité des eaux de drainage interagissant avec ces types de roches, d'où la nécessité de bien comprendre les processus en amont et en aval de ce phénomène. De même, la prédiction de la chimie des eaux de drainage est une étape importante pour une définition des mesures de mitigation.

L'objectif principal de cette thèse est d'évaluer le comportement géochimique de rejets miniers ayant un potentiel de séquestration de carbone et de comprendre aussi l'impact de ce potentiel sur la qualité des eaux de drainage. Les matériaux étudiés ici sont ceux du projet nickélifère Dumont de Royal Nickel Corporation (maintenant RNC Minerals). Le site de la future mine est situé à 25 kilomètres de la ville d'Amos (Québec) et vise à exploiter un gisement de nickel associé à des sulfures de nickel et à l'awaruite, un alliage fer-nickel dont très peu d'informations sont disponibles sur son comportement environnemental. La compréhension des caractéristiques des eaux de drainage en contact avec des matériaux de ce type peut aider à mieux comprendre les processus impliqués dans la carbonatation passive des rejets ultramafiques comme ceux du projet Dumont.

Comme la mine n'est pas encore en activité, les résidus ont été produits en usine pilote, alors que les stériles ont été échantillonnés en vrac après un dynamitage. Les autres lithologies étudiées proviennent d'échantillons de carottes sélectionnés pas les géologues de RNC minerals. Les matériaux ont été soumis à des essais cinétiques au laboratoire (mini-cellule, cellule humide, colonne) et sur le terrain (cellule expérimentale) afin d'évaluer leur comportement géochimique. Des concentrés de sulfures et d'awaruite ont été produits et soumis aussi à des essais en mini-cellule afin d'évaluer leur potentiel de génération de métaux dans les lixiviats. Une caractérisation détaillée a été réalisée sur les matériaux frais et post-essais afin d'évaluer les changements de leurs caractéristiques chimiques et minéralogiques.

Les résultats des essais cinétiques indiquent que les résidus de Dumont ainsi que les lithologies des stériles qui séquestrent du carbone ont des eaux de drainage alcalines

avec un pH qui oscille près des limites permises (9,5) par la Directive 019 et le REMM. Malgré un pH alcalin, aucun métal n'est présent dans les lixiviats à des concentrations qui depassent les limites de la Directive 019. La principale préoccupation concernant les eaux de drainage des matériaux de Dumont est le pH élevé. Cependant, avec les pluies acides de la région de l'Abitibi-Témiscamingue et le CO_2 qui peut se dissoudre dans le bassin de rétention des eaux de drainage, le pH pourrait se maintenir à l'intérieur des limites permises.

La comparaison des résultats obtenus à différentes échelles montrent que les différences aux niveaux des essais cinétiques ont un impact sur les taux de génération des métaux. Le ratio solide-liquide et la température sont les principaux paramètres qui induisent cette différence. Cependant, les qualités des eaux de drainage générées sont similaires. En outre, les essais en colonne sont les essais cinétiques à privilégier puisqu'ils génèrent des résultats plus proches de ceux des cellules expérimentales de terrain.

Les essais cinétiques et les différentes caractérisations ont confirmé le potentiel de séquestration du carbone des matériaux de Dumont. La dissolution du CO_2 et l'oxydation des traces de sulfures induisent l'altération de la serpentine et de la brucite et conduisent à la précipitation de carbonates de magnésium hydratés. La précipitation des minéraux secondaires induit une cimentation à la surface des matériaux. Cette cimentation pourrait permettre de réduire considérablement les émanations de poussières de la mine. Dans les conditions des essais cinétiques, les matériaux de Dumont pourraient séquestrer de manière passive entre 600 – 2200 g de $CO_2/m^2/an$. La brucite est le principal minéral impliqué dans la séquestration du carbone malgré la prédominance de la serpentine. En effet, la consommation de la brucite coïncide avec le plafonnement de la quantité de carbone dans les matériaux. Le potentiel de séquestration du CO_2 des matériaux ultramafiques de Dumont peut être augmenté de manière significative. Pour cela, il apparaît primordial de favoriser la carbonatation de la brucite. Une méthode de co-disposition résidus et stériles pourrait permettre d'augmenter les flux de CO_2 séquestrés et en même temps assurer une meilleure stabilité physique des rejets.

Malgré l'augmentation des teneurs en carbone dans les matériaux de Dumont avec la précipitation des carbonates secondaires, le potentiel de neutralisation (PN) d'acide n'augmente pas pour autant. En effet, la consommation de la brucite, qui est aussi réactive que les carbonates, induit une diminution du PN des matériaux.

La présente étude a montré que la séquestration du carbone par des rejets ultramafiques pouvait conduire à la production d'un drainage alcalin. Ce phénomène est donc important à considérer dans la prédiction du comportement géochimique de tels rejets. Les résultats de cette thèse pourront aider RNC Minerals à mieux définir

un plan de gestion qui permettrait d'atténuer ses impacts sur l'environnement et de compenser ses émissions de CO_2 de gaz à effet de serre.

Mots-clés : Drainage alcalin; rejets miniers ultramafiques; carbonatation minérale; brucite; serpentine, prédiction de la qualité d'eau, essais cinétiques.

CHAPITRE I

INTRODUCTION GÉNÉRALE

1.1 Problématique des rejets miniers

L'industrie minière est une source non négligeable de revenus pour beaucoup de pays dont le Canada. Son apport dans l'économie du Canada et du Québec en termes de revenus, de création d'infrastructures et d'emplois est indéniable. Cependant, les réels avantages que peuvent apporter l'exploitation de ressources naturelles divisent l'opinion (Beaupré, 2012). En effet, l'industrie minière est le secteur d'activité qui produit les plus grandes quantités de rejets dans le monde (Blowes *et al.* 2003; Aubertin *et al.* 2002). En plus des problématiques liées aux bruits et aux vibrations, aux émissions de gaz à effet de serre, de poussières et à l'utilisation d'importantes quantités d'eau et d'énergie, l'aspect le plus préoccupant demeure cependant les volumes importants de rejets qui sont produits durant le cycle de vie de la mine. Ces volumes importants de rejets, en plus d'avoir une forte emprise sur le térritoire, induisent une réduction importante de la végétation ainsi qu'une diminution de la qualité et du niveau des eaux de surfaces et souterraines (Chamley, 2002).

Des quantités importantes de rejets sont produites lors de l'excavation des roches pour pouvoir accéder aux zones minéralisées. Lors de cette phase, les roches stériles sont produites en quantités importantes. Les stériles miniers sont des roches qui n'ont qu'une faible valeur économique et sont caractérisés par leur granulométrie très étalée, allant du µm au m, et sont empilées dans les haldes à stériles (Aubertin *et al.* 2002). Ces haldes peuvent être immenses et s'élever sur plusieurs dizaines de mètres de hauteur. Le traitement et le broyage des roches ayant des teneurs plus élevées en

métaux dans les usines de concentration vont produire les rejets de concentrateur (aussi appelés résidus miniers) qui peuvent être déchargés sous forme de pulpe (mélange d'eau de procédé et de matières solides fines) dans les parcs à résidus. La méthode d'exploitation (mine souterraine versus à ciel ouvert) influe sur les quantités de rejets générées (Aubertin *et al.* 2002).

Généralement, les stériles et les parcs à résidus occupent de larges surfaces. Seulement au Québec, par exemple, les surfaces occupées par les rejets miniers (rejets de concentrateur et stériles) sont estimées à plus 13 000 hectares (Aubertin *et al.* 2002). En plus de cette forte emprise des rejets sur le térritoire, s'ajoute l'instabilité physique que peuvent représenter les ouvrages servant à entreposer les rejets miniers. En effet, ces grandes quantités de rejets mélangés souvent avec beaucoup d'eau, exercent des contraintes importantes sur les digues qui peuvent alors céder.

De plus, certaines roches excavées stables sous terre, peuvent devenir chimiquement instables une fois exposées à l'air et à l'eau. Cette instabilité se traduit par l'oxydation des sulfures dont les plus communs dans les rejets miniers sont la pyrite et la pyrrhotite (Gunsinger *et al.* 2006; Aubertin *et al.* 2002; Blowes *et al.* 2003*)*. L'oxydation de ces sulfures entraîne la production d'acide et de lixiviats pouvant montrer des valeurs de pH inférieures à 6,5 et peuvent même, dans certains cas, atteindre des pH négatifs, comme c'est le cas à Iron Mountain Mine (Nordstrom *et al.* 2000). Les eaux de drainage acide sont aussi caractérisées par des fortes concentrations en métaux (par ex. : Fe, Al, Mn, Zn, Cu, Cd, Hg, Pb, Co, Ni, Ta, As, pour n'en nommer que quelques-uns) et en sulfates; un phénomène appelé le drainage minier acide (DMA). Ces eaux minières contaminées sont très dommageables pour les écosystèmes. Les conséquences pour l'environnement peuvent s'étaler sur plusieurs décennies et sont très coûteuses.

Les processus d'oxydation des sulfures sont largement décrits dans la littérature (e.g. Blowes *et al.* 2003; Dold, 2010; Evangelou et Zhang, 1995; Blowes et Ptacek, 1994; Morin et Hutt, 1997; Nordstrom et Southam, 1997; Taylor *et al.* 1984). La pyrite est le sulfure le plus souvent utilisé pour décrire les réactions d'oxydation car c'est le sulfure le plus répandu dans les rejets miniers. L'oxydation de la pyrite se déroule en trois étapes. La première étape est la phase d'oxydation directe par l'oxygène en présence d'eau (Équation 1.1) qui génère de l'acide et des ions fer ferreux (Fe^{2+}) :

$$2FeS_2 + 7O_2 + 2H_2O \rightarrow 2Fe^{2+} + 4SO_4^{2-} + 4H^+ \quad (1.1)$$

Le fer ferreux est à son tour oxydé par l'oxygène pour donner le fer ferrique (Fe^{3+}) (Équation 1.2) :

$$Fe^{2+} + 1/4O_2 + H^+ \rightarrow Fe^{3+} + 1/2H_2O \quad (1.2)$$

A pH suffisamment élevé (> 3,5), le fer ferrique précipite, on parle d'hydrolyse du fer qui peut aussi générer 3 moles de H^+ (Équation 1.3) :

$$Fe^{3+} + 3H_2O \rightarrow Fe(OH)_3 + 3H^+ \quad (1.3)$$

Lorsque le fer ferrique ne précipite plus à cause du faible pH, il se comporte comme un oxydant pour la pyrite; c'est l'oxydation indirecte de la pyrite (Équation 1.4) :

$$FeS_2 + 14Fe^{3+} + 8H_2O \rightarrow 15Fe^{2+} + 2SO_4^{2-} + 16H^+ \quad (1.4)$$

La réaction globale peut alors s'écrire de la manière suivante (Équation 1.5) :

$$4FeS_2 + 15O_2 + 14H_2O \rightarrow 4Fe(OH)_3 + 8H_2SO_4 \quad (1.5)$$

De plus, les réactions 1.1 et 1.2 peuvent être catalysées par les bactéries qui colonisent le milieu (Blowes *et al.* 2003*)*. Comme le montre l'équation 1.4, l'oxydation indirecte génère beaucoup plus d'acide que l'oxydation de la pyrite par l'oxygène (Mylona *et al.* 2000). Même si l'oxydation de la pyrite est la plus souvent

citée en exemple, d'autres sulfures sont aussi susceptibles de s'oxyder et peuvent, pour certains, générer de l'acide et des contaminants (e.g., Aubertin *et al.* 2002; Blowes *et al.* 2003; Sharer *et al.* 2000). L'oxydation de la pyrrhotite, par exemple, est beaucoup plus rapide que celle de la pyrite (Aubertin *et al.* 2002). Les autres sulfures que l'on peut aussi retrouver dans les rejets miniers sont la pentlandite, la sphalerite et l'arsénopyrite, entre autres. Quelques facteurs sont connus pour leur influence sur la cinétique des processus d'oxydation et, par conséquent, sur l'étendue et la qualité du DMA. Il peut s'agir du type de sulfure (Evangelou et Zhang, 1995; Keith et Vaughan, 2000) et leur distribution, la granulométrie des rejets, la surface exposée, les conditions hydrauliques, l'alimentation en O_2 et enfin la présence de certaines bactéries (Aubertin *et al.* 2002; Moon *et al.* 2007; Paktunc, 1999; Keith et Vaughan, 2000; Blowes *et al.* 1998; Blowes *et al.* 2003).

En réaction à l'oxydation des sulfures, certains minéraux présents dans les rejets peuvent s'altérer et consommer l'acidité générée (Sharer *et al.* 2000; Blowes *et al.* 1998; Lindsay *et al.* 2009). Il s'agit principalement des carbonates et, dans une moindre mesure, des silicates et des aluminosilicates (Blowes *et al.* 2003; Jurjovec *et al.* 2002; Blowes *et al.* 1998; Plante *et al.* 2010a; Heikkinen et Räisänen, 2008; Jambor *et al.* 2002; Sherlock *et al.* 1995). Les réactions de neutralisation de l'acide par la calcite et la dolomite sont données respectivement aux équations 1.6 et 1.7 (Aubertin *et al.* 2002). Le pH peut ainsi être maintenu à des valeurs neutres voire même alcalines, ce qui contribue à limiter la mobilité des métaux dans les eaux de drainage.

$$2CaCO_3 + H_2SO_4 \rightarrow 2Ca^{2+} + 2HCO_3^- + SO_4^{2-} \quad (1.6)$$

$$CaMg(CO_3)_2 + H_2SO_4 \rightarrow Ca^{2+} + Mg^{2+} + 2HCO_3^- + SO_4^{2-} \quad (1.7)$$

La dissolution des silicates et moins rapide que celle des carbonates, cependant sa contribution dans la neutralisation de l'acide générée par l'oxydation des sulfures

mérite d'être considérée (Jambor *et al.* 2002; Sherlock *et al.* 1995). La dissolution des silicates se fait généralement de façon incongruente, libérant ainsi préférentiellement un élément au détriment d'un autre. La réaction de neutralisation de l'acide par la serpentine est donnée par l'équation 1.8 (Lin et Clemency, 1981) et celle de l'anorthite (Sherlock *al.*, 1995) est donnée par l'équation 1.9 :

$$Mg_3Si_2O_5(OH)_4 + 6H^+ \rightarrow 3Mg^{2+} + 2H_4SiO_4 + H_2O \quad (1.8)$$

$$CaAl_2Si_2O_8 + 2H^+ + H_2O \rightarrow Ca^{2+} + Al_2Si_2O_5(OH)_4 \quad (1.9)$$

Cependant, il peut arriver que les concentrations de certains métaux dans les effluents dépassent les normes de rejets même si les pH ne sont pas acides. En effet, certains métaux demeurent relativement solubles à des pH neutres voire alcalins, comme c'est le cas par exemple du Ni, du Zn et de l'arsenic, entre autres. De plus, la plupart des métaux ont un comportement amphotérique, comme le montre la Figure 1.1, avec une solubilité maximale aux pH acide et alcalin, et faible à pH neutre.

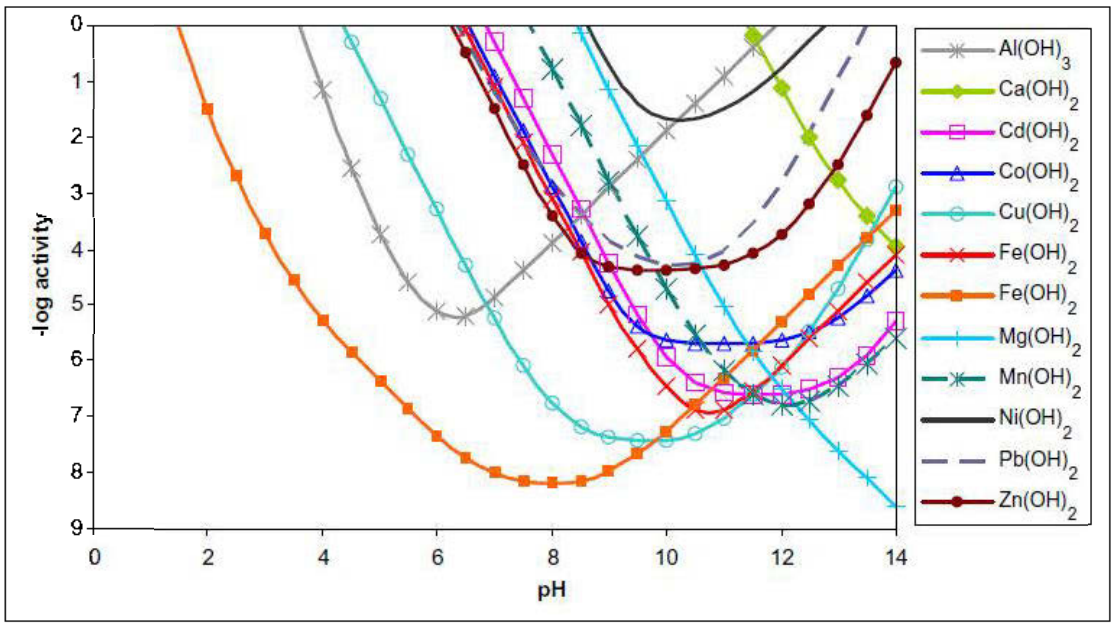

Figure 1.1 Solubilité de quelques hydroxydes métalliques en fonction du pH (tirée de Cravotta III, 2008)

Comme le montre la Figure 1.2, il existe principalement trois types de drainages dépendamment du pH des eaux minières: (1) le drainage minier acide (pH < 6), (2) le drainage minier alcalin (pH > 9-10) (González *et al.* 2012; Rose et Cravotta, 1998; Aubertin *et al.* 2002; Banks *et al.* 2002) et (3) le drainage neutre contaminé (DNC; Nicholson 2004) (6 < pH < 9-10). Le DMA et le DNC sont les deux types de drainage les plus fréquents et leurs processus de formation sont relativement bien connus. Trois raisons sont généralement évoquées pour expliquer la survenue du DNC : (1) la neutralisation de l'acide par les minéraux neutralisants qui maintient le pH à des valeurs neutres mais que certains métaux demeurent solubles et dépassent ainsi les normes de rejets, (2) l'oxydation de certains sulfures qui libèrent des métaux sans pour autant générer d'acide et enfin (3), l'application d'une méthode de restauration peu efficace sur des rejets sulfureux (Nordstrom *et al.* 2015; Bussiere *et al.* 2005). Le DMA et le DNC sont beaucoup plus problématiques et ont donc reçu beaucoup plus d'intérêt que le drainage alcalin.

Le drainage alcalin est pour le moment relativement peu connu et sa survenue est assez rare. Ce type de drainage peut apparaîttre lorsque les minéraux contenus dans les rejets miniers sont fortement neutralisants (Banks *et al.* 2002). Nordstrom *et al.* (2015) ont répertorié quatre autres situations pouvant entrainer la production d'eaux minières alcalines : (1) la faible perméabilité de roches riches en feldspaths pouvant réagir en système fermé, entrainant la précipitation de la calcite et, par conséquent, la mobilisation des ions bicarbonates, (2) l'évolution d'une eau souterraine de type bicarbonate de sodium par échange ionique, réduction du sulfate et par l'oxydation du carbone organique, (3) l'altération de la marne-calcaire et, enfin, (4) la dissolution du villiaumite (NaF).

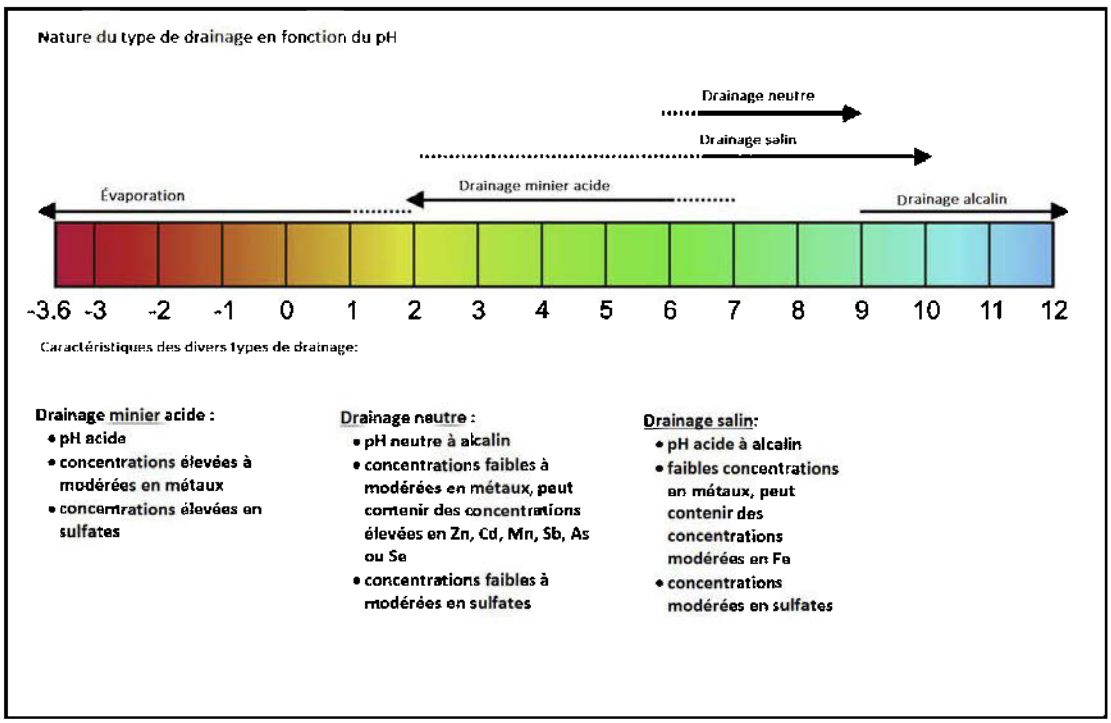

Figure 1.2 Gamme de pH des différents types de drainage et leurs caractéristiques. Adaptée de Nordstrom *et al.* (2015)

Les réactions d'oxydation et de neutralisation vont générer des qnantités significatives de cations et d'anions, favorisant ainsi la précipitation d'une large

gamme de minéraux secondaires plus ou moins solubles (Blowes *et al.* 2003, Aubertin *et al.* 2002; Blowes *et al.* 1998; Moncur *et al.* 2005). Parmi les minéraux secondaires, on trouve des minéraux sulfatés, comme le gypse ($CaSO_4.2H_2O$) (Lindsay *et al.* 2009), la barite ($BaSO_4$), la jarosite ($KFe^{3+}{}_3(SO_4)_2(OH)_6$) (Moncur *et al.* 2005) ou des oxyhydroxydes de fer (goethite, lepidocrocite et ferrihydrite) et d'aluminium, des carbonates comme la sidérite ($FeCO_3$), mais aussi des sulfures secondaires, comme la pyrite (Paktunc et Davé, 2002), la marcassite (Blowes *et al.* 2003) et la covellite (Dold & Fontbote, 2002; Gunsinger *et al.* 2006; Moncur *et al.* 2005). La précipitation de ces minéraux secondaires est un processus important dans l'atténuation de la présence des métaux lourds dans les eaux de drainage (Carbone *et al.* 2013; Wilkin, 2008; Giere *et al.* 2003; Al et Blowes, 2000). De plus, certains métaux peuvent être retenus dans la phase cristalline de certains minéraux secondaires, on parle alors de co-précipitation (Lottermoser, 2010). D'autres métaux peuvent être adsorbés par les oxyhydroxydes de fer ou d'aluminium (Al et Blowes, 2000; Lindsay *et al.* 2009; Moncur *et al.* 2009) ou même solubilisés par complexation par les acides organiques. Dans les parcs à rejets miniers, l'accumulation des minéraux secondaires se traduit par la formation d'une zone indurée et cimentée dont la caractérisation donne une idée du degré d'altération des rejets, mais aussi des processus de rétention des contaminants (Blowes *et al.* 1991; McGregor et Blowes, 2002; Johnson *et al.* 2000; Blowes *et al.* 2003; Moncur *et al.* 2005). Toutefois, la stabilité de ces phases dépend essentiellement du pH et du potentiel redox (Eh). Les métaux peuvent être ainsi remobilisés lorsque les conditions géchimiques changent (Dold et Fontbote, 2002; Gunsinger *et al.* 2006; Hageman & Smith, 2005; MEND, 1995; Moncur *et al.* 2009; Moncur *et al.* 2005; Rose et Cravotta III, 1998).

Les cycles de séchage et mouillage causés par les évènements de pluie et d'évaporation peuvent aussi jouer sur la mobilité des métaux (Stillings *et al.* 2008; Moncur *et al.* 2005). Les précipitations favorisent la dissolution des minéraux secondaires solubles, modifiant ainsi la chimie des eaux de drainage (Hageman et

Smith, 2005). À l'inverse, l'évapo-concentration favorisera la concentration des ions, leur permettant ainsi d'atteindre leur limite de solubilité et de précipiter. Le climat constitue donc un facteur important qui influence l'évolution des concentrations des contaminants dans les eaux de drainage (Dold et Fontbote, 2002; MEND, 1995; Moncur *et al.* 2005; Sáinz *et al.* 2002). Pour prédire le comportement géochimique des rejets miniers ainsi que l'évolution de la qualité des eaux de drainage; la compréhension et la prise en compte de tous les processus géochimiques traités dans cette section sont essentielles.

1.2 Prédiction du comportement géochmique des rejets miniers

Afin d'atténuer les impacts négatifs tout le long du cycle de vie de la mine, il est important de bien comprendre et caractériser les rejets dans le but d'identifier des mesures de mitigation adéquates. La prédiction du comportement géochimique de rejets miniers est une étape importante dans l'élaboration du plan de gestion des rejets miniers. Cependant, comme nous l'avons vu précédemment, les processus géochimiques impliqués dans l'altération des rejets et la production de drainages contaminés sont nombreux et complexes. Tous les facteurs externes et processus géochimiques impliqués sont difficiles à tenir en compte au laboratoire et difficiles à intégrer aussi dans un seul type d'outils, ce qui rend difficile la prédiction de la qualité des eaux de drainage à long terme par les outils existants (Sapsford et Williams, 2005).

La compréhension et la prédiction du drainage minier acide ont fait l'objet de plusieurs travaux de recherche lors de ces dernières décennies (e.g. Kleinmann *et al.* 1981; Evangelou, et Zhang, 1995; Gunsinger *et al.* 2006; Akcil et Koldas, 2006; 1994; Blowes *et al.* 2003) afin de mieux cerner le problème. Cette plus grande attention s'explique en partie par le fait que les coûts de traitement des eaux contaminées et des travaux de restauration des sites miniers confrontés à ce problème sont très importants (Aubertin *et al.* 2002). Ainsi, deux types d'essais ont étés conçus,

dont les essais statiques (e.g., Jambor *et al.* 2002, 2003, 2007; Sobek *et al.* 1978; Miller *et al.* 1991; Lawrence and Wang, 1997; Skousen *et al.* 1997; Duncan et Bruynesteyn, 1979) et les essais cinétiques (e.g., MEND, 2009; Frostad *et al.* 2002; Villeneuve 2004). Les essais statiques sont utilisés durant les phases de développement des projets miniers.

Le principe des essais statiques est de faire le bilan instantané entre le potentiel de neutralisation (PN) et le potentiel d'acidification (PA) (Price *et al.* 1997), d'où son nom *Acid-Base Accounting* (ABA), en anglais. Ils sont largement utilisés du fait de leur rapidité et de leur simplicité (Blowes *et al.* 2003). On distingue les essais statiques chimiques et les essais statiques minéralogiques (Plante, 2005; Bouzahzah, 2013).

Les méthodes les plus populaires sont le pH de la pâte (MEND, 1991) et l'ABA de Sobek *et al.* (1978). La mesure du pH de pâte est une méthode rapide pour vérifier la prédominance des sels acides en mesurant le pH d'une suspension du rejet, alors que le bilan acide-base se fait généralement en 2 étapes : (1) la détermination du potentiel d'acidité (PA) et (2) la détermination du potentiel de neutralisation (PN). Le PA est déterminé par calcul en utilisant la teneur en soufre total ou en soufre sous forme de sulfure. Le PN calculé à partir du carbone inorganique total est appelé Pouvoir de Neutralisation des Carbonates (PNC) (Frostad *et al.* 2003; Plante *et al.* 2012), alors que le PN selon la méthode de Sobek et ses dérivés se fait par titrage acido-basique (Sobek *et al.* 1978; Miller *et al.* 1991; Lawrence and Wang, 1997; Skousen *et al.* 1997; Kwong and Ferguson, 1997). Le PN peut aussi être calculé en se basant sur la minéralogie. Il se fait en sommant le potentiel de neutralisation de chaque minéral pris individuellement. Il est aussi possible de faire un ABA à partir de la minéralogie de l'échantillon. Dans ce cas, le PA et le PN minéralogiques utilisent les résultats des caractérisations minéralogiques, et leur fiabilité en dépendent fortement (Plante *et al.*

2012). Pour plus de détails sur les essais, le lecteur intéressé pourra se référer à la thèse de Bouzahzah (2013) et sur l'article de Plante *et al.* (*2012*).

L'interprétation des résultats des essais statiques consiste à faire la différence entre le PN et le PA, appelé PNN (pouvoir net de neutralisation) ou le rapport entre les deux, qui est le NPR (« Neutralization potential ratio »; Price *et al.* 1997; MEND, 2009). La zone d'incertitude du PNN est comprise entre -20 et +20 kg $CaCO_3$/t. Un rejet ayant un PNN > 20 kg $CaCO_3$/t est considéré comme non générateur d'acidité, alors que si son PNN < -20 kg $CaCO_3$/t, il est considéré comme générateur d'acidité (Aubertin *et al.* 2002). Lorsqu'il s'agit du critère du NPR (PN/PA), le rejet est considéré comme potentiellement générateur d'acide lorsque le ratio est inferieur à 1 et potentiellement non-générateur si le rapport est supérieur à 2. Enfin, un échantillon dont le NPR se situe entre 1 et 2 est classé comme incertain (MEND, 2009).

Cependant, cette classification varie de manière importante selon les juridictions, ce qui fait que la définition des critères et de la zone d'incertitude est très controversée (Rousseau, 2012; Plante, 2004). La classification selon le NPR ne fait pas l'unanimité et est aussi problématique (Plante, 2004; Price *et al.* 1997; MEND, 2009). Dans tous les cas, les résultats de l'ABA doivent prendre en compte les résultats des caractérisations minéralogiques pour une meilleure interprétation (Rousseau, 2012; Bouzahzah, 2013; Maest et Kuipers, 2005) et le choix d'un essai statique devrait être basé sur la minéralogie (Plante *et al.* 2012). En plus d'une large zone d'incertitude, les essais statiques ne donnent pas d'informations sur les cinétiques et les taux de réaction (Miller *et al.* 1991). De plus, les lixiviats ne sont pas analysés pour les éléments dissous, d'où la pertinence des essais cinétiques. Le rapport du MEND (2009) suggère de conduire des essais cinétiques même si les resultats de l'ABA classe un échantillon comme non générateur d'acide, du fait que les eaux de drainage neutres ou alcalines peuvent être problématiques.

Les essais cinétiques durent plus longtemps que les essais statiques et leur réalisation est plus complexe et plus coûteuse. Ils sont basés sur une altération accélérée des rejets dans des conditions naturelles ou forcées (Bouzahzah, 2013; Bradham et Caruccio, 1990; Villeneuve, 2004). Beaucoup de données peuvent être générées permettant de calculer les taux de réaction et d'avoir une idée sur la qualité des eaux par le suivi géochimique des lixiviats obtenus. Il existe plusieurs types d'essais cinétiques : (1) l'essai en cellule humide (ASTM D 5744); (2) l'essai en mini-cellule d'altération; (3) l'essai en colonne; (4) les essais en flacons agités; (5) l'essai de confirmation *British Columbia Research* (BCR); (6) le réacteur Soxhlet; et enfin (7) les essais *in situ*. Tous ces essais sont similaires dans leur principe mais peuvent varier considérablement en termes de complexité, de durée et pour la qualité des données générées (MEND, 1991; Lapakko, 2002).

L'essai en cellule humide (Morin et Hutt, 1998) est le seul essai cinétique normé (ASTM D 5744-96, 1998; D 5744-07, 2007). L'essai a pour but d'accélérer l'altération des rejets en les soumettant à des cycles de séchage et de mouillage. Un rinçage marque la fin de chaque cycle. Cependant, dans le cas des essais en colonne (Benzaazoua *et al.* 2004) et en mini-cellule d'altération (Plante *et al.* 2010b; Villeneuve, 2004), le cycle de séchage et de mouillage se fait sans air sec. L'échantillon est rincé périodiquement afin de récupérer les lixiviats. L'analyse de ces lixiviats permet d'apprécier les cinétiques des réactions d'oxydation et de neutralisation. De plus, les essais en colonne peuvent être utilisés pour tester des scénarios de restauration (Demers *et al.* 2008). L'évaluation des scénarios de restauration peut se faire aussi directement sur le terrain. On parle alors d'essais cinétiques *in situ*; leur mise en œuvre est complexe et plus coûteuse (par ex., les parcelles expérimentales) et les processus géochimiques n'y sont pas accélérés, puisque les rejets sont lixiviés au gré des précipitations. Ils permettent cependant d'avoir des qualités d'eau des lixiviats plus réalistes et peuvent être utiles pour la modélisation numérique (Demers *et al.* 2013; Molson *et al.* 2008).

Comme pour les essais statiques, des approches ont été proposées pour interpréter les résultats des essais cinétiques (Villeneuve, 2004). Les données obtenues sont utilisées pour estimer les taux d'oxydation des sulfures à partir des sulfates et les taux de dissolution des minéraux neutralisants, ainsi que de suivre l'évolution de la qualité des eaux de drainage en fonction du temps (Villeneuve, 2004). A partir des résultats des essais en cellule humide, la norme ASTM D5744-96 (1998) propose le calcul d'un temps d'épuisement à partir des taux de production des sulfates, de calcium et de magnésium. Benzaazoua *et al.* (2004) proposent une méthode d'évaluation du potentiel de génération d'acide à long terme basée sur l'utilisation d'une courbe d'oxydation-neutralisation sur laquelle on place les teneurs initiales en soufre et en Ca+Mg+Mn. Cependant, les approches présentées visent exclusivement à évaluer le potentiel de génération d'acide des rejets miniers.

Les limites des essais cinétiques apparaissent souvent quand les teneurs en sulfures des rejets sont faibles (Li, 2000; Morin, 2003; Plante *et al.* 2011a; Walker *et al.* 2012). Dans ces conditions, les réponses géochimiques des rejets de ce type soumis aux essais sont bien plus faibles (Plante *et al.* 2011a) que sur le terrain. Un autre facteur limitant la fiabilité des outils de prédiction à statuer sur les cas de DNC, c'est l'apparition des phénomènes de sorption qui prennent place quand le pH est proche de la neutralité. Ces conditions retardent l'établissement d'un DNC. Il apparait donc que le DNC est difficile à prédire avec les outils conçus pour la prédiction du DMA. Toujours dans le domaine de la prédiction, les modèles numériques dont *MIN3P* (Demers *et al.* 2013; Molson *et al.* 2008) sont aussi de plus en plus utilisés, mais exigent des données solides pour la validation.

Les résultats obtenus lors des essais cinétiques sont souvent différents de ceux obtenus sur le terrain (Maest et Kuipers, 2005; Plante *et al.* 2014), et ceci pour plusieurs raisons : les essais de laboratoire ne prennent pas en compte tous les facteurs du terrain (Ardau *et al.* 2009). De plus, la comparaison des résultats des

essais cinétiques entre eux donne parfois des résultats contradictoires (Benzaazoua *et al.* 2001; 2004), démontrant ainsi l'impact des variations des conditions opératoires sur les résultats obtenus (Frostad *et al.* 2002, Bouzahzah, 2013; Sapsford *et al.* 2009). Dans ce contexte, il est important de développer de nouveaux outils ou d'adapter les outils existants afin de corriger les lacunes identifiées. Dans le même temps, lors de l'interprétation des résultats, il importe de tenir compte des facteurs liés aux effets d'échelles et aux phénomènes de sorption (par ex., cas de la mine Tio; Plante 2010c). Ainsi dans le cas de rejets ayant un potentiel de séquestration de carbone, les processus impliqués sont à prendre en compte dans la prédiction de leur comportement.

1.3 Séquestration du carbone par les rejets miniers

1.3.1 Généralités

Des stations de suivi de la concentration du CO_2 dans l'atmosphère indiquent que la barre des 400 ppm a été atteinte (The New York Times, 2013) et devrait être une moyenne générale dans 2 ou 3 ans (R.F.I., 2013). La concentration en CO_2 de l'atmosphère est passée de 280 ppm avant la révolution industrielle à 379 ppm en 2005 (IPCC, 2007). Cette augmentation rapide et inquiétante du CO_2 dans l'atmosphère a mobilisé les pouvoirs publics pour prendre des dispositions afin de contenir le problème, surtout que le CO_2 est le responsable principal mis en cause dans le dérèglement du climat observé. Cette volonté de freiner l'augmentation de la température s'est ainsi traduite par plusieurs rencontres et décisions importantes. La première conférence mondiale sur le climat s'est tenue à Genève (Suisse) en 1979 et a abouti à la création du Groupe d'experts intergouvernemental sur l'évolution du climat (GIEC ou IPCC en anglais) en 1988. Depuis sa création, le GIEC a produit plusieurs évaluations et rapports qui ont permis de mieux comprendre les risques liés aux changements climatiques et les principales stratégies de mitigation envisageables. Il y a eu aussi d'autres dates importantes où des décisions ont été prises : Rio (1992),

Kyoto (1997), Bali (2007), Durban (2011) et Doha (2012). À la fin 2015, il y a eu la grande conférence des Nations Unies sur le climat à Paris (COP21). Toutes ces rencontres ont abouti à établir des accords et de redéfinir des priorités et des politiques visant à réduire l'impact de l'activité humaine sur le climat.

De manière plus concrète, diverses approches ont été proposées afin de limiter l'augmentation du CO_2 anthropique (principal gaz à effet de serre) dans l'atmosphère. Globalement, les voies proposées peuvent être classées dans trois axes : (1) la promotion de l'utilisation des sources d'énergies renouvelables au détriment de sources fossiles, (2) une meilleure efficacité énergétique, et (3) la séquestration du carbone (Huijgen and Comans, 2003; IPCC, 2005). Cependant, chacune de ces voies a des avantages et des limitations (voir Huijgen and Comans, 2003). Pour résumer, les sources d'énergies fossiles sont, pour l'instant, moins coûteuses que les sources renouvelables. Ces dernières représentent quand même des alternatives pour le futur. Cependant, à court terme, l'on ne semble pas être sur la voie d'abandonner les sources d'énergies fossiles (IPCC, 2005). La séquestration du CO_2 qui est proposée peut se faire de plusieurs manières : le piégeage du CO_2 dans des formations géologiques ou dans les océans, et le piégeage sous formes de minéraux carbonatés stables. Cependant, l'envoi du CO_2 dans les océans peut malheureusement causer des baisses de pH localisées et des perturbations sur les écosystèmes marins (IPCC, 2005), en plus de son potentiel qui est relativement faible (Huijgen and Comans, 2003). Le piégeage du CO_2 dans les réservoirs géologiques pose le problème du transport mais aussi le risque de fuite de gaz (IPCC, 2005). D'ailleurs, pour rappeler ce risque, le cas du lac Nyos (Cameroun) est très souvent cité en exemple. La fuite soudaine de CO_2 y a causé la mort de plus d'un millier de personnes en 1986, sans parler des dommages sur la faune (Kling *et al.* 1987). Par conséquent, le stockage du CO_2 dans des réservoirs pose un problème de sécurité et nécessite un suivi quasi-permanent (Huijgen and Comans, 2003; IPCC, 2005) et donc coûteux, au contraire de la fixation du CO_2 par des sources riches en métaux alcalins et surtout alcalino-

terreux. Il s'agit principalement des roches riches en magnésium et en calcium, excluant les carbonates.

1.3.2 Carbonatation minérale

La fixation chimique du CO_2 par les sources de métaux divalents menant à la formation de carbonates est appelée carbonatation minérale. Seifritz (1990) a été le premier à émettre l'idée d'utiliser les minéraux silicatés pour fixer du CO_2 alors que Lackner *et al.* (1995) ont proposé les premières approches pour concrétiser cette idée. Cette méthode est considérée comme un moyen sûr et durable pour piéger du CO_2 selon Lackner (1995). En effet, la séquestration du carbone par les minéraux silicatés est un processus naturel et ne nécessite pas de suivi à long terme, contrairement au piégeage du CO_2 dans des réservoirs (Harvey *et al.* 2013) ou dans les océans. La fixation du CO_2 par les matériaux alcalins forme des carbonates stables sur plusieurs millions d'années (Allen and Brent, 2010; Teir *et al.* 2006; Lackner *et al.* 1995). Ce processus se déroule dans la nature de manière très lente (Wilson *et al.* 2009a). De plus, la vitesse de séquestration du carbone par les roches mafiques et utlramafiques est plus lente que la vitesse des émissions de CO_2 par les activités humaines. Cependant, plusieurs facteurs peuvent limiter le potentiel de séquestration du carbone par les minéraux, comme la passivation des surfaces des minéraux silicatés lors de leur altération (Assima *et al.* 2012), l'absence ou un excès d'eau, ou même l'apport en CO_2 (Assima *et al.* 2013a, 2014; Awoh *et al.* 2013; 2014).

Pour tirer profit au maximum de ce potentiel, nombreux sont les travaux de recherche qui ont évalué diverses approches afin d'accélérer les réactions et ainsi profiter au maximum de ce potentiel (*e.g.* Matter *et al.* 2016; Bobicki *et al.* 2015; Harrison *et al.* 2012; Power *et al.* 2013, 2009; Zhang *et al.* 2012; Jacobs et Hitch, 2011; Krevor and Lackner, 2011; Orlando *et al.* 2011; Larachi *et al.* 2010; Teir *et al.* 2007; Karam *et al.* 2006; Lackner *et al.* 1995). Diverses techniques plus ou moins complexes ont alors été proposées ou sont en cours de développement. Généralement, elles

consistent à extraire les cations divalents (Mg^{2+} ou Ca^{2+}) et à les faire réagir avec le CO_2 en une ou plusieurs étapes, avec ou sans eau, et dans des conditions de températures et de pressions très élevées. Les températures dépassent généralement les 100°C et les pressions peuvent aller jusqu'à 300 bars ou plus (Orlando *et al.* 2011; Zevenhoven *et al.* 2006).

Comme on peut s'y attendre, ces techniques sont très coûteuses car nécessitant souvent des apports considérables d'énergie et de produits chimiques (Muriithi *et al.* 2013; Nduagu *et al.* 2012a, 2012b). Leur applicabilité à l'échelle industrielle tardent ainsi à se mettre en œuvre (Power *et al.* 2013). N'empêche, plusieurs groupes de recherche s'attellent à réduire le temps de réaction et à tirer avantage au maximum de la carbonatation minérale. Le lecteur intéressé par les différentes techniques de carbonatation minérale trouvera des informations pertinentes dans les revues de littérature proposée par de Bobicki *et al.* (2012), Olajire *et al.* (2013) et Huijgen and Comans, (2003). Ces auteurs présentent les différents types de sources utilisables dans la carbonatation minérale, ainsi qu'une description des techniques et des procédés utilisés et les performances associées.

La carbonatation minérale passive du CO_2 dans des conditions ambiantes par les minéraux silicatés et autres hydroxydes de calcium ou de magnésium a connu un regain d'intérêt lors des dix dernières années. La raison principale est que ces sources de cations divalents sont disponibles en quantités importantes dans des rejets industriels (e.g. scories d'aciéries, cendres d'incinérateurs, rejets de cimenteries) (Muriithi *et al.* 2013; Santos *et al.* 2012; Bobicki *et al.* 2012; Bertos *et al.* 2004; Huntzinger *et al.* 2009), dans les roches mafiques et ultramafiques et, enfin, dans des rejets miniers (Bobicki *et al.* 2012). De plus, les coûts reliés au minage et au broyage peuvent être *de facto* absorbés par les opérations minières (Lackner *et al.* 1995). De ce fait, l'utilisation des rejets miniers comme sources de magnésium ou de calcium est très attrayante d'un point de vue économique. De plus, lorsque ces rejets miniers

ou industriels sont exposés sur de larges surfaces, la consommation du CO_2 est beaucoup plus importante et ces piles de rejets deviennent de gigantesques réacteurs naturels (Thom *et al.* 2013; Hitch *et al.* 2010; Wilson *et al.* 2009a). La carbonatation minérale des rejets miniers riches en certains minéraux silicatés peut ainsi contribuer à diminuer significativement l'empreinte carbone des industries minières. À titre d'exemple, Wilson *et al.* (2014) avance que les émissions de CO_2 des opérations de la mine Mount Keith (Australie) pourraient être compensées par la carbonatation de seulement 11 % de ses résidus ultramafiques.

Les travaux récents sur des sites miniers et au laboratoire ont permis d'améliorer les connaissances sur les mécanismes et les facteurs affectant les processus de carbonatation des rejets miniers dans les conditions environnementales et, surtout, de prendre conscience de leur potentiel encore inexploité (Power *et al.* 2014). Même si la plupart des travaux se concentrent sur la carbonatation accélérée, quelques groupes de recherche se sont intéressés aux mécanismes de la carbonatation minérale passive des rejets miniers et industriels.

1.3.3 Les mécanismes de la carbonatation minérale passive

Le calcium et le magnésium sont généralement les éléments les plus prisés dans la carbonatation puisque qu'ils sont plus courants et disponibles en quantités importantes dans les roches mafiques et ultramafiques (Goff et Lackner, 1998; Lackner *et al.* 1995; Tomsich *et al.* 2014). En effet, ces deux métaux alcalino-terreux se retrouvent dans la croûte terrestre à des pourcentages qui avoisinent les 2 % (Mg) et 3 % (Ca) (Goff et Lackner, 1998). Cependant, l'utilisation des silicates magnésiens comme une source de cations divalents est plus attractive que l'utilisation des silicates de calcium, puisque les premiers contiennent plus de métal divalent (Goff and Lackner, 1998). De ce point de vue, les silicates magnésiens sont très prisés : il s'agit principalement de la forstérite (Mg_2SiO_4) et les trois formes de la serpentine ($Mg_3Si_2O_5(OH)_4$) que sont la lizardite, le chrysotile et l'antigorite. Ces minéraux

possèdent des propriétés thermodynamiques et chimiques nécessaires pour la fixation du CO_2 (Goff and Lackner, 1998). La brucite ($Mg(OH)_2$) est aussi un minéral qui est très réactif par rapport au CO_2 pour former des carbonates stables. Ceci explique les nombreuses études qui portent sur l'altération de ces minéraux dans diverses conditions (e.g. Pokkrovsky et Schott, 2004; Pokkrovsky et Schott, 2000; Schaef *et al.* 2011; Teir *et al.* 2007; Thom *et al.* 2013; Daval *et al.* 2013).

La séquestration du carbone par les minéraux silicatés comme la serpentine, l'olivine, le talc, ou les hydroxydes comme la brucite, peut se faire de manière naturelle, quand ces minéraux se retrouvent exposés à l'air et à l'eau (Seifritz, 1990; Lackner *et al.* 1995). Ce processus présente une certaine analogie avec l'oxydation des sulfures dans les conditions environnementales. L'altération des silicates magnésiens et calciques ou des hydroxydes de magnésium se traduit par la libération du magnésium ou du calcium dans l'eau. La vitesse d'altération des minéraux séquestreurs de carbone peut être augmentée lorsque les rejets sont finement broyés et exposés sur de larges surfaces. La précipitation des carbonates de magnésium ou de calcium est le fruit d'un ensemble de processus qui est entamé lors de la dissolution du CO_2 dans l'eau interstitielle, produisant ainsi des ions carbonates (CO_3^{2-}) et bicarbonates (HCO_3^-), mais aussi des ions H^+ capables de réagir avec certains silicates et la brucite. Le milieu se retrouve alors chargé en cations divalents (Ca^{2+} ou Mg^{2+}) et en anions (CO_3^{2-} et HCO_3^-). Lorsque ces éléments deviennent saturés, ils précipitent pour former des carbonates de Mg ou de Ca hydratés (Équation 1.10; Power *et al.* 2014). Globalement, les processus peuvent être considérés comme une réaction acide-base (Huijgen and Comans, 2003). De plus, la réaction de carbonatation entre les silicates et le CO_2 est exothermique.

$$5Mg^{2+} + 4CO_3^{2-} + 2OH^- + 4H_2O \xrightarrow{Évaporation} Mg_5(CO_3)_4(OH)_2 \cdot 4H_2O \qquad (1.10)$$

Le pH est un facteur important à considérer. D'une part, la dissolution du CO_2 est beaucoup plus importante à pH alcalin. À l'inverse, la dissolution des silicates est beaucoup plus rapide quand le pH est bas (White and Brantley, 1995; Luce *et al.* 1972), Cependant, la précipitation des carbonates est favorisée à pH alcalin (> 8-9) puisque les ions CO_3^{2-} et HCO^- sont les espèces dominantes du CO_2 à ces pH (Teir *et al.* 2007), comme le montre la Figure 1.3. La présence d'eau est aussi une condition *sine qua none* pour la carbonatation minérale. Cependant, les pores ne doivent pas être totalement saturés pour permettre la migration du CO_2 et sa dissolution dans l'eau. Une saturation partielle des rejets est optimale pour la carbonatation de rejets ultramafiques (Assima *et al.* 2012; 2013a; Pronost *et al.* 2011; Awoh *et al.* 2013).

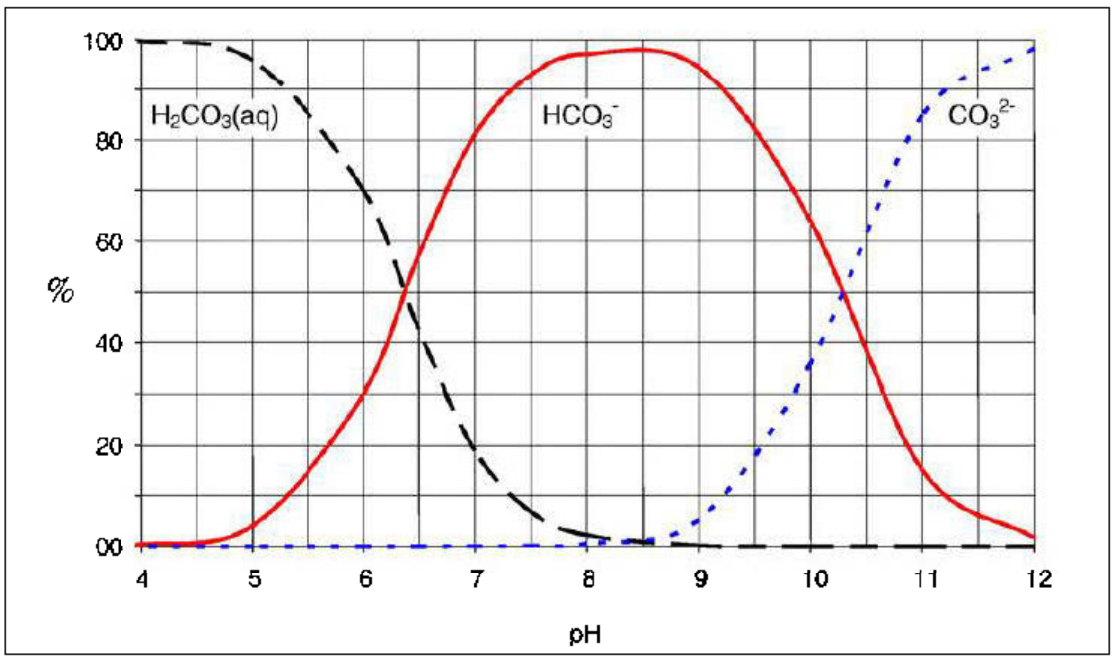

Figure 1.3 Distribution des espèces de carbonates dissous à l'equilibre en fonction du pH (tirée de Teir *et al.* 2007)

Comme le montre l'équation 1.10, l'hydromagnésite, un carbonate de magnésium hydraté, précipite. D'autres carbonates de magnésium hydratés peuvent aussi précipiter dépendamment de la température, de la pression partielle de CO_2 et de la

salinité. Les carbonates les plus communs sont l'hydromagnésite ($Mg_5(CO_3)_4(OH)_2 \cdot 4H_2O$), la nesquehonite ($MgCO_3 \cdot 3H_2O$), la dypingite ($Mg_5(CO_3)4(OH)_2 \cdot 5H_2O$), la lansfordite ($MgCO_3 \cdot 5H_2O$) et la pyroaurite ($Mg_6Fe_2(CO_3)(OH)_{16} \cdot 4H_2O$). De ces carbonates de magnésium, l'hydromagnésite est le plus stable dans les conditions environnementales, après la magnésite ($MgCO_3$) (Langmuir, 1965).

La Figure 1.4 est tirée des travaux de Wilson *et al.* (2009a) sur les rejets des mines de Cassiar et Clinton Creek (Canada). Les auteurs y expliquent les mécanismes de formation des carbonates sur les piles de rejets ultramafiques. Ils suggèrent deux différents types d'occurrence des carbonates magnésiens. La nesquehonite précipite sous forme de croûtes sur les surfaces verticale et horizontale de la pile de rejets. Les auteurs suggèrent que sa formation est favorisée principalement par l'évaporation intense dont sont sujettes les surfaces exposées à l'air. Par contre, l'hydromagnesite et la dypingite sont détectées à quelques centimètres sous la surface, plus humide. La présence des carbonates sous la surface jusqu'à plus de 2 m de profondeur témoigne de la progression du CO_2 jusqu'à l'intérieur des résidus, malgré la cimentation observée en surface (Wilson *et al.* 2009a). D'après les auteurs, cela montre que l'évaporation n'est pas le seul facteur responsable de la précipitation des carbonates de magnésium. Une hypothèse plausible est que ces carbonates sont issus de la transformation de la nesquehonite. En effet, la nesquehonite peut se transformer en hydromagnésite puis en dypingite, lorsque la température augmente et/ou lorsqu'il y a variation de la pression partielle de CO_2 (Langmuir, 1965).

Comme le montre la Figure 1.4, la précipitation des carbonates peut souder les grains entre eux et induire une cimentation à la surface des rejets. Ce phénomène est similaire au développement de zones indurées qu'on retrouve souvent dans les empilements de rejets miniers sulfurés, du fait de la précipitation des minéraux secondaires issus des processus d'oxydation des sulfures et de dissolution des

minéraux acidivores. La présence des carbonates en dessous de la zone cimentée démontre que la carbonatation se poursuit en profondeur malgré la diminution de porosité induite par la cimentation des rejets.

La carbonatation des rejets ultramafiques peut être influencée par plusieurs facteurs, en plus du pH et du degré de saturation en eau mentionnés précédemment. Au premier plan, il y a les caractéristiques des rejets, notamment leur distribution granulométrique, l'hydrologie et la composition minéralogique (Power *et al.* 2013; Assima *et al.* 2012; 2013a; Wilson *et al.* 2009a). Les travaux d'Assima *et al.* (2012) ont montré que la présence de fer dans les rejets ultramafiques pouvaient constituer un frein à la carbonatation. En effet, la précipitation des hydroxydes de fer peut passiver la surface des grains de serpentine et ainsi diminuer leur réactivité. La dissolution incongruente de la serpentine, qui libère préférentiellement le magnésium, peut aussi entrainer la diminution de leur réactivité du fait de la passivation des surfaces par la silice (Assima *et al.* 2012; Luce *et al.* 1972). Enfin, la précipitation des carbonates de magnésium hydratés peut aussi passiver la surface de la brucite ou de la serpentine (Zarandi *et al.* 2016).

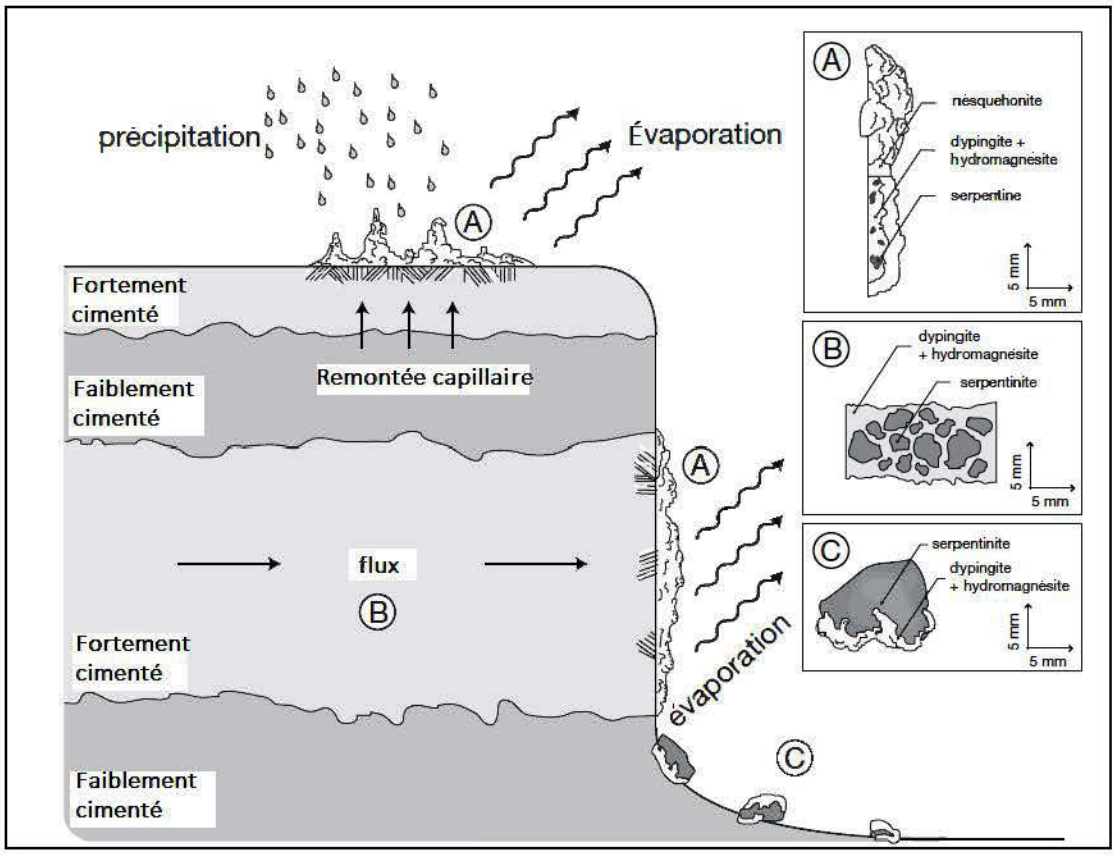

Figure 1.4 Figure conceptuelle illustrant les mécanismes de formation des carbonates de magnésium sur une pile de résidus ultramafiques (adaptée de Wilson *et al.* 2009a). Le schéma montre la précipitation de carbonates de magnésium à différents degrés d'hydratation : A) précipitation de croûtes de nesquehonite sur les surfaces horizontale et verticale, B) Grains de serpentine cimentés par l'hydromagnésite et la dypingite et C) précipitation de dypingite et d'hydromagnésite autour des grains de serpentine

Quelques auteurs ont aussi souligné l'importance de la présence de la brucite dans les rejets ultramafiques. Il est déjà connu que la réactivité de la brucite est de plusieurs ordres de grandeurs plus élevée que les minéraux silicatés réactifs par rapport au CO_2 (Figure 1.5). Assima *et al.* (2014c) et Pronost *et al.* (2011) avancent que c'est la teneur en brucite qui détermine la quantité maximale de CO_2 séquestrée. Cependant,

des taux de carbonatation élevés ont été mesurés pour des rejets ultramafiques qui contenaient pas ou peu de brucite (Wilson *et al.* 2009a, 2009b; Oskierski, *et al.* 2013).

Les processus impliqués dans la carbonatation peuvent aussi être accélérés par l'activité bactérienne. D'ailleurs, des auteurs ont même suggéré l'utilisation des bactéries pour promouvoir la carbonatation des rejets ultramafiques (Power *et al.* 2014).

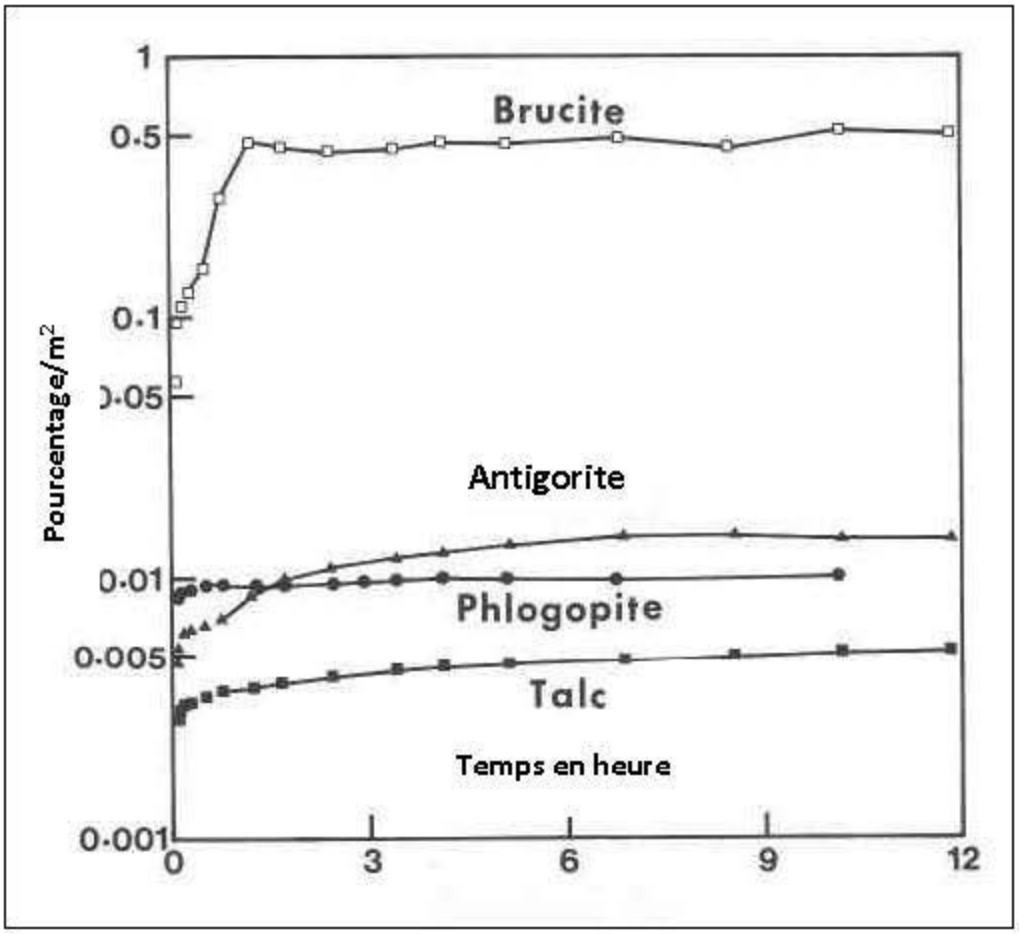

Figure 1.5 Pourcentage de Mg libéré lors de la dissolution de la brucite, de la phlogopite, du talc et de l'antigorite. À noter que les pourcentages sont normalisés par rapport à la surface specifique de chaque minéral. Adaptée de Lin and Clemency (1981)

1.3.4 Synthèse des travaux sur la carbonatation minérale des rejets miniers ultramafiques

Certains métaux de base comme le nickel, le cuivre, le platine ou certains minéraux de valeurs comme la chrysotile (amiante), le diamant et la chromite peuvent se retrouver associés à des gisements de roches mafiques et ultramafiques. Leur exploitation conduit ainsi à la production de grandes quantités de rejets riches en

silicates de magnésium ou en brucite (Power *et al.* 2014; Wilson *et al.* 2009a; Vogeli *et al.* 2011; Beinlich and Austrheim, 2012). De même, ces éléments réactifs au CO_2 peuvent aussi se retrouver dans des rejets industriels issus des cimenteries et des fonderies. Ces minéraux deviennent alors une source importante de cations divalents (Mg^{2+} et Ca^{2+}) lors de leur altération.

Comparée à la carbonatation accélérée, très peu de travaux se sont penchés sur la séquestration du carbone *in situ* par des rejets miniers riches en minéraux séquestreurs de carbone. Les données de ces rares travaux sont synthétisées dans le Tableau 1.1. Au Canada, il y a eu les travaux sur les rejets de la mine Diavik (Territoires du Nord-ouest; Wilson *et al.* 2011; Wilson *et al.* 2009b), les mines Clinton Creek et Cassiar en Colombie Britannique (Wilson *et al.* 2009a; Wilson, 2006), et aussi sur les rejets d'une ancienne mine d'amiante à Thetford Mines au Québec (Assima *et al.* 2013; 2012; Pronost *et al.* 2012; Beaudoin *et al.* 2008; Lechat *et al.* 2016). À Clinton Creek (Yukon) et à Cassiar (Colombie Britanique), des études isotopiques du carbone et de l'oxygène ont été utilisées afin de démontrer que c'est le carbone atmosphérique qui est séquestré (Wilson *et al.* 2009a). Parmi ces mines au Canada, seule Diavik, dont l'exploitation a débuté en 2003, est encore active.

À Thetford Mines, la formation des carbonates de magnésium hydratés a été rapportée dans le début des années 2000 (Huot *et al.* 2003). Récemment, un groupe de recherche de l'Université Laval a découvert des évents d'air chauds qui s'échappent des piles de rejets miniers, appauvris en CO_2 et montrant des températures qui dépassent la température ambiante (Pronost *et al.* 2012), rappelant que la réaction de carbonatation de la serpentine est exothermique (Équation 1.11; tirée de Power *et al.* 2009).

$$Mg_3Si_2O_5 + 3CO_2 \rightarrow 3MgCO_3 + 2SiO_2 \quad \Delta H = -67\ kJ/mol \qquad (1.11)$$

Ailleurs dans le monde, des rejets miniers présentent des propriétés similaires. En Norvège, des signes de carbonatation ont été observés sur les parois d'une ancienne mine souterraine de chromite, qui est dans un gisement ultramafique, fermée depuis 1920 (Beinlich and Austrheim, 2012). Les carbonates de magnésium hydratés tapissent les galeries sur des épaisseurs allant du mm au cm. L'eau se déchargeant de la mine est alcaline avec un pH variant entre 9,4 et 10,6, avec des concentrations de Mg qui se situent entre 15 et 90 mg/L (Beinlich and Austrheim, 2012). D'ailleurs, cette étude est l'une des rares à rapporter des données liées à la qualité des eaux minières de rejets miniers avec un potentiel de séquestration de carbone, après les travaux de Rollo et Jamieson (2006). En Australie, la néoformation de carbonates de magnésium hydratés a été rapportée sur deux sites miniers. Il s'agit de la mine de nickel de Mount Keith (Wilson *et al.* 2014) qui est active depuis 1994, et la mine de chrysotile de Woodsreef (Oskierski, *et al.* 2013), fermée depuis 1983. La quantité de CO_2 piégée par les rejets de Mount Keith est estimée à 39 800 tonnes annuellement, ce qui représente un taux de carbonatation de l'ordre de 2400 g CO_2/m^2/année (Wilson *et al.* 2014). Des changements dans la gestion des résidus pourraient contribuer à accélérer grandement le taux de carbonatation des rejets et à diminuer significativement l'empreinte carbone de cette mine, d'après les simulations de Wilson *et al.* (2014). À l'ancienne mine d'amiante de Woodsreef en Australie, d'importantes croûtes de carbonates de magnésium se sont formées à la surface des résidus, témoignant d'une importante altération de la serpentine et de la brucite. Oskierski *et al.* (2013) estiment qu'en 29 années d'exposition, les rejets de Woodsreef ont séquestré entre 1400 et 70 000 tonnes de CO_2 sous forme de carbonates de magnésium (hydromagnesite et pyrauorite). Sur ce site, le taux de carbonatation est estimée entre 99 et 4876 g CO_2/m^2/ année.

Il y a une différence évidente au niveau des taux de carbonatation des rejets miniers pour les différents sites miniers présentés ici. Les principales raisons sont, entre autres, la distribution granulométrique des rejets, la surface exposée, la méthode de

déposition (en surface ou submergé, compactage), la composition minéralogique des rejets (incluant la quantité de brucite), ainsi que des facteurs liés au climat tels l'hydrologie et l'évaporation, qui diffèrent selon les sites. Le taux de consommation de CO_2 observé à Clinton Creek est plus élevé que pour les autres sites et est essentiellement dû au fait que les résidus, déjà très fins, ne sont pas ennoyés (Power *et al.* 2014).

Jusqu'à maintenant, les auteurs se sont très peu intéressés aux caractéristiques des eaux minières qui intéragissent avec les rejets mafiques et ultramafiques, ainsi que l'impact des processus de formation des carbonates de magnésium hydratés sur les eaux de drainage, son évolution et son impact sur une modification éventuelle des caractéristiques intrinsèques des rejets ultramafiques. D'ailleurs, une meilleure connaissance des caractéristiques des eaux de drainage pourrait aider à mieux comprendre les processus qui contrôlent la carbonatation puisque nous avons vu que l'eau y joue un rôle important.

Les carbonates formés ou même les processus en amont peuvent favoriser l'établissement de conditions de DNC ou de drainage alcalin. Aux pH alcalin ou neutre, certains métaux sont toujours solubles dans l'eau et peuvent donc se retrouver dans les eaux de drainage à des concentrations supérieures aux limites permises par la législation. La séquestration du carbone est donc un phénomène géochimique important à considérer dans la prédiction de la qualité de l'eau de drainage de rejets miniers serpentinifères.

Tableau 1.1 Les sites miniers qui ont fait l'objet d'études pour leur carbonatation minérale

	Clinton Creek (Canada)	**Diavik (Canada)**	**Mount Keith (Australie)**	**Woodsreef Chrysotile Mine (Australie)**	**Feragen ultramafic body (Norvége)**	**Thetford mine (Canada)**
Situation	Parc à résidus, Fermée depuis 1978	Parc à résidus; Mine active depuis 2003	Parc à résidus; Mine active depuis 1994)	Parc à résidus; Fermée depuis 1983	Galeries; Fermées depuis 1920	Rejets d'usinage; Fermée depuis 1956
Minéralogie	Chrysotile ~ 88%	Lizardite + Forsterite ~ 73%	serpentine ~ 81 %	Serpentine (lizardite et chrysotile)	Serpentine (chrysotile et lizardite) et Olivine	Lizardite, antigorite, et chrysotile > 90%
Teneur en brucite	n.d	n.d	1.0–2.5 wt.%	Trace	Trace	Trace
Principaux carbonates identifiés	Nesquehonite , dypingite, hydromagne-site, lansfordite.	Nesquehonite	Hydromagne-site	Hydromagne-site et Pyroaurite	Lansfordite et nesquehonite,	Hydromagne-site
pH des eaux de drainage ou de procédé	Non rapporté	~ 8	5 – 8 (eau des pores)	Non rapporté	9.4 – 10.6	Non rapporté
Concentrat-ions d'éléments rapportés (mg/L)	Mg + Ca: 160 (eau des pores)	Mg + Ca: 40 (eaux de procédés)	Mg + Ca: 3500 (eaux de procédés)	Non rapporté	Eau miniere : Mg^{2+}: 15.6 – 88.5; Si : 0 – 9.3; Ca : 0.36 – 1.02; SO_4^{2-} : 0.67 – 1.34	Non rapporté
Taux de carbonatat-ion passive des rejets (g CO_2/m^2/ an)	6200	374 - 418	2400	99 - 4876	n.d	978
Références	Wilson *et al.* 2009a	Wilson *et al.* 2011; 2009b; Baker *et al.* 2003	Wilson *et al.* 2014; Bea *et al.* 2011	Oskierski, *et al.* 2013	Beinlich et Austrheim 2012	Pronost *et al.* 2012; Beaudoin *et al.* 2008

1.4 Le Projet Dumont de RNC Minerals

Le site faisant l'objet de la présente étude est le projet Dumont de Royal Nickel Corporation (RNC), une mine à ciel ouvert en développement, située à 25 km à l'ouest de la ville d'Amos, dans la région de l'Abitibi-Témiscaminque, au Québec. La

région a une longue histoire minière avec plusieurs mines, dont certaines sont toujours actives. Le site du projet Dumont a un climat continental avec des moyennes de températures variant entre -17.3°C en janvier à 17.2°C au mois de juillet. La moyenne annuelle de la température est de 1.2°C. Les précipitations totales entre 2011 et 2014 varient entre 840 et 960 mm (Environnement Canada), alors que la précipitation moyenne annuelle est de 918 mm (Staples *et al.* 2013).

Le gisement est la troisième plus importante réserve de nickel au monde, et potentiellement une des plus vastes exploitations de métaux de base du Canada. La mine prévoit de traiter 52 500 tonnes de minerai par jour dans les 5 premières années avant de passer à 105 000 tonnes par jour après la cinquiéme année d'opération, à une teneur moyenne de 0,27 % Ni avec une récupération d'environ 66 % (Staples *et al.* 2013). La durée de vie prévue de la mine est de 33 années. L'usine devrait produire environ deux gigatonnes de rejets de concentrateur et de stériles. La fosse qui sera creusée devrait être l'une des plus profondes du Québec (environ 560 m) et aura une longueur de 4,9 km par 1,4 km de largeur. Le minerai exploité est dans un gisement de nickel dont la minéralisation est de 2 types : sous forme de sulfures de nickel (pentlandite, $(Fe,Ni)_9S_8$, heazlewoodite, Ni_3S_2, millérite, NiS), et d'alliage fer-nickel (awaruite, Ni_3Fe). D'ailleurs, peu d'informations sont disponibles sur le comportement géochimique de l'awaruite dans les conditions environnementales.

Le gisement se trouve dans une zone minéralisée de dunite serpentinisée, composée majoritairement de lizardite et de minéraux mineurs dont la magnétite, la brucite, la chlorite, la diopside et la chrysotile. La géologie et la formation du gisement de Dumont sont présentées plus en détails dans Sciortino *et al.* (2015).

Les études préliminaires ont écarté la possibilité de génération du DMA (Staples *et al.* 2013) mais mettent en exergue un fort potentiel de séquestration de carbone des rejets (Pronost *et al.* 2011). L'évaluation du potentiel de séquestration de carbone par les rejets de concentrateur de Dumont a été faite par l'université Laval, avec des

essais en eudiométrie. Ces essais permettent de mesurer la diminution (donc la consommation) du CO_2 initialement injecté dans un compartiment contenant des résidus (environ 5 g). Cependant les conditions de réalisation de ces essais reflètent peu les conditions de terrain (quantité, hétérogénéité, etc.).

1.5 Objectifs et hypothèses de la thèse

Cette thèse s'inscrit dans un projet plus global impliquant l'Université du Québec en Abitibi-Témiscamingue (UQAT), l'Université Laval (U LAVAL) et un partenaire industriel qui est la société RNC Minerals. Ainsi, ce projet interdisciplinaire implique l'engagement de trois étudiants au doctorat, d'un étudiant au DESS (Diplôme d'Études Supérieures Spécialisées) et, enfin, d'un stagiaire postdoctoral. Ce partenariat a pour but de caractériser le potentiel de séquestration du CO_2 des matériaux de Dumont et l'impact de ce phénomène sur la qualité des eaux de drainage. Les étudiants au doctorat à l'Université Laval (A. Gras et A. Entezari Zarandi) s'intéressent principalement aux aspects fondamentaux de la séquestration du carbone par les matériaux du projet Dumont de RNC. Le stagiaire postdoctoral (S. Awoh) et l'étudiant au DESS (A. Ibrahim Saïb) ont pour objectif de développer une méthode de quantification du CO_2 séquestré par les rejets en s'inspirant de l'essai de consommation d'oxygène qui a été développé pour évaluer la réactivité des rejets miniers sulfurés.

L'objectif principal de cette thèse est d'améliorer la prédiction du drainage contaminé neutre ou alcalin de rejets miniers serpentinifères ayant un potentiel de séquestration en carbone. Les objectifs spécifiques visés par ce projet de recherche peuvent être résumés de la façon suivante :

1. Évaluer la qualité des eaux de drainage des matériaux du projet Dumont à partir d'essais cinétiques de laboratoire et en cellules de terrain;

2. Évaluer le comportement géochimique des concentrés de minerai d'awaruite et des sulfures de nickel (pentlandite et heazlewoodite);
3. Évaluer le potentiel de séquestration de carbone et son influence sur la qualité des eaux de drainage des matériaux, à partir d'essais cinétiques de laboratoire et en cellules de terrain;
4. Évaluer les effets d'échelle entre les résultats du laboratoire et en cellules de terrain.

Les hypothèses s'énoncent comme suit :

1. La séquestration du CO_2 par les matériaux du projet Dumont est significative et les carbonates formés sont stables;
2. Les essais en colonne peuvent reproduire de manière adéquate l'altération des rejets miniers ultramafiques;
3. Les processus qui mènent à la formation des carbonates peuvent favoriser l'établissement des conditions de DNC ou de drainage alcalin;
4. À des pH neutres et alcalins, certains métaux sont solubles et il y a donc possibilité de production d'eau minière contaminée;
5. Puisque les conditions de réalisation des essais cinétiques au laboratoire sont différentes de celles du terrain, on peut s'attendre à des différences dans la qualité d'eau entre le laboratoire et le terrain.

1.6 Structure de la thèse

Afin d'atteindre les objectifs de cette thèse, des essais cinétiques ont été réalisés au laboratoire et sur le terrain. Également, une caractérisation détaillée a été réalisée sur les matériaux de Dumont, en amont et en aval des essais cinétiques. La présente thèse est composée de six chapitres. Après ce premier chapitre qui fait office d'introduction, le chapitre suivant traite des résultats des essais en colonne et en mini-cellules d'altération sur les résidus de concentrateur produits en usine pilote, ainsi que

des concentrés de minerai (awaruite et sulfures de nickel). Ces essais cinétiques combinés à une caractérisation détaillée ont permis de mieux comprendre l'étendue de la carbonatation minérale des rejets, son influence sur la qualité des lixiviats et aussi les modifications induites sur les propriétés intrinsèques des rejets. Le chapitre III présente les résultats des essais cinétiques en colonne, de caractérisation des stériles et des principales lithologies rencontrées sur le site du projet Dumont. Le chapitre IV présente une comparaison des résultats des essais cinétiques aux différentes échelles (laboratoire et terrain), ainsi qu'une évaluation de l'influence de la température, la surface spécifique et le ratio liquide-solide sur la qualité des eaux de drainage et sur le potentiel de séquestration de carbone. Le chapitre V est consacré à une discussion de certains aspects, dont l'influence de la formation des carbonates sur le pouvoir de neutralisation (PN), ainsi que la méthode d'entreposage des rejets qu'il faudrait privilégier pour favoriser la fixation du CO_2 par les matériaux de Dumont. Enfin, le dernier chapitre présente les principales conclusions et recommandations que l'on peut tirer de cette thèse. Les chapitres II, III et IV ont été rédigés sous forme d'articles qui ont été soumis dans des revues internationales avec comité de lecture.

1.7 Avancements et contributions scientifiques anticipées

Les principales avancées des vingt dernières années dans le domaine de la carbonatation minérale passive des rejets miniers ultramafiques ont été acquises principalement à partir de travaux *in situ* sur des empilements de rejets qui ont pris plusieurs décennies à s'altérer et à générer toutes ces données utilisables aujourd'hui. Cependant, jusqu'à maintenant, les essais de laboratoire (eudiométrie et réacteurs) utilisés pour l'étude de la carbonatation des rejets ultramafiques se font dans des conditions peu représentatives des conditions de stockage des rejets. De plus, ces essais ne s'intéressent pas à la qualité des lixiviats en contact avec les rejets.

Les essais cinétiques réalisés dans cette thèse permettent de générer, dans des délais relativement courts (environ une année ou moins), des données similaires à celles du terrain. En effet, ces essais permettent d'évaluer des phénomènes de carbonatation, son évolution et son impact sur la qualité des eaux de drainage et sur les propriétés des rejets, afin de mieux comprendre ces phénomènes mais aussi de proposer, à partir de ces résultats, des méthodes de déposition qui favorisent la séquestration du carbone par les rejets ultramafiques. Pour la première fois, des essais cinétiques sont donc utilisés afin de répondre à ces objectifs. De plus, ces travaux permettront de fournir des informations pertinentes sur le comportement géochimique de l'awaruite, pour lequel très peu d'informations sont trouvées dans la littérature. Enfin, les résultats de cette thèse devraient permettre d'améliorer la compréhension de l'effet d'échelle dans les études de prédiction du comportement géochimique de rejets serpentinifères. Ces résultats pourront également aider les minières qui produisent des rejets ultramafiques à mieux profiter de leur potentiel de séquestration de CO_2. Ainsi, les conclusions de ces travaux seront applicables à divers sites miniers dont les rejets ont un potentiel de séquestration de carbone. Les résultats permettront de jeter les bases d'une approche pour la prédiction de la qualité des eaux de drainage de rejets miniers séquestreurs de carbone.

CHAPITRE II

KINETIC TESTING TO EVALUATE THE MINERAL CARBONATION AND METAL LEACHING POTENTIAL OF ULTRAMAFIC TAILINGS: CASE STUDY OF THE DUMONT NICKEL PROJECT, AMOS, QUEBEC

Cet article a été accepté pour publication à la revue "*Applied Geochmistry* ", en Mars 2017

Auteurs

Kandji, El Hadji Babacar [(a)], Plante, Benoit [(a),] Bussière, Bruno [(a)], Beaudoin, Georges [(b)], Dupont, Pierre-Philippe [(c)]

[(a)] Research Institute in Mining and Environment (RIME), UQAT (Université du Québec en Abitibi-Témiscamingue), 445 boulevard de l'Université, Rouyn-Noranda, Québec, J9X 5E4, Canada.

[(b)] Department of Geology and Geological Engineering, Université Laval, Québec, Québec G1V 0A6, Canada.

[(c)] Royal Nickel Corporation, 42 Rue Trudel, Amos, Québec, J9T 4N1, Canada

Résumé

Les rejets miniers ultramafiques sont connus pour leur capacité à réagir avec le CO_2 pour former des carbonates de magnésium hydratés stables. Cette étude porte sur l'évaluation du comportement géochimique des résidus miniers ultramafiques provenant du projet nickélifère de Dumont (Royal Nickel Corporation, Québec, Canada), en utilisant des essais cinétiques, afin d'évaluer le potentiel de carbonatation et l'impact de ce dernier sur la qualité des eaux de drainage à long terme. L'altération et le potentiel de génération de contamination de l'awaruite, de la pentlandite et de la heazlewoodite, les principales sources de Ni dans ces matériaux, ont également été étudiés. Un essai en colonne et des essais à plus petite échelle (mini-cellules d'altération) ont été utilisés pour simuler l'altération passive des rejets miniers ultramafiques, ainsi que pour les concentrés d'awaruite et de sulfures de Ni. Les résultats des essais cinétiques confirment que les résidus Dumont ont un fort potentiel de séquestration du carbone. Les taux de carbonatation calculés varient entre 600 et 2200 g de $CO_2/m^2/an$. Les résultats montrent aussi que la teneur en brucite est le principal paramètre contrôlant la séquestration du CO_2 par les rejets de concentrateur de Dumont. La dissolution de la brucite et de la serpentine est causée par la dissolution du CO_2 et potentiellement par l'acide généré par l'oxydation de sulfures. La dissolution rapide de la brucite induit un pH alcalin dans les lixiviats. Ce pH élevé semble être un frein à la mobilité des métaux; Ni, Zn, Fe et le Cu semblent être immobilisés dans la phase solide immédiatement après leur libération par l'oxydation des sulfures. L'awaruite semble être stable et ne libère pas de métaux dans les conditions des essais cinétiques. Les rejets de concentrateur de Dumont ne sont pas générateurs d'acide et leur potentiel de séquestration du CO_2 joue un rôle important dans la qualité des lixiviats.

Abstract

Ultramafic mine waste are known to react passively with CO_2 to form stable hydrated magnesium carbonates. This study focuses on the evaluation of ultramafic mine tailings from the Dumont project (RNC Minerals, Quebec, Canada), using kinetic tests, in order to assess its carbonation potential and its impact on the long-term quality of drainage water. The weathering and potential of generation of contamination from awaruite, pentlandite, and heazlewoodite, the main sources of Ni in the studied materials, were also investigated. A column test and small scale weathering cell tests were used to simulate the passive weathering of ultramafic mine wastes, as well as for concentrates of awaruite and Ni-sulfides. Results of kinetics tests confirm that the Dumont tailings have a significant carbon sequestration potential which range from 8.5 and 33.6 $kgCO_2/t$. The surface-normalized carbonation rates vary from 600 to 2200 g of CO_2/m^2/year. Results show that the brucite content is the main parameter controlling the CO_2 uptake by the Dumont waste. Weathering of brucite and serpentine are driven by CO_2 dissolution and acid generated by sulfide oxidation. Rapid dissolution of brucite induces alkaline pH in the leachates. This high pH prevents metal mobility; Ni, Zn, Fe, and Cu are suggested to be retained within the waste immediately upon their release by sulfides oxidation. The Ni-Fe alloy awaruite is stable and does not release metals in kinetic tests. The Dumont tailings are found to be non-acid generating and CO_2 sequestration is shown to play a significant role in drainage water quality.

Keywords: Kinetic column test; Mineral carbonation; Ultramafic tailings; brucite; Alkaline drainage; Mine waste; Awaruite; Heazlewoodite.

2.1 Introduction

The environmental impact of mine waste produced by base metal mines is highly linked to the geology, the type of mineralization, and the processing methods.

Exploitation of base metals leads to production of 2 main types of mine wastes: tailings and waste rock. The latter is characterized by the size of particles (from um to m) and its heterogeneity (Paktunc, 1999), while tailings coming from the ore processing plant and depleted in valuable minerals have a grain size distribution similar to silty sand and are discharged as a pulp with a relatively high proportion of water (Bussière, 2007). Weathering of minerals that compose the mine waste is of major concern for environmental issues. Contaminated drainage such as acid-mine drainage (AMD), contaminated neutral drainage (CND), and alkaline drainage are produced through weathering of metal sulfides exposed to the atmospheric conditions (water and air). The geochemistry of drainage water is also highly influenced by mineralogy, as well as by other processes such as specific surface area, drying and wetting, bacterial activity, and temperature (Stillings *et al.* 2008; Blowes *et al.* 2003).

Some base metal and minerals such as nickel, platinum group metals, chrysotile (or serpentines), diamond, chromite, and talc are sometimes associated with ultramafic rocks (Power *et al.* 2014; Vogeli *et al.* 2011; Hitch *et al.* 2010;). Their exploitation can lead to the exposition of large quantities of mafic and ultramafic mine wastes to the earth's surface conditions. Some minerals (e.g. serpentines, brucite, and olivine) contained in ultramafic rocks are known to react with CO_2 in ambient conditions to form stable magnesium carbonates (Lackner *et al.* 1995). Passive carbonation of serpentine and brucite is a slow process, but the large surface exposition of the mine waste could significantly increase the carbon sequestration potential. This could potentially represent a significant carbon sink to attenuate the carbon footprint of mining activities (Hitch *et al.* 2010).

Passive carbonation is occurring in at least seven well-documented, active or abandoned mines in Canada, Australia, and Norway (Wilson *et al.* 2014; Oskierski *et al.* 2013; Bea *et al.* 2012; Beinlich and Austrheim 2012; Pronost *et al.* 2012; Wilson, *et al.* 2009a, 2009b; Beaudoin *et al.* 2008; Wilson *et al.* 2006). These studies on

carbonation of mine wastes are mainly focused on understanding the carbonation process, the rate, the characterization, the identification, and the stability of carbonates formed, and carbon isotopic disequilibrium. Also, laboratory studies on ambient carbonation of ultramafic mine wastes helped to understand the main factors influencing the carbonation process such as mineralogy, temperature, wetting, and CO_2 partial pressure (Harrison *et al.* 2015; Assima *et al.* 2014a, 2014b, 2013a, 2012; Pronost *et al.* 2011; Hänchen *et al.* 2008; Golubev *et al.* 2005). Also, the stability of secondary Mg carbonates was investigated (Morgan *et al.* 2015; Teir *et al.* 2006). These phenomena can influence the quality of water (Beinlich and Austrheim, 2012; Rollo and Jamieson, 2006). For example, the formation of secondary Mg carbonates can increase the pH up to values of 9 to 10, as for kimberlite process waters (Rollo and Jamieson, 2006), for water in contact with ultramafic mine wastes in Mount Keith, Australia (Bea *et al.* 2012), and a chromite mine shaft in Norway (Beinlich and Austrheim, 2012). At alkaline pH values, several metals and metalloids are still soluble. Thus, predicting the geochemical behavior of ultramafic mine waste is a crucial step for management planning, but this aspect has not been investigated in details in the literature.

The objectives of this study are to evaluate (1) the geochemical behavior of ultramafic mine tailings at the lab scale, and (2) the impact of carbonation on drainage water quality. Additionally, the tailings studied here are characterized by the presence of awaruite, a nickel-iron alloy for which very little information is available. That is why for this study, kinetic tests were performed on a sulfide concentrate and on an awaruite concentrate, in order to increase the geochemical response of the Ni source terms. Furthermore, the weathering of awaruite is not well known and data generated in this study will help to better understand its weathering. This study provides a new approach, with the use of column tests to study the carbon sequestration potential of ultramafic mine wastes and the impact of passive carbonation on the quality of mine drainage.

2.2 Materials and methods

2.2.1 Dumont mine project: Location and geology

The Dumont mine project is a large nickel deposit located near the town of Amos (Quebec, Canada), approximately 120 km northeast of Rouyn-Noranda and 85 km northwest of Val d'Or. While the presence of ultramafic and mafic rocks has been known on the Dumont property since 1935, the presence of nickel within the rock sequence was only discovered in 1956. The existence and potential of the large low-grade nickel mineralization was first recognized in 1970 (RNC, 2013). The production is planned to begin in 2017 and the mine will be exploited for 33 years, producing more than 2 billion tons of ultramafic waste rocks and tailings. The climate at the Dumont site is continental and the mean temperatures range from -17.3°C in January to 17.2°C in July, for an annual mean temperature of 1.2°C. The total average annual precipitation is 918 mm (RNC, 2013).

The Dumont sill is one the mafic to ultramafic intrusive bodies found between Val d'Or, Québec and Timmins, Ontario (RNC, 2013). It is composed a lower ultramafic zone, about 450 m in thickness, and an upper mafic zone with a thickness of around 250 m. The ultramafic zone is divided into the lower peridotite, dunite, and upper peridotite subzones. Cumulus nickel (Ni) sulfide and alloy minerals occur in parts of the dunite subzone and locally in the lower peridotite to form the Dumont deposit. Nickel mineralization is characterized by disseminated blebs of pentlandite ($(Ni,Fe)_9S_8$), heazlewoodite (Ni_3S_2), and the ferronickel alloy, awaruite ($Ni_{2.5}Fe$), occurring in various proportions throughout the sill. Nickel can also occur in the crystal structure of several silicate minerals, including olivine and serpentine (Sciortino *et al.* 2015; RNC, 2013). Nickel occurring in this mode would not be recoverable through the flotation and magnetic separation methods considered by RNC for the Dumont project, and will report to the mine wastes.

2.2.2 Dumont Tailings

Since the mining activities have not started yet, representative samples of tailings were produced from various bench scale metallurgical tests. The environmental geochemical characterization of the Dumont materials indicates that they will be non-acid-generating due to their low sulfide content and their high neutralization potential. Previous studies show that the Dumont tailings have the ability to fix CO_2 (Awoh *et al.* 2013; Pronost *et al.* 2011), due to their high serpentine and brucite contents. The carbonates formed during eudiometer carbonation tests are dypingite ($Mg_5(CO_3)_4(OH)_2 \cdot 5H_2O$) and nesquehonite ($Mg(HCO_3)(OH)_2H_2O$) (Pronost *et al.* 2011). Awoh *et al.* (2013) developed an innovative CO_2 consumption test in order to quantify the CO_2 flux circulating through the materials. Results of the various laboratory and in situ CO_2 consumption tests suggest that the Dumont wastes sequester CO_2 fluxes of up to 1400 g/m^2/year in typical ambient conditions. These studies have also shown that the non-ultramafic lithologies of the Dumont deposit do not consume CO_2. The CO_2 consumption tests also show that a specific water content (between 25 and 28 wt. %) is required for optimal carbonation of Dumont waste rock (Awoh *et al.* 2013).

2.2.3 Awaruite and Ni sulfide concentrates production

Recent studies shows that the geochemical response of laboratory kinetic tests on mine wastes with very low sulfide content can be underestimated in comparison to the field results (Plante *et al.* 2011b). The main nickel-bearing phases of the Dumont sill were concentrated and submitted to weathering cell tests in order to investigate their geochemical behavior. Studying these concentrates separately from the gangue minerals will enable to increase their geochemical responses and highlight the potential contaminants they might generate in the tailings and waste rocks of the Dumont mine. The concentrates of Ni-sulfides (pentlandite and heazlewoodite) and awaruite were prepared by various metallurgical separations mimicking the expected

Dumont process plant. The final nickel concentrate is made up of streams from 3 separate circuits; nickel sulfide cleaners, awaruite cleaners and the slimes cleaners. The samples in this study came from the nickel sulfide cleaners and the awaruite cleaners. The heazlewoodite and pentlandite are recovered in the sulfide rougher concentrate by flotation in the rougher flotation circuit. The sulfide rougher concentrate is then cleaned using subsequent flotation stages to remove excess gangue material and achieve final concentrate grade. The awaruite is recovered after the rougher using a magnetic separation process. This produces a magnetic concentrate, which is reground to liberate any locked sulfide for subsequent recovery. Once the sulfides are removed, the awaruite is separated from the gangue by a flotation process. The awaruite rougher concentrate is then cleaned using flotation to an acceptable concentrate grade and reports to the final concentrate (RNC, 2013; Personal communication).

2.2.4 Chemical, mineralogical and physical characterization methods

All samples were characterized physically and chemically. Elemental compositions of tailings and concentrates were determined by ICP-AES following an acid digestion (HNO_3-Br_2-HF-HCl). Silica was determined using whole-rock analyses (X-ray fluorescence), since it is partially evaporated during the acid digestion. The whole-rock analysis of major elements of the Dumont samples was performed by X-ray fluorescence (XRF) following a Lithium borate fusion on pulverized sample aliquots (85 % < 200 mesh) by Acme Analytical Laboratories (Vancouver) Ltd. The XRF analysis for the sulfide concentrate and the alloy was done at the RIME-UQAT laboratory on a pulverized aliquot of the sample. The detection limits of the whole rock analyses ranged between 0.001 and 0.1 wt.%. The ICP-AES was also used to analyze the leachates for various elements. The total carbon and sulfide content were determined by using a LECO carbon/sulfur analyzer (Maxxam Analytical, QC, Canada) with a reported detection limit of 0.05 wt.%. The neutralization potential of tailings samples was evaluated with the modified Sobek acid-base accounting (ABA)

method (Lawrence and Scheske, 1997). The alkalinity measurements of leachates kinetic testing were done by titration with sulfuric acid (0.02 N).

The mineralogical composition of the samples was determined by X-ray diffraction (XRD) and microscopic observations. XRD patterns were collected using a Bruker AXS Advance D8 with a copper cathode, acquired at a rate of 0.02°s-1 between 2Θ values of 5° and 70°. The DiffracPlus EVA software (v. 9.0) was used to identify the mineral species, and the quantitative mineralogical compositions were evaluated using the TOPAS software (v. 2.1) with a Rietveld (1993) refinement. The scanning electron microscope (SEM) observations were performed by using an Hitachi S-3500 N SEM equipped with an energy dispersive spectroscopy (EDS) Oxford X-Max 20 mm^2 Silicon Drift Detector (SDD) microanalysis system. The SEM observations were performed at approximately 15 mm working distance and a 100-150 µA current at 20 kV.

Initial and post-testing samples were submitted to Diffuse Reflectance Infrared Fourier Transform (DRIFT) spectroscopy to characterize the secondary Mg carbonates formed. The DRIFT spectra were collected on a Bruker Optics Tensor 27 Fourier Transform Infrared Spectrometer. The spectra were acquired with 200 scans at a resolution of 1 cm^{-1} from 400 to 4000 cm^{-1}, with the aperture set to 4 mm. The samples were ground and sieved to <45 µm and the spectra were obtained on samples diluted to 15 wt.% with spectrograde KBr powder (Harrick Scientific Products) and dried in the oven. During the spectra acquisition, the sample room was purged with nitrogen to prevent atmospheric CO_2 contamination.

The specific gravity (Gs) of the samples were determined using a Micromeritics Accupyc 1330 helium pycnometer (the accuracy is within 0.03 % of reading plus 0.03 % of nominal full-scale sample chamber volume; ASTM Standard D4892, 2014). The specific surface area (SSA) was determined with a Micromeritics Surface Area Analyser using the BET method. Finally, the grain-size distribution was

determined by laser diffraction using a Malvern Instruments Mastersizer S particle size analyzer (Merkus, 2009).

2.2.5 Kinetic column test

Kinetic tests are often used to evaluate the long-term geochemical behavior of mine waste (US EPA, 1994). These tests attempt to mimic natural weathering of mine waste (Bradham and Caruccio, 1991). Such tests provide information on the sulfide oxidation rate and weathering characteristics of waste (Benzaazoua *et al.* 2004; US EPA, 1994), and are also used to provide an indication of drainage water quality. For these purposes, the Dumont tailings samples were submitted to two types of laboratory kinetic tests: column and weathering cell tests. Approximately 8 kg of tailings was deposited as a pulp in a Plexiglas column, with 14 cm internal diameter and 60 cm in height. The inside wall of the column was coated with grease to avoid preferential flow paths to develop along the sides. A porous ceramic plate was installed at the bottom of the column in order to control the suction potential at a value of 1 m below the tailings. The initial height of the sample in the column at the beginning of the tests was around 35 cm, and it consolidated to near 24 cm after approximately one week. The column was flushed from the top with 2 L of deionized water (pH 5.5-6.0) once per month. The liquid-to solid ratio used in this study is representative to the Amos rainfall. The leachates were recovered after a contact time of 3-4 hours and analyzed for pH, conductivity, and dissolved species. The column was run for over 2 years. Between each flushes, the material is let open to the atmosphere (temperatures between 20-22 C).

2.2.6 Weathering cells

The geochemical behavior of the awaruite and Ni-sulfides concentrates were evaluated using small scale leaching cells called weathering cells (Plante *et al.* 2015; 2011a; Hakkou *et al.* 2008; Cruz *et al.* 2001). Weathering cells are small-scale humidity cells and were used mainly because they require fewer samples compared to

column and humidity cell tests. However, the high liquid-to-solid ratio of weathering cell could exaggerate the dissolution of minerals involved in the neutralization of acid (Villeneuve *et al.* 2003). Weathering cell tests were also conducted on Dumont tailings samples in five replicates and dismantled after different durations (28, 59, 108, 143, 178 days), in order to evaluate the carbonation rate and the weathering characteristics at different times. Approximately 65 g samples (~ 1 cm thickness) were deposited in Buchner funnels with a 0.45 µm pore size glass-fiber filter. The Buchner funnels were also coated with grease for the concentrate samples to hold the filter paper and avoid preferential flow on the sides, while for the tailings samples, glue was used to hold the filter. Each cell was flushed twice per week with 50 ml of deionized water. The contact time between tailings and water is 3-4 hours. After, leachates recovery, the tailings were allowed to dry under ambient air (temperatures ranging between 20-22 °C) between flushes (Plante *et al.* 2011a).

Leachate compositions from kinetics tests (Column and weathering cells) were modelled by thermodynamical equilibrium with Visual Minteq version 3.0 (US EPA, 1999) in order to calculate the saturation indices (SI) of selected minerals and the speciation of dissolved elements.

2.3 Results

2.3.1 Characterization of the Dumont samples

Results of chemical and physical properties of tailings are presented in Table 2.1. The tailings contain 42.49 Wt.% of MgO, 35.10 Wt.% of SiO_2, and 5.82 Wt.% Fe_2O_3. While the theoretical ratio of MgO/SiO_2 in serpentine in weight equals 1.0, it is higher (1.2) for the tailings, suggesting an excess of Mg which can be attributed to brucite, $Mg(OH)_2$. The tailings sample contains 0.18 % of total carbon and 0.17 % of total sulfide.

The elemental composition of the concentrate samples are given in Table 2.2. The Ni concentration is almost the same for the 2 samples (38.0 % and 38.1 %). The Ni-sulfides concentrate has higher sulfur (22.30 %) than the awaruite sample (0.96 %). The Fe content in the sulfide concentrate (30.0 %) is associated with Ni-sulfide and magnetite, while it is associated with awaruite and magnetite in the awaruite concentrate (46.0 %). The other metals are present in low concentrations: Zn (0.16 – 0.24 %), Cu (0.55 – 1.18 %), and Co (0.23 – 0.67 %). Despite the process cleaner to remove the gangue minerals, there remain some amounts of serpentine and brucite in the concentrates, as shown by the Mg (2.73 – 3.16 %) and Si (2.73 – 4.25 %) concentrations. Others elements are also detected as traces but are not shown, such as Al, Ba, Cr, Mn, Pb, and Ti. Ca (Not shown) concentrations are below the detection limit (< 0.01 %).

The acid-base accounting (ABA) of tailings and concentrates are shown respectively in Tables 2.1 and 2.2. The acid-potential (AP) of Dumont tailings is equal to 5.3 kg $CaCO_3$/t, while for awaruite and sulfide concentrates it is respectively 133 and 697 kg $CaCO_3$/t. The neutralization potential (NP) of the tailings, awaruite and sulfide samples are respectively 191, 21, and 42 kg $CaCO_3$/t. Thus, the NNP balance (NP-AP) indicates that the Dumont tailing are not acid generating (NNP>20 kg $CaCO_3$/t), while the concentrate samples are potentially acid generating (NNP<-20 kg $CaCO_3$/t) according to the criteria defined by SRK (1989).

Table 2.1 Whole rock analysis and physicals parameters of Dumont tailings samples

Majors elements in %											
SiO_2	Al_2O_3	Fe_2O_3	CaO	MgO	Na_2O	K_2O	MnO	TiO_2	P_2O_5	Cr_2O_3	V_2O_5
35,10	0.22	5.82	0.05	42.49	<0.01	<0.01	0,11	<0.01	0.05	0.24	<0.002
Trace elements in ppm											
Co	Cu	Fe	Hg	Ni	Pb	K	Ti	Zn	TOT/C	TOT/S	SO_4
84	48	37000	0.04	2600	<5	<40	38	44	1500	1700	610
Physical properties of Dumont tailings and ABA results (AP, NP, NNP in kg $CaCO_3$/t, NP/AP Unitless)											
Gs	Ss (m^2/g)	D_{10} (µm)	D_{60} (µm)	D_{90} (µm)	C_u	%< 100 (µm)	AP	NP	NP/AP	NNP	
2.58	13.2	2.2	49.8	191	22.7	76	5.31	191	36	186	

The physical characterisation of the tailings shows that the specific surface area (SSA) and the relative density (G_s) of the samples are respectively 13.2 m^2/g and 2.58. The grain size parameters D_{10}, D_{60}, and D_{90} are respectively 2.2, 49.8, and 191 µm, where D_{10}, D_{60}, and D_{90} corresponds to 10 %, 60 % and 90 % of particles passing on the cumulative curve respectively. The C_u (D_{60}/D_{10}) is equal to 22.7. The relative density of the awaruite and sulfide concentrate is respectively 5.52 and 4.59. Grain size parameters are also given for awaruite concentrate and Ni-sulfides concentrate respectively (C_u: 3.52 – 3.27; D_{10}: 34.6 – 28.5 µm; D_{60}: 122 – 93.1 µm; D_{90}: 206 – 185 µm).

Table 2.2 Chemical composition of nickel sulfide and awaruite concentrates

Chemical composition (wt.%)									
	Ni	Zn	Co	Cu	Fe	Mg	C	S	Si
Sulfide Concentrate	38.0	0.24	0.67	1.18	30.0	2.73	0.12	22.30	2.73
Awaruite concentrate	38.1	0.16	0.23	0.55	46.0	3.16	0.14	0.96	4.25
ABA characterization results AP, NP and NNP in Kg $CaCO_3$/t and physicals parameters									
	AP	NP	NNP	NP/AP	G_s	C_u	D_{10} (µm)	D_{60} (µm)	D_{90} (µm)
Sulfide concentrate	697	42	-655	0.06	4.59	3.27	28.5	93.1	185
Awaruite concentrate	133	21	-112	0.16	5.52	3.52	34.6	122	206

The mineralogical compositions of the samples are shown in Table 2.3. It confirms that the tailings contain mainly serpentine and brucite with 79.7 % and 11.2 %, respectively. The brucite content calculated here is similar to the results found by Assima *et al.* (2013b) in his studies for an accurate quantification of native brucite by using a combination of isothermal and nonisothermal thermogravimetric analyses with mass spectrometry. By this method, Assima *et al.* (2013b) conclude that the Dumont tailing sample contain 10.88 % of brucite. The Dumont samples contain traces of awaruite and Ni-sulfides (heazlewoodite and pentlandite) but were not detected by X-Ray diffraction. Tailings samples contain near 5 % of magnetite and small amounts of chlorite (1.4 %), chromite (0.3 %), and diopside (0.2 %).

Awaruite is the main mineral in the awaruite concentrate sample, which also contains some residual gangue minerals such as serpentine and brucite. Magnetite was also detected by XRD and by SEM. Pentlandite and heazlewoodite were also detected. The sulfide concentrate mainly contains pentlandite, heazlewoodite, and magnetite. Serpentine and brucite are also present in low concentrations, and SEM characterizations show the presence of awaruite, chalcocite, and sphalerite in traces. Native copper was also detected as traces in both concentrate samples.

Table 2.3 Quantitative Mineralogy of Dumont Tailings, awaruite and sulfur concentrate (in wt.%)

Minerals	Formula	Tailings sample	Awaruite Concentrate	Sulfur Concentrate
Serpentine	$Mg_3Si_2O_5(OH)_4$	79.7	< 12	< 10
Brucite	$Mg(OH)_2$	11.2	< 7	< 6.5
Magnetite	Fe_2O_4	4.9	~ 40	22.86
Chlorite	$(Fe,Mg)_5Al(Si_3Al)O_{10}(OH,O)$	1.4	-	-
Diopside	$CaMgSi_2O_6$	0.2	-	-
Chromite	$FeCr_2O_4$	0.3	-	-
Awaruite	$Ni_{2.5}Fe$	< 0.4	~ 50	
Pentlandite	$(Fe,Ni)_9S_8$	< 0.6	Trace	40.72
Heazlewoodite	Ni_3S_2	< 0.4	Trace	32.84

2.3.2 Geochemistry of the Dumont tailings leachates from column

Leachates generated in each cycle were analyzed for pH, conductivity, and for the concentration of various elements. The evolution of some of these parameters (pH, electrical conductivity, SO_4, Mg, Ca, and alkalinity) is shown in Figure 2.1. The pH of the leachates shows 2 plateaus: one at a pH value near 7.5 during the first 200 days, after which it increases gradually from 200 to 500 days to reach the second plateau at pH 9.0-9.5 (Figure 2.1a). In contrast, the electrical conductivity values (Figure 2.1b) are higher during the first 200 days but decrease and stabilize near 600 µS/cm. Figure 2.1c shows a slow increase of alkalinity values up to approximately 300 mg $CaCO_3$/L. Interestingly, the alkalinity and pH values both increase at approximately 200 days, suggesting that the buildup of secondary carbonates gets significant enough to influence pH and alkalinity values from this moment on. Sulfate (SO_4) in leachates increases during the first 300 days (50 – 310 mg/L) then decreases afterwards to reach 100 mg/L. The Mg concentrations are relatively constant through the entire kinetic test (~100 mg/L). In contrast, Ca concentrations decrease from 60 mg/L to stabilize near 3 mg/L after 300 days. Other

elements were also analyzed but are not shown in Figure 2.1. Al concentrations range between 0.05-0.3 mg/l, whereas Ni concentrations were generally less than the detection limit (0.004 mg/L). For other metals such as Fe, Zn, Cu and Co, their concentrations were below the detection limit (respectively 0.006, 0.005, 0.003, and 0.004 mg/L) for most of the tests.

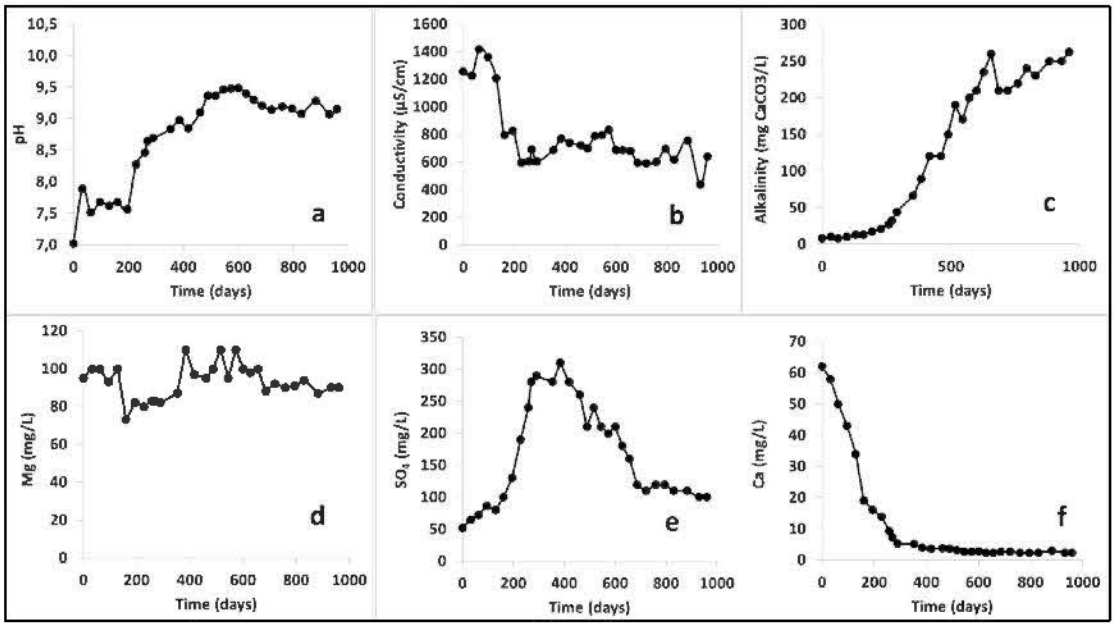

Figure 2.1 Geochemistry of leachates from column: pH (a), Conductivity (b), Alkalinity (c), Mg (d), SO_4 (e), and Ca (f)

2.3.3 Geochemistry of tailings, awaruite, and sulfides concentrates leachates from weathering cells

The geochemical results of the weathering cells are presented in Figure 2.2. The pH remains near-neutral throughout the tests, but shows a decreasing tendency (awaruite: pH 9.3 – 8.5; sulfide: 9.0-7.4). Leachates from tailings weathering cells have a higher pH ranging from 9.15 to 9.71. The Eh is similar for the 2 concentrates and vary from 165 to 700 mV, while for tailings, the Eh was not measured. The electrical conductivity values decrease during the test (awaruite: 950 to 220 µS; sulfide: 870 to

460 µS; tailings: 1220 to 600 µS). Sulfate in leachates is higher for the Ni-sulfides concentrate than for the awaruite and tailings. For the sulfide sample, sulfate concentrations increase from 200 to 600 mg/L and stabilize after 50 days around these values, while awaruite concentrate and tailings shows a decreasing trend (200 to 20 mg/L). The Ni levels in leachates of the sulfides concentrate gradually increase to 10 mg/L in the first 100 days, after which they abruptly reach values between 40 – 50 mg/L, while they oscillate around 1 mg/l for the awaruite concentrate, whereas Ni in the tailings weathering cell leachates does not exceed 0.02 mg/L. The Zn concentrations in the leachates stabilize at approximately 0.01 mg/L for the awaruite concentrate while they show a behavior similar to that of Ni for the sulfide sample, gradually reaching 0.05 mg/L after 100 days and quickly reaching 0.15-0.20 mg/L after 100 days. Zn was not detected in the tailings weathering cell leachates. The Ni and Zn concentrations rapidly increase at the same time (100 days) even if the pH does not vary significantly during this period. The Mg concentrations are higher at the beginning of the test before it decrease and stabilize after 100 days (Tailings: 235 to 130 mg/L; awaruite: 156 to 32 mg/L; sulfides concentrate: 100 to 40 mg/L). The calcium levels decrease rapidly and stabilize at around 0.2 mg/L for the concentrates and near 3 mg/L. Co and Cu concentrations in the leachates (not shown) stabilize at concentrations below the detection limit (0.003-0.004 mg/L for Cu and Co respectively). The Si concentrations (not shown in Figure 2.2) were measured in both kinetic tests (column and weathering cells). In the column test, the Si concentrations are oscillating near 50 mg/L while they vary between 20 and 60 mg/L in the concentrates leachates (awaruite and sulfides). These high concentrations of Si in the column and weathering cells leachates were attributed to the silicone grease used to coat the inside of the column walls and the weathering cells. This was confirmed by conducting a weathering cell on the tailings without using silicon grease, in which the Si concentrations measured were below 3 mg/L.

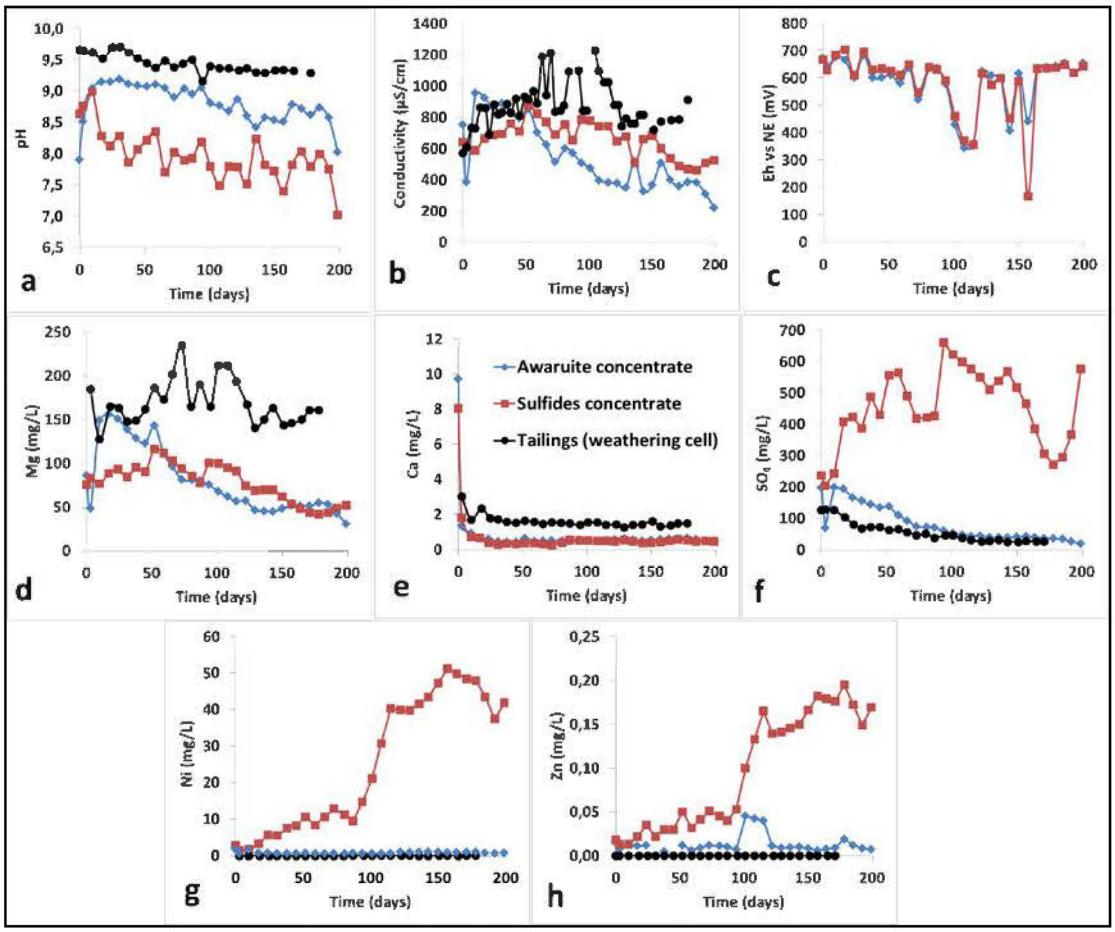

Figure 2.2 Weathering cells results for tailings, awaruite and Ni-sulfides concentrates: pH (a), conductivity (b), Eh (c), Mg (d), Ca (e), SO_4 (f), Ni (g), and Zn (h)

2.4 Discussion

2.4.1 Awaruite and sulfide concentrates behaviour

Sulfate and metal concentrations detected in the weathering cell leachates (Figure 2.2) show that sulfides within the awaruite and sulfide concentrate samples are subject to oxidation. However, in the awaruite sample, sulfate concentrations gradually decrease, which shows that sulfide oxidation slows, most probably because

of surface passivation and/or depletion of fines particles of sulfide minerals. In contrast, sulfide oxidation in the sulfide concentrate remains high throughout the test and release noticeable Ni and Zn concentrations. These results suggest that both the sulfides and awaruite minerals may release Ni and Zn during weathering. However, Ni is soluble under near-neutral conditions up to pH values around 8.5, over which its solubility decreases significantly, while Zn remains soluble up to pH values of 9.0-9.5 (Cravotta III, 2008). It is thus possible that Ni and Zn are generated from the awaruite concentrate, but that Ni is immediately precipitated or sorbed within the sample, while Zn remains in solution. The sulfate detected in the awaruite cell leachates suggests that Ni and Zn come from the oxidation of traces sulfides present in the awaruite concentrate. It is therefore likely that awaruite will be unaffected by oxidation and the only acid and metals producers will be the traces of sulfides present in the alloy concentrate. It is interesting to specify that no information could be found on awaruite weathering, most studies focusing on its occurrence and formation in the environment. Pentlandite is with pyrrhotite, the main sources of Ni in mine waste pores-water (Heikkinen and Räisänen 2008; Gunsinger *et al.* 2006; Johnson *et al.* 2000; McGregor *et al.* 1998). Pentlandite can be oxidized by oxygen (Equation 2.1) in acidic conditions or by ferric ions (Equation 2.2) in near-neutral conditions (Kodali *et al.* 2004; Aubertin *et al.* 2002). Direct oxidation of pentlandite by oxygen (Equation 2.1) is not acid-generating but can release nickel in the leachates. However, pentlandite oxidation by ferric ions will generate acid upon oxidation of native sulfur (S^0) generated (Equation 2.2) to sulfate (Equation 2.3).

$$(Ni,Fe)_9S_8 + \frac{141}{8}O_2 + \frac{13}{4}H_2SO_4 \rightarrow \frac{9}{2}NiSO_4 + \frac{9}{4}Fe_2(SO_4)_3 + \frac{13}{4}H_2O \quad (2.1)$$

$$Ni_9S_8 + 9Fe_2(SO_4)_3 \rightarrow 9NiSO_4 + 18FeSO_4 + 8S^0 \quad (2.2)$$

$$S^0 + \frac{3}{2}O_2 + H_2O \rightarrow H_2SO_4 \quad (2.3)$$

Magnetite, also found in the awaruite concentrate sample, has a high resistance to oxidation (Lindsay *et al.* 2015), except under extremely low-pH conditions (Moncur *et al.* 2009). Such conditions in the future tailings impoundment are unlikely to occur. The lower pH (less than 8.5) in the sulfides concentrate leachates than in the alloy cell facilitates the solubilisation of Ni and Zn. Levels of these two elements increase abruptly at approximately 100 days, when the pH values decrease below 8.

Serpentine minerals weather through exchange reactions between H^+ and Mg^{2+} (equation 2.4) as reported by Luce *et al.* (1972). Despite its slow weathering rate, serpentine may buffer the acidity generated by sulfide as reported for the Hitura sulfide mine tailings (Heikkinen and Räisänen, 2008). However, in the Dumont sill case, the neutralization of acid is more likely to be provided mainly by brucite, which is more reactive than serpentine (Lin and Clemency, 1981; Bales and Morgan 1985). This may explain the increasing concentration of Mg in the leachates for the first 50 days before it decreases and stabilizes at 60 mg/L. Moreover, the high concentrations of Mg versus Si in the tailings weathering cell leachates is an indication of the higher reactivity of brucite over serpentine, and also of the incongruent dissolution of serpentine.

$$Mg_3Si_2O_5(OH)_4 + 6H^+ \rightarrow 3Mg^{2+} + 2H_4SiO_4 + H_2O \quad (2.4)$$

Cumulative-normalized loadings of neutralization products (Mg, Ca, and Mg+Ca+Si) and oxidation products (S, Ni, and Zn) versus time are shown in Figure 2.3. Cumulative-normalized evolution of the neutralization products (Mg, Ca, and Mg+Ca+Si) versus time are similar for the awaruite and sulfide samples, but the awaruite sample releases slightly more Mg than the sulfide concentrate. The combined Mg+Ca+Si, loadings are much more similar. The cumulative-normalized sulfates, Ni, and Zn loadings are significantly lower for the awaruite than for sulfides

concentrate. An inflection point at around 100 days is noticed in almost all curves but is more pronounced for the sulfides concentrate. As shown in Figure 2.2, an abrupt increase of Ni and Zn was noticed in the sulfide weathering cell leachates at the same time (100 days). The solubilization of Ni and Zn seem to be promoted when pH values are <8.

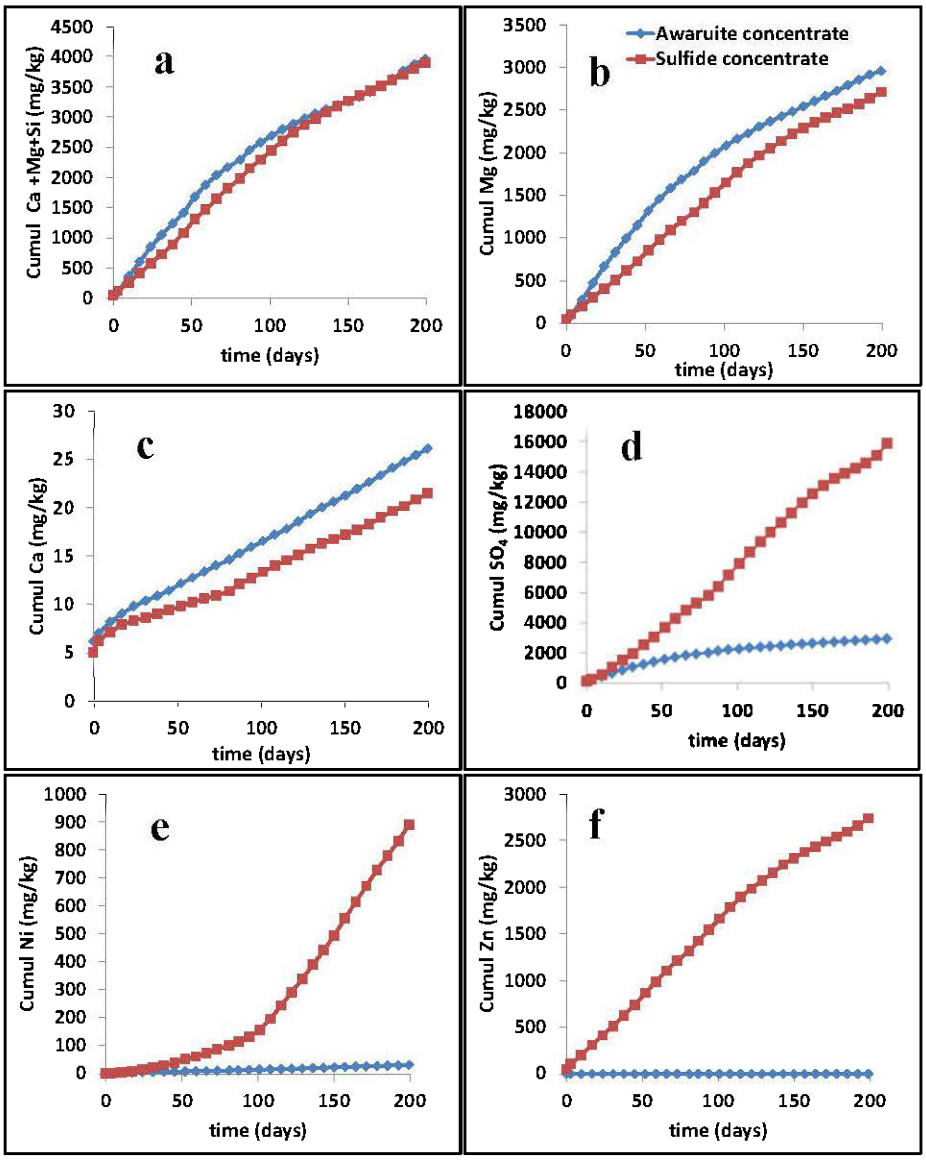

Figure 2.3 Cumulative and normalized weathering cell loadings for neutralization (a, b, and c) / oxidation (d, e, and f)-related elements for awaruite and sulfide concentrates

The release rates of S, Ni, Mg, Ca, Si and Zn calculated from the cumulative-normalized loading of S, Ni, Mg, Ca, Si and Zn after 100 days are given in Table 2.4. For the sulfides concentrate, the oxidation-related products are released at higher

rates (SO_4: 77.86 mg/kg/day; Ni: 7.6 mg/kg/day; Zn: 3.67 mg/kg/day) than for the awaruite concentrate (SO_4: 6.69 mg/kg/day; Ni: 0.17 mg/kg/day; Zn: 0.002 mg/kg/day). Despite this difference in the release rates of products related to the oxidation of sulfides, the neutralization-related products are released in the leachates in the same order of magnitude for both samples. Mg is released for the sulfide and awaruite samples at a rate of 10.3 and 8.9 mg/kg/day respectively. This similitude in the geochemical responses of the neutralization minerals (serpentine and brucite) from the two samples suggests that in addition to the acidity generated by sulfide oxidation, the acidity generated from CO_2 dissolution might also be controlling the Mg loadings in the leachates. Indeed, serpentine and brucite could react with CO_2 under environmental conditions to form Mg-carbonates (Lechat *et al.* 2016; Wilson *et al.* 2014; Oskierski *et al.* 2013; Wilson *et al.* 2011, 2009a; 2009b; Beaudoin *et al.* 2008) as shown in equation 2.5.

$$Mg_3Si_2O_5(OH)_4 + 3CO_2 \rightarrow 3MgCO_3 + 2SiO_2 + 2H_2O \quad (2.5)$$

Table 2.4 Elemental release rates (mg/kg/day) and associated determination coefficients (R^2) from weathering cells tests (>100 days)

	Neutralization related products		**Oxidation related products**		
	Mg	Ca	SO_4	Ni	Zn
Sulfides concentrate	10.3	0.08	77.86	7.6	3.67
R^2	0.984	0.998	0.988	0.998	0.997
Awaruite concentrate	8.9	0.098	6.69	0.17	0.002
R^2	0.999	0.999	0.995	0.998	0.927

2.4.2 Dumont tailings behavior

The presence of sulfate in the tailings column and weathering cell leachates suggest that sulfide oxidation is occurring. The trends observed for sulfates in the leachates may be due to the partial inhibition of sulfide oxidation by surface passivation due to the growth of secondary minerals. As for sulfates, metals are also generated during sulfide oxidation, as shown by the awaruite and sulfides concentrate cells. Ni and Zn are sporadically detected in the weathering cells leachates but were below the detection limit for the Dumont tailings column. These results indicate that most of the metals generated by sulfide oxidation will remain in the solid and will not be leached in the drainage waters, or that they are generated at concentrations below the detection limit. These metals are commonly precipitated mainly in the form of (oxy)hydroxides, especially at such high pH values (Blowes *et al.* 2003), or by sorption phenomena (Plante *et al.* 2011a; Heikkinen *et al.* 2009; Heikkinen and Räisänen, 2008; Gunsinger *et al.* 2006). Generally, the mobility of metal ions is reduced at high pH, as many attenuation processes are pH dependent (e.g. precipitation, co-precipitation, and sorption; Lindsay *et al.* 2015; Moncur *et al.* 2009; Wilkin, 2008; Gunsinger *et al.* 2006; Jurjovec *et al.* 2002; Johnson *et al.* 2000). Johnson *et al.* (2000) reported an abrupt decrease of Ni concentrations (300 to 0.5 mg/L) in the Nickel Rim tailings impoundment (Sudbury, Canada) for a small pH increase from 5 to 5.8. Likewise, in the study of Langman *et al.* (2015), Ni was released from pentlandite oxidation and immediately adsorbed or precipitated with Fe mineral phases.

The acidity generated by sulfide oxidation is neutralized by brucite and serpentine, and despite the varying sulfates concentrations, Mg concentrations in the leachates remain relatively constant. The major source of Mg may be primarily brucite dissolution because of its higher dissolution rate than serpentine (Bales and Morgan, 1985; Lin and Clemency, 1981). However, it is difficult to point out the exact contribution of brucite and serpentine, since both minerals release Mg during

weathering. In addition, Mg concentrations may also be controlled by secondary precipitation of carbonates, as will be discussed later on. Si in the tailings weathering cell leachates (below 3 mg/L) is provided mainly by the dissolution of serpentine which is known to have an incongruent dissolution with preferential release of Mg over Si. Bea *et al.* (2012) suggest that Si is retained in the solid in the form of chalcedony (SiO_2) in the tailings impoundment at Mount Keith (Australia). Water drainage from the Clinton Creek and Cassiar mine wastes are reported to be saturated with respect to chalcedony (Wilson *et al.* 2009a). Precipitation of chalcedony was also suggested by thermodynamic equilibrium calculations with Visual Minteq on the column leachates of the present study.

Figure 2.4 presents the cumulative elemental releases for Mg, Ca, K, Al, and SO_4 (normalized to the sample mass, in mg/kg) in column leachates versus time. The cumulative Mg loadings in the leachates are linear, while Ca, K, and Al show an inflection point before they become linear. The inflection points observed for Ca, K, and Al correspond to the point where the pH values reach 8.5 and higher. This suggests an initial transition phase characterised by rapid dissolution of fine-grained particles as observed in previous studies (Plante *et al.* 2011b; Hakkou *et al.* 2008; Benzaazoua *et al.* 2004). The almost linear trend observed for Mg during both kinetics tests contrasts with the other elements cited earlier and traduces either a constant weathering rate of serpentine and brucite, or a control of Mg concentrations by secondary precipitation of Mg-carbonate minerals.

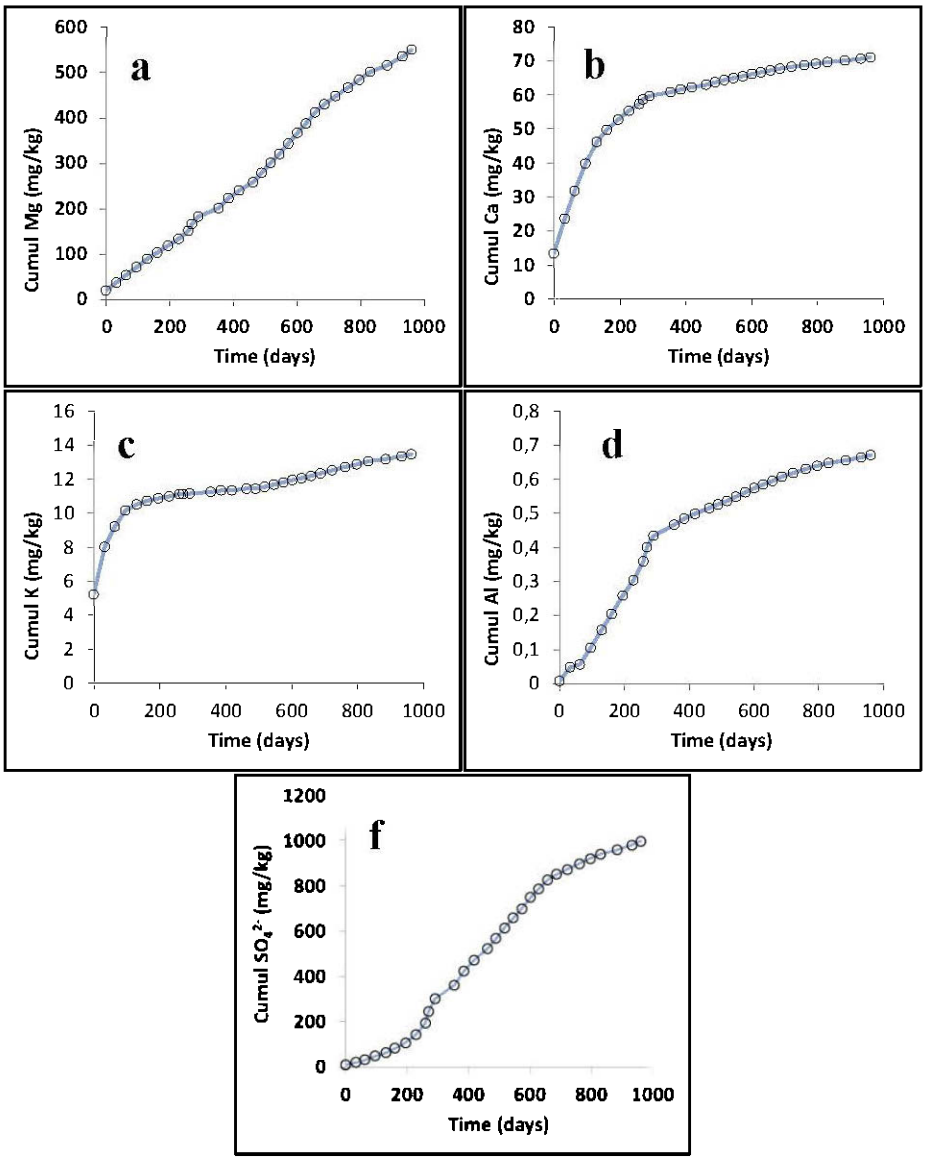

Figure 2.4 Cumulative and normalized column loadings for Mg (a), Ca (b), K (c), Al (d), and SO_4 (f)

The slope of the normalized-cumulative releases versus time in the leachates gives the release rate of an element (Sapsford *et al.* 2009). Mg is released at higher rates in both tests (0.6 mg/kg/day in column and 22.4 mg/kg/day in weathering cell leachates), while the sulfates release rate are higher in the weathering cell (4.78 mg/kg/day) than in the column (1.05 mg/kg/day), as shown in Table 2.5. The

higher release rates observed in the weathering cell than in the column confirms that weathering cell is more aggressive than column tests (Villeneuve *et al.* 2003) due principally to its higher liquid-to-solid ratio and leaching frequency.

Table 2.5 Elemental release rate and associated determination coefficients from column and weathering cell test results (> 300 days for column and > 50 days for weathering cell)

	Column		Weathering cell	
	Mg	**SO_4**	**Mg**	**SO_4**
Release rate (mg/kg/day)	0.6	1.05	22.4	4.78
R^2	0.9845	0.9423	0.998	0.983

2.4.3 Thermodynamic equilibrium calculations

Thermodynamic equilibrium calculations using the leachate compositions generated during kinetics tests (column and weathering cell) suggest the precipitation of various secondary minerals such as Ni-hydroxide ($Ni(OH)_2$), nickel-carbonate ($NiCO_3$), chalcedony (SiO_2), magnesite ($MgCO_3$) and barite ($BaSO_4$). In the weathering cells of awaruite and sulfides concentrates, Ni is suggested to precipitate in the form of $Ni(OH)_2$ and in $NiCO_3$, suggesting that Ni is retained in the solid. Barite, chalcedony, and magnesite are also saturated. Due to the absence of Fe and Zn in the leachates, the related secondary minerals were not taken into account in this geochemical calculation. However, the high pH prevailing in the leachates will favor the precipitation of iron in (oxy)hydroxides or carbonates.

For the tailings column and weathering cell, saturation indices (SI) calculated using Visual MINTEQ (USEPA, 1999) are presented in Figure 2.5. Leachates are always supersaturated in chalcedony but are undersaturated with respect to hydromagnesite ($4MgCO_3 \cdot Mg(OH)_2 \cdot 4H_2O$) and nesquehonite ($MgCO_3 \cdot 3H_2O$ or

$Mg(HCO_3)(OH)\cdot 2(H_2O)$). However, magnesite is undersaturated at the beginning of the test, but becomes supersaturated after 300 days, corresponding to the pH and alkalinity increase. Chalcedony and nesquehonite are undersaturated for the weathering cells, while magnesite and hydromagnesite are supersaturated. This is consistent with the fact that precipitation of Mg carbonates is generally favored at high pH (Krevor & Lackner 2011; Ferrini *et al.* 2009; Teir *et al.* 2009, 2007; Park and Fan, 2004). However, in practice magnesite and many others minerals fail to precipitate in ambient conditions even if they are supersaturated (Saldi *et al.* 2009), due to kinetic barriers (Gautier *et al.* 2014; Saldi *et al.* 2009; Hänchen *et al.* 2008). Felmy *et al.* (2012) succeeded to produce magnesite at temperatures below 35°C but they used a water-saturated supercritical CO_2. Thus, at low temperatures, hydrated carbonates such as hydromagnesite, lansfordite ($MgCO_3\cdot 5(H_2O)$), and less stable nesquehonite, precipitate much more easily than magnesite. This explains why these hydrous Mg-carbonates are observed to precipitate during in-situ passive carbonation of ultramafic mine wastes (Lechat *et al.* 2016; Wilson *et al.* 2014; Wilson *et al.* 2011; Oskierski *et al.* 2013; Pronost *et al.* 2011; Wilson, *et al.* 2009a;). Nesquehonite and lansfordite are observed to precipitate as secondary Mg carbonates along the walls of chromite mine shafts in the Feragen ultramafic body (Norway; Beinlich and Austrheim, 2012). Yet, thermodynamic equilibrium calculations performed in this mine water suggested that they were undersaturated with respect to nesquehonite and lansfordite. Only magnesite was suggested to be supersatured (SI: 0.18 to 1.63) in all samples, while the calculated SI of hydromagnesite oscillated between positive and negative values (SI: -6.86 to 1.13; Beinlich and Austrheim, 2012). Thus, hydrated magnesium carbonates (hydromagnesite, dypingite, or nesquehonite) are more likely to precipitate rather than magnesite under the conditions of kinetic testing. Post-testing characterizations were used to verify this hypothesis.

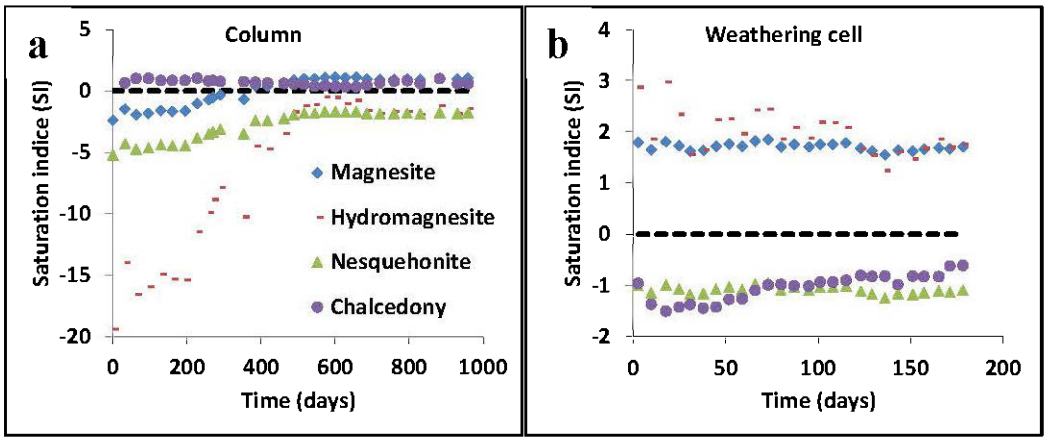

Figure 2.5 Saturation indices evolution calculated with Visual Minteq for tailings column (a) and weathering cell leachates (b); dashed line represent the equilibrium point

2.4.4 Post testing results

At the end of the kinetics tests, the column and weathering cells were dismantled. The column was dismantled in successive layers (0 – 2 cm, 2 – 4 cm, 4 – 6 cm, 6 – 8 cm, 8 – 10 cm, 10 – 17 cm, and 17 – 24 cm). The weathering cells were dismantled in a single sample. Each layer was characterized to determine their final content of various elements. Figure 2.6 shows the total carbon content.

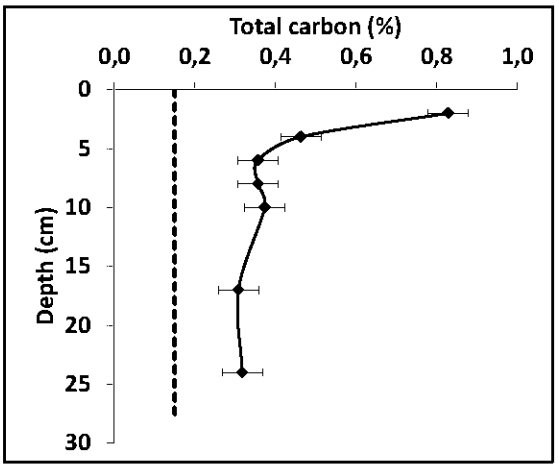

Figure 2.6 Carbon profiles after column dismantling. Dashed line show the initial carbon

The total carbon (Figure 2.6) increases significantly from 0.15 % (initial concentration) to reach the maximum value (0.83 %) in the top 2 cm of the column, while for the other layers below, the carbon contents are respectively 0.46 % and 0.36 %. The last layer at the bottom of the column contains 0.32 % carbon, suggesting that the carbonation process occurs throughout the whole depth but is more concentrated at the surface. Therefore, a significant increase of the carbon content was obtained, demonstrating the ability of the Dumont wastes to fix CO_2. The sulfates (not shown) were completely removed on the surface of the tailings (first 6 cm from the top column), and was equal to 0.01 % at the bottom of the column, which is less than the initial concentration in the fresh tailings (0.06 %). These results suggest that that there is no sulfate precipitated at the surface despite the oxidation of sulfides occurring within the first cm's of the column.

X-ray diffraction (Figure 2.7) performed on each layer shows the appearance of a peak of quartz or chalcedony and a less pronounced peak of hydromagnesite on the first layer, with a significant decrease of the main brucite peak. The other deeper layers (not shown) tend to be closer to the initial tailings. Previous studies performed

on the Dumont tailings have observed the precipitation of nesquehonite and dypingite rather than hydromagnesite, and demonstrated the prevalent role of brucite in the carbon capture. Pronost *et al.* (2011) found that nesquehonite was the main carbonate formed during eudiometer tests at 21°C, while dypingite is the main carbonate formed at 33°C. Assima *et al.* (2014a) also observed that nesquehonite is the main Mg carbonate precipitated on Dumont samples under various temperatures ranging from 10 to 40 °C. Precipitation of hydromagnesite was reported in almost all studies involving in-situ passive carbonation of mines wastes (Wilson *et al.* 2009a; Wilson *et al.* 2014; Oskierski *et al.* 2013; Beaudoin *et al.* 2008). Thus, the fact that the kinetic tests of the present study mainly generate hydromagnesite is questionable and need further investigations, in light of the contradictory evidence found in the literature.

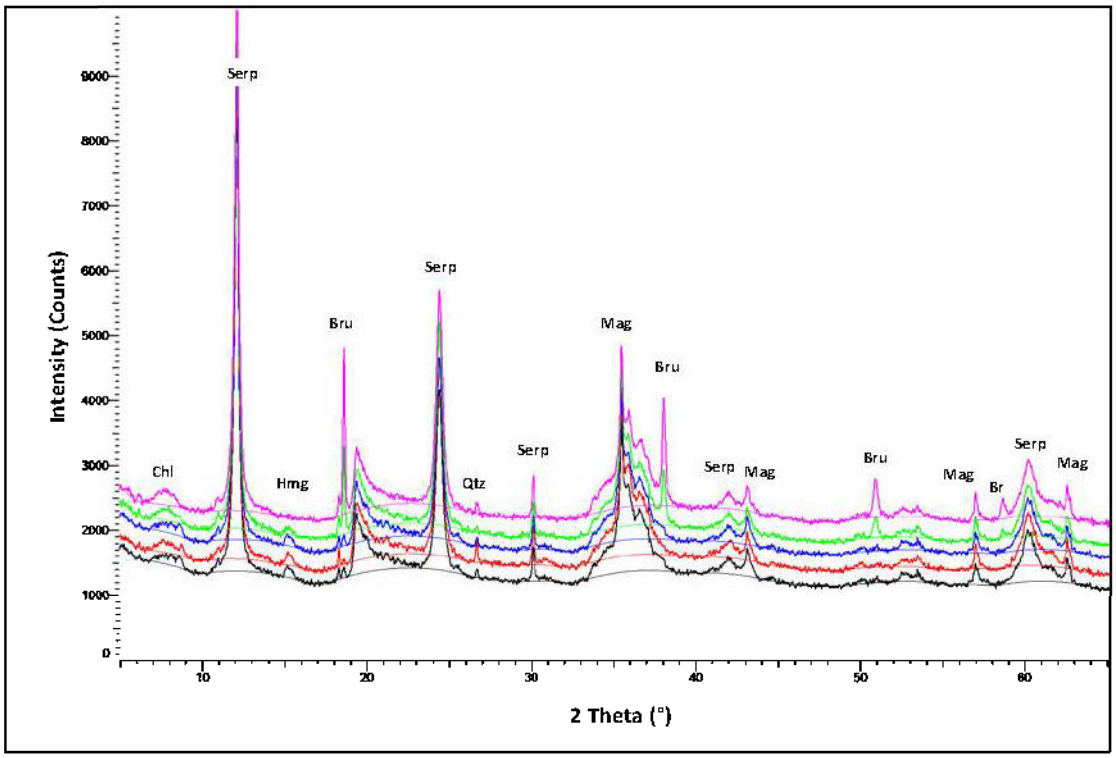

Figure 2.7 XRD Patterns of fresh tailings (Pink), tailings from the column surface (Black), and tailings from the posttesting weathering cell tests (Green: 28 days, blue: 59 days, and red: 178 days). Abbreviations refer to serpentine (Serp), hydromagnesite (Hmg), brucite (Bru), Quartz or chalcedony (Qtz), magnetite (mag), and chlorite (Chl)

Weathering cells were conducted in five replicates and dismantled after different durations (28, 59, 108, 143, and 178 days). The total carbon content was analyzed on each dismantled weathering cell. After 28 days of weathering cell testing, the carbon concentration increased from 0.15 to 0.58 %, and it reached approximately 1 % for 59 days and longer tests (Figure 2.8). Since the pH of the weathering cell leachates remains high (> 9), and alkalinity and Mg concentrations remain at similar concentrations during the whole test (refer to Figure 2.1), the conditions for carbonate growth are present during the whole test duration. However, the fact that there is no

6200 g of CO_2/m^2/year) than in other mine sites where passive carbonation was reported. Therefore, brucite-free ultramafic minerals are also able to sequester CO_2 from the atmosphere in ambient conditions (Assima *et al.* 2014c), sometimes as fast as for brucitic materials, because carbonation is dependent on other factors such as specific surface area and water content, which are highly variable and site-specific.

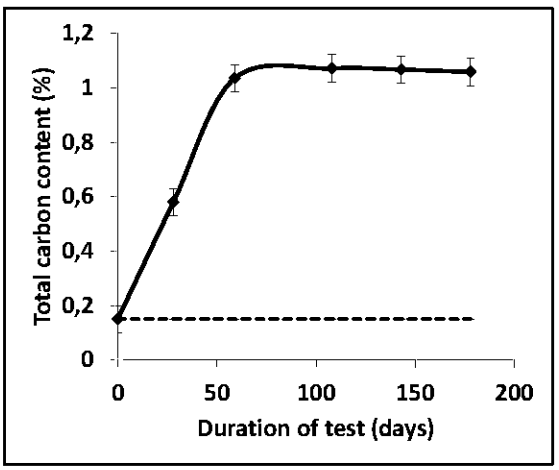

Figure 2.8 Final carbon content in tailings samples submitted to weathering cells conduct for 28, 59, 108, 143, and 178 days. Dashed line represents the initial total carbon content in the fresh tailings

2.4.4.1 Secondary Mineral Characterization

Weathered tailings from the columns and weathering cells were collected and examined under a scanning electron microscope (SEM) in the secondary electrons mode. Observations show that grains are coated with secondary carbonates that have grown over the gangue minerals, often cementing grains together. The secondary products cementing the grains mainly show 2 different habitus: (i) an amorphous phase having a chemical composition close to that of serpentine (Figure 2.9a), (ii) a flaky, rosette-like shape (Figure 2.9b, 2.9c, and 2.9d). The two latter shapes are sometimes attributed to hydromagnesite or dypingite. Dypingite is a transitional product of the transformation of nesquehonite into hydromagnesite (Morgan *et al.*

2015; Hopkinson *et al.* 2008); both minerals have similar habitus and chemical compositions, and are therefore difficult to differentiate. The former phase may be a thin coating of amorphous secondary carbonates over serpentine, which would explain its chemical composition analyzed by energy dispersive spectroscopy (EDS).

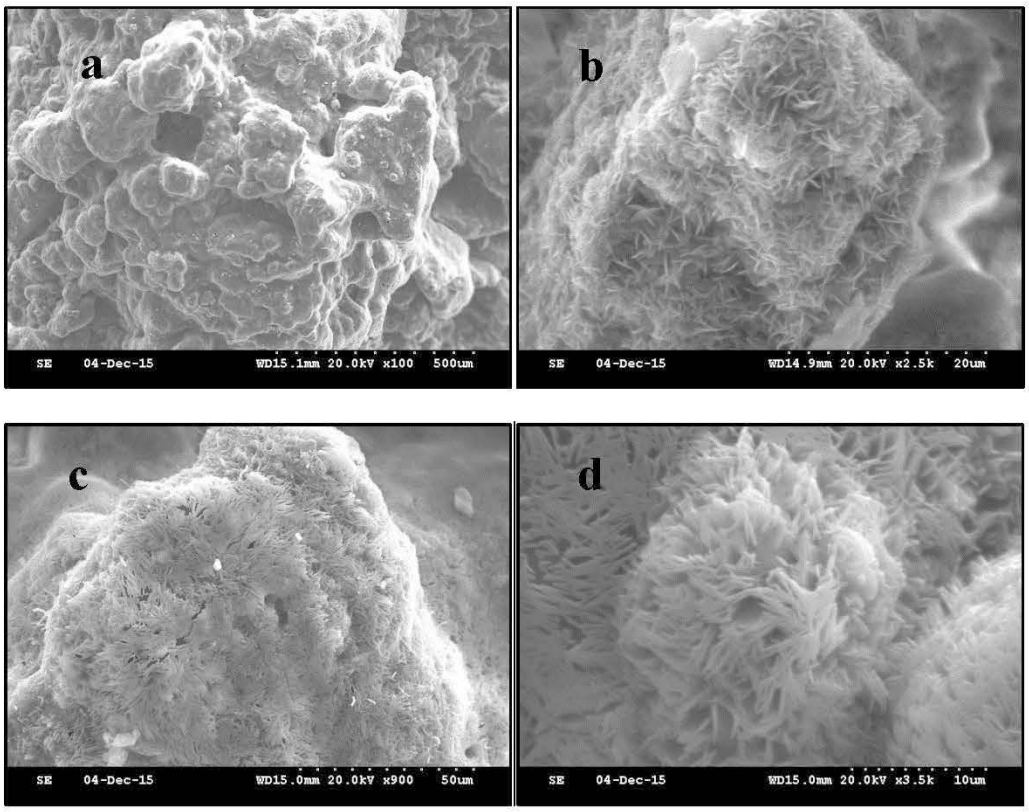

Figure 2.9 SEM images of weathered tailings: (a) amorphous secondary precipitates coating serpentine; (b) flaky, rosette-like secondary carbonates; (c) and (d) needles of secondary carbonates

The DRIFT collected for the fresh tailings, the weathered tailings (at the column surface), and the weathering cells after dismantling are shown in Figure 2.10. The most significant differences for the fresh and weathered tailings appear between 1400 and 1500 cm^{-1} (Figure 2.10b), which is in the range of the asymmetric CO_3^{2-} stretching vibrations modes (v_3) for various hydrated magnesium carbonates such as

nesquehonite, dypingite, huntite ($CaMg_3(CO_3)_4$), and hydromagnesite (Morgan *et al.* 2015; Frost and Palmer, 2011; Hopkinson *et al.* 2008; Kloprogge *et al.* 2003; White, 1971), and of other unidentified carbonate minerals ($MgCO_3 \cdot x(H2O)$) observed by Zhang *et al.* (2006). Thus, the couplet of bands located at ~1428 and ~1484 cm^{-1} appearing in the infrared spectrum of weathered tailings can be assigned to the asymmetric CO_3^{2-} stretching vibration modes of secondary carbonates, which are close to those reported for hydromagnesite and dypingite (1420 – 1480 cm^{-1}) (Hopkinson *et al.* 2008; Botha and Strydom, 2003; White, 1971).

A series of band appear at 802 (the strongest one-Figure 2.10a), 852, and 885 cm^{-1} and are attributed to the out-of-plane ν_2 CO_3^{2-} bending modes, for which it is reported to equal to ~850 cm^{-1} for nesquehonite (Morgan *et al.* 2015; Frost and Palmer, 2011; Ferrini *et al.* 2009; Kloprogge *et al.* 2003), while these bands are split for hydromagnesite and dypingite to 800 (strongest), 850 and 880 cm^{-1} (Frost *et al.* 2009; Hopkinson *et al.* 2008). The presence of hydromagnesite is also supported by the appearance of an absorption band near 802 cm^{-1} which is characteristic of the C-O out-of-plane bending vibration (ν_2) of hydromagnesite (Zhang *et al.* 2006; White, 1971) and suggests the absence of nesquehonite, for which the strongest ν2 band is near 850 cm^{-1} (Morgan *et al.* 2015; Zhang *et al.* 2006). The split of the C-O stretching vibration (ν_3; 1400-1500 cm^{-1}) observed for the weathered tailings spectrum was reported to be indicative of the presence of the bicarbonate ion (HCO_3^-) either than carbonate (CO_3^{2-}; Botha and Strydom, 2003; White, 1971). The C-O Symmetric Stretching mode (ν_1) normally located around 1000 and 1120 cm^{-1} for various hydrated Mg carbonates (Frost *et al.* 2009; Hopkinson *et al.* 2008) cannot be resolved in the obtained DRIFT spectra, as they are probably merged in the broad bands already present in both fresh and weathered samples attributed to symmetric stretching vibrations of Si-O-Si and Si-O bonds (Liu *et al.* 2010; Golightly and Arancibia, 1979). Another band near 1648 cm^{-1} can be seen for both the fresh and

weathered samples, which can be attributed to H_2O bending mode (White, 1971) and may vary from 1640 to 1650 cm^{-1} depending on the type of hydrated carbonate.

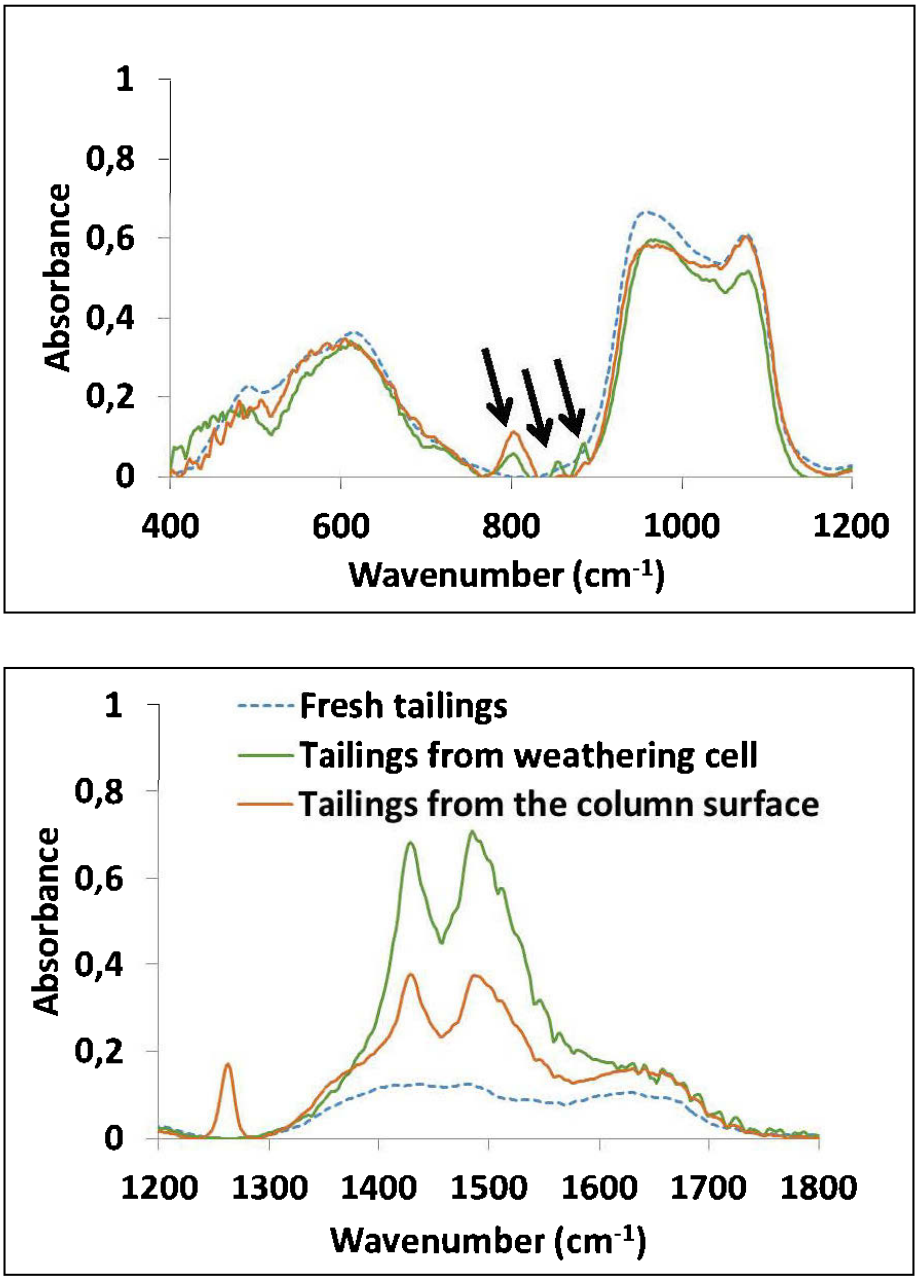

Figure 2.10 DRIFT results for fresh and weathered tailings: (a) 400-1200 cm^{-1}; (b) 1200-1900 cm^{-1}

2.4.5 Estimating carbonation rate and capacity of the Dumont tailings

Based on the increase of total carbon at the end of kinetic tests (Figure 2.6), it is possible to estimate the carbon sequestration capacity of the Dumont tailings as well as the rate of mineral carbonation. For the column test, the carbonation capacity of the Dumont tailings is 8.5 $kgCO_2/t$, corresponding to a carbonation rate of 3.2 $kgCO_2/t/year$. On the other hand, the calculated CO_2 uptake using the weathering cells is higher than for the column and vary from 16 to 33.6 $kgCO_2/t$, which corresponds to a rate of 68.3 to 205 $kgCO_2/t/year$. The higher carbonation rate of the tailings within the weathering cell is explained by many factors: (1) the higher liquid-to-solid ratio (LSR) and the more frequent flushing for the weathering cell test compared to the column test; (2) the higher ratio of surface exposed to mass of tailings for the weathering cell (1.2 cm^2/g) than for the column (0.02 cm^2/g); (3) the carbonation rate at the surface of exposed tailings declines as soon as the brucite is consumed, after which the carbonation is limited by CO_2 diffusion deeper into the tailings. As a consequence, a high ratio of surface to thickness of tailings should be privileged in order to increase their CO_2 uptake capacity.

The theoretical maximum CO_2 uptake of Dumont tailings based on its brucite content (around 11 %) is estimated to be near 70 $kgCO_2/t$. Tailings in the column reach near 12 % of its theoretical carbonation capacity after 2.5 years (8.5 $kgCO_2/t$), whereas with the weathering cell, 48 % of the theoretical carbonation capacity was achieved (33.6 $kgCO_2/t$) in just half a year. The operation of the Dumont mine project will produce at least 500 Mt of ultramafic tailings in 33 years and will emit around 127 700 $tCO_2eq/year$ (Personal communication). Based on the carbonation rates obtained from the kinetic tests conditions, the estimated quantities of CO_2 sequestered by the ultramafic Dumont tailings are potentially up to 4 times greater than the projected annual emissions of this future mine. Thus, passive carbonation of the Dumont tailings could potentially offset the CO_2 emissions of the future mine.

However, the conventional deposition of mine tailings will not help to achieve their fully carbonation potential (Power et al., 2014). According to the design of the tailings storage facility of the Dumont nickel project, part of the tailings will be submerged (RNC, 2013). Thus, expressing the carbonation rate by surface of tailings exposed is more relevant to assess the carbonation potential of the future Dumont tailings exposed in the tailings impoundment. The rates calculated earlier were normalized with the exposed surfaces of column and weathering cells. The surface-normalized rates range from 600 to 2200 gCO_2/m^2/year. These rates are comparable to those reported for the ultramafics mine sites where passive carbonation was reported. Power et al., (2014) reported the following rates: Mount Keith, Australia: 2400 gCO_2/m^2/year; Clinton Creek, Australia: 6200 gCO_2/m^2/year; Diavik, Canada: 374 – 418 gCO_2/m^2/year. In addition, the carbonation rates of the Woodsreef Asbestos Mine waste (Australia) were reported to range between 99 and 4876 gCO_2/m^2/year (Oskierski et al., 2013).

2.5 Summary and conclusions

The column and weathering cell tests performed on the Dumont tailings show that they do not release Ni during weathering, but release sulfates upon sulfide oxidation. However, Fe and Zn are not found in the leachates, whereas Ni is sporadically found in the leachates but is mainly below detection limit. In addition, weathering cell tests on awaruite and sulfides concentrates, suggest that awaruite is stable in the conditions of kinetic testing, and that the metals and sulfates generated in the leachates come from the oxidation of sulfide minerals. CO_2 dissolution and acid generated by sulfide oxidation drive brucite and serpentine dissolution, which generate significant alkalinity and a rise of pH in the leachates. Brucite and serpentine weather to release Mg, which reacts with CO_3^{2-} and HCO_3^- to form hydrated magnesium carbonate. The low concentrations of Si in weathering cells leachates (without grease) reveal

that the faster dissolution of brucite and the incongruent dissolution of serpentine lead to the release of more Mg than Si.

The significant carbon sequestration capacity is highlighted by a carbon content increase, mainly at the surface of the tailings column. This carbon sequestration potential seems to be provided mainly by brucite, which is suggested to be the primary carbon sink, as carbonation seems to decrease as soon as brucite is depleted in the wastes, as shown by weathering cell tests. Compared to other ultramafic mine wastes subject to passive mineral carbonation, the Dumont wastes have the greatest capacity to store CO_2 because of their higher brucite content, approximately 11 %, far superior to the 2.5 % from Mount Keith (Australia). However, the rate of carbonation obtained from the kinetics tests (2200 g of CO_2/m^2/year) is of the same order than within the other studies reported. The control of brucite on the carbonation potential of Dumont is consistent with other mine sites.

The high pH values (9-10) prevailing during the tests impedes metals mobility such as Ni, Zn, and Fe generated by sulfide oxidation. Furthermore, the Dumont mine tailings will not be acid generating and, therefore, contaminated drainage is not expected, other than slightly alkaline pH values that might need treatment before discharge.

Post-testing characterizations (XRD, DRIFT, and SEM) reveal that hydromagnesite is the main carbonate formed during tailings weathering in the conditions of laboratory kinetic testing, while previous studies on the Dumont tailings performed at high CO_2 partial pressure showed that nesquehonite and dypingite formed. However, the conditions of the kinetic tests used in the present study are closer and probably more representative of field conditions. The results obtained here are comparable to those found in the literature on in-situ passive sequestration of carbon from ultramafic mine wastes. Thus, it appears that the kinetic column tests performed can be used to predict

the dissolution and carbonation rates in conditions relevant to in situ CO_2 sequestration.

Acknowledgments

The authors thank RNC Minerals and the Natural Sciences and Engineering Research Council (NSERC) for their contributions to a Research and Collaborative Grant, the RIME-UQAT and RNC Minerals staff. The URSTM (UQAT) staff is also acknowledged for their laboratory support during this project.

References

Assima, G.P., Larachi, F., Beaudoin, G., Molson, J., 2014a. Impact of temperature and oxygen availability on the dynamics of ambient CO2 mineral sequestration by nickel mining residues. Chemical Engineering Journal, 240, pp.394–403.

Assima, G.P., Larachi, F., Beaudoin, G., Molson, J., 2014b. Emulation of ambient carbon dioxide diffusion and carbonation within nickel mining residues. Minerals Engineering, 59, pp.39–44.

Assima G. P., Larachi F., Molson J. and Beaudoin G., 2014c. Comparative study of five Quebec ultramafic mining residues for use in direct ambient carbon dioxide mineral sequestration. Chem. Eng. J. 245, 56–64.

Assima, G.P., Larachi, F.; Beaudoin, G., Molson, J., 2013a. Dynamics of carbon dioxide uptake in chrysotile mining residues – Effect of mineralogy and liquid saturation. International Journal of Greenhouse Gas Control, 12, pp.124–135.

Assima, G.P., Larachi, F., Beaudoin, G., Molson, J., 2013b. Accurate and direct quantification of native brucite in serpentine ores New methodology and implications for CO2 sequestration by mining residues. Thermochimica Acta, 566, pp.281–291.

Assima, G.P., Larachi, F., Beaudoin, G., Molson, J., 2012. CO2 Sequestration in Chrysotile Mining Residues: Implication of Watering and Passivation under Environmental Conditions. Industrial & Engineering Chemistry Research, pp.2–10.

ASTM Standard D4892, 2014. Standard test method for density of solid pitch (Helium Pycnometer Method). West Conshohocken, PA, (www.astm.org).

Aubertin, M., Bussière, B. & Berner, L., 2002. Environnement et gestion des résidus miniers. Les Presses Internationales Polytechnique, Montreal, Canada. Manuel sur Cédérom.

Awoh, A.S., Plante, B., Bussière, B., Mbonimpa, M., 2013. CO2 consumption test for the quantification of the mineral carbonation potential of mine waste rock. In Canadian Geotechnical Conference.

Bales, R.C. & Morgan, J.J., 1985. Dissolution kinetics of chrysotile at pH 7 to 10. Geochimica et Cosmochimica Acta, 49(11), pp.2281–2288.

Bea, S.A., Wilson, S.A., Mayer, K.U., Dipple, G.M., Power, I.M., Gamazo, P., 2012. Reactive Transport Modeling of Natural Carbon Sequestration in Ultramafic Mine Tailings. Vadose Zone Journal, 11(2).

Beaudoin, G., Hébert, R. & Constantin, M., 2008. Spontaneous carbonation of serpentine in milling and mining waste, southern Québec and Italy. Proceedings of Accelerated Carbonation for Environmental and Materials Engineering (ACEME2008), pp.73–82.

Beinlich, A. & Austrheim, H., 2012. In situ sequestration of atmospheric CO 2 at low temperature and surface cracking of serpentinized peridotite in mine shafts. Chemical Geology, 332-333, pp.32–44.

Benzaazoua, M., Bussière, B., Dagenais, A.-M., Archambault , M., 2004. Kinetic tests comparison and interpretation for prediction of the Joutel tailings acid generation potential. Environmental Geology, 46(8 SPEC.ISS.), pp.1086–1101.

Blowes, D.W., Ptacek, C.J., Jambor, J.L., Weisener., C.G., 2003. The Geochemistry of Acid Mine Drainage. Treatise on Geochemistry: Second Edition, 11, pp.131–190.

Botha, A. & Strydom, C. A., 2003. DTA and FT-IR analysis of the rehydration of basic magnesium carbonate. Journal of Thermal Analysis and Calorimetry, 71, pp.987–995.

Bradham, W. & Caruccio, F., 1991. A comparative study of tailings analysis using acid/base accounting, cells, columns and Soxhlets. In C. Vol. 1. CANMET,

Ottawa, ed. 2nd Int Conf Abatement of Acidic Drainage. Montréal, pp. 157–173.

Bussière, B., 2007. Hydro-geotechnical properties of hard rock tailing from metal mines and emerging geo-environmental disposal approaches. Canadian Geotechnical Journal, 44(9), 1019-1052.

Cravotta III, C. A. 2008. Dissolved metals and associated constituents in abandoned coal-mine discharges, Pennsylvania, USA. Part 2: Geochemical controls on constituent concentrations. Applied Geochemistry 23(2): 203-226.

Cruz, R., Bertrand, V., Monroy, M., González, I., 2001. Effect of sulfide impurities on the reactivity of pyrite and pyritic concentrates: A multi-tool approach. Applied Geochemistry 16:803–819.

Felmy A. R., Qafoku O., Arey B. W., Hu J. Z., Hu M., Schaef H. T., Ilton E. S., Hess N. J., Pearce C. I., Feng J. and Rosso K. M., 2012. Reaction of water-saturated supercritical CO2 with forsterite: evidence for magnesite formation at low temperatures. Geochim. Cosmochim. Acta 91, 271–282.

Ferrini, V., De Vito, C. & Mignardi, S., 2009. Synthesis of nesquehonite by reaction of gaseous CO2 with Mg chloride solution: its potential role in the sequestration of carbon dioxide. Journal of Hazardous Materials, 168(2-3), pp.832–837.

Frost, R.L. & Palmer, S.J., 2011. Infrared and infrared emission spectroscopy of nesquehonite Mg(OH)(HCO3)·2H2O-implications for the formula of nesquehonite. Spectrochimica acta. Part A, Molecular and biomolecular spectroscopy, 78(4), pp.1255–60.

Frost, R.L., Bahfenne, S. & Graham, J., 2009. Infrared and infrared emission spectroscopic study of selected magnesium carbonate minerals: artinite and dypingite. Spectrochim. Acta, 71A, pp.1610–1616.

Gautier, Q., Bénézeth, P., Mavromatis, V., Schott, J., 2014. Hydromagnesite solubility product and growth kinetics in aqueous solution from 25 to 75 °C. Geochimica et Cosmochimica Acta, 138, pp.1–20.

Golightly, J.P. & Arancibia, O.N., 1979. The chemical composition and infrared spectrum of Nickel- and iron-substituted serpentine from a nickeliferous laterite profile, Sorobako Indonesia. Canadian Mineralogist 17, 719-728.

Golubev, S.V, Pokrovsky, O.S. & Schott, J., 2005. Experimental determination of the effect of dissolved CO2 on the dissolution kinetics of Mg and Ca silicates at 25 °C. Chem. Geol., 217, pp.227–238.

Gunsinger, R., Ptacek, C.J., Blowes, D.W., Jambor, J.L., Moncur, M.C., 2006. Mechanisms controlling acid neutralization and metal mobility within a Ni-rich tailings impoundment. Applied Geochemistry, 21, pp.1301–1321.

Hakkou, R., Benzaazoua, M. & Bussière, B., 2008. Acid mine drainage at the abandoned kettara mine (Morocco): 2. mine waste geochemical behavior. Mine Water and the Environment, 27(3), pp.160–170.

Hänchen, M., Prigiobbe, V., Baciocchi, R., Mazzotti, M., 2008. Precipitation in the Mg-carbonate system-effects of temperature and CO2 pressure. Chemical Engineering Science, 63(4), pp.1012–1028.

Harrison, A.L., Dipple, G.M., Power, I.M., Mayer, U.K., 2015. Influence of surface passivation and water content on mineral reactions in unsaturated porous media: Implications for brucite carbonation and CO2 sequestration. Geochimica et Cosmochimica Acta, 148, pp.477–495.

Heikkinen, P., Räisänen, M., Johnson, R., 2009. Geochemical characterization of seepage and drainage water quality from two sulphide mine tailings impoundments: acid mine drainage vs. neutral mine drainage. Mine Water Environ 28:30–49

Heikkinen, P.M. & Räisänen, M.L., 2008. Mineralogical and geochemical alteration of Hitura sulphide mine tailings with emphasis on nickel mobility and retention. Journal of Geochemical Exploration, 97(1), pp.1–20.

Hitch, M., Ballantyne, S.M. & Hindle, S.R., 2010. Revaluing mine waste rock for carbon capture and storage. International Journal of Mining, Reclamation and Environment, 24(1), pp.64–79.

Hopkinson, L., Rutt, K.. & Cressey, G., 2008. The transformation of nesquehonite to hydromagnesite in the system CaO-MgO-H2O-CO2: an experimental spectroscopic study. Journal of Geology, 116(4), pp.387–400.

Johnson, R.H., Blowes, D.W., Robertson, W.D., Jambor, J.L., 2000. The hydrogeochemistry of the Nickel Rim mine tailings impoundment, Sudbury, Ontario. Journal of Contaminant Hydrology, 41(1-2), pp.49–80.

Jurjovec, J., Ptacek, C.J., & Blowes, D.W., 2002. Acid neutralization mechanisms and metal release in mine tailings : A laboratory column experiment. Geochimica et Cosmochimica Acta, 66(9), pp.1511–1523.

Kloprogge, J.T., Martens, W.N., Nothdurft, L., Duong, L.V., Webb, G.E., 2003. Low temperature systhesis and characterization of nesquehonite. Journal of Materials Science Letters, 22(11), pp.27–32.

Kodali, B., Rao, B.M., Narasu, L.M., Pogaku, R., 2004. Effect of biochemical reactions in enhancement of rate of leaching. Chemical Engineering Science, 59(22-23), pp.5069–5073.

Krevor, S. & Lackner, K.S., 2011. Enhancing serpentine dissolution kinetics for mineral carbon dioxide sequestration. International Journal of Greenhouse Gas Control, 5(4), pp.1073–1080.

Lackner, K.S.,Wendt, C.H., Butt, D.P., Joyce, E.L., Sharp, D.H., 1995. Carbon dioxide disposal in carbonate minerals. Energy 20, 1153–1170.

Langman, J.B., Blowes, D.W., Veeramani, H., Wilson, D., Smith, L., Sego, D.C., Paktunc, D., 2015. The mineral and aqueous phase evolution of sulfur and nickel with weathering of pyrrhotite in a low sulfide, granitic waste rock. Chemical Geology, 401, pp.169–179.

Lawrence, R.W. & Scheske, M., 1997. A method to calculate the neutralization potential of mining wastes. Environmental Geology, 32(September), pp.100–106.

Lechat, K., Lemieux, J.M., Molson, J., Beaudoin, G., Hébert, R., 2016. Field evidence of CO2 sequestration by mineral carbonation in ultramafic milling wastes, Thetford Mines, Canada. Int. J. Greenhouse Gas Control, 47 (2016), pp. 110–121.

Lin, F.C. & Clemency, C. V., 1981. The dissolution kinetics of brucite, antigorite, talc, and phlogopite at room temperature and pressure. American Mineralogist, 66(7-8), pp.801–806.

Lindsay, M.B.J., Moncur, M.C., Bain, J.G., Jambor, J.L., Ptacek, C.J., Blowes, D.W., *et al.* 2015. Geochemical and mineralogical aspects of sulfide mine tailings. Applied Geochemistry, 57, pp.157–177.

Liu, K., Chen, Q., Hu, H., Yin, Z., 2010. Characterization and leaching behaviour of lizardite in Yuanjiang laterite ore. Applied Clay Science. 47. pp. 311–316.

Luce, R.W., Bartlett, R.W. & Parks, G.A., 1972. Dissolution Kinetics of Magnesium Silicates. Geochimica Et Cosmochimica Acta, 36(1), p.35–&.

Mcgregor, R.G., Blowes, D.W., Jambor, J,L., Robertson, W.D., 1998. Mobilization and attenuation of heavy metals within a nickel mine tailings impoundment near Sudbury, Ontario, Canada. Environmental Geology, pp.305–319.

Merkus, H., 2009. Particle size measurements: fundamentals, practice, quality. Particle Technology Series, 17(Springer), 519. http://doi.org/ISBN 978-1-4020-9016-5.

Moncur, M.C., Jambor, J.L., Ptacek, C.J., Blowes, D.W., 2009. Mine drainage from the weathering of sulfide minerals and magnetite. Applied Geochemistry, 24(12), pp.2362–2373.

Morgan, B., Wilson, S.A., Madsen, I.C., Gozukara, Y.M., Habsuda, J., 2015. Increased thermal stability of nesquehonite (MgCO3·3H2O) in the presence of humidity and CO2: Implications for low-temperature CO2 storage. International Journal of Greenhouse Gas Control, 39, pp.366–376.

Oskierski, H.C., Dlugogorski, B.Z. & Jacobsen, G., 2013. Sequestration of atmospheric CO2 in chrysotile mine tailings of the Woodsreef Asbestos Mine, Australia: Quantitative mineralogy, isotopic fingerprinting and carbonation rates. Chemical Geology, 358, pp.156–169.

Paktunc, A. D., 1999. Characterization of mine wastes for prediction of acid mine drainage. In Environmental impacts of mining activities (pp. 19-40). Springer Berlin Heidelberg.

Park, A.H.A. & Fan, L.S., 2004. CO2 mineral sequestration: Physically activated dissolution of serpentine and pH swing process. Chemical Engineering Science, 59(22-23), pp.5241–5247.

Plante, B., Benzaazoua, M., Bussière, B., Kandji, E.B., Chopard, A., Bouzahzah, H., 2015. Use of EDTA in modified kinetic testing for contaminated drainage prediction from waste rocks: case of the Lac Tio mine. Environmental Science and Pollution Research, pp.1–15.

Plante, B., Benzaazoua, M. & Bussière, B., 2011a. Kinetic Testing and Sorption Studies by Modified Weathering Cells to Characterize the Potential to Generate Contaminated Neutral Drainage. Mine Water and the Environment, 30(1), pp.22–37.

Plante, B., Benzaazoua, M. & Bussière, B., 2011b. Predicting Geochemical Behaviour of Waste Rock with Low Acid Generating Potential Using Laboratory Kinetic Tests. Mine Water and the Environment, 30(1), pp.2–21.

Power, I. M., McCutcheon J., Harrison A. L., Wilson S. A., Dipple G. M., Kelly S., Southam C., Southam G., 2014 Strategizing carbon-neutral mines: A case for pilot projects. Minerals 4, 399–436.

Pronost, J., Beaudoin, G., Lemieux, J.-M., Hébert, R., Constantin, M., Marcouiller, S., Klein, M., Duchesne, J., Molson, J.W., Larachi, F., Maldague, X., 2012. CO2-depleted warm air venting from chrysotile milling waste (Thetford Mines, Québec, Canada): evidence for in situ carbon capture from the atmosphere. Geology 40, 275–278.

Pronost, J., Beaudoin, G., Tremblay, J., Larachi, F., Hébert, R., Constantin, M., Duchesne, J., 2011. Carbon sequestration kinetics and storage capacity of ultramafic mining waste. Environmental Science & Technology 45, 9413–9420.

Rietveld HM, 1993. The Rietveld method. Oxford University Press, (Oxford, UK).

RNC, 2013. Technical Report on the Dumont Ni Project , Launay and Trécesson Townships , Quebec , Canada,

Rollo, H.A. & Jamieson, H.E., 2006. Interaction of diamond mine waste and surface water in the Canadian Arctic. Applied Geochemistry, 21(9), pp.1522–1538.

Saldi G. D., Jordan G., Schott J., Oelkers E. H., 2009. Magnesite growth rates as a function of temperature and saturation state. Geochim. Cosmochim. Acta 73, 5646–5657.

Sapsford, D.J., Bowell. R.J., Dey, M., Williams, K.P., 2009. Humidity cell tests for the prediction of acid rock drainage. Minerals Engineering, 22(1), pp.25–36.

Sciortino, M., Mungall, J.E. & Muinonen, J., 2015. Generation of High-Ni Sulfide and Alloy Phases During Serpentinization of Dunite in the Dumont Sill, Quebec. Economic Geology, 110, pp.733–761.

Smith, L.J.D., Bailey, B.L., Blowes, D.W., Jambor, J.L., Smith, L., Sego, D.C., 2013. The Diavik Waste Rock Project: initial geochemical response from a low sulfide waste rock pile. Applied Geochemistry. 36, 210–221.

SRK, 1989. Draft acid rock drainage technical guide. Prepared by Steffen, Robertson and Kirsten (BC) Inc. in association with Norecol Environmental Consultants and Gormely Process Engineering. Technical Guide, Vancouver, Canada.

Stillings, L.L., Foster, A.L., Koski, R.A., Munk, L., Shanks III, W.C., 2008. Temporal variation and the effect of rainfall on metals flux from the historic Beatson mine, Prince William Sound, Alaska, USA. Applied Geochemistry. 23, 255–278.

Teir, S., Elanova, S., Fogelholm, C.J., Zevenhoven, R., 2009. Fixation of carbon dioxide by producing hydromagnesite from serpentinite. Applied Energy, 86(2), pp.214–218.

Teir, S., Kuusik, R., Fogelholm, C.J., Zevenhoven, R., 2007. Production of magnesium carbonates from serpentinite for long-term storage of CO2. International Journal of Mineral Processing, 85(1-3), pp.1–15.

Teir, S., Elanova, S., Fogelholm, C.J., Zevenhoven, R., 2006. Stability of calcium carbonate and magnesium carbonate in rainwater and nitric acid solutions. Energy Conversion and Management, 47(18-19), pp.3059–3068.

US EPA, 1999. MINTEQA2, Metal speciation equilibrium model for surface and ground water, version 4.0. Available at: http://epa.gov/ceampubl/.

US EPA, 1994. Technical Document Acid Mine Drainage Prediction. Environmental Protection, (December), p.52. Available at: U.S. Environnmental Protection Agency.

Villeneuve, M., Bussière, B., Benzaazoua, M., Aubertin,M., Monroy, M., 2003. The Influence of Kinetic Test Type on the Geochemical Response of Low Acid Generating Potential Tailings, Tailings and Mine Waste '03. Sweets & Zeitlinger, Vail, CO., USA 269–279.

Vogeli, J., Reid, D.L., Becker, M., Broadhurst, J., Franzidis, J.-P., 2011. Investigation of the potential for mineral carbonation of PGM tailings in South Africa. Minerals Engineering, 24(12), pp.1348–1356.

White, W.B., 1971. Infrared characterization of water and hydroxyl ion in the basic magnesium carbonate. The American Mineralogist, 56(100), pp.46–53.

Wilkin, R.T., 2008. Contaminant Attenuation Processes at Mine Sites. Mine Water and the Environment, 27(4), pp.251–258.

Wilson, S. A., Harrisson, A.L., Dipple, G.M., Power, I.M., Barker, S.L.L., Mayer, K.U., Fallon, S.J., Raudsepp, M., Southam, G., 2014. Offsetting of CO2 emissions by air capture in mine tailings at the Mount Keith Nickel Mine, Western Australia: Rates, controls and prospects for carbon neutral mining. International Journal of Greenhouse Gas Control, 25, pp.121–140.

Wilson, S.A., Dipple, G.M., Power, I.M., Barker, S.L.L., Fallon, S.J., Southam, G., 2011. Subarctic weathering of mineral wastes provides a sink for atmospheric CO2. Environmental Science and Technology, 45(18), pp.7727–7736.

Wilson, S. A., Dipple, G.M., Power, I.M., Thom, J.M., Anderson, R.G., Raudsepp, M., Gabites, J.E., Southam, G., 2009a. Carbon dioxide fixation within mine wastes of ultramafic-hosted ore deposits: Examples from the Clinton Creek and Cassiar Chrysotile deposits, Canada. Economic Geology, 104(1), pp.95–112.

Wilson, S. A., Raudsepp, M. & Dipple, G.M., 2009b. Quantifying carbon fixation in trace minerals from processed kimberlite: A comparative study of quantitative methods using X-ray powder diffraction data with applications to the Diavik Diamond Mine, Northwest Territories, Canada. Applied Geochemistry, 24(12), pp.2312–2331.

Wilson, S.A., Raudsepp, M. & Dipple, G.M., 2006. Verifying and quantifying carbon fixation in minerals from serpertine-rich mine tailings using the Rietveld method with X-ray powder diffraction data. American Mineralogist, 91(8-9), pp.1331–1341.

Zhang, Z., Zheng, Y., Ni, Y., Liu, Z., Chen, J., Liang, X., 2006. Temperature- And pH-dependent morphology and FT-IR analysis of magnesium carbonate hydrates. Journal of Physical Chemistry B, 110(26), pp.12969–12973.

CHAPITRE III

GEOCHEMICAL BEHAVIOR OF ULTRAMAFIC WASTE ROCKS WITH CARBON SEQUESTRATION POTENTIAL: A CASE STUDY OF THE DUMONT NICKEL PROJECT, AMOS, QUEBEC

Article publié dans "Environmental Science and Pollution Research International".
March 2017. doi: 10.1007/s11356-017-8735-9. pp 1–18.

Auteurs

Kandji, El Hadji Babacar [(a)], Plante, Benoit [(a)], Bussière, Bruno [(a)], Beaudoin, Georges [(b)], Dupont, Pierre-Philippe [(c)]

[(a)]Research Institute in Mining and Environment (RIME), UQAT (Université du Québec en Abitibi-Témiscamingue), 445 boulevard de l'Université, Rouyn-Noranda, Québec, J9X 5E4, Canada.

[(b)]Department of Geology and Geological Engineering, Université Laval, Québec, Québec G1V 0A6, Canada.

[(c)]RNC Minerals, Rue Trudel, Amos, Quebec, J9T 4N1, Canada.

Résumé

L'impact de la séquestration du CO_2 par les rejets miniers ultramafiques sur la qualité des eaux de drainage a été étudié via des essais cinétiques en colonne, au laboratoire sur des échantillons de stériles. Les rejets étudiés proviennent du projet nickélifère Dumont de Royal Nickel Corporation, Québec, Canada. Les résultats des essais ont démontré que la dissolution du CO_2 induit l'altération de la serpentine et de la brucite, générant ainsi des concentrations élevées en Mg et en HCO_3^- dans les lixiviats, avec des valeurs de pH comprises entre 9 et 10 qui favorisent la précipitation de carbonates secondaires de magnésium. Ces valeurs de pH empêchent la mobilisation de nombreux métaux; Fe, Ni, Cu et Zn ont été trouvés à des concentrations négligeables dans les lixiviats. Les caractérisations post-démantèlement des colonnes sur les rejets via les analyses chimiques, la spectroscopie infrarouge à transformée de Fourier (DRIFT) et les observations au microscope électronique à balayage (MEB), ont confirmé la précipitation des carbonates de magnésium hydratés, tel que suggéré par les calculs d'équilibre thermodynamique. La formation des carbonates de magnésium secondaires a induit une cimentation des rejets en surface, ce qui entraîne le développement d'une zone indurée.

Abstract

The geochemical behavior of ultramafic waste rocks and the effect of carbon sequestration by these waste rocks on the water drainage quality were investigated using laboratory-scale kinetic column tests on samples from the Dumont Nickel Project (RNC Minerals, Québec, Canada). The test results demonstrated that atmospheric CO_2 dissolution induced the weathering of serpentine and brucite within the ultramafic rocks, generating high concentrations of Mg and HCO_3^- with pH values ranging between 9 and 10 in the leachates that promote the precipitation of secondary Mg-carbonates. These alkaline pH values appear to have prevent the mobilization of many metals; Fe, Ni, Cu, and Zn were found at negligible

concentrations in the leachates. Post-testing characterization using chemical analyses, diffuse reflectance infrared Fourier transform (DRIFT), and scanning electron microscope (SEM) observations, confirmed the precipitation of secondary hydrated Mg-carbonates as predicted by thermodynamic calculations. The formation of secondary Mg-carbonates induced cementation of the waste particles, resulting in the development of a hardpan.

Keywords: Alkaline drainage, carbon sequestration, hydrated magnesium carbonate, kinetic column test, prediction, ultramafic waste rock.

3.1 Introduction

Significant amounts of ultramafic rocks are scattered in the earth's crust. Ultramafic rocks are rich in minerals with the capacity to react with CO_2 during the weathering process (Goff and Lackner 1998; Lackner *et al.* 1995). These rocks are sometimes produced as wastes when they are associated with base metal deposits. Consumption of atmospheric CO_2 by precipitation of secondary Mg or Ca carbonates, or mineral carbonation, is a slow process under natural environmental conditions, and likely occurs in mine wastes in the following steps: 1) dissolution of CO_2 into interstitial waters; 2) dissolution of silicates or hydroxides in carbonic acid, which releases Mg^{2+} or Ca^{2+}; and 3) reactions between Mg^{2+} or Ca^{2+} with HCO_3^- or CO_3^{2-} form stable carbonates under ambient conditions (Gras *et al.* 2017; Harrison *et al.* 2012; Wilson *et al.* 2009a). Extensive carbonation has been noted at: Clinton Creek and Cassiar mines, Canada (Wilson *et al.* 2009a); Thetford Asbestos mine, Canada (Beaudoin *et al.* 2008); Woodsreef Absestos mine, Australia (Oskierski *et al.* 2013); Mount Keith Nickel mine, Australia (Wilson *et al.* 2014); and in chromite mine shafts in Norway (Beinlich and Austrheim 2012). Despite the slow rate of the carbonation process, the exposition of large amounts of finely crushed rocks over large surface areas could

considerably increase the total carbon fixed by ultramafic mine wastes. Such passive mineral carbonation of mine wastes could, at least in part, reduces the carbon footprint of mining activities (Hitch *et al.* 2010).

Existing literature on passive carbon sequestration by ultramafic mine wastes focuses mainly on understanding the process, estimation of sequestration potential, or evaluation of factors that potentially affect sequestration potential and evolution, such as temperature, surface passivation, or degree of saturation (Lechat *et al.* 2016; Assima *et al.* 2014a, 2012; Pronost *et al.* 2011; Wilson *et al.* 2009a, b; Beaudoin et al. 2008; Bea *et al.* 2012). These studies also evaluated the processes controlling carbonate formation and stability, as well as the CO_2 sources via radiocarbon data (Oskierski *et al.* 2013; Wilson *et al.* 2010, 2009a). Some studies were conducted under laboratory conditions in order to better understand the fundamental aspects of passive mineral carbonation processes, as well as the main parameters controlling CO_2 uptake (Zarandi *et al.* 2016; Assima *et al.* 2014a, 2014b, 2013, 2012). However, these laboratory studies were performed mainly in small samples (less than 100 g) using fine grain sizes (below 2 mm) and in conditions that are not representative of field conditions in terms of quantity, heterogeneity, and CO_2 partial pressure. Other studies aimed to develop industrial techniques to increase or accelerate the carbon sequestration of mine wastes, and to move up to the industrial scale (Harrison *et al.* 2012, 2012; Power *et al.* 2013; Krevor and Lackner 2011; Larachi *et al.* 2010). Likewise, pre-treatment of ultramafic mine waste through chemical and mechanical activations was also considered recently in order to increase their CO_2 sequestration potential (Li and Hitch 2017, 2016a, 2016b).

Because CO_2 sequestration by mine waste involves the extensive dissolution of certain silicate minerals, the dissolution of CO_2, and the precipitation of secondary carbonates, it may have an effect on water drainage quality. This was first described by Rollo and Jamieson (2006), who stated that mineral carbonation (dissolution of

CO_2) is possibly responsible for the dissolution of serpentine in diamond mine wastes and for the precipitation of secondary carbonates. This was later confirmed by Wilson *et al.* (2009b) who also added that this phenomenon could increase the neutralization potential of the kimberlite processing wastes by 1 to 2 %. Waters interacting with ultramafic mine wastes in Mount Keith mine (Australia; Bea *et al.* 2012) and in chromite mine shafts in Norway (Beinlich and Austrheim 2012) were alkaline, with pH values up to 10. It was also demonstrated that nesquehonite [$MgCO_3 \cdot 3H_2O$], a secondary carbonate precipitated upon carbon sequestration, remove metals from solution by adsorption and ionic exchange (Hamilton *et al.* 2017).

Therefore, it is important to consider these aspects when predicting the geochemical behavior of ultramafic mine wastes. The aim of this work is to evaluate the geochemical behavior of ultramafic waste rocks from the Dumont Nickel Project by using long-term kinetic column tests in order to predict the quality of the water that will leach out of the future mine wastes.

Previous work on the Dumont materials

The serpentinized rocks of the future Dumont tailings and waste rocks will possess a significant carbon sequestration potential as suggested by previous studies (Kandji *et al.* 2017; Gras *et al.* 2017; Zarandi *et al.* 2016; Assima *et al.* 2014b, 2014c; Pronost *et al.* 2011). However, these studies only focused on the carbonation of tailings, not on waste rocks. The study of Pronost *et al.* (2011) demonstrated that the Dumont tailings reached approximately 8 wt % of CO_2 upon carbonation in eudiometers (Pronost *et al.* 2011). A study of Zarandi *et al.* (2017) highlighted the transformation of secondary nesquehonite formed during the mineral carbonation of the Dumont tailings into hydromagnesite [$4MgCO_3 \cdot Mg(OH)_2 \cdot 4H_2O$] and dypingite [$Mg_5(CO_3)4(OH)_2 \cdot 5(H_2O)$]. A paper focusing on the geochemical behavior of the Dumont tailings and the potential of generation of contaminants of the two main sources of nickel, using the same methodology as this present paper, is currently

under review (Kandji *et al.* 2017). The main findings of this study are that, in contrast to Ni-sulfides, awaruite [Ni_3Fe] does not release Ni or Fe during its weathering. Therefore, the low Ni concentrations found in the tailings' leachates are suggested to come from the oxidation of Ni-sulfides. This study also highlighted the fact that brucite [$Mg(OH)_2$] seems to be the main mineral controlling the maximum CO_2 uptake in the Dumont tailings, and carbon sequestration stagnated as soon as brucite was depleted in the tailings samples.

3.2 Materials and methods

3.2.1 Dumont Nickel Project site

RNC Minerals, a Canadian mineral resource company, plans to operates a nickel mine, in which the mineralization is comprised primarily of nickel sulfides: pentlandite [$(Fe,Ni)_9S_8$], heazlewoodite [Ni_3S_2], and millerite [NiS]; and iron-nickel alloy (awaruite, [Ni_3Fe]) (Sciortino *et al.* 2015). The Dumont site (Figure 3.1) is located 25 km west of the Amos, Quebec (Canada). The climate in this area is temperate continental and the mean annual temperature is approximately 1.2°C. The monthly mean temperature ranges from -17.3 to 17.2°C in January and July, respectively. The total average annual precipitation is 918 mm (RNC 2013). The deposit is in a mineralized zone of serpentinized dunite, which is mainly composed of lizardite with minor minerals including magnetite, brucite, chlorite, diopside, and chrysotile (< 2 %) (RNC 2013). The exploitation of the Dumont mine is expected to produce more than 2 billion tons of ultramafic waste rocks and tailings.

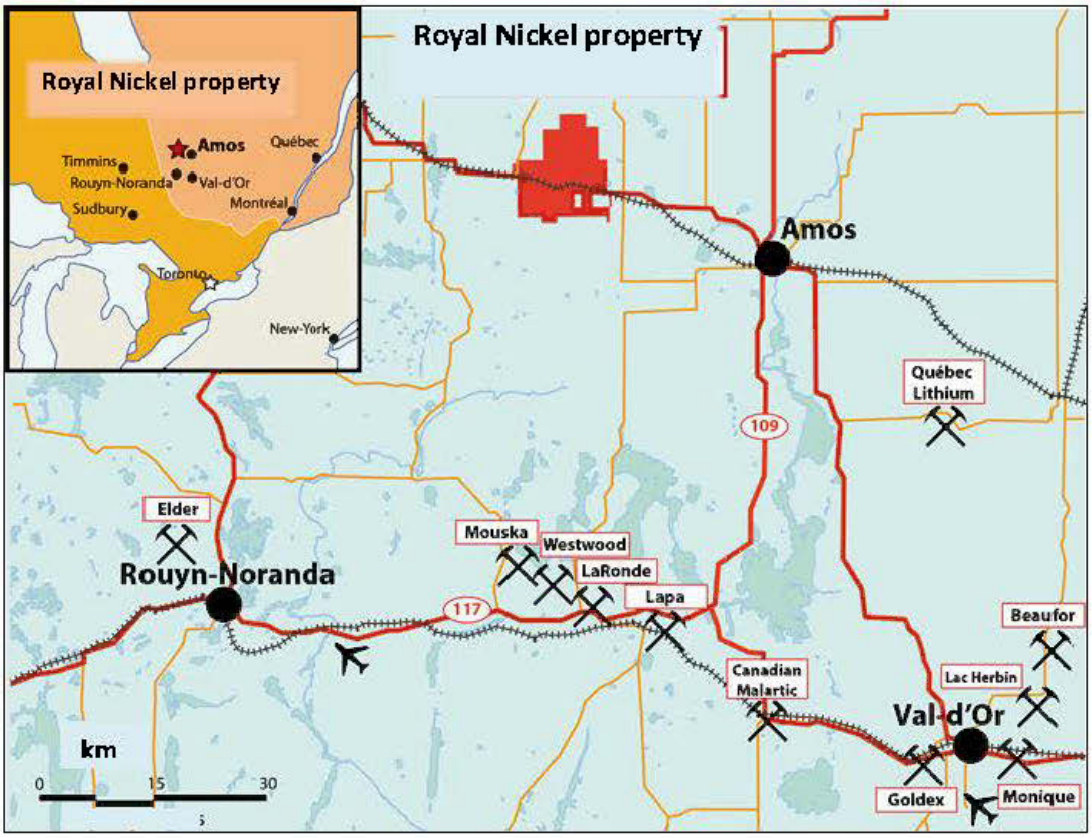

Figure 3.1 Dumont Nickel Project site location (from RNC, 2013)

3.2.2 Sampling and samples characterization methods

One ultramafic waste rock and five samples of the main lithologies found in the Dumont Nickel Project were sampled for this study: low-grade dunite, upper peridotite, footwall ultramafic (which is dominantly peridotite), gabbro, and volcanic basalt. The ultramafic waste rock of the future Dumont mine site was a bulk sample from a blasted outcrop consisting mainly of dunite and peridotite. The fraction below 2 cm was selected for this study. The five main lithologies were sampled from representative sections of drill cores and crushed to < 2 cm.

The chemical composition of all samples was determined by inductively coupled plasma atomic emission spectroscopy (ICP-AES) analysis following acid digestion

(HNO_3-Br_2-HF-HCl). The acid-extractable sulfates were determined after extraction with 40 % HCl (Sobek *et al.* 1978). The whole-rock composition was determined by X-ray fluorescence (XRF) following a lithium borate fusion on pulverized sample aliquots (85 % < 200 mesh) by Acme Analytical Laboratories Ltd (Vancouver, Canada), with detection limits between 0.001 and 0.1 % on the oxides. The total carbon and sulfur content of the Dumont samples was determined using a LECO carbon/sulfur analyzer (Maxxam Analytical, Quebec, Canada) with a reportable detection limit of 0.05 % for carbon and 0.009 % for sulfur. The acid-base accounting (ABA) was determined using the Lawrence and Wang (1997) procedure. The neutralization potential (NP) was determined through titration to an endpoint pH of 8.3. The acid generation potential (AP) was calculated by using the sulfide sulfur portion, obtained by subtracting the sulfate sulfur from the total sulfur. Both AP and NP results are expressed in kg $CaCO_3$/t.

Leachates from the column tests were collected and an aliquot was filtered, acidified with 2 % HNO_3, and analyzed for various elements using ICP-AES and inductively coupled plasma mass spectrometry (ICP-MS). The pH, conductivity, acidity, and alkalinity were also measured on the leachates. Alkalinity and acidity were measured by acid base titration to pH endpoints of 4.5 and 8.3, respectively.

The mineralogical composition of the Dumont samples was determined with mineralogical reconciliation of X-ray diffraction (XRD) and XRF data, microscopic observations, and chemical composition results. The XRD patterns were collected using a Bruker AXS Advance D8 with a copper cathode, acquired at steps of $0.02°s^{-1}$ between 2Θ values of 5° and 70°. The DiffracPlus EVA software (v. 9.0) was used to identify the mineral species, and the semi-quantitative mineralogical compositions were evaluated using the TOPAS software (v. 2.1) with a Rietveld (1993) refinement. The XRD was used to evaluate the general mineralogical composition of the materials (detection limit in the range of 1-2 %), while the SEM was used to detect

mineral phases that remained undetected by the XRD, either because they were below the detection limit or amorphous. Scanning electron microscope (SEM) observations were performed with a Hitachi S-3500 N SEM equipped with an energy dispersive spectroscopy (EDS) Oxford X-Max 20 mm^2 silicon drift detector (SDD) microanalysis system. SEM observations were performed at, approximately, a 15 mm working distance and a 100 – 150 μA current at 20 kV.

Fresh and weathered (post-testing) samples were submitted to diffuse reflectance infrared Fourier transform (DRIFT) spectroscopy to characterize the secondary Mg-carbonates formed. The DRIFT spectra were collected on a Bruker Optics Tensor 27 Fourier transform infrared spectrometer. The spectra were collected over 200 scans from 400 to 4000 cm^{-1} with a resolution of 1 cm^{-1}, with the aperture set to 4 mm. The samples were sieved to < 45 μm and the spectra were obtained on samples diluted to approximatively 15 wt.% with oven-dried spectrograde KBr powder. During the spectra acquisition, the sample room was purged with nitrogen gas to prevent atmospheric CO_2 contamination.

The physical properties of the initial samples were determined prior to kinetic testing. The specific gravity (G_s) of the samples was determined using a Micromeritics Accupyc 1330 helium pycnometer (the accuracy is within 0.03 % of the reading plus 0.03 % of nominal full-scale sample chamber volume; ASTM Standard D4892 2014). The grain-size distribution was determined by sieving for the fractions between 2 cm and 355 μm (ASTM D 6913-04 2009) and by a laser diffraction grain-size analyzer for the fraction below 355 μm using a Malvern Instruments Mastersizer S (Merkus 2009). The specific surface area (SSA) of each material was calculated using the equation proposed by Chapuis and Légaré, (1992) using the material density and the grainsize distribution.

3.2.3 Kinetic column tests description

Column tests were used to study the geochemical behavior of the Dumont samples. In contrast to humidity cells tests, column tests are not standardized, but are generally considered to be much more representative of field conditions (Plante *et al.* 2014; Benzaazoua *et al.* 2004). The reproducibility of such tests was demonstrated by Demers *et al.* (2008). The columns were constructed from 1 m high, 14 cm internal diameter Plexiglas tubes, and were filled (without compaction) to a height of approximately 70 cm, which corresponded to masses between 17.1 and 19.1 kg. The columns were flushed from the top with 2 L of deionized water (pH 5.5 – 6.0) twice per month, which is representative of the average monthly rainfall in the field area. The leachates were recovered after a contact time of a few hours and analyzed for parameters including pH, conductivity, and dissolved species. The column tests were performed over a duration of approximately 1 year. Between each flush, the material was left open to ambient laboratory conditions. Thermodynamic equilibrium calculations for the collected leachates were performed using Visual MINTEQA2 version 3.1 (USEPA 2006) in order to calculate the saturation indices (SI) of selected minerals. The default thermodynamic database was updated for some selected magnesium carbonates; Table 3.1 shows the thermodynamic data used and the corresponding references.

Tableau 3.1 Thermodynamic data used to update Vminteq database of selected minerals

Minerals	**-Log(Ks)**	**$\Delta_r H°_{298.15}$ (kJ mol^{-1})**	**References**
Magnesite	7.80	-1111.75	Bénézeth et al. (2011)
Hydromagnesite	37.08[a]	-6516.0 [b]	[a]Gautier et al. (2014) [b]Königsberger et al. (1999)
Nesquehonite	5.59[a]	-1977.3[b]	[a]Langmuir (1965) [b]Robie & Hemingway (1995)
Lansfordite	5.46[a]	-2574.3[b]	[a] Langmuir (1965) [b]Königsberger et al. (1999)
Artinite	17.2[a]	-2920.6[b]	[a] Langmuir (1965) [b]Robie & Hemingway (1995)

3.2.4 Physical and chemical characterization results

The main physical parameters are summarized in Table 3.2, while grain-size curves for all samples are shown in Figure 3.2. The waste rocks were finer than the other samples, having > 9 % of particles smaller than 300 µm, while the lithology samples all had 3 % or fewer particles smaller than 300 µm. This significant difference is due to the sampling and preparation methods used; i.e., crushing the drill core samples of the lithologies generated less fines than blasting of the waste rock bulk sample. The D_{10}, D_{30}, and D_{60} values (corresponding to 10 %, 30 % and 60 % of particles passing on the cumulative curves, respectively) were all higher for the lithology samples than for the waste rock sample, which also emphasizes the physical differences among these materials. The specific gravity (G_s) of the samples were similar for all ultramafic samples (between 2.6 and 2.7) while they were slightly higher for the gabbro and volcanic samples (2.97 and 3.04). The calculated SSA range from 1.44 to 5.94 m^2/kg.

Results of major and minor elements are presented in Table 3.2. These results, combined with XRD analysis, allowed for the identification and quantification of the minerals present in the samples. The ultramafic lithologies (low-grade dunite, upper peridotite, and footwall ultramafic) contained between 34 % and 43 % MgO. The gabbro and volcanic samples contained 10 % and 6 % MgO, respectively. All tested samples contained between 34 % (footwall ultramafic) and 49 % (gabbro) SiO_2. While the theoretical ratio of MgO/SiO_2 in serpentine equals 1.00, it was > 1.00 in the low-grade dunite (1.2), upper peridotite (1.1), and footwall ultramafic (1.2) samples, suggesting an excess of Mg which can be attributed to brucite, $Mg(OH)_2$. Iron was present in all samples, with Fe_2O_3 concentrations between 6 % and 12 %. The gabbro and volcanic samples also contained more Al_2O_3 (13 % and 14 %, respectively) and CaO (12 % and 10 %, respectively) compared to the other samples (Al_2O_3: 0.2 – 3 %; CaO: 0.05 – 0.9 %), revealing the differences in mineralogical compositions between the non-ultramafic samples of gabbro and volcanic in comparison to the other materials. High loss on ignition values (LOI; 12 – 15 %) were common for ultramafic rocks, while they were near 3 and 5 % respectively for the gabbro and volcanic sample. The highest concentration of carbon was detected in the volcanic sample (8000 ppm), due to the presence of calcite [$CaCO_3$]. The waste rock, low-grade dunite, upper peridotite, gabbro, and footwall ultramafic contained similar carbon concentrations (between 1200 and 1700 ppm). The samples contained low sulfur concentrations, between 200 and 800 ppm. The sulfate was below the detection limit (5 ppm) for upper peridotite, footwall ultramafic, and low-grade dunite, and between 10 and 100 ppm for the gabbro, volcanic, and waste rock samples. The five ultramafic samples had high NP (96 – 147 kg $CaCO_3$/t), but for the gabbro and volcanic samples, the NP were 13 and 55 kg $CaCO_3$/t, respectively. In contrast, the AP was negligible for all samples (< 3 kg $CaCO_3$/t). Thus, with the exception of the gabbro, all samples were considered to be non-acid generating as the difference between NP and AP (net neutralization potential, or NNP) was high (52 to

145 of kg $CaCO_3$/t). The NNP of the gabbro fell inside the uncertainty zone (± 20 kg$CaCO_3$/t) according to the criteria defined by SRK (1989).

Tableau 3.2 Physical and chemical characteristics of the six samples studied

	Ultramafic Waste Rock	Upper Peridotite	Footwall Ultramafic	Low-grade Dunite	Gabbro	Volcanic
D_{10} (µm)	350	2800	1800	1400	4500	3000
D_{50} (µm)	5500	10000	9000	9000	12000	11000
D_{90} (µm)	15000	16000	16000	16000	18000	16000
% < 300 µm	9.3	2.0	2.6	3.4	1.0	1.9
G_s	2.66	2.71	2.65	2.60	3.04	2.97
SSA (m2/kg)	5.94	1.44	1.97	2.36	1.94	2.04
MgO (wt. %)	34.06	38.97	40.64	42.68	9.96	6.00
SiO_2 (wt. %)	41.40	35.83	34.17	34.53	49.27	47.93
Al_2O_3 (wt. %)	3.08	1.27	0.58	0.23	13.41	14.07
Fe_2O_3 (wt. %)	7.07	9.59	9.42	6.71	9.41	12.62
CaO (wt. %)	0.86	0.69	0.16	0.15	11.97	9.78
Na_2O (wt. %)	0.74	< 0.01	< 0.01	< 0.01	1.64	1.99
K_2O (wt. %)	0.25	< 0.01	< 0.01	< 0.01	0.18	0.28
MnO (wt. %)	0.09	0.14	0.12	0.11	0.18	0.22
TiO_2 (wt. %)	0.13	0.05	0.02	< 0.01	0.40	0.87
P_2O_5 (wt. %)	0.02	< 0.01	< 0.01	< 0.01	0.03	0.08
Cr_2O_3 (wt. %)	0.16	0.72	0.99	0.49	0.07	0.03
LOI (wt. %)	12.31	12.94	14.11	15.41	2.72	5.3
Total (wt. %)	**100.18**	**100.2**	**100.21**	**100.3**	99.**22**	99.**18**
S (ppm)	400	500	200	500	500	800
SO_4(ppm)	100	< 5	< 5	< 5	10	10
C (ppm)	1700	1600	1200	1200	1200	8000
Ni (ppm)	2200	1800	2300	2800	100	100
Zn (ppm)	30	30	33	30	100	32
Pb (ppm)	10	< 5	< 5	< 5	100	< 5
Cu (ppm)	50	8	10	10	100	93
Co (ppm)	70	100	100	100	100	29
NP (kg $CaCO_3$/t)	120	96	139	147	13	55
AP (kg $CaCO_3$/t)	1.3	1.6	0.6	1.6	1.6	2.5
NNP (kg $CaCO_3$/t)	118.7	98.4	138.4	145.4	11.4	52.5

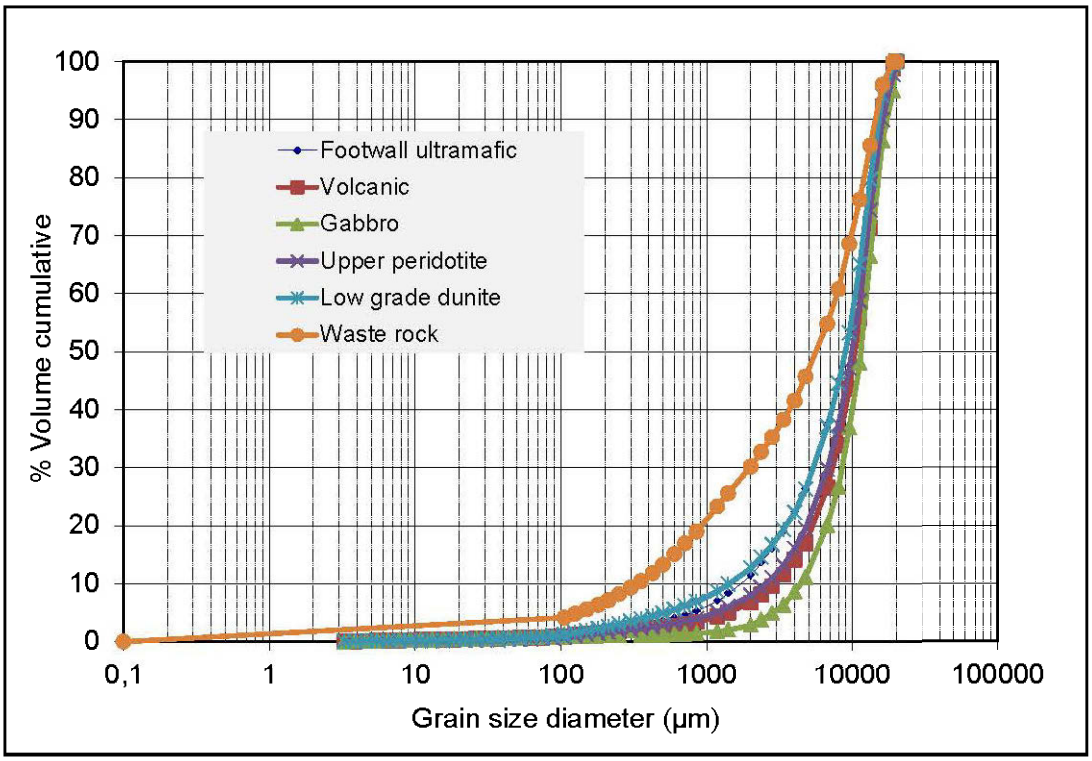

Figure 3.2 Grain-size distribution of studied samples

The XRD results indicated that the bulk of the ultramafic samples, such as waste rock, low-grade dunite, upper peridotite, and footwall ultramafic, were comprised of approximately 60 – 80 % serpentine (lizardite; $[(Mg,Fe)_3Si_2O_5(OH)_4]$, as shown in Table 3.3. Brucite $[Mg(OH)_2]$, the most reactive mineral with respect to acidity (Lin and Clemency 1981; Bales and Morgan 1985), was present in all four ultramafic samples in concentrations varying from 4 to 11 %. Other minerals included magnetite $[Fe_3O_4]$ and chlorite $[(Fe,Mg,Al)_6(Si,Al)_4O_{10}(OH)_8]$. The waste rock sample also contained albite $[NaAlSi_3O_8]$ and quartz $[SiO_2]$. The gabbro and volcanic materials contained predominantly hornblende $[Ca_2[Mg_4(Al,Fe)]Si_7AlO_{22}(OH)_2]$, albite, and epidote $[Ca_2(Fe,Al)Al_2(SiO_4)(Si_2O_7)O(OH)]$, with lesser amounts of quartz, biotite $[K(Mg,Fe)_3(OH,F)_2(Si_3AlO_{10})]$, and diopside $[CaMgSi_2O_6]$. The volcanic sample also contained around 7 % calcite. No serpentine and brucite were detected in the

gabbro and volcanic samples. The waste rock sample appeared to be a mix of all lithologies, however, hornblende, magnesite, and epidote were not detected. Small quantities of carbonate were present in all samples, as shown by the total carbon content and the DRIFT analyses performed on the fresh materials.

Table 3.3 Mineralogical composition of Dumont Nickel Project samples (in wt.%)

Minerals and Formulas	**Waste Rock**	**Upper Peridotite**	**Ultramafic Footwall**	**Low-grade Dunite**	**Gabbro**	**Volcanic**
Lizardite + Chrysotile $Mg_3Si_2O_5(OH)_4$	60 – 80				-	-
Brucite $Mg(OH)_2$	4 – 11				-	-
Magnetite Fe_3O_4	1 – 6				-	-
Chlorite $(Fe,Mg,Fe)_5Al(Si_3Al)O_{10}(OH,O)_8$	2 – 12				6 – 10	
Chromite $FeCr_2O_4$	0.2 – 2				~0.1	-
Diopside $CaMgSi_2O_6$	1 – 2				~8	
Calcite $CaCO_3$	-	-	-	-	-	~7
Quartz SiO_2	~8	-	-	-	6 – 16	
Albite $NaAlSi_3O_8$	~7	-	-	-	15 – 17	
Biotite Mica $K(Mg,Fe)_3(OH,F)_2(Si_3AlO_{10})$	~2	-	-	-	~2	
Hornblende $Ca_2[Mg_4(Al,Fe)]Si_7AlO_{22}(OH)_2$	-	-	-	-	19 – 46	
Epidote $Ca_2(Fe,Al)Al_2(SiO_4)(Si_2O_7)O(OH)$	-	-	-	-	15 – 18	
Rutile TiO_2	-	-	-	-	~1	

3.3 Results and discussion

3.3.1 Geochemistry of columns leachates

Results of the water quality analysis from the column tests are summarized in this section. Selected parameters (i.e., pH, electrical conductivity, alkalinity, sulfate, Mg, Ca, Si, Al, and Na) are shown in Figure 3.3. Others parameters (HCO_3^-, CO_3^{2-}, As, Ni, Zn, and Cr) are shown in Figure 3.4. Elements not shown (i.e., Cu, Co, Fe, Pb, and Ba) were generally below the detection limit of the ICP. Ni and Zn were periodically found in all leachates and ranged from 0.001 to 0.01 mg/L and 0.001 to 0.13 mg/L, respectively. Arsenic was found only in the gabbro leachates at concentrations ranging from 0.001 to 0.008 mg/L. Strontium (not shown) was present in all leachates between 0.003 mg/L and 0.2 mg/L.

The geochemical behavior of the ultramafic samples (waste rock, low-grade dunite, upper peridotite, and footwall ultramafic) was similar. The pH of the ultramafic samples remained alkaline during the kinetic tests (9.5 – 10); values were periodically around 8.3. The volcanic and gabbro samples had lower pH values which varied from 8.0 to 8.5. The waste rock leachates' pH was slightly higher than the other ultramafic samples. The electrical conductivity of the leachates from ultramafic samples was highest in the earliest leachates (near 4000 µS/cm) and stabilized near 500 µS/cm. For the gabbro and volcanic rocks, the electrical conductivity was low, with values near 100 µS/cm. The waste rock sample generated higher alkalinity values than the other samples, with higher values at the beginning of the test, which stabilized near 300 mg $CaCO_3$/L after approximately 75 days. Alkalinity stabilized at less than 100 mg $CaCO_3$/L for all other samples. The concentrations of HCO_3^- and CO_3^{2-} were calculated based on the alkalinity and pH values of the leachates. In the range of pH values prevailing in the leachates, HCO_3^- is the dominant carbonate species, except for the waste rocks leachates for which CO_3^{2-} is the dominant carbonate ion, because of their higher alkalinity and pH values.

Magnesium was the most concentrated element in the leachates and showed a significant difference between ultramafic and non-ultramafic materials. Magnesium concentrations in leachates from the waste rock, low-grade dunite, peridotite, and footwall ultramafic columns varied from 400 mg/L to around 100 mg/L, with the highest values obtained during the first 100 days, while for the gabbro and volcanic samples, Mg concentrations varied between 1 and 5 mg/L. However, Si concentrations in the leachates were highest for volcanic and gabbro with a relatively constant concentration varying from 2 to 4 mg/L, while for ultramafic samples, Si was detected only after 280 days of testing. The Ca concentrations in the low-grade dunite leachates reached 80 mg/l in the beginning of the test but decreased and stabilized near 30 mg/l after approximately 100 days, while they did not exceed 2 mg/L for the waste rock sample. Other samples produced lower Ca concentrations (upper peridotite and footwall ultramafic: 30 – 10 mg/L, gabbro and volcanic: around 10 mg/L). As for Si, the gabbro and volcanic samples produced the highest Al concentrations, which ranged between 0.1 to 0.2 mg/L, while the other samples only periodically generated Al in the leachates. Na levels stabilized at around 10 mg/L for gabbro, volcanic, and waste rock samples.

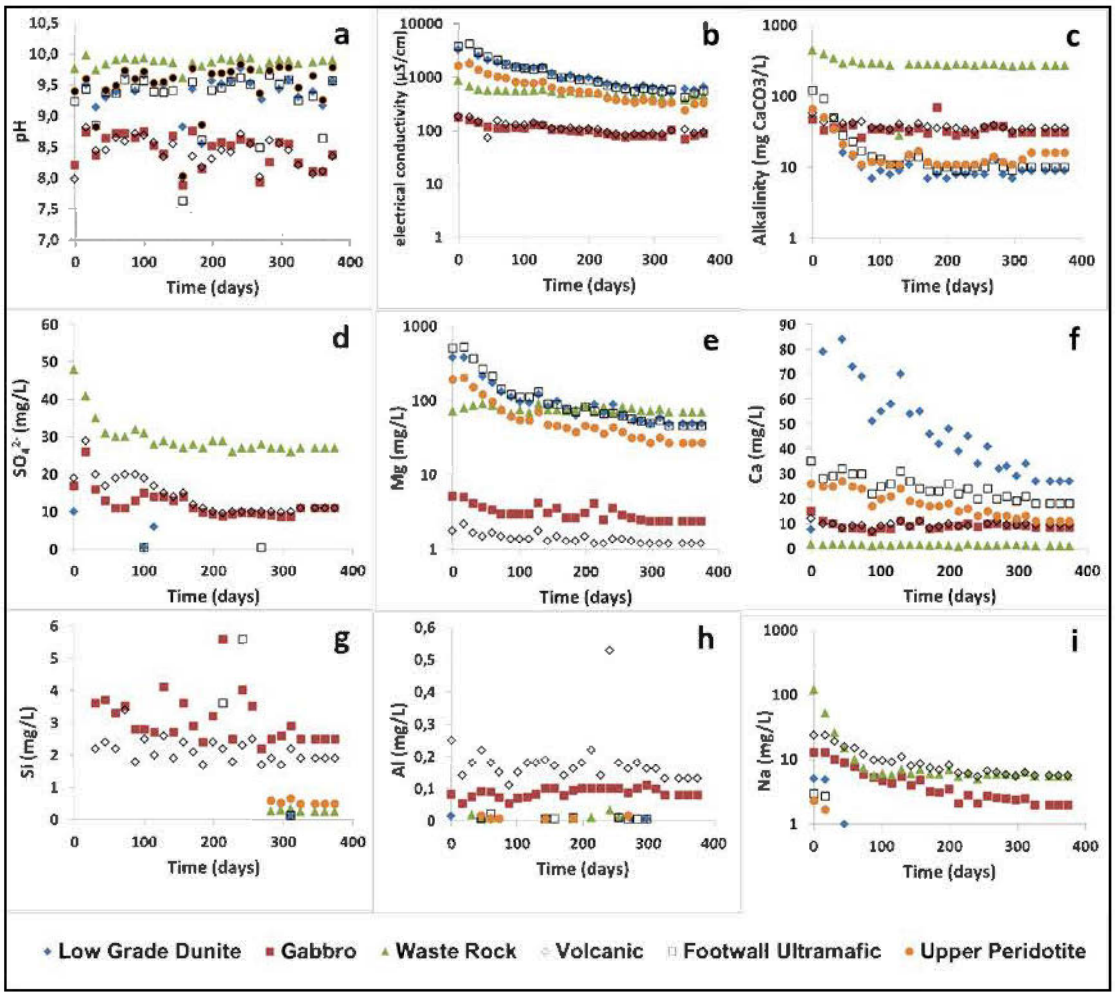

Figure 3.3 Evolution of (a) pH, (b) conductivity, (c) alkalinity, (d) sulfates, (e) Mg, (f) Ca, (g) Si, (h) Al, and (i) Na concentrations in kinetic column tests for six Dumont samples. Note the log scale for electrical conductivity, alkalinity, Mg, and Na

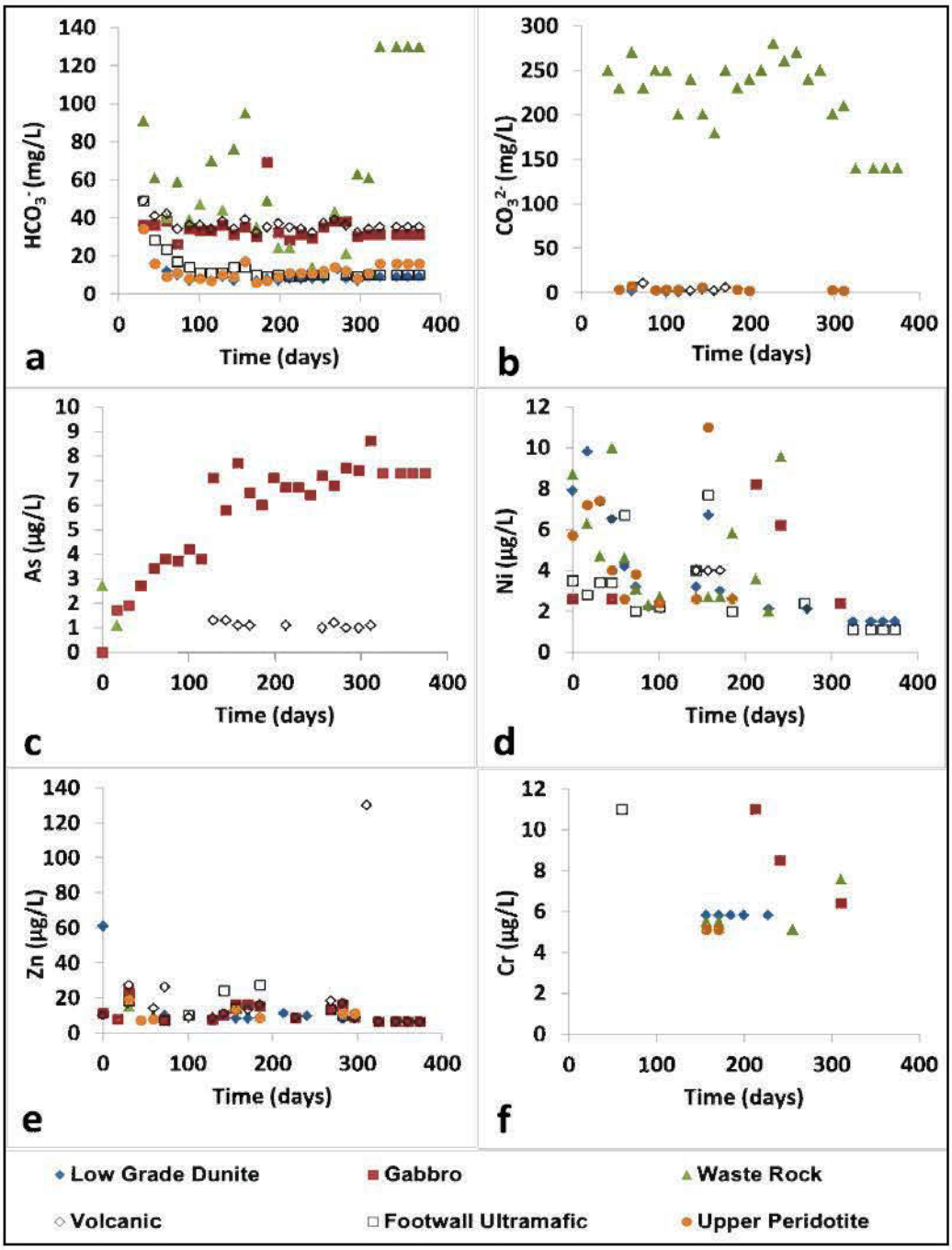

Figure 3.4 Evolution of (a) HCO_3^-, (b) CO_3^{2-}, (c) As, (d) Ni, (e) Zn, and (f) Cr concentrations in kinetic column tests for six Dumont samples

Sulfate was only detected in the leachates from the waste rock, gabbro, and volcanic samples. The highest concentrations were detected for waste rock leachates (25-50 mg/L), while the gabbro and volcanic samples generated sulfate at similar, but lower, concentrations (10-30 mg/L). The sulfate concentrations stabilized after 100 days for all samples. Many results (e.g. electrical conductivity, alkalinity, sulfate, Mg, Al, and Na) showed higher values in the first flushes of kinetic testing followed by a rapid decrease and stabilizing to lower values. This phenomenon was also observed in several previous studies and was explained by a combination of factors: the early dissolution of fine particles, the rapid dissolution of the most reactive phases, and the passivation of sulfide minerals (e.g., Plante et al. 2011; Hakkou et al. 2008; Benzaazoua et al. 2004; Scharer et al. 1991; Furrer and Stumm 1986). The Dumont samples contained sulfur at trace levels (below 800 ppm) and sulfates (from sulfate-bearing minerals) were detected only in the waste rock, gabbro, and volcanic samples, while concentrations were below the detection limit (< 5 ppm) for the other samples (upper peridotite, low-grade dunite, and footwall ultramafic). The higher concentrations of sulfate in the waste rock leachates are explained by its finer grain-size distribution (Table 3.2).

Another possible reason for the higher sulfate concentrations in the waste rock leachates may be due to their higher sulfate (from sulfate-bearing minerals) content (100 mg/kg) in the solids compared to the gabbro and volcanic samples (10 mg/kg). In the gabbro and volcanic leachates, the cumulative-normalized loadings of sulfate (30-40 mg/kg) exceeded the sulfate content in the initial samples (10 mg/kg), which confirm that sulfate in the leachates come from both sulfide oxidation and dissolution of soluble sulfate-bearing minerals.

The cumulative-normalized loadings of sulfate in leachates were calculated by summing the punctual loadings of sulfate after each flush and dividing by the total sample mass. The same process was used for other elements such as Mg, Si, and Ca

(Figure 3.5). The slopes of the stabilized portion of theses curves give the elemental release rates (presented in Table 3.4). The release rates (in mol/m^2/s) were normalized by the estimated SSA values of each sample. Acid generated by sulfide oxidation and by the dissolution of CO_2 was neutralized by brucite and silicate minerals. Serpentine and brucite were the phases that were most likely to neutralize acid, and their weathering was highlighted by the fact that Mg was the dominant element in the leachates of the ultramafic samples. The weathering of serpentine minerals is known to be incongruent (Thom et al. 2013; Lin and Clemency 1981; Luce et al. 1972), preferentially releasing Mg over Si, especially at high pH (Daval et al. 2013). In the early dissolution step, there is a rapid exchange of Mg^{2+} and H^+ at the surface. However, the dissolution of serpentine is expected to become near-congruent in the long-term (Luce et al. 1972). This may explain the fact that Si was only detected in the ultramafic samples after about 280 days, suggesting that serpentine started to release Si late in the kinetic tests. The stoichiometric ratio of Mg and Si in serpentine is ~1.5 and contrast with the high Mg/Si shown in Table 3.4, which range between 114 and 12780 for ultramafic materials. The higher ratios obtained in the ultramafic material leachates is caused by the incongruent dissolution of serpentine, which leads to the formation of a silica-rich layer (Luce et al. 1972). The reaction of serpentine with H^+ is given in Equation 3.1:

$$Mg_3Si_2O_5(OH)_4 + 6H^+ \rightarrow 3Mg^{2+} + 5H_2O + 2SiO_2 \qquad (3.1)$$

Serpentine minerals (lizardite, antigorite, and chrysotile) and brucite consume CO_2: the global reaction for serpentine is given in Equation 3.2 as an example. The same process was suggested to induce the dissolution of chrysotile and CO_2 in mine wastes at the Ekati Diamond mine in Canada (Rollo and Jamieson 2006).

$$5Mg_3Si_2O_5(OH)_4 + 12H_2CO_3 + 13H_2O \rightarrow 3Mg_5(OH)_2(CO_3)_4 \cdot 4H_2O + 10H_4SiO_4 \qquad (3.2)$$

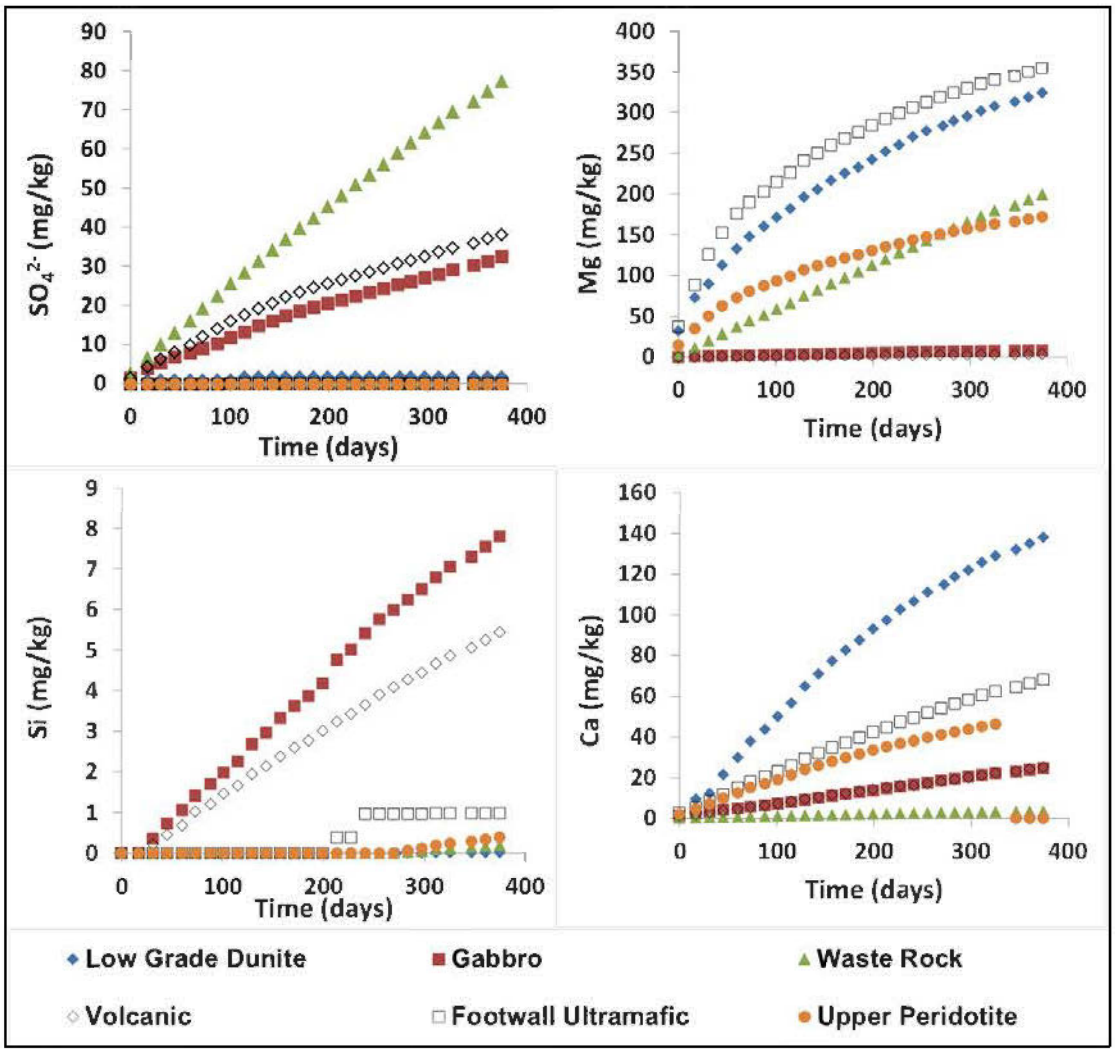

Figure 3.5 Cumulative and normalized column loadings for SO_4, Mg, Si, and Ca

The rate of brucite dissolution is higher than that of serpentine (Pokrovsky and Schott, 2004; Paktunc, 1999; Lin and Clemency 1981), and thus, its contribution to Mg in the leachates is greater than that of serpentine (Pronost et al. 2011) and explains the higher Mg/Si ratios obtained in the leachates. In the gabbro and volcanic leachates, the presence of Mg, Ca, K, Al, and Si demonstrated the dissolution of other

silicate minerals. In addition to brucite and serpentine, Mg can be generated by the dissolution of hornblende, chlorite, and diopside. In the waste rock sample, diopside can release Mg, but in lesser amounts than brucite. Albite (plagioclase) (Blum and Stillings, 1995), diopside (pyroxene), hornblende (amphibole) (Schott et al. 1981), and epidote dissolve nonstoichiometrically, releasing cations (Mg, Ca, or Al) preferentially over silica in the leachates. This behavior is generally accepted for the majority of silicates (White 2003; White and Brantley 1995).

The Dumont samples had low sulfide contents and sulfate (from sulfate-bearing minerals) was present in traces and was below the detection limit (< 5 ppm) in some of the samples (upper peridotite, low-grade dunite, and footwall ultramafic). Sulfate was also absent from the low-grade dunite, upper peridotite, and footwall ultramafic leachates. Based on the low sulfide and sulfate contents of the materials and on the low sulfate values generated in the leachates, it appears that metal release from sulfide oxidation is not a major concern in the Dumont wastes. Thus, extensive dissolution of serpentine and brucite, as shown by the high concentrations of Mg in the leachates, appears to be primarily driven by the carbonic acid derived from CO_2 dissolution in the pore-water of the ultramafic columns (waste rock, low-grade dunite, upper peridotite, and footwall ultramafic) which in turn enhanced the dissolution of brucite and serpentine to produce Mg-carbonates (Gras *et al.* 2017; Rollo and Jamieson 2006). Mg in the gabbro and volcanic leachates was significantly lower than those of the ultramafic samples, due to the absence of serpentine and brucite.

It is possible to estimate the brucite and serpentine weathering rates (Table 3.4) based on the Mg and Si release rates in the leachates. However, the rates estimated in the present study are conservative because: 1) part of the released Mg precipitate as secondary minerals; 2) it is impossible to discriminate the specific contributions of brucite and serpentine to the Mg released in the leachates; and 3) the Si is released incongruently from serpentine weathering. The estimated brucite weathering rates

(based on Mg release rates) range from 4.2×10^{-11} to 1.2×10^{-10} mol/m^2/s. These rates are within the lower range of dissolution rates (between 10^{-8} and 10^{-11} mol/m^2/s at alkaline pH) reported for brucite by Pokrovsky and Schott (2004), probably because of Mg precipitation. The serpentine weathering rates (based either on the Mg or Si release rates) range between 10^{-11} mol/m^2/s (based on Mg) and 10^{-13} to 10^{-15} mol/m^2/s (based on Si), also within the lower range of those with found in the literature (10^{-11} to 10^{-13} mol/m^2/s; Daval *et al.* 2013; Thom *et al.* 2013), because of Mg and Si precipitations, or because of the incongruent release of Si.

Table 3.4 Calculated elemental release rates (in mol/m^2/s), serpentine dissolution rates based on Mg and Si, brucite release rates based on Mg, and the ratio between Mg/Si (n/d: not determined; r: release rate)

	Ultramafic waste rock	Upper peridotite	Footwall ultramafic	Low-grade dunite	Gabbro	Volcanic (Basalt)
Mg	4.2×10^{-11}	9.3×10^{-11}	1.2×10^{-10}	1.1×10^{-10}	5.2×10^{-12}	2.1×10^{-12}
Ca	4.4×10^{-13}	2.2×10^{-11}	2.4×10^{-11}	3.9×10^{-11}	9.7×10^{-12}	9.1×10^{-12}
Si	4.2×10^{-14}	2.9×10^{-13}	1.0×10^{-12}	8.7×10^{-15}	4.7×10^{-12}	3.0×10^{-12}
SO_4	3.9×10^{-12}	n/d	n/d	n/d	4.5×10^{-12}	4.5×10^{-12}
Mg/Si	1005	326	115	12780.1	1.1	0.7
Serpentine dissolution rates (based on the Mg and Si release rates) *						
r(Mg)	1.4×10^{-11}	3.1×10^{-11}	4.0×10^{-11}	3.7×10^{-11}	n/d	n/d
r(Si)	2.1×10^{-14}	1.4×10^{-13}	5.2×10^{-13}	4.4×10^{-15}	n/d	n/d
Brucite dissolution rates**						
r(Mg)	4.2×10^{-11}	9.3×10^{-11}	1.2×10^{-10}	1.1×10^{-10}	n/d	n/d

*Assuming that all Mg and Si come from serpentine dissolution exclusively
** Assuming that all Mg comes from the dissolution of brucite exclusively

Thermodynamic equilibrium calculations

Thermodynamic equilibrium calculations performed using data from the column leachates (Figure 3.6) suggest that various anhydrous carbonates in the ultramafic materials (waste rock, low-grade dunite, upper peridotite, and footwall ultramafic) are

saturated, including: magnesite, calcite [$CaCO_3$], aragonite [$CaCO_3$], dolomite [$CaMg(CO_3)_2$], and huntite [$CaMg_3(CO_3)_4$]. However, higher saturation indices were calculated for hydromagnesite [$4MgCO_3 \cdot Mg(OH)_2 \cdot 4H_2O$] and artinite [$Mg_2CO_3(OH)_2 \cdot 3H_2O$], while nesquehonite [$MgCO_3 \cdot 3H_2O$] or [$Mg(HCO_3)(OH) \cdot 2H_2O$] and lansfordite [$MgCO_3 \cdot 5H_2O$] were always suggested to be undersaturated during the tests for all samples. For the gabbro and volcanic samples, only hydromagnesite and artinite are suggested to be saturated. A previous study on the Dumont tailings (Kandji *et al.* 2017) showed that magnesite was suggested to precipitate, while hydromagnesite and nesquehonite were not saturated. However, the XRD and SEM characterizations showed that hydrated Mg-carbonates precipitated rather than magnesite, because its precipitation is kinetically limited (Gautier *et al.* 2014; Saldi *et al.* 2009; Hänchen *et al.* 2008), as is also the case for dolomite. Artinite is a low temperature magnesium carbonate (Langmuir, 1965) and its formation is expected at temperatures below 15°C (Königsberger *et al.* 1999).

In the waste rock sample, barite ($BaSO_4$) was calculated to be saturated or close to saturation (SI: -0.4 to 0.1), as for gabbro and volcanic samples (SI: -0.5 to 0.2). The high pH values prevailing in the leachates promoted the precipitation of many metals as oxyhydroxides; Ni hydroxide [$Ni(OH)_2$] was suggested to be saturated or close to saturation for all samples (SI: -10.8 to 0.8). No Fe-minerals were also suggested to be saturated, as Fe was not detected in the leachates and, thus, not included in the thermodynamic equilibrium calculations. However, Fe-hydroxides have very low solubility, especially at high pH, so its precipitation is still possible despite the fact that Fe concentrations in solution are below the detection limit. Precipitation of barite or any Fe and Ni-secondary minerals were not confirmed by XRD and mineralogical observations, because their presence in the materials is too scarce. Indeed, the main source of Fe and Ni are the very low sulfide contents and oxidation rates occurring in the materials, which generate concentrations of secondary minerals too scarce for their detection, even under the SEM.

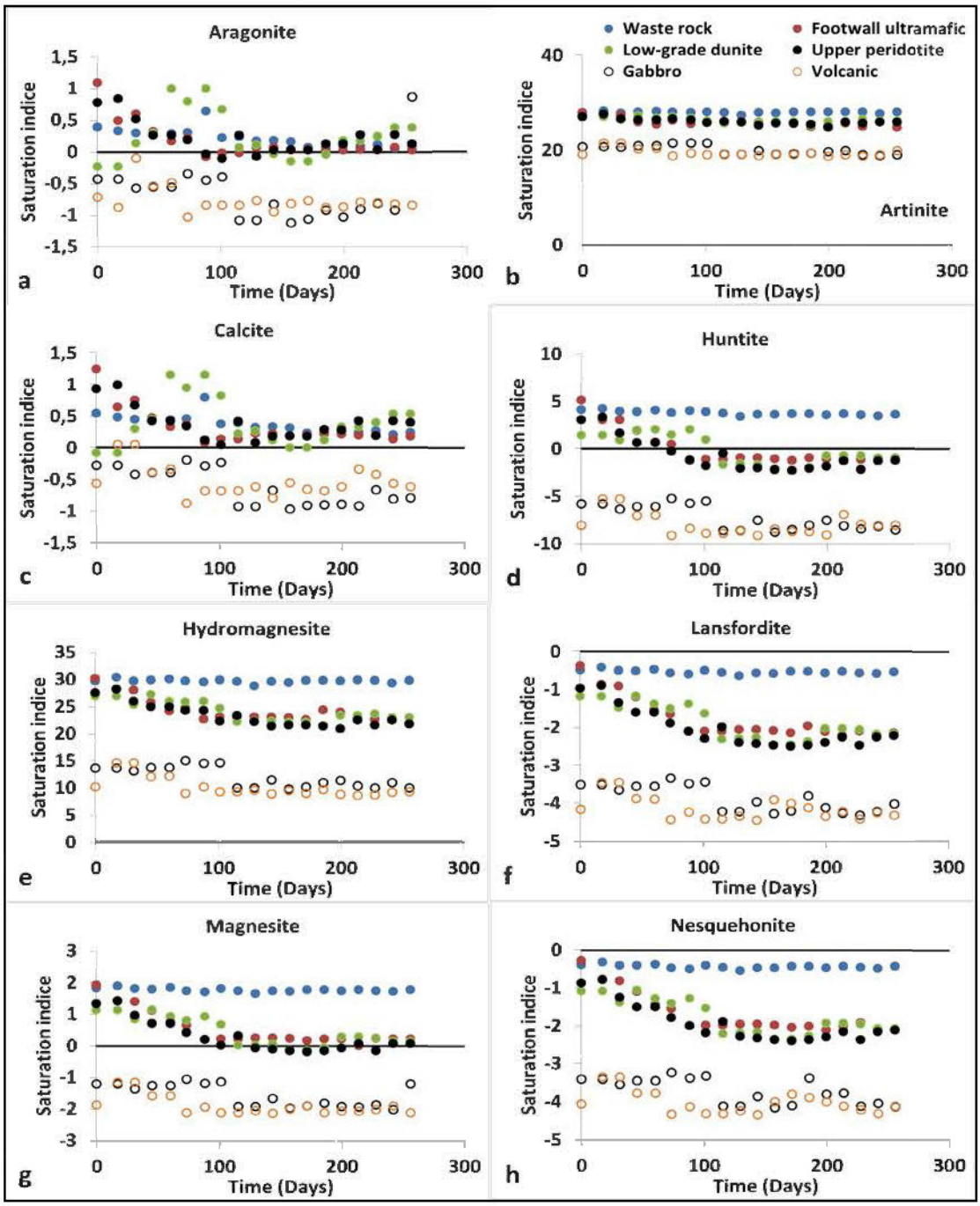

Figure 3.6 Evolution of the saturation index (SI) of selected minerals for: (a) waste rock, (b) upper peridotite, (c) footwall ultramafic, and (d) low-grade dunite

3.3.2 Post kinetic tests characterization results

At the end of the kinetic tests, the columns were dismantled in different layers (Figure 3.7) and were characterized to validate geochemical calculation results and better understand the geochemical behavior of the materials. Samples from each layers were analyzed to determine the total carbon contents (Table 3.5). An enrichment was observed at the surface of the ultramafic materials, while for the gabbro and volcanic samples, the increase in total carbon was considered negligible. This increase was more significant for the < 2 mm fraction, suggesting that the precipitates were formed preferentially from the reaction of finer particles, or that the precipitates were relatively fine grained. For the layers deeper than 10 cm, the increase of total carbon was negligible (not shown); this suggests that carbon fixation by the ultramafic materials was relatively fast, since CO_2 was sequestered before it migrated deeper into the column. Similarly, accumulation of secondary carbonates was limited within the first 25 cm of the ultramafic tailings pile at Mount Keith (Wilson *et al.* 2014).

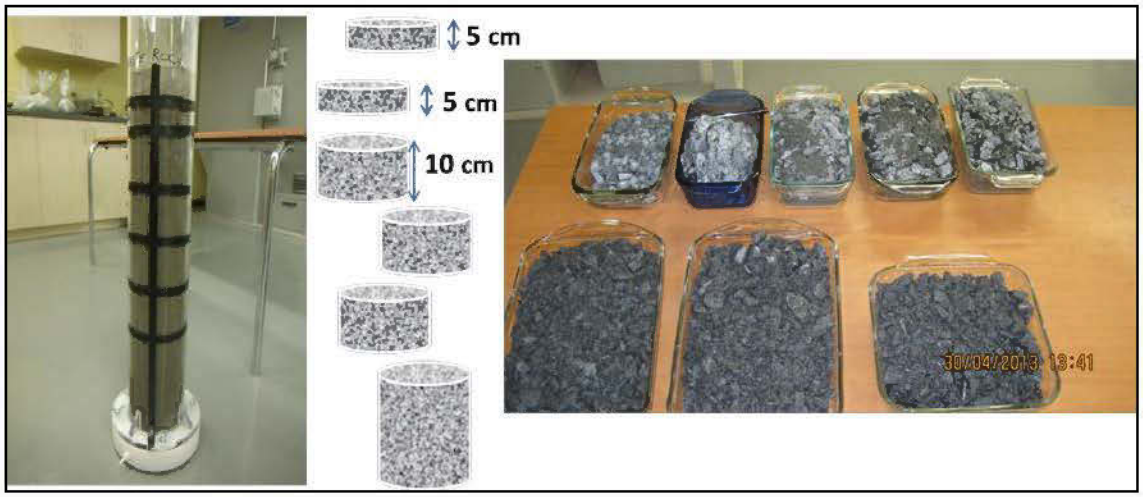

Figure 3.7 Post column test dismantling

The carbonation capacity calculated from the final carbon content gives approximately between 0.60 and 1.75 g of CO_2 per kg of waste per year. However,

when only the first 10 cm of the column is considered (the section exposed to atmospheric conditions the most), the calculated capacity is between 4.00 and 11.00 g of CO_2/kg of waste per year. It appears that the carbonation capacity of the ultramafic Dumont materials could be enhanced by maximizing its surface of exposition. Similarly, Wilson *et al.* (2014) suggested a low deposition rate of the Mount Keith ultramafic mine tailings in thin layers in order to increase their carbon sequestration potential. This approach is hardly feasible for coarse materials such as waste rock. However, the conventional approach of waste rock deposition could be an advantage, as the high porosity of conventional waste rock piles allow considerable gas and water transport (e.g., Amos *et al.* 2015). The typical example is the case of Thetford Mines wastes (Quebec, Canada), where diffuse warm air vents depleted in CO_2 were discovered (Pronost *et al.* 2012). Direct reaction between Mg-rich minerals and CO_2 in moist air was suggested to be a possible cause of CO_2 depletion in the air vents (Pronost *et al.* 2012). Finally, another drawback of the carbonation of ultramafic waste rock is the size distribution of the rock which varies from micrometers to meters.

Table 3.5 Carbon enrichment in the first 10 centimeters of the columns

	Ultramafic Waste Rock	**Upper Peridotite**	**Footwall Ultramafic**	**Low-grade Dunite**	**Gabbro**	**Volcanic (Basalt)**
Initial % C	0.17	0.16	0.12	0.12	0.13	0.80
Final % C (first layer)	0.48	0.30	0.23	0.24	0.16	0.98
Initial % C (< 2 mm)	0.19	0.18	0.15	0.14	0.17	1.2
Final % C (< 2 mm)	0.64	0.44	0.48	0.55	0.18	1.1

For the materials that sequestered CO_2, cementation was observed at approximately 5 cm below the surface (Figure 3.8). These clumps were hard, requiring a hammer to separate the particles. The same phenomenon has been observed at both active and

historical mine sites where the passive carbonation of ultramafic wastes takes place (Wilson *et al.* 2009a, 2009b; Beaudoin *et al.* 2008). In Thetford Mines, for example, chrysotile mine wastes were subjected to weathering for many decades and the waste surfaces were cemented by hydromagnesite (Beaudoin *et al.* 2008).

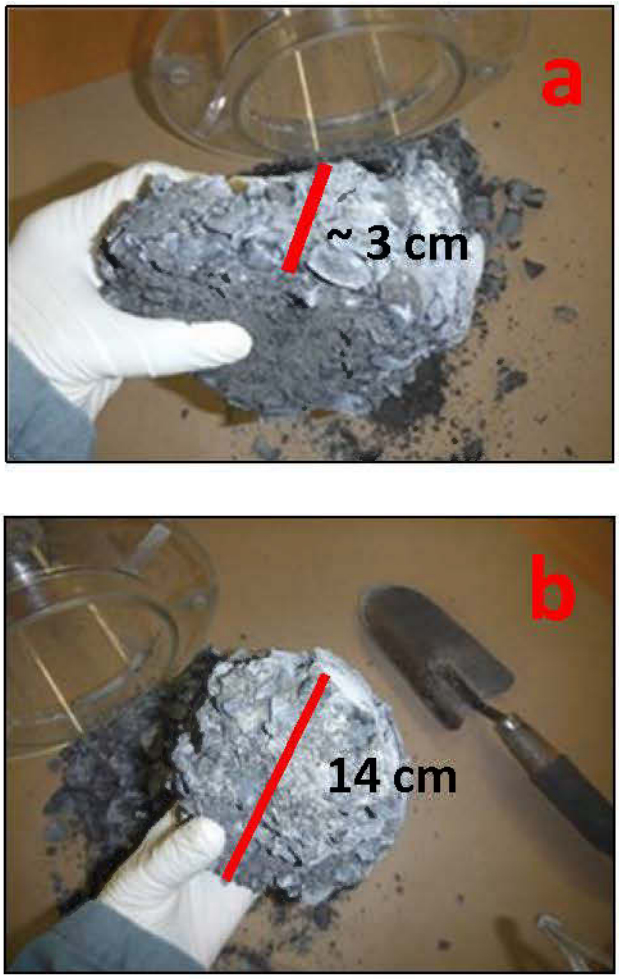

Figure 3.8 Cemented layer observed at approximately 5 cm below the surface of the columns of all ultramafic samples (waste rock, upper peridotite, footwall ultramafic, and low-grade dunite); (a) side view, (b) top view

The agglomerated particles were sampled and imaged by SEM, and were found to be cemented by secondary Mg-carbonates (Figure 3.9). The main carbonates showed

flaky-like structures typical of hydromagnesite or dypingite. These minerals (hydromagnesite and dypingite) had relatively similar habits and chemical compositions (Botha and Strydom 2001; Davies and Bubela 1973), and were, therefore, difficult to differentiate under the SEM.).

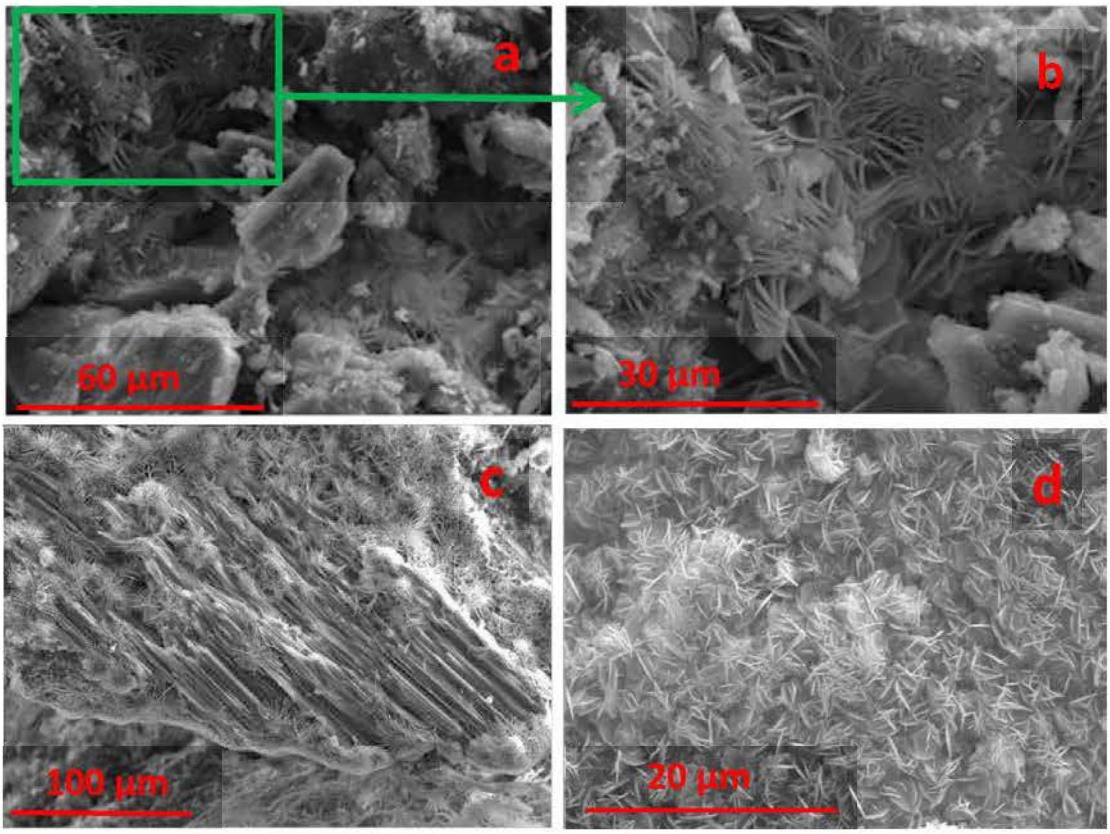

Figure 3.9 SEM images of secondary carbonates cementing the particles at the end of the column tests; (a) flaky secondary carbonates between primary particles, (b) enlargement of the area highlighted in (a), (c) flaky secondary carbonates covering a serpentine particle, (d) close-up view of flaky secondary carbonates covering a serpentine particle

XRD analyses were also performed on samples from the first 10 cm of the columns in order to identify possible secondary Mg-carbonates. The fraction below 2 mm was selected as it was richer in carbon; however, the XRD analyses were unable to

identify any Mg-carbonates, likely because their concentrations were below the detection limit. Indeed, the SEM observations suggest that the secondary carbonates are well crystallized; therefore, their detection with the XRD should be possible if their concentrations were high enough. Figure 3.10 shows the comparison of XRD patterns obtained from the fresh and weathered (fraction below 2 mm) samples of footwall ultramafic as an example. The XRD analyses also indicated that brucite is still present within the first 10 cm of the ultramafic materials after one year of kinetic testing. This may indicate that carbonation should continue at the surface and may explain the fact that after one year, the reaction front did not move downwards. Another constraint of carbonation ingress on the column may be due to the cementation at the column surface that reduced its permeability; other studies reported the ability of cemented layers in tailings impoundments to reduce oxygen transport into tailings (Kohfahl *et al.* 2010; Gilbert *et al.* 2003; Blowes *et al.* 1991).

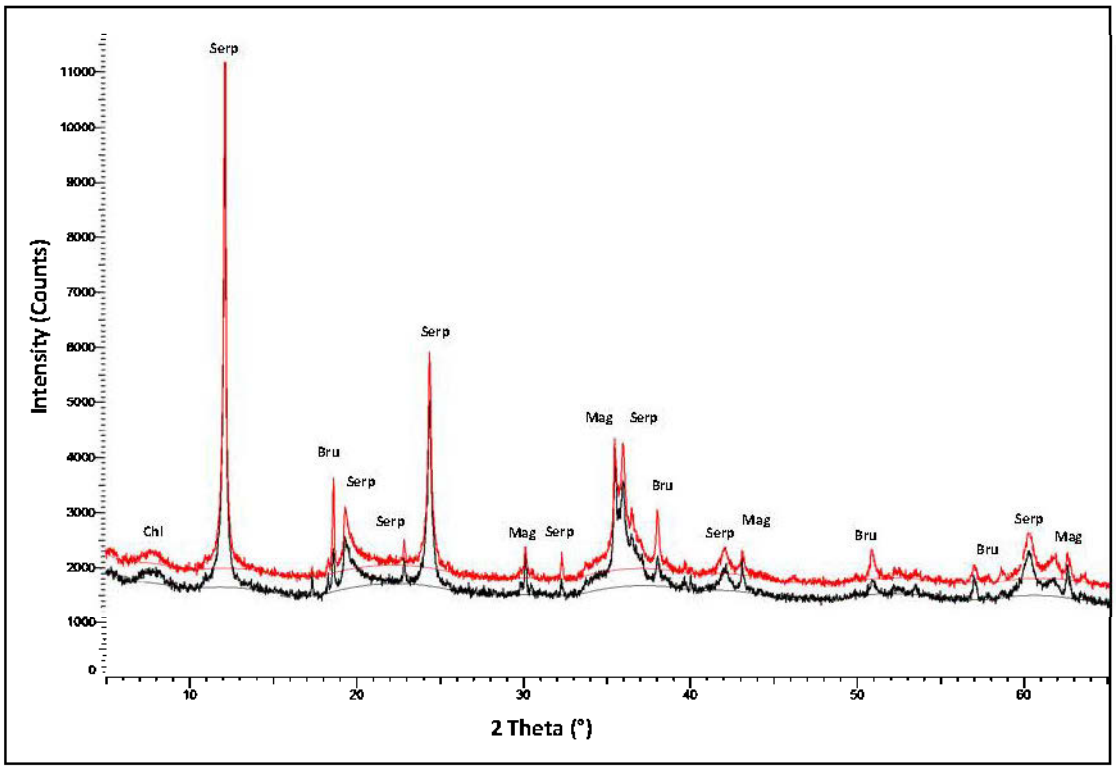

Figure 3.10 XRD patterns of fresh (red) and weathered (black) footwall ultramafic samples. Abbreviations refer to serpentine (Serp), magnetite (Mag), brucite (Bru), and chlorite (Chl)

The saturation degree (Sr) also has a significant effect on the passive carbonation of ultramafic mine wastes (Harrison *et al.* 2016, 2015; Assima *et al.* 2012). Low and high saturation degrees decrease the carbonation of ultramafic mine waste. The saturation degrees (Figure 3.11) were determined after dismantlement of the column tests (nearly 2 weeks after the last flush, thus at equilibrium with the atmosphere). Results indicate that both the top and the bottom of the column are unsaturated, the top of the column being dryer than the bottom. The Sr is below 20 % for all samples but the waste rocks, for which the Sr is between 10 % (Top) and 50 % (bottom). This difference in the Sr between materials is due to the fact that the waste rock sample contains more fine particles (Figure 3.2). This range of saturation degrees within the

columns is favorable to carbonation (Harrison *et al.* 2015; Assima *et al.* 2012). The fact that no significant carbon enrichment was noticed below 10 cm from the surface of the waste rocks suggests that the CO_2 was consumed readily at the top of the column by brucite.

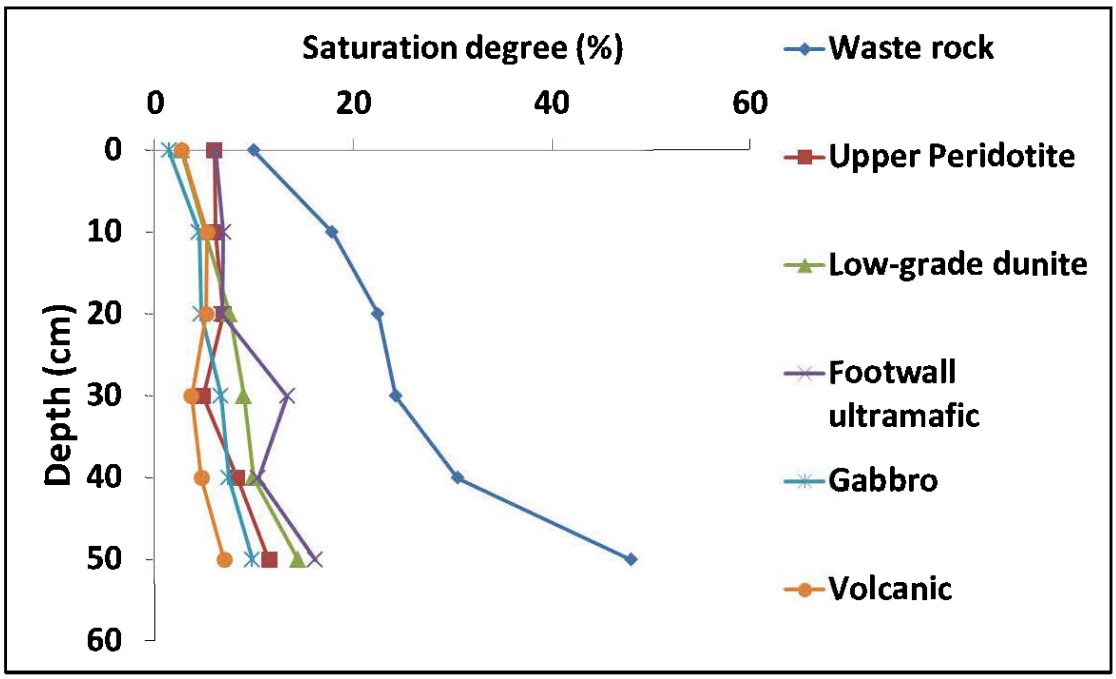

Figure 3.11 Water saturation profile upon column dismantling

DRIFT characterization

Initial samples and samples from the surfaces of each column after dismantlement were submitted to DRIFT analyses in order to highlight the Mg carbonate growth (Figure 3.12). Only the range from 1200 to 1900 cm^{-1} was considered here, as it contained the main absorption bands characteristic of the asymmetric CO_3^{2-} stretching vibrations modes (v_3) (White 1971). For the weathered ultramafic samples, broad bands (~1428 and ~1485 cm^{-1}) appeared upon weathering. For the gabbro and volcanic samples, there were negligible changes on the carbonates band. The broad

bands for volcanic samples (fresh and weathered) were similar to the ν_3 absorption band of calcite, which confirms the presence of calcite in the initial volcanic sample.

For samples that sequestered CO_2, the couplet of bands located at ~1428 and ~1484 cm^{-1} appearing in the DRIFT spectrum of weathered materials can be assigned to the asymmetric CO_3^{2-} stretching vibration modes of secondary carbonates, which are close to those reported for hydromagnesite and dypingite (1420 – 1480 cm^{-1}) (Hopkinson *et al.* 2008; Botha and Strydom 2003; Canterford and Tsambourakis 1984; White 1971; Raade 1970). The spectra reported here are also similar to those observed by Zarandi *et al.* (2017) in long-term carbonation experiments on the Dumont tailings (two years of watering and drying under ambient temperature).

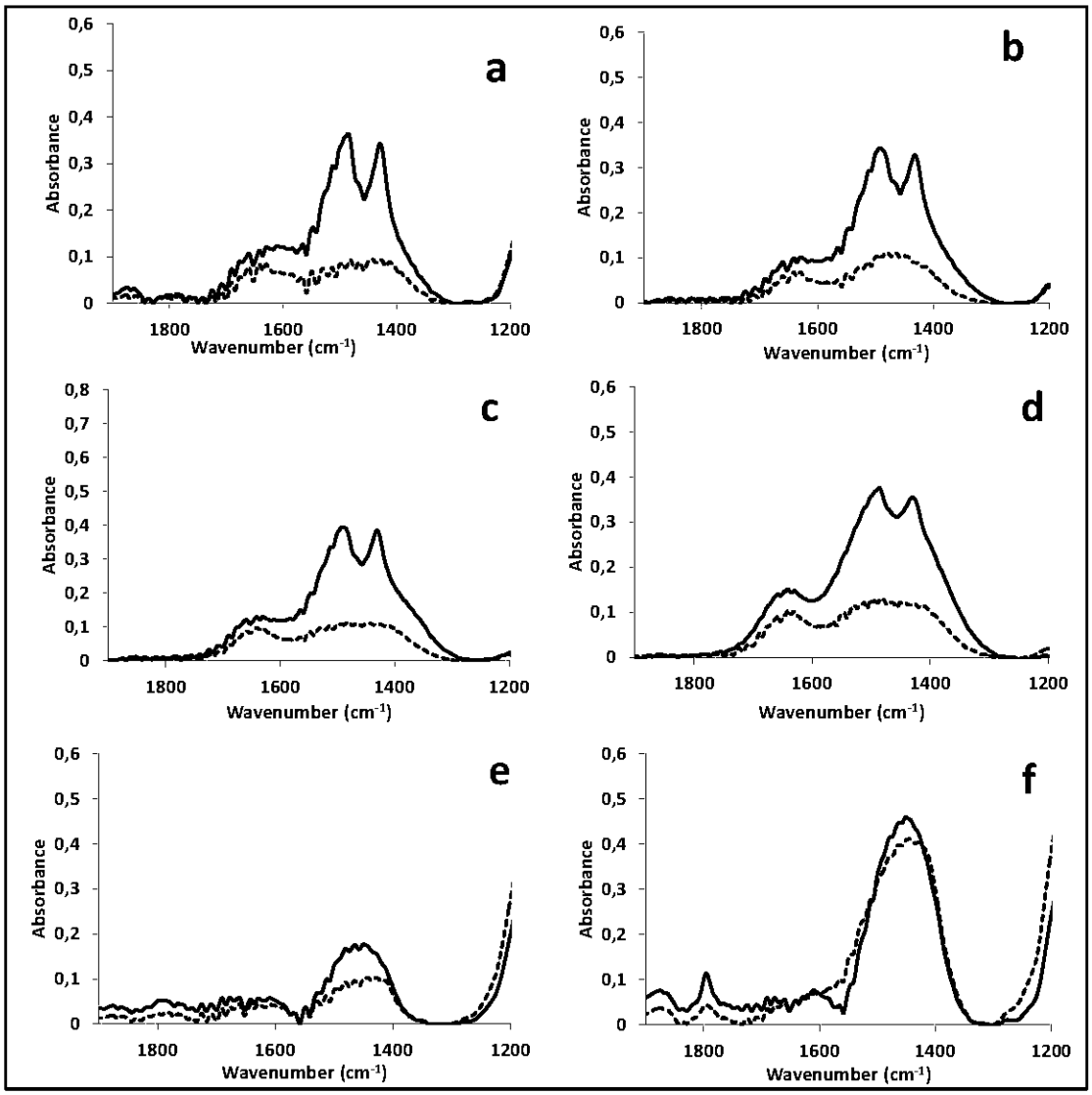

Figure 3.12 Partial DRIFT spectra of fresh (dashed line) and weathered (solid line) samples: (a) waste rock, (b) upper peridotite, (c) footwall ultramafic, (d) low-grade dunite, (e) gabbro, and (f) volcanic

Figure 3.13 compares the spectra obtained from the footwall ultramafic samples (fresh and weathered) versus the reference spectra of nesquehonite, magnesite, and hydromagnesite taken from the RRUFF online database (in the 1200 and 1900 cm^{-1} range). Some studies have investigated the transformation of nesquehonite into

hydromagnesite (Morgan *et al.* 2015; Botha and Strydom 2003, 2001; Davies and Bubella 1973). These studies show that the asymmetric CO_3^{2-} stretching mode (ν_3) of nesquehonite initially appears as a broad band split into three peaks (1408, 1471, and 1515 cm^{-1}) that merge during its transformation into hydromagnesite (Morgan *et al.* 2015; Botha and Strydom 2003, 2001). During this transformation, appearance of some transitional hydrated Mg-carbonates, such as dypingite, was observed (Morgan *et al.* 2015; Botha and Strydom 2003, 2001). Unfortunately, no DRIFT spectrum of dypingite was found, but it was reported to be similar to that of hydromagnesite (Hopkinson *et al.* 2008 White 1971; Raade 1970). The DRIFT spectra observed by Morgan *et al.* (2015) showed that during the decomposition of nesquehonite, these three peaks, observed initially for nesquehonite, merged into two closest peaks as observed in the present study. Observation of the three peaks of nesquehonite show that they tended to merge again to give only one peak as for the reference spectra of hydromagnesite taken from the RRUFF database (Figure 3.13), which probably represents a well-crystallized carbonate, as well as the spectra obtained by White (1971). However, Raade (1970) and Botha and Strydom (2003) observed a couplet of peaks for a hydromagnesite at 1420 and 1484 cm^{-1} for the asymmetric CO_3^{2-} stretching vibration modes and not only a single peak as for the reference hydromagnesite presented in Figure 3.13. Botha and Strydom (2003) stated that this split is characteristic of the presence of the bicarbonate ion rather than the carbonate ion in the hydromagnesite structure.

Davies and Bubella (1973) found that synthesized nesquehonite easily transforms (within few days) in water at 52°C to hydromagnesite and to another Mg-carbonate with a diffraction pattern close to dypingite. Nesquehonite forms at ambient temperature and seems to be stable below at least 50°C (Ballirano *et al.* 2010; Zhang *et al.* 2006; Botha and Strydom 2001; Davies and Bubella 1973; Langmuir 1965). However, hydromagnesite is more common at the earth's surface than nesquehonite, since it is more stable (Langmuir 1965). This suggests that the transformation of

nesquehonite into hydromagnesite can occur over time under ambient conditions. There is also evidence of this transformation occurring under ambient conditions in natural environments such as the Atlin hydromagnesite-magnesite playas in Canada (e.g., Power *et al.* 2007, 2009). However, nesquehonite and lansfordite were found to precipitate and persist at the Feregan chromite mine shafts, Norway (Beinlich and Austrheim 2012), as well as in Diavik and Clinton Creek, Canada (Wilson *et al.* 2010, 2009a, b), where temperatures are low (below 12°C in Feregan; Diavik and Clinton Creek have subarctic climates). Moreover, carbonation of the Dumont tailings performed under controlled conditions with eudiometer tests (Pronost et al. 2011) and reactors (Zarandi *et al.* 2016; Assima *et al.* 2014c) resulted mainly in the precipitation of nesquehonite and dypingite rather than hydromagnesite. However, it should be mentioned that these experiments were conducted in a very short-term (less than 48 hours) compared to the one-year column tests used in the present study. More recently, Zarandi *et al.* (2017) reported evidence of nesquehonite transformation into hydromagnesite and dypingite on the surface of already carbonated layers of Dumont tailings submitted to wetting and drying episodes. Dypingite has also been observed to form directly at ambient conditions (e.g., Wilson *et al.* 2010). Thus, it can be hypothesized that during the kinetic column tests, nesquehonite or dypingite first formed during earlier stages and converted into hydromagnesite or another intermediate, with the bicarbonate ion in the structure of the carbonate mineral.

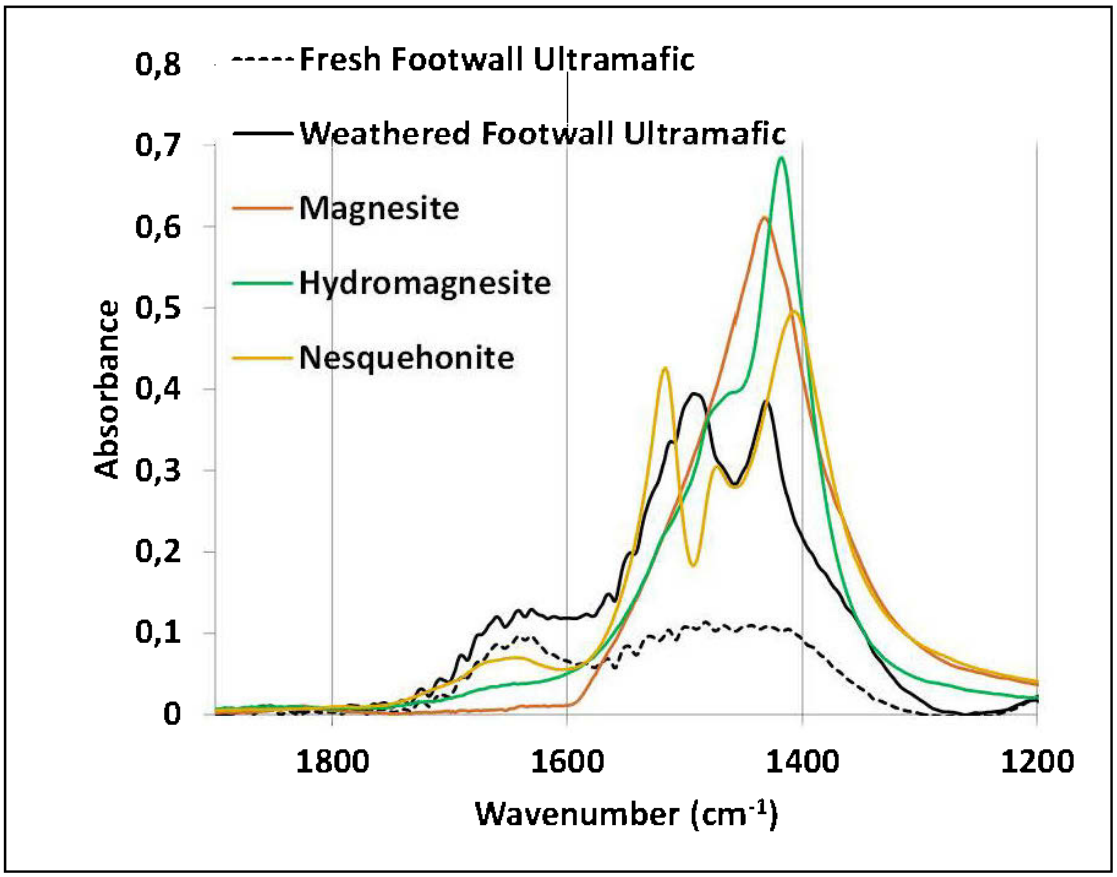

Figure 3.13 Magnesite, hydromagnesite, and nesquehonite partial DRIFT spectra taken from the RRUF online database compared to the footwall ultramafic spectra

Effect of mineral carbonation on water quality

Accumulation of nesquehonite in the ultramafic mine wastes of the Diavik mine (Canada) was suggested to induce an increase of its neutralization potential (NP; Wilson *et al.* 2009b). However, it should be noted that the Kimberlite wastes from Diavik, in contrast to the Dumont wastes, did not contain brucite. The minerals responsible for nesquehonite precipitation at Diavik were serpentine and forsterite, which are less reactive than common carbonates such as calcite (Paktunc, 1999). It is thus logical to expect an increase in the NP of mine wastes containing minerals like

serpentine and forsterite, which could even contribute to increase the lag time before AMD generation in potentially acid-generating materials. However, brucite is the primary mineral involved in the carbonation of the Dumont wastes (Assima *et al.* 2014c; Pronost *et al.* 2011). The replacement of brucite by secondary magnesium carbonates should theoretically not induce a net increase of NP, since brucite is more reactive than carbonates (Paktunc, 1999).

In addition to favoring metal oxyhydroxide formation, the secondary carbonates formed probably reduced metal mobility by adsorption and ionic exchange (Hamilton *et al.* 2017), although they were not detected in the secondary carbonates of the present study because of the low concentrations of metals generated by sulfide oxidation. Overall, the low metal concentrations in the Dumont wastes leachates are explained by 1) low sulfide oxidation rates; 2) oxyhydroxide precipitation of the leached metals ay these pH values; and 3) adsorption/ionic exchange of the leached metals on the secondary carbonates formed upon CO_2 sequestration. The main concern for the Dumont waste leachates is their pH values (9 – 10), which sometimes exceed the 9.5 limit that is required in Québec (Directive 019) and Canada (Metal Mining Effluent Regulations).

3.4 Conclusion

Kinetic column tests were conducted to evaluate the geochemical weathering of ultramafic and non-ultramafic mine waste rocks of a future open-pit mine for the Dumont deposit. The Dumont ultramafic mine wastes have a significant potential to sequester CO_2 in the form of stable Mg-carbonates.

Leachates generated by the wastes that sequestered CO_2 were alkaline (pH: 9 – 10) and were dominated by Mg, bicarbonate ions, Na, and Ca. On the contrary, the non-CO_2 sequestering gabbro and volcanic rock leachates had near-alkaline pH (8 – 8.5) with low amounts of Mg, Si, Ca, and Al. The high pH values prevailing in the

ultramafic leachates were due the extensive dissolution of brucite and, in turn, the alkaline pH and elevated Mg concentrations in the leachates were an indication of CO_2 capture through the precipitation of hydrated Mg-carbonates, as demonstrated by the post testing results. The low sulfide contents and its marginal oxidation were an indication that brucite and serpentine weathering were mainly driven by CO_2 dissolution in the pore waters. Serpentine showed an incongruent dissolution as suggested by the lack of Si in the leachates. Metals such as Ni, Al, and Zn were found in trace concentrations in the leachates and thermodynamic calculations suggest that metal hydroxides may form, although they were not directly observed because of their scarcity. The only parameter that could be of environmental concern in the leachates was the high pH, which reached values of up to 10.

The post characterization results showed a significant carbon increase in the solid samples for the ultramafic materials, while gabbro and volcanic showed a negligible increase of carbon contents. The hydrated Mg-carbonates were demonstrated to be dypingite or hydromagnesite. Cementation of the grains upon carbon sequestration was observed and might reduce wind erosion and dust generation from future waste rock piles and tailings ponds.

Although the sulfide concentration within the studied materials were low, the present study suggests that ultramafic materials generate high pH and alkalinity values that might be useful to mitigate or provide a longer lag time prior to AMD generation from more sulfidic mine wastes through an increase in NP. The high pH values generated by the weathering of ultramafic materials could also reduce metal leaching in near-neutral conditions by inducing the precipitation of a variety of metal oxyhydroxides of lower near-neutral solubility. In addition, the secondary carbonates generated will passivate the sulfide mineral surfaces, thus reducing the metal leaching and acid generation at the source, and retain a portion of the leached metals by adsorption and ionic exchange. Further studies on more sulfidic ultramafic mine

wastes are needed in order to clarify the influence of the mineralogical composition – namely the initial brucite content and the precipitation of secondary carbonates – on the extent of these potential benefits to mine water quality. The present study highlights the importance of taking into account the carbon sequestration potential in mine wastes in water quality predictions.

Acknowledgments

The authors thank RNC Minerals and the Natural Sciences and Engineering Research Council (NSERC) for their contributions to a Research and Collaborative Grant, the Research Institute in Mining and Environment (RIME-UQAT) and RNC Minerals staff. The URSTM (UQAT) staff is also acknowledged for their laboratory support during this project.

References

Amos, R.T., Blowes, D.W., Bailey, B.L., Sego, D.C., Smith, L., Ritchie, A.I.M. (2015). Waste-rock hydrogeology and geochemistry. Applied Geochemistry 57, pp 140-156.

Assima, G.P., Larach,i F., Beaudoin, G., Molson, J. (2014a). Impact of temperature and oxygen availability on the dynamics of ambient CO2 mineral sequestration by nickel mining residues. Chemical Engineering Journal, 240, pp 394–403

Assima, G.P., Larachi, F., Beaudoin, G., Molson, J. (2014b). Emulation of ambient carbon dioxide diffusion and carbonation within nickel mining residues. Minerals Engineering, 59, pp 39–44

Assima, G.P., Larachi, F., Molson, J., Beaudoin ,G. (2014c). Comparative study of five Québec ultramafic mining residues for use in direct ambient carbon

dioxidemineral sequestration. Chem Eng J 245, 56–64, http://dxdoiorg/101016/jcej201402010

Assima, G.P., Larachi, F., Beaudoin, G., Molson, J. (2013a.) Dynamics of carbon dioxide uptake in chrysotile mining residues – Effect of mineralogy and liquid saturation. International Journal of Greenhouse Gas Control, 12, pp 124–135

Assima, G.P., Larachi, F., Beaudoin ,G., Molson, J. (2012). CO2 Sequestration in Chrysotile Mining Residues: Implication of Watering and Passivation under Environmental Conditions. Industrial & Engineering Chemistry Research, pp 2–10

ASTM Standard D4892. (2014). Standard test method for density of solid pitch (Helium Pycnometer Method) West Conshohocken, PA, (http://wwwastmorg)

ASTM Standard D6913-04. (2009). Standard test methods for particle-size distribution (gradation) of soils using sieve analysis. Annual Book of ASTM Standards vol. 0409

Bales, R.C., Morgan, J.J., (1985). Dissolution kinetics of chrysotile at pH 7 to 10. Geochimica et Cosmochimica Acta, 49(11), pp 2281–2288

Ballirano, P., De Vito, C., Ferrini, V., Mignardi, S. (2010). The thermal behaviour and structural stability of nesquehonite, MgCO3·3H2O, evaluated by in situ laboratory parallel-beam X-ray powder diffraction: new constraints on CO2 sequestration within minerals. J Hazard Mater 178, 522–528

Bea, S.A., Wilson, S.A., Mayer, K.U., Dipple, G.M., Power, I.M., Gamazo, P. (2012). Reactive Transport Modeling of Natural Carbon Sequestration in Ultramafic Mine Tailings. Vadose Zone Journal, 11(2)

Beaudoin, G., Hébert, R., Constantin, M. (2008). Spontaneous carbonation of serpentine in milling and mining waste, southern Québec and Italy. Proceedings of

Accelerated Carbonation for Environmental and Materials Engineering (ACEME2008), pp 73–82

Beinlich, A. & Austrheim, H. (2012). In situ sequestration of atmospheric CO2 at low temperature and surface cracking of serpentinized peridotite in mine shafts. Chemical Geology, 332-333, pp 32–44

Bénézeth, P., Saldi, G. D., Dandurand, J. L., & Schott, J. (2011). Experimental determination of the solubility product of magnesite at 50 to 200 C. Chemical Geology, 286(1), 21-31

Benzaazoua, M., Bussière, B., Dagenais, A-M., Archambault, M. (2004). Kinetic tests comparison and interpretation for prediction of the Joutel tailings acid generation potential. Environmental Geology, 46(8 SPECISS), pp 1086–1101

Blowes, D. W., Reardon, E. J., Jambor, J. L., & Cherry, J. A. (1991). The formation and potential importance of cemented layers in inactive sulfide mine tailings. Geochimica et Cosmochimica Acta, 55(4), 965-978

Blum, A.E., Stillings, L.L. (1995)., Feldspar dissolution kinetics. Rev Mineral Geochem 31:291–351

Botha, A., Strydom, C.A. (2003). DTA and FT-IR analysis of the rehydration of basic magnesium carbonate. Journal of Thermal Analysis and Calorimetry, 71, pp 987–995

Botha, A., Strydom, C.A., (2001). Preparation of a magnesium hydroxy carbonate from magnesium hydroxide. Hydrometallurgy 62, 175–183

Canterford, J.H., Tsambourakis, G., Lambert, B. (1984). Some observations on the properties of dypingite, Mg5(CO3)4(OH)2·5H2O, and related minerals. Miner Mag 48 (1984) 437–442

Chapuis, R.P., and Légaré, P.P. (1992). A simple method for determining the surface area of fine aggregates and fillers in bituminous mixtures. Effects of aggregates and mineral filler on asphalt mixture performance, ASTM STP 1147, pp. 177-186

Daval, D., Hellmann, R., Martinez, I., Gangloff, S., & Guyot, F. (2013). Lizardite serpentine dissolution kinetics as a function of pH and temperature, including effects of elevated pCO 2. Chemical geology, 351, 245-256

Davies P.J., Bubela, B., (1973). The transformation of nesquehonite into hydromagnesite. Chemical Geology, 12(4), 289-300

Demers, I., Bussière, B., Benzaazoua, M., Mbonimpa, M., Blier, A., (2008). Column test investigation on the performance of monolayer covers made of desulphurized tailings to prevent acid mine drainage. Minerals Engineering 21, 317-329

Furrer, G., Stumm, W. (1986). The coordination chemistry of weathering: I. Dissolution kinetics of δ-Al 2 O 3 and BeO. Geochimica et Cosmochimica Acta, 50(9), 1847-1860

Gautier, Q., Bénézeth, P., Mavromatis, V., Schott, J. (2014). Hydromagnesite solubility product and growth kinetics in aqueous solution from 25 to 75 °C. Geochimica et Cosmochimica Acta, 138, pp 1–20

Gilbert, S. E., Cooke, D. R., & Hollings, P. (2003). The effects of hardpan layers on the water chemistry from the leaching of pyrrhotite-rich tailings material. Environmental Geology, 44(6), 687-697

Goff, F., Lackner, K.S. (1998). Carbon dioxide sequestering using ultramafic rocks. Environmental Geosciences, 5(3), 89-101

Gras, A., Beaudoin, G., Molson, J.W.H., Plante, B., Bussière, B., Lemieux, J.M., Dupont, P.P., (2017). Isotopic evidence of passive mineral carbonation in mine wastes from the Dumont Nickel Project (Abitibi, Quebec). To be published

Hakkou, R., Benzaazoua, M., Bussière, B., (2008). Acid mine drainage at the abandoned kettara mine (Morocco): 2. mine waste geochemical behavior. Mine Water and the Environment, 27(3), pp 160–170

Hamilton, J. L., Wilson, S. A., Morgan, B., Turvey, C. C., Paterson, D. J., MacRae, C., ... & Southam, G. (2016). Nesquehonite sequesters transition metals and CO 2 during accelerated carbon mineralisation. International Journal of Greenhouse Gas Control, 55, 73-81

Hänchen ,M., Prigiobbe, V., Baciocchi, R., Mazzotti, M., (2008). Precipitation in the Mg-carbonate system-effects of temperature and CO2 pressure. Chemical Engineering Science, 63(4), pp 1012–1028

Harrison, A. L., Dipple, G. M., Power, I. M., & Mayer, K. U. (2016). The impact of evolving mineral–water–gas interfacial areas on mineral–fluid reaction rates in unsaturated porous media. Chemical Geology, 421, 65-80

Harrison, A. L., Dipple, G. M., Power, I. M., & Mayer, K. U. (2015). Influence of surface passivation and water content on mineral reactions in unsaturated porous media: implications for brucite carbonation and CO 2 sequestration. Geochimica et Cosmochimica Acta, 148, 477-495

Harrison, A. L., Power,, IM., Dipple, G.M. (2012). Accelerated carbonation of brucite in mine tailings for carbon sequestration. Environmental science & technology, 47(1), 126-134

Hitch, M., Ballantyne, S.M, Hindle, S.R., (2010). Revaluing mine waste rock for carbon capture and storage. International Journal of Mining, Reclamation and Environment, 24(1), pp 64–79

Hopkinson, L., Rutt, K., Cressey, G., (2008). The transformation of nesquehonite to hydromagnesite in the system CaO-MgO-H2O-CO2: an experimental spectroscopic study. Journal of Geology, 116(4), pp 387–400

Kandji, E.H.B., Plante, B., Bussière, B., Beaudoin, G., Dupont, P.P. (2017) Kinetic testing to evaluate the mineral carbonation and metal leaching potential of ultramafic tailings: case study of the Dumont Nickel Project, Amos, Québec. To be published

Kohfahl, C., Graupner, T., Fetzer, C., & Pekdeger, A. (2010). The impact of cemented layers and hardpans on oxygen diffusivity in mining waste heaps A field study of the Halsbrücke lead–zinc mine tailings (Germany). Science of the total environment, 408(23), 5932-5939

Königsberger, E., Königsberger, L. C., & Gamsjäger, H. (1999). Low-temperature thermodynamic model for the system Na 2 CO 3− MgCO 3− CaCO 3− H 2 O. Geochimica et Cosmochimica Acta, 63(19), 3105-3119

Krevor, S., Lackner, K.S., (2011). Enhancing serpentine dissolution kinetics for mineral carbon dioxide sequestration. International Journal of Greenhouse Gas Control, 5(4), pp 1073–1080

Lackner, K.S., Wendt, C.H., Butt, D.P., Joyce, E.L., Sharp, D.H., (1995). Carbon dioxide disposal in carbonate minerals. Energy 20, 1153–1170

Langmuir, D., (1965). Stability of carbonates in the system MgO–CO2–H2O. The Journal of Geology, 730-754

Larachi, F., Daldoul, I., Beaudoin, G. (2010). Fixation of CO2 by chrysotile in low-pressure dry and moist carbonation: Ex-situ and in-situ characterizations. Geochimica et Cosmochimica Acta, 74(11), 3051-3075

Lawrence, R.W., Wang, Y. (1997). Determination of neutralization potential in the prediction of acid rock drainage. Proc, 4th International Conf on Acid Rock Drainage (ICARD) Vancouver, Canada, pp 451–464

Lechat, K., Lemieux, J.M., Molson, J., Beaudoin, G., Hébert, R. (2016). Field evidence of CO2 sequestration by mineral carbonation in ultramafic milling wastes, Thetford Mines, Canada. Int J Greenhouse Gas Control, 47 (2016), pp 110–121

Li, J., & Hitch, M. (2017). Structural and chemical changes in mine waste mechanically-activated in various milling environments. Powder Technology, 308, 13-19

Li, J., & Hitch, M. (2016a). Carbon dioxide adsorption isotherm study on mine waste for integrated CO 2 capture and sequestration processes. Powder Technology, 291, 408-413

Li, J., & Hitch, M. (2016b). Mechanical activation of ultramafic mine waste rock in dry condition for enhanced mineral carbonation. Minerals Engineering, 95, 1-4

Lin, F.C., Clemency, C.V. (1981). The dissolution kinetics of brucite, antigorite, talc, and phlogopite at room temperature and pressure. American Mineralogist, 66(7-8), pp 801–806

Luce, R.W., Bartlett, R.W., Parks, G.A. (1972). Dissolution Kinetics of Magnesium Silicates. Geochimica Et Cosmochimica Acta, 36(1), p35

Merkus, H. (2009). Particle size measurements: fundamentals, practice, quality. Particle Technology Series, 17(Springer), 519. http://doi.org/ISBN 978-1-4020-9016-5

Morgan, B., Wilson, S.A., Madsen, I.C., Gozukara, Y.M., Habsuda, J. (2015). Increased thermal stability of nesquehonite ($MgCO_3 \cdot 3H_2O$) in the presence of humidity and CO_2: Implications for low-temperature CO_2 storage. International Journal of Greenhouse Gas Control, 39, pp 366–376

Oskierski, H.C., Dlugogorski, B.Z., Jacobsen, G, (2013). Sequestration of atmospheric CO_2 in chrysotile mine tailings of the Woodsreef Asbestos Mine, Australia: Quantitative mineralogy, isotopic fingerprinting and carbonation rates. Chemical Geology, 358, pp 156–169

Paktunc, A. D. (1999). Characterization of mine wastes for prediction of acid mine drainage. In Environmental impacts of mining activities (pp. 19-40). Springer Berlin Heidelberg

Plante, B., Bussière, B., Benzaazoua, M. (2014). Lab to field scale effects on contaminated neutral drainage prediction from the Tio mine waste rocks. J Geochem Explor 137:37–47

Plante, B., Benzaazoua, M., Bussière, B. (2011). Predicting Geochemical Behaviour of Waste Rock with Low Acid Generating Potential Using Laboratory Kinetic Tests. Mine Water and the Environment, 30(1), pp 2–21

Pokrovsky, O. S., & Schott, J. (2004). Experimental study of brucite dissolution and precipitation in aqueous solutions: surface speciation and chemical affinity control. Geochimica et Cosmochimica Acta, 68(1), 31-45

Power, I., Harrison, A.L., Dipple, G.M., Wilson, S.A., Kelemen, P.B., Hitch, M., Southam, G. (2013). Carbon mineralization: From natural analogues to engineered systems. Reviews in Mineralogy & Geochemistry, Mineralogical Society of America, Vol. 77, pp. 305-360

Pronost, J., Beaudoin, G., Lemieux, J.-M., Hébert, R., Constantin, M., Marcouiller, S., Klein, M., Duchesne, J., Molson, J.W., Larachi, F., Maldague, X. (2012). CO2-depleted warm air venting from chrysotile milling waste (Thetford Mines, Québec, Canada): evidence for in situ carbon capture from the atmosphere. Geology 40, 275–278

Pronost ,J., Beaudoin, G., Tremblay, J., Larachi, F., Hébert, R., Constantin, M., Duchesne, J. (2011). Carbon sequestration kinetics and storage capacity of ultramafic mining waste. Environmental Science & Technology 45, 9413–9420

Raade G. (1970). Dypingite, a new hydrous basic carbonate of magnesium from Norway. American Mineralogist, 55: 1457-1465

Rietveld, H.M. (1993). The Rietveld method. Oxford University Press, (Oxford, UK)

RNC. (2013). Technical Report on the Dumont Ni Project, Launay and Trécesson Townships, Quebec, Canada

Robie, R. A., & Hemingway, B. S. (1995). Thermodynamic properties of minerals and related substances at 298.15 K and 1 bar (10^ 5 Pascals) pressure and at higher temperatures (No. 2131). USGPO; For sale by US Geological Survey, Information Services

Rollo, H.A., Jamieson, H.E. (2006). Interaction of diamond mine waste and surface water in the Canadian Arctic. Applied Geochemistry, 21(9), pp 1522–1538

Saldi, GD., Jordan, G., Schott, J., Oelkers, E.H. (2009). Magnesite growth rates as a function of temperature and saturation state. Geochim Cosmochim Acta 73, 5646–5657

Scharer, J.M., Garg, V., Smith, R., Halbert, B.E. (1991). Use of steady state models for assessing acid generation in pyritic mine tailings. Proceedings, 2nd ICARD, Montreal CANMET, Ottawa, Vol 2, pp 211–229

Schott J., Berner, R.A., Sjoberg, E.L. (1981). Mechanism of pyroxene and amphibole weathering–I experimental studies of iron-free minerals. Geochim Cosmochim Acta 45:2123–2135

Sciortino, M., Mungall, J.E., Muinonen, J. (2015). Generation of High-Ni Sulfide and Alloy Phases During Serpentinization of Dunite in the Dumont Sill, Quebec. Economic Geology, 110, pp 733–761

Sobek, A.A., Schuller, W.A., Freeman, J.R., Smith, R.M. (1978) Field and laboratory methods applicable to overburdens and mine soils. EPA-600/2-78-054 US Gov Print Office, Washington, DC

SRK. (1989). Draft Acid Rock Drainage Technical Guide, Vancouver, Canada

Thom, J. G., Dipple, G. M., Power, I. M., & Harrison, A. L. (2013). Chrysotile dissolution rates: Implications for carbon sequestration. Applied geochemistry, 35, 244-254

USEPA. (2006). MINTEQA2, Metal speciation equilibrium model for surface and ground water, version 3.1 Available at: https://vminteq.lwr.kth.se/

White, A.F. (2003). Natural weathering rates of silicate minerals In: Holland, HD, Turekian, KK (Ex Eds), Treatise on Geochemistry vol 5 Drever, JI (Ed) Surface and Ground Water, Weathering, and Soils, Elsevier, New York, 133–168

White, A.F., Brantley, S.L. (1995). Chemical Weathering Rates of Silicate Minerals. Rev Mineral, Mineralogical Society of America, vol. 31

White, W.B. (1971). Infrared characterization of water and hydroxyl ion in the basic magnesium carbonate. The American Mineralogist, 56(100), pp 46–53

Wilson, S.A., Harrison, A.L., Dipple, G.M., Power, I.M., Barker, S.L.L., Mayer, K.U., Fallon, S.J., Raudsepp, M., Southam, G. (2014.) Offsetting of CO2 emissions by air capture in mine tailings at the Mount Keith Nickel Mine, Western Australia: Rates, controls and prospects for carbon neutral mining. International Journal of Greenhouse Gas Control, 25, pp 121–140

Wilson, S.A., Barker, S.L., Dipple, G.M., Atudorei, V. (2010). Isotopic disequilibrium during uptake of atmospheric CO2 into mine process waters: Implications for CO2 sequestration. Environmental science & technology, 44(24), 9522–9529

Wilson, S. A., Dipple, G.M., Power, I.M., Thom, J.M., Anderson, R.G., Raudsepp, M., Gabites, J.E., Southam, G., (2009a) Carbon dioxide fixation within mine wastes of ultramafic-hosted ore deposits: Examples from the Clinton Creek and Cassiar Chrysotile deposits, Canada Economic Geology, 104(1), pp 95–112

Wilson, S.A., Raudsepp, M., Dipple, G.M. (2009b). Quantifying carbon fixation in trace minerals from processed kimberlite: A comparative study of quantitative methods using X-ray powder diffraction data with applications to the Diavik Diamond Mine, Northwest Territories, Canada. Applied Geochemistry, 24(12), pp 2312–2331

Zarandi, A. E., Larachi, F., Beaudoin, G., Plante, B., & Sciortino, M. (2017). Nesquehonite as a carbon sink in ambient mineral carbonation of ultramafic mining wastes. Chemical Engineering Journal, 314, 160-168

Zarandi A.E., Larachi, F., Beaudoin, G., Plante, B., Sciortino, M. (2016). Multivariate study of the dynamics of CO2 reaction with brucite-rich ultramafic mine tailings. International Journal of Greenhouse Gas Control, 52, 110-119

Zhang Z, Zheng Y, Ni Y, Liu Z, Chen J, Liang X (2006) Temperature And pH-dependent morphology and FT-IR analysis of magnesium carbonate hydrates. Journal of Physical Chemistry B, 110(26), pp 12969–12973

CHAPITRE IV

SCALE EFFECTS ON THE PREDICTION OF WATER DRAINAGE QUALITY OF ULTRAMAFIC MINE WASTE WITH CARBON SEQUESTRATION POTENTIAL

Cet article est en préparation pour être soumis au *Journal of Geochemical Exploration.*

Auteurs

Kandji, El Hadji Babacar (a), Plante, Benoit (a), Bussière, Bruno (a), Beaudoin, Georges (b), Dupont, Pierre-Philippe (c)

(a) Research Institute in Mining and Environment (RIME), UQAT (Université du Québec en Abitibi-Témiscamingue), 445 boulevard de l'Université, Rouyn-Noranda, Québec, J9X 5E4, Canada.

(b) Department of Geology and Geological Engineering, Université Laval, Québec, Québec G1V 0A6, Canada.

(c) Royal Nickel Corporation, Rue Trudel, Amos, Quebec, J9T 4N1, Canada

Résumé

La prédiction de la qualité de drainage des eaux de rejets miniers dans des conditions de laboratoire est particulièrement difficile en raison des nombreuses différences entre les conditions du terrain et du laboratoire. De plus, l'altération des rejets miniers peut être influencée par plusieurs processus qui peuvent avoir un impact significatif sur la qualité des eaux de drainage, tels que les phénomènes de sorption ou la précipitation des minéraux secondaires. C'est le cas des rejets ultramafiques qui possèdent un potentiel important de séquestration du CO_2. Cette étude vise à mieux comprendre les effets d'échelle sur le comportement géochimique de rejets miniers ayant un potentiel de séquestration de carbone. Afin d'atteindre cet objectif, différents essais cinétiques ont été effectués sur des rejets de concentrateur et des stériles au laboratoire (mini-cellules d'altération, cellules humides et essais en colonne) et sur le terrain (cellules expérimentales). Les résultats des essais cinétiques ont été comparés entre eux et les principaux paramètres qui peuvent potentiellement avoir un effet sur les résultats ont été évalués. Les résultats indiquent que les principaux paramètres qui ont un impact sur le comportement géochimique des matériaux de Dumont sont le rapport liquide-solide (RLS) et la température. Un RLS élevé semble augmenter les taux de libération des éléments liés aux minéraux de la gangue, alors que la température semble avoir un effet sur le type de carbonates de magnésium qui précipite durant l'essai cinétique. En outre, le type de test cinétique utilisé semble aussi avoir un effet sur la dynamique de la carbonatation minérale des rejets de concentrateur de Dumont.

Abstract

The prediction of water drainage quality of mine waste in lab conditions is particularly challenging because of differences between the field and lab conditions. In addition, mine waste weathering is subject to processes that may have a great impact on the water drainage quality, such as sorption phenomena or secondary

minerals precipitation. This is particularly the case for ultramafic mine waste that possess a significant potential for mineral carbonation. This study aims to better understand the scale effects on the geochemical behavior of mine waste with the ability to sequester CO_2. In order to reach this objective, various kinetic tests were conducted on ultramafic tailings and waste rock in the laboratory (weathering cells, humidity cells, and column tests) and in the field (experimental field cells). The results of kinetic tests were compared and the main parameters that potentially have an effect on the results were evaluated. Results indicate that the main parameters that have an impact on the geochemical behavior of these materials are the liquid to solid ratio (LSR) and the temperature. A high LSR seems to increase the release rates of elements from the gangue minerals, while the temperature has an effect on the type of magnesium carbonates precipitated during kinetic testing. Additionally, the type of kinetic test used seems to have an effect on the dynamics of mineral carbonation of ultramafic mine tailings.

Keywords: kinetic tests; ultramafic mine waste; scale-up; carbon sequestration; mine drainage.

4.1 Introduction and background

A considerable amount of mine wastes (tailings and waste rock) are produced through the exploitation of base metals. Exposition of waste rocks and tailings to earth surface conditions can lead to poor quality mine drainage (Nordstrom *et al.* 2015; Cravotta III, 2008; Blowes *et al.* 2003; Nordstrom, & Alpers, 1999) causing serious environmental impacts if effluents are not treated (Blowes *et al.* 2003; Nordstrom & Alpers, 1999). Moreover, the water treatment and the mine site rehabilitation costs are increasing with pressure of regulation authorities and the population. For this reason, accurate prediction of the geochemical behavior (the quality of mine waste effluents) of mine waste is a crucial step for pre-mine management. With static and kinetic tests, valuable data is generated that help to plan and operate the management

of mine wastes and to minimize the production of poor water drainage quality (SRK, 1989). Consequently, a fail on prediction could lead to miss management of the wastes and contaminated drainage waters.

To date, the common approach used to characterize mine wastes is to conduct various lab tests (e.g., Acid-base Accounting and kinetic tests) and to scale results to the field. However, this approach is challenging because of the uncertainties related to differences between lab and field conditions. The complexity of field conditions (the heterogeneity of waste, the high residence time of water, the temperature variations, and waste quantity) (Plante *et al.* 2014; Sapsford *et al.* 2009; Price, *et al.* 1997; SRK, 1989; Frostadt & Lawrence, 2005; Malmstrom *et al.* 2000) is difficult to take into account in a kinetic test in laboratory conditions. In addition, some geochemical processes such as sorption and dissolution-precipitation of secondary minerals can influence the water quality (MEND, 2009; Blowes *et al.* 2003), whereas the magnitude of these phenomena could also be greatly influenced by the scale of the kinetics tests. For example, the precipitation of secondary minerals is reported to be favored in the field because of the longer water-rock interaction and the lower liquid-to-solid ratio (LSR; Ardau *et al.* 2009), while small scale kinetic tests are often seen to exaggerate the dissolution of neutralizing minerals (Plante *et al.* 2014; Villeneuve *et al.* 2009; Hakkou *et al.* 2008; Benzaazoua *et al.* 2004). Moreover, small-scale weathering cells have the advantage to be cheaper and less time-consuming compared to field testing. Because of the factors listed earlier, the results obtained in the laboratory must be taken with caution and interpreted by recognizing scale-up issues between lab and field. It is thus important to better understand the scale effects of kinetic tests in the geochemical behavior of CO_2 capturing ultramafic mine wastes.

This paper aims at investigating the scale effects on the geochemical behavior of ultramafic mine waste. Specifically, the water quality results for waste rock and tailings obtained with various kinetic tests in the laboratory (columns, humidity cells,

and weathering cells) and in situ (field experimental cells) were compared in order to identify the main factors responsible for the differences observed at each scale. The mine waste studied here are those from the Dumont Nickel Project located near Amos (Québec, Canada), a Ni deposit in an ultramafic formation. The future mine will be operated by RNC minerals during an expected life-of-mine of 33 years. This future open pit mine will produce more than 2 billion tons of ultramafic mine wastes rich in minerals such as brucite and serpentine, which have the ability to react with CO_2 under ambient conditions (Assima *et al.* 2014; Pronost *et al.* 2011). Previous studies on the Dumont tailings highlighted their potential for carbon sequestration. Mg-carbonates growth was shown to develop between gangue minerals (brucite and serpentine) and sometimes cemented the grains, leading to a hardpan (Kandji *et al.* 2017a, 2017b). Brucite, which was found to be the main mineral involved in the carbon sequestration, is rapidly consumed and replaced by hydromagnesite ($Mg_5(CO_3)_4(OH)_2 \cdot 4(H_2O)$) or dypingite ($Mg_5(CO_3)4(OH)_2 \cdot 5(H_2O)$) in the process. The dissolution of brucite and serpentine is induced through the acidity generated by CO_2 dissolution in the pore-water. The products of these reactions (Mg^{2+}, HCO_3^- and CO_3^{2-}) combine and precipitate as hydrated Mg-carbonates. The mineral carbonation of magnesium silicate minerals within mine wastes is a slow process under environmental conditions (Assima, *et al.* 2012). However, the large quantity of already pulverized waste could increase the potential for carbon sequestration of ultramafic mine wastes (Hitch *et al.* 2010).

4.2 Materials and methods

4.2.1 Tailings and waste rock samples

Since the mining activities have not started yet, the tailings samples were produced from combined bench scale metallurgical tests. The waste rock sample was taken from a bulk sample blasted from an outcrop at the Dumont site. The mine site is located in the Abitibi-Témiscamingue region with a continental climate showing an

annual mean temperature of 1.2°C. The mean temperatures are ranging from -17.3 to 17.2°C in January and July, respectively (RNC, 2013). The total annual precipitation in 2011, 2012, 2013, and 2014 is respectively 848 mm, 893 mm, 967 mm, and 925 mm (Environment Canada).

4.2.2 Characterization methods

The tailings and waste rock samples were characterized physically and chemically prior to the kinetic tests. Their elemental composition was determined by ICP-AES (Perkin Elmer Optima 3100 RL) following an acid digestion (HNO_3-Br_2-HF-HCl). The whole-rock analysis was performed by X-ray fluorescence (XRF) following a lithium borate fusion on pulverized sample aliquots (85 % < 200 mesh) by Acme Analytical Laboratories (Vancouver) Ltd. The total sulfide and carbon content were determined using a LECO induction furnace carbon/sulfur analyzer (Maxxam Analytical, QC, Canada) with a detection limit of 0.05 % for carbon and 0.009 % for sulfur. The neutralization potential was evaluated using the modified Sobek acid-base accounting (ABA) method (Lawrence & Scheske, 1997). The alkalinity measurements of kinetic testing leachates were done by titration with 0.02 N sulfuric acid.

X-ray diffraction (XRD), chemical composition, and microscopic observations were used to determine the mineralogical composition of tailings and waste rock (fraction below < 2 cm fraction). The XRD patterns were collected using a Bruker AXS Advance D8 with a copper cathode, acquired at a rate of $0.02°s^{-1}$ between 2Θ values of 5° and 70°. The DiffracPlus EVA software (v. 9.0) was used to identify the mineral species, and the quantitative mineralogical compositions were evaluated using the TOPAS software (v. 2.1) with a Rietveld (1993) refinement.

The specific gravities (G_s) were determined by using a Micromeritics Accupyc 1330 helium pycnometer (the accuracy is within 0.03 % of reading plus 0.03 % of nominal full-scale sample chamber volume; ASTM Standard D4892 2014). The grain size

distribution of the tailings and for the < 355 µm fraction of the waste rock samples was determined with a Malvern Instruments Mastersizer S particle size analyzer (Merkus, 2009). For the fraction between 2 cm and 355 µm of the waste rock samples, the grain size distribution was determined by sieving (ASTM D 6913-04 2009). The specific surface area (SSA) of the tailings sample was determined with a Micromeritics Surface Area Analyzer using the BET (Brunauer *et al.* 1938) method. The SSA of the waste rock samples (fraction below 2 cm) was calculated using the Equation 4.1, where ρ (kg/m^3) is the material density (ρ, in kg/m^3), (P_D - P_d) is the percentage by weight smaller than size D and larger than next size d (m) (Chapuis et Légaré, 1992)

$$SSA = 6/\rho \sum \left(\frac{P_D - P_d}{d}\right) \tag{4.1}$$

4.2.3 Weathering cell tests description

The weathering cells (Bouzahzah *et al.* 2015; Plante *et al.* 2011; Villeneuve *et al.* 2009; Hakkou *et al.* 2008) require 67 g of sample laid out as a thin layer placed in a 100 mm diameter Buchner funnel equipped with a 0.45 µm glass-fiber filter held in place with silicon grease. A conical vacuum flask is placed at the bottom of the Buchner to collect the leachates. The flushes were done with 50 mL of deionized water (contact time: 3 hours) twice a week (typically on Mondays and Thursdays), and the samples were left to dry under ambient laboratory conditions between each flushes. The recovered leachates were analyzed for pH, conductivity, alkalinity, and dissolved species using the methods described in the previous section. The weathering cell tests were run for 25 weeks.

4.2.4 Humidity cell tests description

Humidity cell tests (ASTM D5744-07, 2007) were also used to evaluate the geochemical behavior of the Dumont materials. The humidity cell tests used here were operated following the MEND procedure (MEND, 2009) by Maxxam Analytical (QC, Canada). One kg of samples (tailings and waste rock) was placed in Plexiglas columns, with 11 cm in diameter and 20 cm high for the waste rock, and 20 cm in diameter and 11 cm high for the tailings sample. The waste rock sample was crushed to < 6.35 mm while the tailings sample was tested as received. The test was conducted for 20 cycles and 60 cycles for the waste rock and tailings, respectively. One cycle consisted of 3 days of dry air circulation through the sample, followed by 3 days of humid air circulation, and flushing on the seventh day. The flush was done using 500 ml of deionized water at the top of the sample for at least 2 hours of contact time. The water is drained and analyzed for the same geochemical parameters as the columns and weathering cell tests. Leachates from kinetic tests were analyzed for various parameters. The pH and the conductivity were measured with an Orion 920A controller equipped with an Orion triode electrode. The dissolved metal concentrations were analyzed with a Perkin Elmer Optima DV ICP-AES following 0.45 µm filtration and acidification at 2 % HNO_3.

Table 4.1 summarizes the main test conditions and part of the physical characteristics of the tailings and waste rock studied. The large disparity between the test conditions will have an effect on the weathering characteristics and drainage chemistry of the leachates.

4.2.5 Column tests description

Aliquots of 8 kg of tailings and 18 kg of waste rock were submitted to laboratory column tests and were deposit as is in the columns. The waste rock column was 1 m high, 14 cm of internal diameter Plexiglas tube filled to a height of approximately 80 cm. The tailings column is a 60 cm high and 14 cm in diameter Plexiglas tube with an initial height of 35 cm; the tailings settled to a final height of 24 cm after one

week. Before the waste deposition, the tailings column was coated with silicon grease in order to avoid preferential flow of water along the interior walls. The 2 columns were trickle-leached from the top with 2 L of deionized water, monthly for tailings and bi-monthly for waste rock. The tests were conducted during two years for the tailings and one year for the waste rock. A porous ceramic plate installed at the bottom of the tailings column enabled to apply a 1 m suction on the materials for drainage. Leachates were recovered after 3 to 4 hours of contact time for the waste rock and after a few days for the tailings, and were analyzed for pH, conductivity, alkalinity, and dissolved species (0.45 µm filtration).

4.2.6 Field experimental cell tests description

Two field experimental cells were constructed at the site of the Dumont project during the summer 2011 (see Bussière *et al.* 2007 for more information on field experimental cells design and construction). The tailings cell contains nearly 2.1 m^3 of tailings while the waste rock cell contains 104 t. The wastes were deposited over a waterproof geomembrane allowing the percolation of precipitations through the waste. The geomembrane was installed in between two compacted sand layers (each 20 cm thick) for protection. A perforated drain runs through the interior of each cell to collect the percolating leachates. The drains are connected to a sealed pipe which discharges water outside the cell to lead to a reservoir for flow measurement and sampling. The tailings field cell has an inverse truncated conical form that is approximately 3 m in diameter at the top (see Appendix A). Since the cell is not filled completely, the exposed surface of the tailings is approximately 2 m in diameter. This induces a high surface reception of precipitation that favors a relatively high LSR. The discharge water was sampled on a bi-monthly basis during the first 2 years, and sporadically during the following years. The pH was measured on site while samples were sent to Maxxam Analytical (QC, Canada) to be analyzed for conductivity, dissolved species (after 0.45 µm filtration), and alkalinity. Details of the field experimental set-up and figures can be found in Gras *et al.* (2015).

Table 4.1 Comparison of the conditions between the tests considered (WR: waste rock; Tails: tailings)

Tests	Weathering cells	Humidity cells	Column test	Field cells
Temperature (°C)	22	20-22	22	Annual ambient mean: 1.4-4.1 (2011-2014)
pH of flushing water	5.5 - 6	5.4 - 5.9	5.5 - 6	5.4
Particle size	WR < 2 mm	WR < 6.35 mm	WR: < 2 cm	WR: < 50 cm
Test duration	WR: 178 days; Tails: 178 days	WR: 133 days; Tails: 427 days	WR: 374 days; Tails: 960 days	4 years
Mass and volume of samples	67 g; 25.2-25.9 cm^3	1 kg; 375.5-387 cm^3	WR: 18 kg; 7.14 dm^3; Tails: 8 kg; 3.08 dm^3	WR: 104 t; 39 m^3; Tails: 5.42 t; 2.1 m^3
SSA (m^2/kg)	WR: 17.4; Tails: 13228	WR: 9.6; Tails: 13228	WR: 5.9; Tails: 13228	WR: 5.9; Tails: 13228
Flush volume and frequency	50 ml; bi-weekly	500 ml; weekly	WR: 2 L; bi-monthly; Tails: 2 L; monthly	Rainfall; WR : 110-126 L/day; Tails: 60-68 L/day
Liquid to solid ratio (L/m^3/week)	WR: 3968; Tails: 3861	WR: 1331,5; Tails: 1292	WR: 140; Tails: 162	WR: 19.8 - 22.7; Tails : 230

4.3 Results

4.3.1 Characterization results

Some of the physical characteristics of waste rock and tailings are summarized in Table 4.1. The SSA of the tailings is 13229 m^2/kg. This high value of the SSA is an indication of the dominance of fibrous minerals (here serpentine) in the Dumont waste. Thus, the calculated SSA of the waste rock sample used for study is probably underestimated because it considers all particles to be spherical. The calculated SSA of the waste rock at different scales are roughly similar: 17.43 m^2/kg for the weathering cell, 9.64 m^2/kg for the humidity cell, and 5.94 m^2/kg for the column test. The Gs (Not shown in the table 4.1) of the tailings is 2.58 while for waste rock it is 2.66. Different grain sizes were used to conduct the kinetics tests: the fractions used are <50 cm, <2 cm, <6.35 mm, and <2 mm for the experimental field cell, column test, humidity cell, and weathering cell, respectively. Since the grain-size distribution of waste rock in the field cell was not determined, we assume that it SSA is the same than for waste rock in the column.

The chemical characterization results for tailings and waste rock are given in Table 4.2. The chemical composition of the waste rock samples is assumed to be the same for all fractions at all scales. The SiO_2 is 35.1 % for tailings and 41.4 % for waste rock, while the MgO is highest for tailings (42.5 %) than for waste rock (34.0 %). Other oxides are also present in lower concentrations: Fe_2O_3 (5.8 % - 7.0 %), Al_2O_3 (0.2 % -3 %), CaO (0.05 % - 0.9 %), and MnO (0.1 %). Ni is the most concentrated trace element detected (2200-2600 ppm), with lesser amounts of Co (70-84 ppm), Cu (48-50 ppm), Zn (30-44 ppm), and Pb (<5 and 10 ppm). The initial total carbon of the tailings and waste rock are similar (1500-1700 pm). The tailings contain more total sulfur (1700 ppm) than the waste rock (400 ppm). The sulfate content is 610 ppm in the tailings and 100 ppm in the waste rock. The acid-base accounting (ABA) indicate

a low AP (1-5 kg CaCO3/t) and a high NP (120-190 kg $CaCO_3$/t); thus, the NNP (NP-AP) indicate that tailings and waste rock are not acid generating.

Table 4.2 Whole rock analysis and physicals parameters of Dumont tailings and waste rock

Majors elements in %											
	SiO_2	Al_2O_3	Fe_2O_3	CaO	MgO	Na_2O	K_2O	MnO	TiO_2	P_2O_5	Cr_2O_3
Tailings	35.10	0.22	5.82	0.05	42.49	<0.01	<0.01	0.11	<0.01	0.05	0.237
Waste rock	41.40	3.08	7.07	0.86	34.06	0.74	0.25	0.09	0.13	0.02	0.16
Trace elements (mg/kg) and acid-base accounting (kg of $CaCO_3$/t)											
	Ni	Co	Cu	Pb	Zn	TOT/C	TOT/S	SO_4	AP	NP	NNP
Tailings	2600	84	48	<5	44	1500	1700	610	5	191	186
Waste rock	2200	70	50	10	30	1700	400	100	1	120	119

The mineralogical composition of the tailings and waste rock is given in Table 4.3. Serpentine is the dominant mineral and reaches near 80 % in the tailings and 61 % in the waste rock. The brucite content is 11.2 % and 5.9 % for tailings and waste rock, respectively. Magnetite is the third dominant mineral in the tailings (4.9 %) but is only 1 % in the waste rock sample. The other minerals detected in the waste rock sample are chlorite (12.4 %), quartz (7.9 %), albite (6.6 %), and biotite mica (2.3 %), with trace levels of awaruite, pentlandite, and heazlewoodite.

Table 4.3 Quantitative mineralogy of the Dumont tailings and waste rock samples (in wt.%)

Minerals	Formula	Tailings sample	Waste rock
Serpentine	$Mg_3Si_2O_5(OH)_4$	79.7	60.8
Brucite	$Mg(OH)_2$	11.2	5.9
Magnetite	Fe_2O_4	4.9	1
Chlorite	$(Fe,Mg)_5Al(Si_3Al)O_{10}(OH,O)$	1.4	12.4
Diopside	$CaMgSi_2O_6$	0.2	2.2
Chromite	$FeCr_2O_4$	0.3	0.2
Awaruite	$Ni_{2.5}Fe$	Trace	Trace
Pentlandite	$(Fe,Ni)_9S_8$	Trace	Trace
Heazlewoodite	Ni_3S_2	Trace	Trace
Quartz	SiO_2	Trace	7.9
Albite	$NaAlSi_3O_8$	-	6.6
Biotite mica	$K(Mg,Fe)_3(OH,F)_2(Si_3AlO_{10})$	-	2.3

4.3.2 Water quality results comparison

Tailings

The results of the kinetics tests on the tailings at the different scales are given in Figures 4.1. At small scales (weathering and humidity cells), the first leachates show an alkaline pH (8.5-10), while for the columns and field cells, the pH start at around 7 and increase gradually and stabilize between 9 and 10. Mg is the dominant element in the leachates and is produced mainly by the dissolution of brucite and serpentine, as shown in previous studies (Kandji *et al.* 2017, 2017b). Extensive weathering of serpentine and brucite is enhanced by the dissolution of CO_2 and the oxidation of the

sulfides present in the samples. The Mg concentrations are generally similar in all tests and stabilize at near 100 mg/l, but in the weathering cell leachates, it is slightly higher (near 200 mg/l). The Ca shows a transition phase early in the kinetic tests and stabilizes near 10 mg/l. Ca is probably produced by the dissolution of diopside. The sulfates produced by sulfide oxidation are present in the leachates for all tests; a remarked trend is observed consisting of an increase followed by a decrease before stabilization. It was suggested that sulfide oxidation is slowed down by the magnesium carbonates growth, which passivates the trace sulfides present in the Dumont samples (Kandji *et al.* 2017a, 2017b). Similarly, studies on ultramafic mine waste carbonation have highlighted the surface passivation of brucite or serpentine by the formation of a silica-rich layer and/or the precipitation of iron hydroxide (Assima *et al.* 2012), and magnesium carbonates precipitation (Zarandi *et al.* 2016).

As for sulfate, Ni is produced by sulfide oxidation and is found sporadically in all leachates, but is mostly below the detection limit (0.004 mg/L). The other metals such as Fe, Zn, Cu, and Pb (not shown) are below the detection limits most of the time (Fe: 0.006 mg/L; Zn: 0.005 mg/L; Cu 0.003 mg/L; Pb 0.02 mg/L). The alkalinity values of the leachates is higher for the small scale tests (weathering and humidity cells) than for columns and field cells; it oscillated near 700 mg $CaCO_3$/l in the weathering cell leachates, while it stabilized at around 400 mg $CaCO_3$/l for humidity cells. In the column and for the experimental field cell, the alkalinity stabilized between 200 and 300 mg $CaCO_3$/l. Despite the dominance of silicate minerals (serpentine, chlorite, etc.) in the gangue, the Si concentrations (not shown) are almost near 1 mg/l at all scales, with the exception of the column (tailings), for which the use of silicon grease is suspected to produce silica in the leachates (between 20 to 80 mg/l). Globally, the waste has the same behavior at each scale, as the concentrations of most species are in the same order of magnitude, after stabilization.

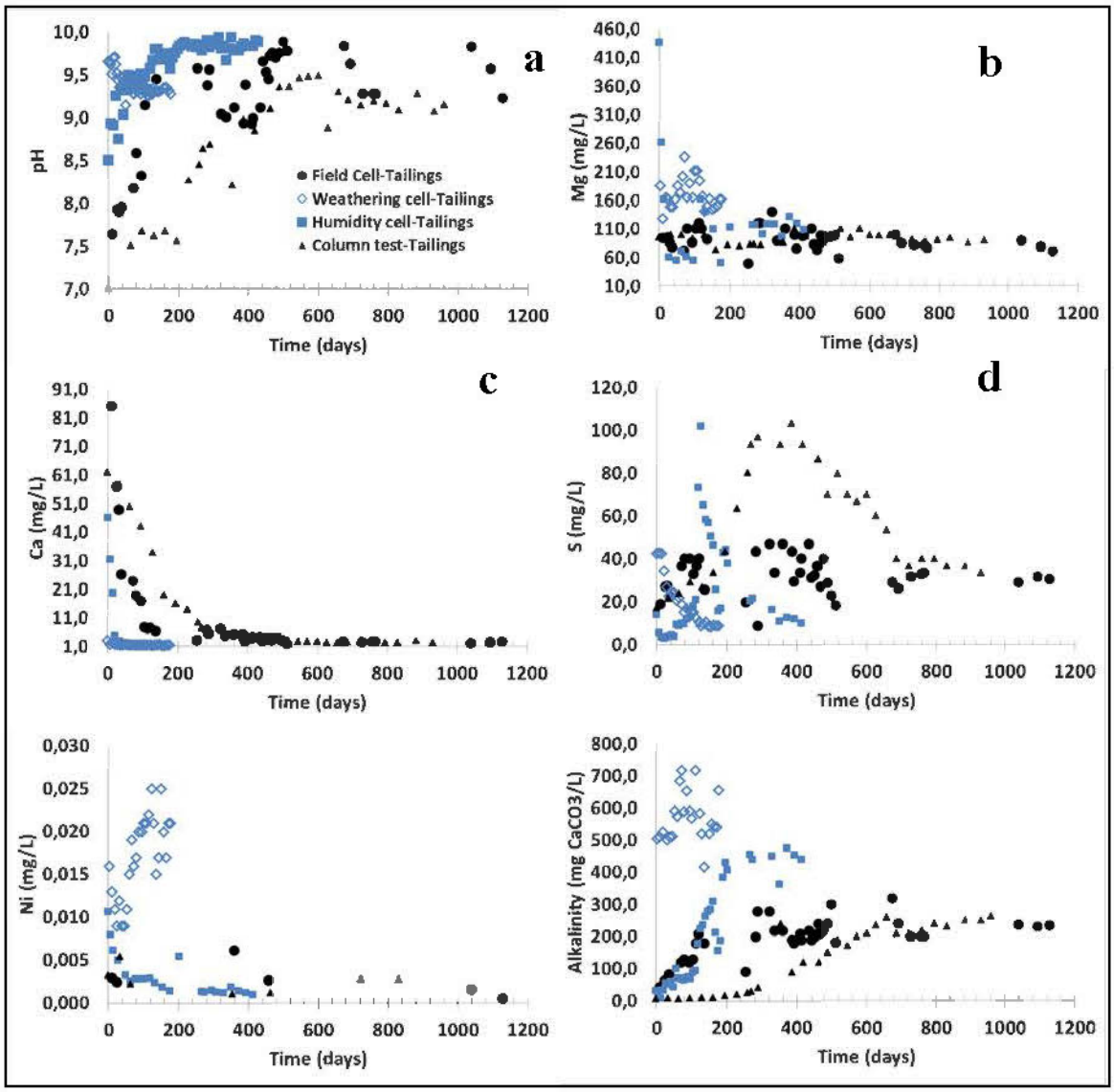

Figure 4.1 Geochemistry comparison for different scales for tailings

Waste rock

As for the tailings, a similar behavior was observed for waste rock at all scales (Figure 4.2). The pH of the waste rock leachates remained circumneutral to alkaline (pH 8 to 10); while Mg concentrations oscillated between 50 and 250 mg/l. Ca concentrations are higher in the field and stabilized at 10 mg/l, while concentrations

are near 1 mg/l for others tests. Sulfates are generated at higher concentrations in column and field tests (20 – 100 mg/l) than in weathering and humidity cells (< 20 mg/l). The alkalinity values range between 200 and 1000 mg/l at all scales. As for tailings, Ni is found sporadically in the leachates and is mostly below the detection limit. Other metals are mainly below the detection limits. For the silica (not shown), the same trend was observed as for the tailings, but this time, grease was used for the weathering cell test, so the concentrations obtained at this scale reached 100 mg/l or higher, while for other scales (column, field and weathering cell) silica concentrations are near 1 mg/l.

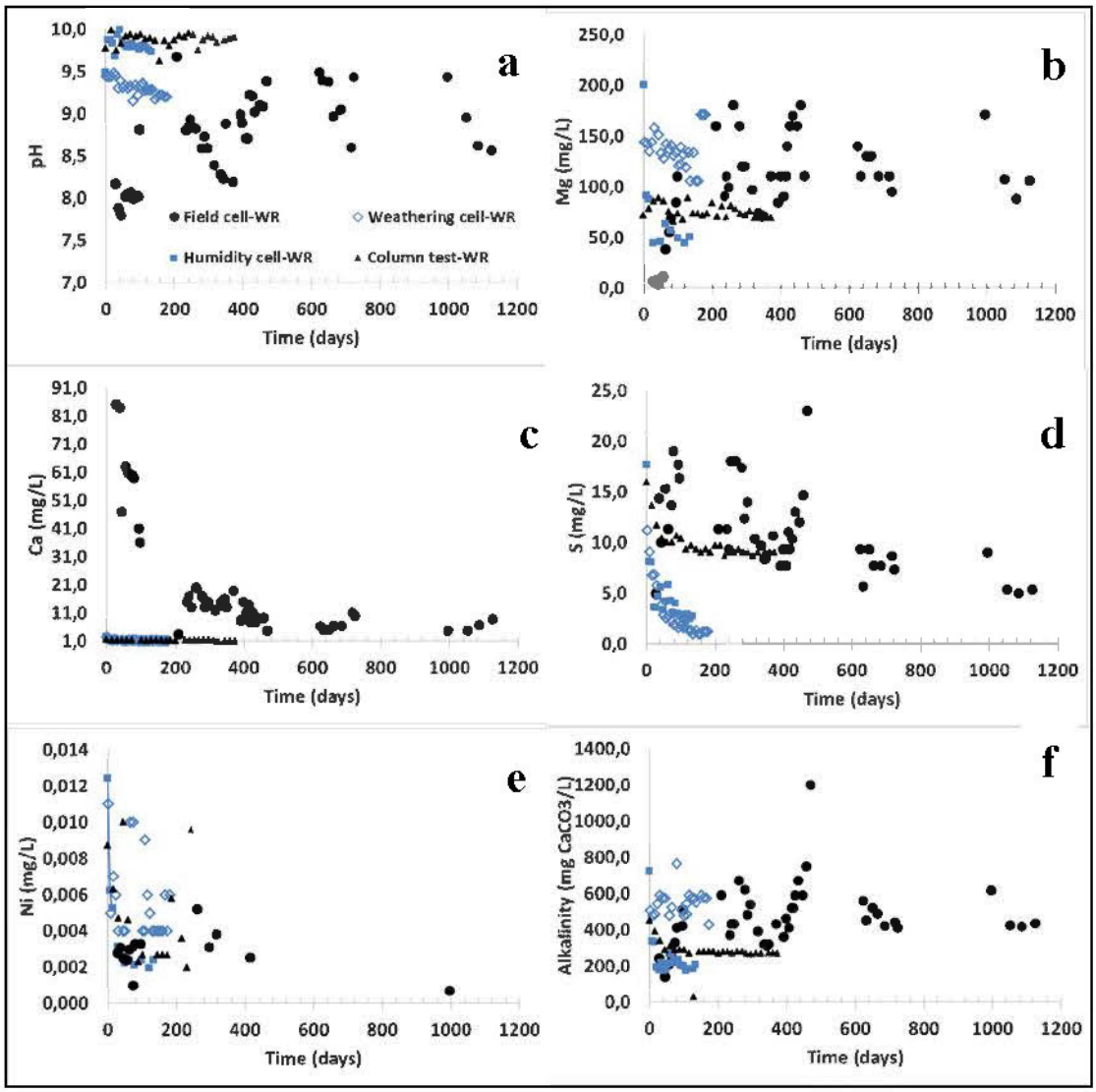

Figure 4.2 Geochemistry comparison for different scales for waste rock

The cumulative loadings normalized by the volume of waste are calculated for the field cells by using the volume (V, m^3) of waste rock or tailings, with the flow rate (Fi, in L/day), concentration (Ci, in mg/l), and the time interval (ti, in days) between each measurement or sampling (i) using Equation 4.2:

$$Cumulative\ mass\ of\ selected\ element = \frac{1}{V}\sum_{i}^{n} F_i \times C_i \times t_i \qquad 4.2$$

In the laboratory tests, the cumulative loadings are calculated by summing the product of the volume of the leachate and the concentration of an element, normalized by the volume of the solid sample (Equation 4.3):

$$Cumulative\ mass\ of\ selected\ element = \frac{1}{V}\sum_{i}^{n} Ci \text{ x } vi \qquad 4.3$$

The evolution of the cumulative and normalized loadings of Mg, Ni, and S calculated for each kinetic tests are shown in Figure 4.3, for waste rock (left) and tailings (right). The Mg, Ni, and S loadings are higher for the small scales kinetics tests (humidity and weathering cells) compared to the column and field tests. The cumulative loadings of the selected elements are following this order: weathering cells > humidity cells > column tests ≥ field cell.

The Mg that leach out of the weathering and humidity cell tests reach more than 8 000 000 mg/m^3 for waste rock and tailings while for the larger scales, Mg loadings are below 4 000 000 mg/m^3 even with their longer test durations. The same trend is observed for Ni and sulfate, which are higher in the small scale cells than in the columns and field cells. The loadings of the selected elements in the columns and field cells leachates are generally within the same order of magnitude.

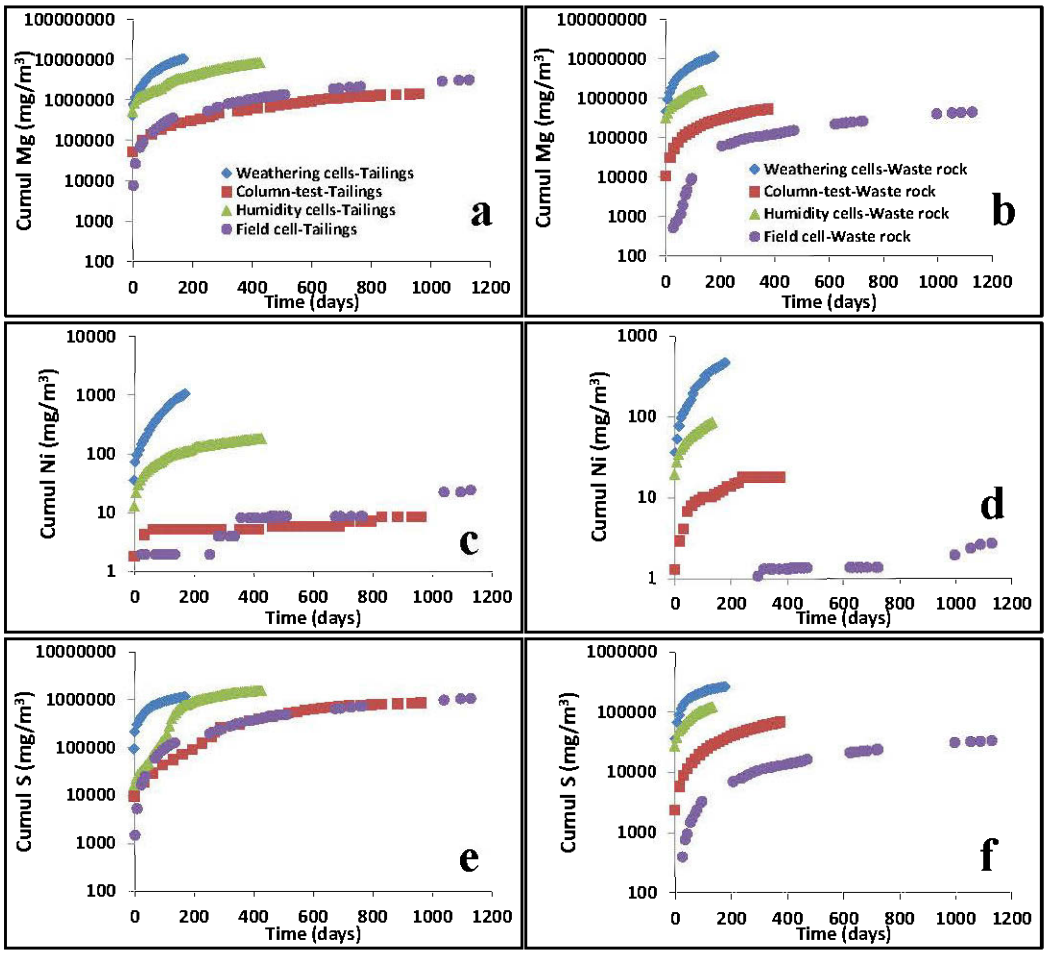

Figure 4.3 Cumulative Mg, Ni, and sulfate loadings in the leachates of the different kinetic tests used for tailings (left) and waste rock (right) (Note the log scale for all elements)

4.4 Discussion

4.4.1 Release rates comparison

The slope of the cumulative loading volume-normalized (mg/m^3) curves versus time (d) represents the release rate ($mg/m^3/d$) of the selected element. The release rates after stabilization were calculated for Al, Ca, Mg, Ni, Si, and sulfate and are summarized in Figure 4.4. These elements are the major cations present in the

leachates along with the bicarbonate ion (HCO_3^-). The release rates obtained show between 1 and 2 orders of magnitude of difference between scales for Al (0.5-5.32 mg/m^3/d), Ca (43-483.6 mg/m^3/d), Mg (1 553-57 725 mg/m^3/d), Ni (0.06-6.71 mg/m^3/d), Si (51.96-414.4 mg/m^3/d), and S (906.5-4105 mg/m^3/d) in tailings. For the waste rock, the release rates show between 2 and over 4 orders of magnitude of difference between scales for Al (0.06-19 mg/m^3/d), Ca (23-634 mg/m^3/d), Mg (413-62 065 mg/m^3/d), Ni (0.006-2.43 mg/m^3/d), Si (1.65-73 618 mg/m^3/d), and S (31.5-749 mg/m^3/d). The release rates calculated for the tailings and waste rock generally follow this order: weathering cells > humidity cells > column tests ≥ field cell. For Mg, the dominant element in the leachates, the release rates decrease from the smallest scale to the biggest for the waste rock sample. However, for tailings, the release rate in the field cell is slightly greater than the release rate in the column. This is possibly explained by the highest LSR observed in the field than in the column test. As explained before, the tailings field cell only contains 2.1 m^3 of material, but the surface of the cell is important (19 m^2) which induces the reception of a high quantity of water during rain and snow events. A higher LSR used in the kinetic tests is known to exaggerate the dissolution of neutralizing minerals (Plante *et al.* 2014; Villeneuve *et al.* 2009). This also contributes to the higher release rates obtained in the weathering and humidity cells for almost all species studied.

Sulfide oxidation is the source of sulfate and Ni in the leachates. The difference of release rates for Ni is more obvious (tailings: 0.06-6.71 mg/m^3/d; waste rock: 0.0066-2.43 mg/m^3/d) than for sulfate (tailings: 906.5-4 105 mg/m^3/d; waste rock: 31.5-749 mg/m^3/d). One possible explanation of these differences is that the retention of Ni and sulfate in the materials (through secondary precipitation or sorption) is promoted and most favored in the columns and field cells than in the small scales tests, because of the smaller LSR for column and field cells.

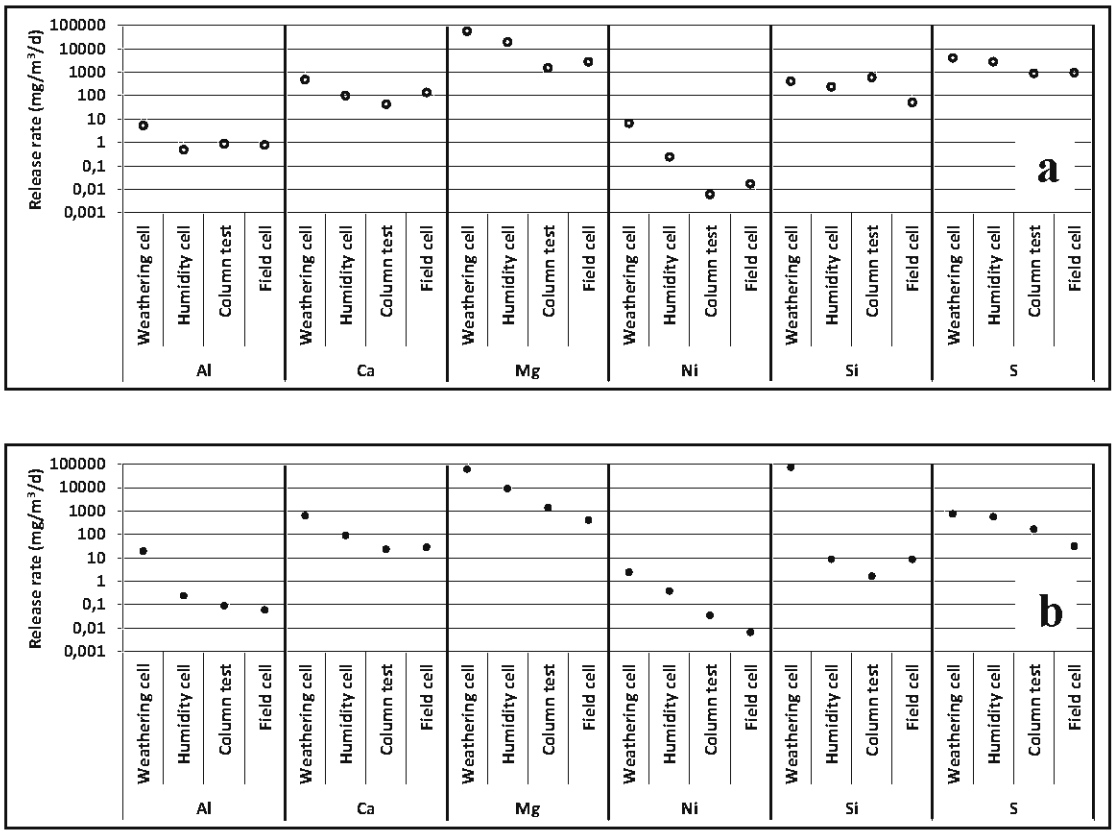

Figure 4.4 Volume-normalized release rate (mg/m^3/d) for selected elements for tailings (a) and waste rock (b); log scale

Since minerals are distributed unevenly within the different grain sizes, the elements leached out of the different minerals may be affected differently by scale effects. This may explain the relatively greater differences for Al, Ca, Mg, Si, and S release rates observed for waste rock than for tailings (Figure 4.4). However, since the mineralogical compositions of the different grain sized were not analyzed, the scale effects between elements are difficult to differentiate in the present study.

4.4.2 Effect of the surface specific on the release rates

The effect of SSA on the release rates between scales was also evaluated by normalizing the release rates to the total surface area. While the same SSA value was used for the tailings at all scales, the calculated SSA of the waste rock vary between 5.41 and 15.9 m^2/kg. These small differences in the SSA between scales does not have a great effect in the surface-normalized release rates, as shown in Figure 4.5. The surface-normalized release rates follow the same order as for the volume-normalized release rates: weathering cells > humidity cells > column tests ≥ field cells. These results therefore need to be interpreted with caution, because the calculation of the SSA of waste rock supposes that the grains have a spherical form, whereas the serpentine that composes the majority of the waste is fibrous and probably have a higher SSA than evaluated. Moreover, similar SSA were assumed for the waste rock in the field cell and in the column, even though the latter only contains particles < 2 cm. It is important to bear in mind the possible bias in the surface-normalized release rates, because the calculation of the SSA did not consider the porosity and surface roughness of the waste rock sample.

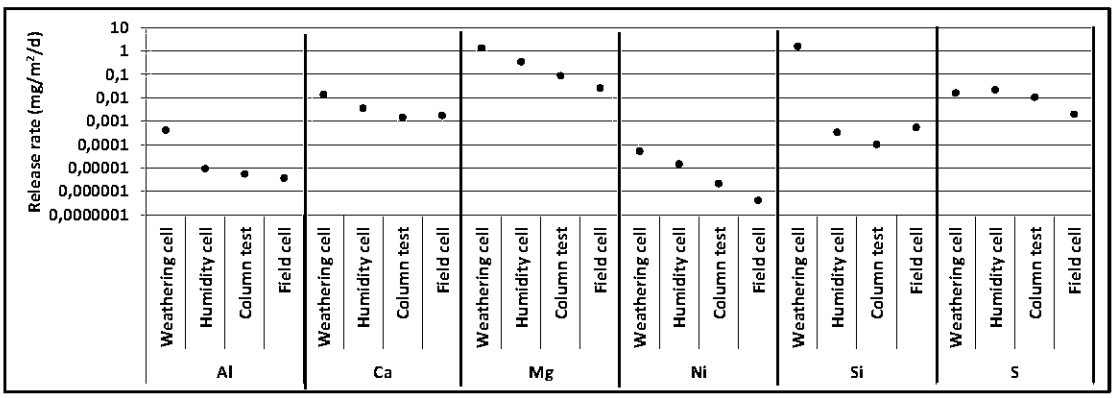

Figure 4.5 Surface-normalized release rate (mg/m^2/d) of selected elements for waste rock, in log scale

4.4.3 Effect of temperature on the release rates

Temperature could have an effect on various geochemical processes that could, in turn, have an effect on the water drainage quality. Temperature has an effect on sulfide oxidation, on silicate weathering, as well as on the gas dissolution in water. The laboratory temperature is near 22°C while in the field, the annual mean temperature from 2011 to 2014 is near 2°C. The temperature difference between the laboratory (weathering cell, humidity cell, and column test) and the field probably affects the weathering behavior of the Dumont ultramafic waste and as well as on the quality of its mine drainage water.

The effect of temperature on sulfide oxidation is generally evaluated by using the Arrhenius relationship between temperature, the reactions rates and the activation energy (Equation 4.4; Plante *et al.* 2014; Ethier *et al.* 2012; Frostadt & Lawrence, 2005).

$$ln\frac{k_2}{k_1} = \frac{E_a}{R}\left(\frac{1}{T_1} - \frac{1}{T_2}\right) \qquad 4.4$$

Where k_1 and k_2 are the rate constants at temperatures T_1 and T_2 (in K); Ea is the activation energy of the reaction (in J/mol); and R is the gas constant, 8.31 J/mol.K. The activation energies reported for pentlandite refer to its transformation into a monosulfide solid solution (MSS) at high temperatures (Xia *et al.* 2012; Etschmann *et al.* 2004). However, very little information on the pentlandite behavior in environmental conditions is available in the literature. For this reason, the activation energy for pyrite oxidation, which is reported to be close to 88 000 j/mol, for pH values between 7-8 (Nicholson *et al.* 1988), is considered for pentlandite. For the range of temperatures prevailing in the field (the mean temperature of the active period from March to November is 7.98°C) and in the laboratory (22°C), the sulfide oxidation in the lab is 5.98 times greater than in the field conditions. Thus, in order to correct the sulfate and Ni release rates in the laboratory tests to meet the field

conditions, the laboratory release rates of these two elements were divided by a factor of 5.98.

As suggested by Morin *et al.* (1995), the rate of neutralization is a response to the rate of acid generation produced by sulfide oxidation. Consequently, it is assumed that neutralizing minerals (here serpentine and brucite, as well as other minor silicates present in the samples) will weather proportionally to sulfide oxidation. Thus, to correct the release rates of Al, Ca, Mg, Ni, Si, and S according to the sulfide oxidation rate, we divided the surface release rates of Al, Ca, Mg, Ni, Si, and S by the same correction factor (5.98).

The Dumont materials contain low sulfide values and previous studies suggest that the CO_2 dissolution is an important factor that drive the dissolution of serpentine and brucite (Kandji, *et al.* 2017a, 2017b). Consequently, the weathering could also be impacted by the temperature-induced dissolved CO_2 variations. Generally, the temperature decrease will increase the dissolution of gases in water. To evaluate the effect of temperature on the CO_2 dissolution, we can apply Henry's law that describes the fraction of gas dissolved in water at a given temperature (Equation 4.5):

$$p = H \times C \qquad 4.5$$

Where p is the pressure of the gas above the solution (atm), H is the Henry coefficient (atm.L/mol), and C is the fraction of the solute in the solution (mol). The Henry's law coefficient is temperature dependent and the relation of Carroll *et al.* (1991) was used to calculate the Henry coefficient at a given temperature (Equation 4.6), where H is expressed in MPa/mole and the temperature is expressed in Kelvin:

$$\ln(H) = -6.8346 + 1.2817\ x10^4/T - 3.7668\ x10^6/T^2 + 2.997\ x10^8/T^3 \qquad 4.6$$

This relationship is valid for low pressures (up to 1 MPa) and temperatures between 0 to 160°C. For the range of temperatures between T_1 (22°C; laboratory) and T_2

(7.98°C; field-unfrozen periods), the fraction of CO_2 dissolved in the pore water is near 1.52 times greater in the field than in the laboratory. This suggests that the acidity generated by CO_2 dissolution will increase the dissolution rate of brucite and serpentine by a factor of up to 1.52.

In summary, the temperature decrease from the laboratory to the field will induces a decrease of the sulfide oxidation rate and the neutralizing minerals dissolution rates by a factor of 5.98. However, the temperature decrease has the opposite effect on the CO_2 dissolution (1.52 times increase). Thus, a global correction factor of 3.93 (5.98/1.52) was applied to the release rates of Al, Ca, Mg, and Si. For the sulfate and Ni release rates, the laboratory release rates were divided by 5.98 to scale them to the field conditions, since the CO_2 dissolution in the pore water has no effect on sulfide oxidation.

The temperature-corrected release rates for each kinetic test are given in Figure 4.6. The temperature correction decreases the laboratory release rates for waste rock and tailings and thus tightens the differences between the laboratory and field scales. The differences of corrected release rates between the scales are now less than two orders of magnitude for the tailings, with the exception of Ni for which the difference is near three orders of magnitude. For waste rock, the differences of release rates between scales are less than two orders of magnitude, with the exception of Si. It is interesting to note that for sulfates, the differences between tests are less than one order of magnitude (tailings and waste rock).

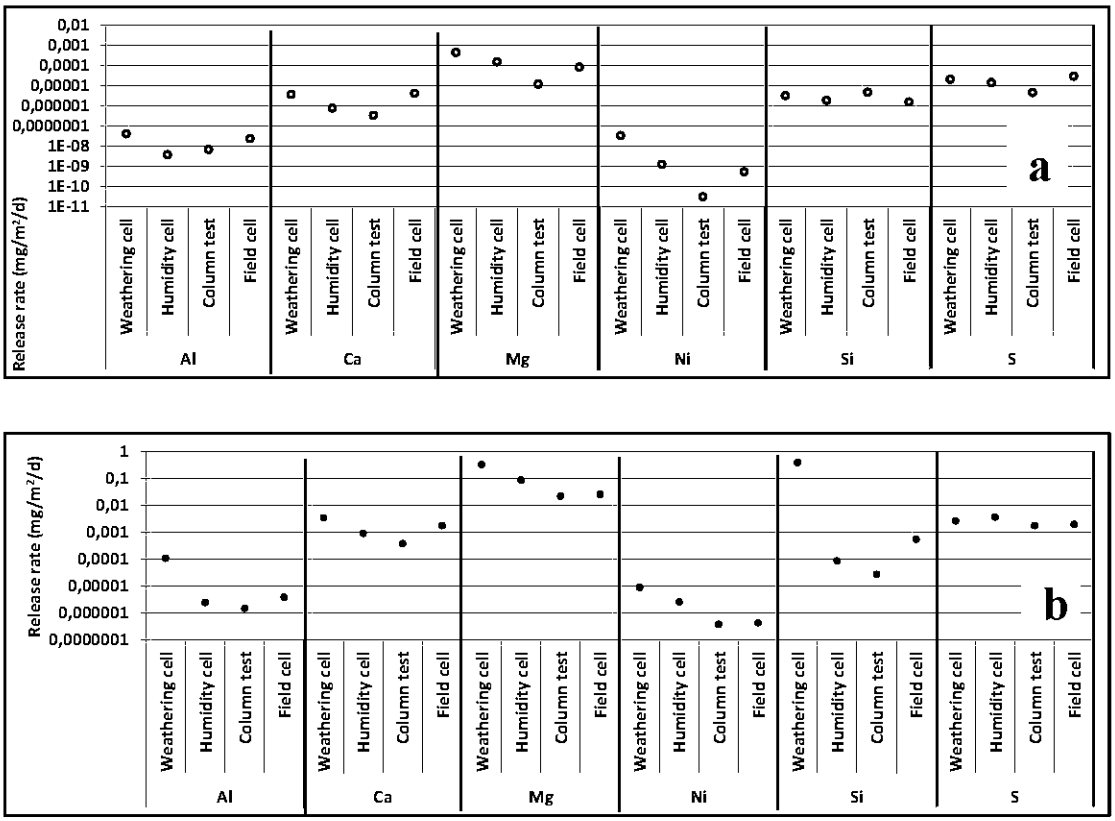

Figure 4.6 Temperature-corrected surface-normalized release rates (mg/m^2/d) of selected elements for waste rock and tailings; log scale

The kinetic tests were performed in the laboratory with a relatively constant temperature (18-22°C; mean 21°C) while in the field, the temperatures range between -33°C and 26.2°C from 2011 to 2014 (Environnement Canada, 2016). Temperature is an important parameter to consider as it has an effect on the oxidation of sulfides (Nordstrom *et al.* 2015; Plante *et al.* 2014; Ethier *et al.* 2012; Frostadt & Lawrence, 2005; Blowes *et al.* 2003) and on the geochemical behavior of neutralization minerals such as carbonates and silicates. However, the Dumont waste contains low sulfide concentrations; it can be assumed that the impact of sulfide oxidation on the silicates and brucite weathering is negligible. CO_2 dissolution can be thus considered to be the main factor controlling serpentine and brucite weathering. Consequently, an effect on

the weathering of silicates and brucite is expected due to the differences of temperature between scales (lab versus field). However, when only the effect of temperature variations on the CO_2 dissolution is considered (neglecting the effect of sulfide oxidation), the differences between the temperature-corrected release rates in the laboratory versus the field are highest than before correction. More detailed investigations should be done, particularly in field conditions, in order to evaluate the effect of seasonal variations on the behavior of ultramafic mine waste and on the water drainage quality.

The post-kinetic testing materials were characterized in order to identify any changes on the weathered samples that may have occurred during testing (Kandji *et al.* 2017a, 2017b). In samples submitted to the laboratory kinetics tests, only dypingite and hydromagnesite were seen to precipitate within the wastes and to cement the particles together at the surface. It was suggested that nesquehonite ($Mg(HCO_3)(OH)\cdot 2(H_2O)$ or $MgCO_3\cdot 3H_2O$), a common low temperature magnesium carbonate, may first form and then transform into more stable carbonates (such as hydromagnesite and dypingite) (Kandji *et al.* 2017a). Moreover, the temperature in the laboratory never drops below 20°C. However, in the field cells, various Mg-carbonates were identified. The characterization of samples taken from the tailings and waste rock cells reveal precipitation of nesquehonite, dypingite, hydromagnesite, and several Mg-Fe carbonates, including brugnatellite ($Mg_6Fe^{3+}(CO_3)(OH)_{13}\cdot 4(H_2O)$) and pyroaurite-sjögrenite ($Mg_6Fe^{3+}{}_2(CO_3)(OH)_{16}\cdot 4(H_2O)$). The morphologies, occurrence, and sequence of formation are detailed in Gras *et al.* (2015).

This difference observed on the type and occurrence of Mg-carbonates between field and laboratory tests can be explained mainly by the mean temperature difference between scales, and possibly by the watering and drying cycles. According to Langmuir (1965), the type of carbonate formed depends on the temperature. This observation is consistent with more recent data from the studies reporting passive

carbonation of ultramafic mine wastes. Indeed, passive carbonation is occurring in at least seven well-documented active or abandoned mines in Canada, Australia, and Norway (Wilson *et al.* 2014; Oskierski, *et al.* 2013; Bea *et al.* 2012; Beinlich & Austrheim, 2012; Pronost *et al.* 2012; Wilson, *et al.* 2009a, 2009b; Beaudoin, *et al.* 2008; Wilson, *et al.* 2006). These closed and active mine sites are subject to various climates from artic (subarctic) arid and semi-arid climates, to continental climates, covering a large range of temperature variations (Table 4.5). For these reported in-situ carbon sequestration observations by ultramafic mine waste, hydromagnesite and nesquehonite were the most common Mg-carbonates found to precipitate in the field. However, for the mines located in colder areas such as the Chromite mine shafts of Feragen (Norway), where the highest monthly average temperature was 12.4°C (from December 2010 to November 2011), the main carbonate observed was lansfordite ($Mg(CO_3)\cdot 5(H_2O)$) (Beinlich & Austrheim, 2012), a low temperature Mg-carbonate. Moreover, nesquehonite was also observed to precipitate in Diavik (North Canada; Wilson *et al.* 2009b), located in a subarctic climate, where the annual mean temperature is -11.8°C (nearby Ekati; Wilson *et al.* 2011). For mine sites located in relatively hot environments such as at the Mount Keith and Woodsreef Chrysotile mines (Australia; mean annual temperature: ~16°C), and at Thedford mines (Canada; mean annual temperature: 3.8°C), more stable Mg-carbonates like dypingite and hydromagnesite, which are the end-products of nesquehonite decomposition (Langmuir, 1965), are observed to precipitate. It appears that the climate seems to have an effect on the type of carbonate formed and probably on the rate of mineral carbonation, since temperature has an effect on the CO_2 solubility as well as on the rate of silicates weathering (White & Brantley, 1995). However, the sequestration of CO_2 into magnesite and hydromagnesite is preferred because these carbonates are thermodynamically more stable than nesquehonite and lansfordite (Langmuir, 1965).

Table 4.4 Climatic data for mine sites that are subject to mineral carbonation of ultramafic waste. These data are taken from climate-data.org

	Climate	T° (min)	T° (max)	T° (mean)	Carbonate minerals identified
Diavik (Canada)	Arid, subarctic; Evaporation ≈ precipitation	-28.2°C	15.4°C	-11.8°C	Nesquehonite
Clinton Creek (Canada)	Subarctic - cold temperate	-30.1°C	15.3°C	-5.4°C	Nesquehonite, dypingite, hydromagnesite, lansfordite.
Feragen (Norway)	Subarctic	-11.3°C	11.4°C	0.3°C	Lansfordite and nesquehonite
Thetford mine (Canada)	Moderate and sub-humid regional climate	-12°C	18.3°C	3.8°C	Hydromagnesite
Mount Keith (Australia)	Desertic	12.3°C	30.6°C	21.7°C	Hydromagnesite
Woodsreef (Australia)	Temperate to subtropical climatic	8.3°C	23.9°C	~16°C	Hydromagnesite and pyroaurite

4.4.4 Effect of the LSR on the release rates

The LSR seems to be an important parameter that influences the geochemical behavior, the release rate, and thus the water quality. The comparison of surface-normalized release rates and temperature corrected surface release rates of Mg, Ca, Ni, and sulfates versus the LSR are given in Figures 7 (tailings) and 8 (waste rock). Generally, the release rates of Mg, Ca, S, and Ni increase with the LSR, with the lowest difference for the tests with low LSR (columns and field cells). However, this trend is not systematically followed for the Ca and sulfates.

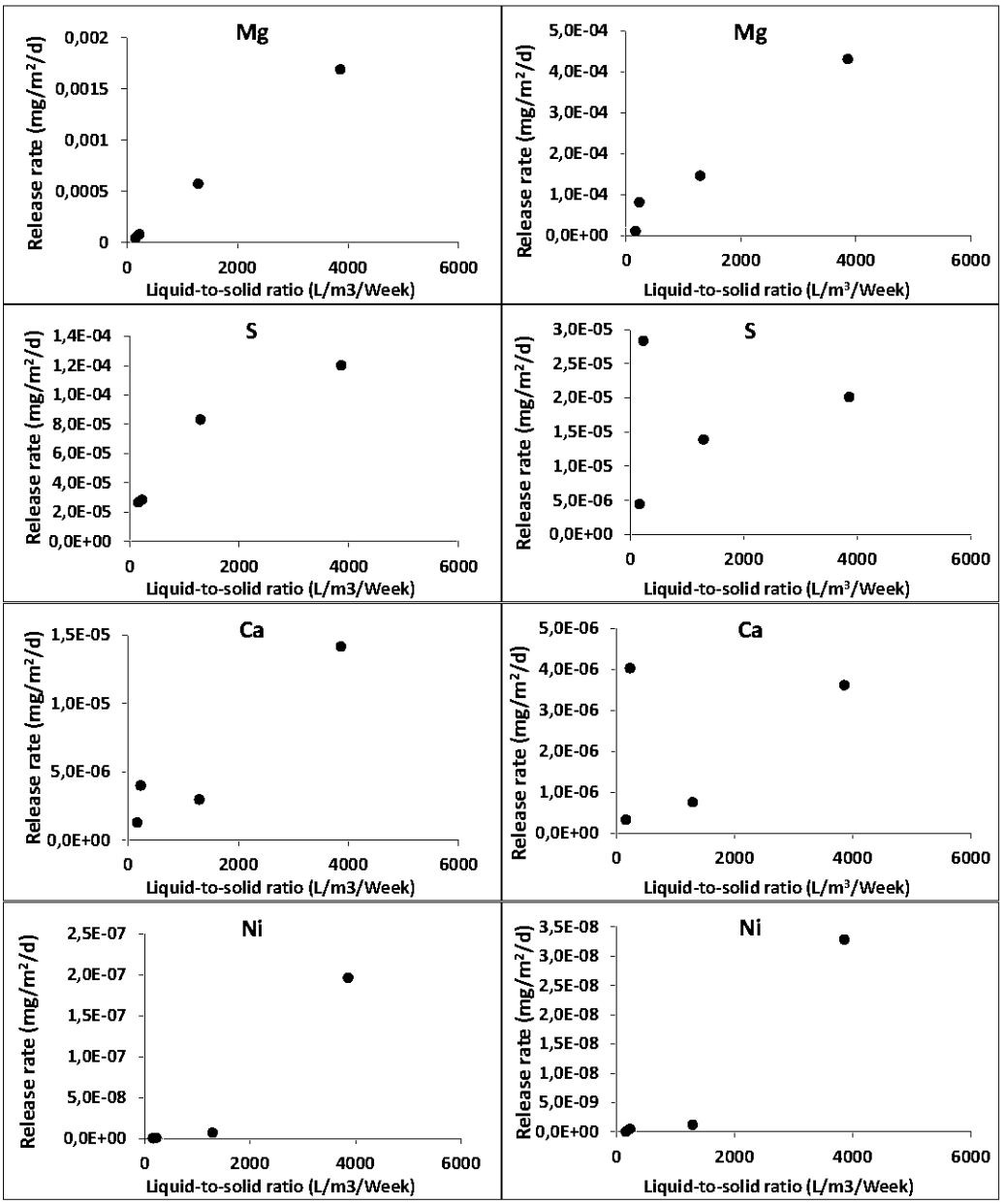

Figure 4.7 Surface-normalized release rates (left) and temperature corrected surface-normalized release rates (right) for tailings versus the LSR

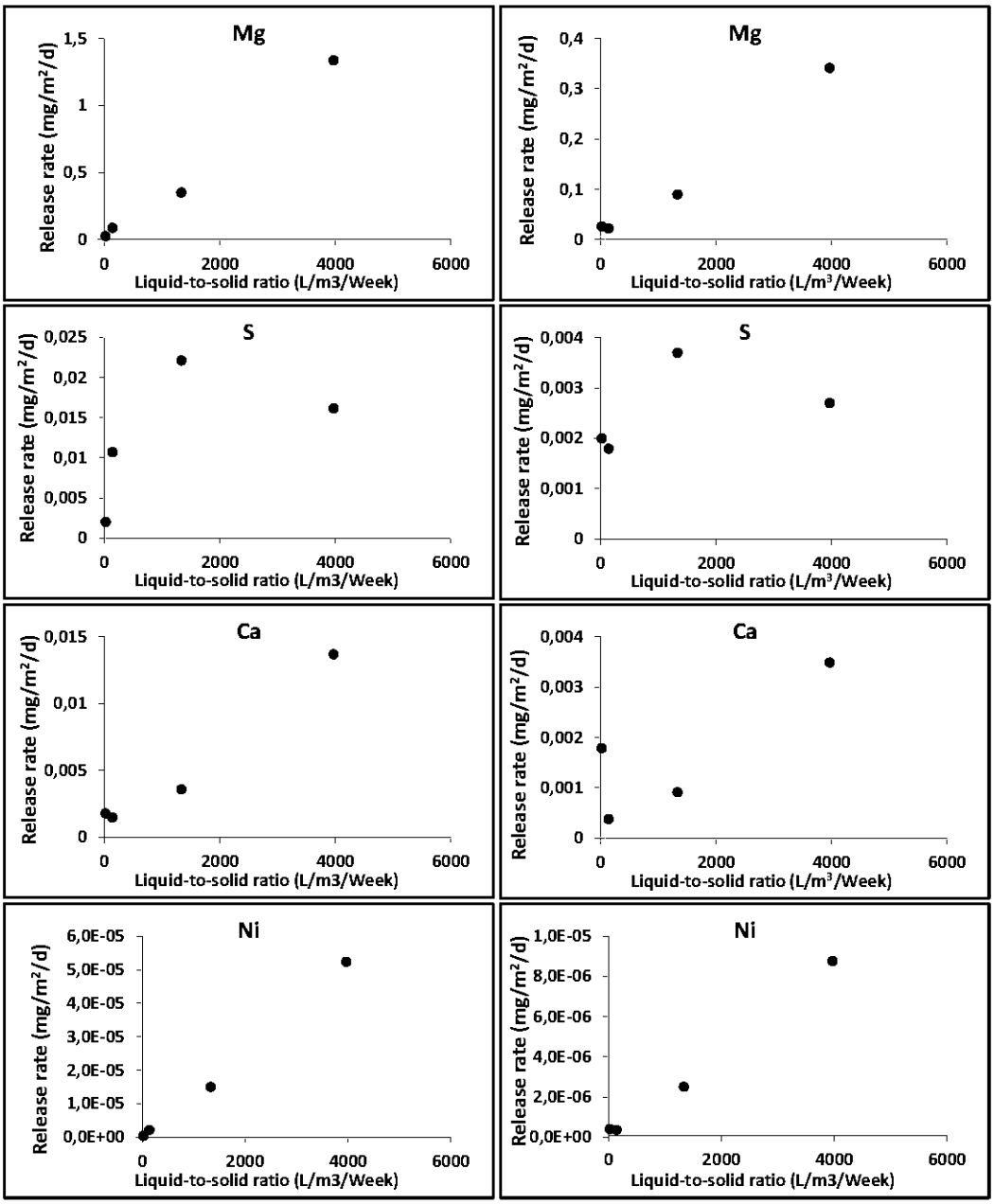

Figure 4.8 Surface-normalized release rates (left) and temperature-corrected of surface-normalized release rates (right) for waste rock versus the LSR

In the field, waste piles are intermittently leached upon rain events. As shown in Table 4.1, lower LSR values prevail in the field and in the column tests (19.8-

230 L/m^3/week). Lower LSR values favor the retention of the weathering products of the primary minerals (Sapsford *et al.* 2009). Thus, the accumulation of these products (for example: Ni^+, Mg^{2+}, Ca^{2+} and SO_4^-, in the case of the oxidation-neutralization processes, Mg^{2+} and CO_3^{2-}/HCO_3^- in the case of mineral carbonation) will generate subsequent precipitation (and accumulation) of secondary minerals such as gypsum, Ni-hydroxide, or hydrated magnesium carbonates. However, in the case of small scale kinetic tests (weathering and humidity cells), the more frequent wetting of the sample will flush out most of the reaction products, which will impede the accumulation of secondary products. According to Ardau *et al.* (2009), the interaction time between water and rock is more prolonged in the field, favoring the precipitation of secondary minerals. Additionally, Assima *et al.* (2012) found that during their carbonation experiment, the precipitation and accumulation of Mg-carbonates is a function of the watering frequency: they showed that the carbon sequestered by their tested ultramafic waste increased by a factor of 20 when small quantities of water were added periodically instead of a single addition of a high water volume. Taken together, these observations suggest that the accumulation of Mg-carbonates should be higher under lower LSR values (field and column) than at higher values (weathering and humidity cells). This hypothesis will be verified in the following section. Thus, kinetic tests with LSR values close to that of the expected field conditions, such as those attainable using column testing, should be preferred in order to simulate the field geochemical conditions.

4.4.5 Comparison of total carbon content between scales

The effect of the type of kinetic tests used on the carbon sequestration capacity of the ultramafic mine tailings is investigated in the present section. The fresh (initial) tailings contains approximately 0.15 % of total carbon (see Table 4.1). The final samples from the weathering and humidity cells were homogenized as a whole, while the tailings column was dismantled in layers (2 cm for the first 2 layers). For the tailings field cell, many cores were sampled at different times and divided in thin

layers for total carbon analyses. The carbon content results in the first layers of each cells are given in Table 4.5. There are no big differences in the amount of total carbon on the surface of the tailings at each test. However, it should be noted that the test durations are not the same for each test. Weathering cells are shorter but showed a greater amount of total carbon. This may suggest that the more frequent watering of the weathering cell accelerates the carbonation of the tailings in comparison to the column and field cell. This implies that even though the high LSR of the smaller scales exaggerate the Mg release in the leachates, it allows the precipitation of more magnesium carbonates than within the bigger scales of the column and field cells.

In addition, a previous study showed that the carbon sequestration of Dumont tailings stagnated as soon as brucite is consumed (Kandji *et al.* 2017a). This may explain the fact that the amount of total carbon on the surface tailings is not higher than 0.8 % in the humidity cell, column, and field cell, despite their longer durations (427, 960, and 1128 days, respectively). The type of kinetic tests used here seems to have an impact on the kinetics of carbon sequestration of the Dumont ultramafic tailings. Thus, it appears that simple kinetic tests such as the weathering cell can be used to evaluate the carbon sequestration potential of ultramafic mine wastes, instead of more complex kinetic tests such as columns and field cells.

Table 4.5 Comparison of the total carbon content on the top 1-2 cm layer of the tailings at each scale studied

	Weathering cell (~1 cm)	Humidity cell (~1-2 cm)	Column test (2 cm)	Field cell (1-2 cm)
Test duration (days)	178	427	960	1128
% of C on the top 1-2 cm layer	1.06	≈0.4**	0.83	~ 0.8*

* Seasonal variations of total carbon content at the tailings surface pile field were observed. The % of total C range from 0.5 to 1 % (Gras *et al.* 2015); ** samples of crusts on the tailings contain around 1.4 % of total carbon.

4.5 Summary and conclusions

The prediction of the drainage quality from ultramafic mine waste was compared by using different kinetics tests at different scales in the laboratory and the field. The laboratory kinetic tests used in this study are the weathering cells, humidity cells, and column tests. In the field, two experimental cells were constructed at the future Dumont mine site. The pH values of the leachates are in the same range for all tests, as are the Mg, alkalinity, and sulfate values, after stabilization. However, Ni was detected more often in the small scale kinetics tests (weathering and humidity cells) than for the column and field cell.

Even if the drainage quality is similar for all tests, differences were noted for the release rates. The differences of the volume-normalized release rates between the laboratory and field reach up to over 4 orders of magnitude. However, these differences are less marked for tailings than for waste rock.

The surface-normalized release rates of waste rock only slightly contribute to decrease the differences observed for the volume-normalized release rates. However, due to the fibrous mineral that composes the Dumont materials, the SSA method calculation underestimates the surface area of the waste rock. The temperature correction applied for laboratory release rates decreased the differences with the field scale. Additionally, the temperature seems to have an effect on the type of magnesium carbonate precipitated.

Despite the temperature and surface corrections of the release rates, differences between scales remain. The LSR seems to be the main parameter that has the most effect on the geochemical behavior of ultramafic mine waste. Since column and field cells have similar LSR, their release rates are closers, generally within an order of magnitude. A high LSR increases the magnesium release rate as well as the total

carbon sequestered. Thus, the type of kinetic test used influences the carbonation dynamics of the tailings.

Overall, this study strengthens the hypothesis that the LSR and temperature are important parameters that influence the geochemical behavior of ultramafic mine wastes. However, column tests are most suited to reproduce the observed field release rates.

Acknowledgments

The authors thank RNC Minerals and the Natural Sciences and Engineering Research Council (NSERC) for their contributions to a Research and Collaborative Grant, the Research Institute in Mining and Environment (RIME-UQAT) and RNC Minerals staff.

References

Ardau, C., Blowes, D. W., & Ptacek, C. J. (2009). Comparison of laboratory testing protocols to fi eld observations of the weathering of sul fi de-bearing mine tailings. Journal of Geochemical Exploration, 100(2–3), 182–191. http://doi.org/10.1016/j.gexplo.2008.06.005

Assima, G. P., Beaudoin, G., & Molson, J. (2012). CO2 Sequestration in Chrysotile Mining Residues: Implication of Watering and Passivation under Environmental Conditions. Industrial & Engineering Chemistry Research, 2–10. http://doi.org/10.1021/ie202693q

Assima, G. P., Larachi, F., Molson, J., & Beaudoin, G. (2014). Comparative study of five Québec ultramafic mining residues for use in direct ambient carbon dioxide mineral sequestration. Chemical Engineering Journal, 245, 56–64. http://doi.org/10.1016/j.cej.2014.02.010

ASTM Standard D4892, (2014). Standard test method for density of solid pitch (Helium Pycnometer Method). West Conshohocken, PA, (www.astm.org)

ASTM Standard D6913-04 (2009) Standard test methods for particle-size distribution (gradation) of soils using sieve analysis. Annual Book of ASTM Standards vol 0409

ASTM. 2007. D5744-07, (2007) Standard Test Method for Accelerated Weathering of Solid Materials Using a Humidity Cell. Annual Book of ASTM Standards

Bea, S.A., Wilson, S.A., Mayer, K. U., Dipple, G. M., Power, I. M., & Gamazo, P. (2012). Reactive Transport Modeling of Natural Carbon Sequestration in Ultramafic Mine Tailings. Vadose Zone Journal, 11(2). http://doi.org/10.2136/vzj2011.0053

Beaudoin, G., Hébert, R., & Constantin, M. (2008). Spontaneous carbonation of serpentine in milling and mining waste, southern Québec and Italy. Proceedings of Accelerated Carbonation for Environmental and Materials Engineering (ACEME2008). Retrieved from http://scholar.google.com/scholar?hl=en&btnG=Search&q=intitle:Spontaneous+carbonation+of+serpentine+in+milling+and+mining+waste,+Southern+Quebec+and+Italy#0

Beinlich, A., & Austrheim, H. (2012). In situ sequestration of atmospheric CO2 at low temperature and surface cracking of serpentinized peridotite in mine shafts. Chemical Geology, 332–333, 32–44. http://doi.org/10.1016/j.chemgeo.2012.09.015

Benzaazoua, M., Bussière, B., Dagenais, A. M., & Archambault, M. (2004). Kinetic tests comparison and interpretation for prediction of the Joutel tailings acid generation potential. Environmental Geology, 46(8), 1086-1101.

Blowes, D. W., Ptacek, C. J., Jambor, J. L., Weisener, C. G., Paktunc, D., Gould, W. D., & Johnson, D. B. (2003). The Geochemistry of Acid Mine Drainage. Treatise on

Geochemistry: Second Edition, 11, 131–190. http://doi.org/10.1016/B978-0-08-095975-7.00905-0

Bouzahzah, H., Benzaazoua, M., Plante, B., & Bussiere, B. (2015). A quantitative approach for the estimation of the " fi zz rating " parameter in the acid-base accounting tests : A new adaptations of the Sobek test. Journal of Geochemical Exploration, 153, 53–65. http://doi.org/10.1016/j.gexplo.2015.03.003

Brunauer, S., Emmett, P.H., Teller, E. (1938). Adsorption of gases in multimolecular layers. J. Am. Chem. Soc. 60 (2), 309–319. http://dx.doi.org/10.1021/ja01269a023.

Bussière, B., Aubertin, M., Mbonimpa, M., Molson, J. W., & Chapuis, R. P. (2007). Field experimental cells to evaluate the hydrogeological behaviour of oxygen barriers made of silty materials. Canadian Geotechnical Journal, 44(3), 245-265.

Carroll, J. J., Slupsky, J. D., & Mather, A. E. (1991). The solubility of Carbon dioxide in water at low pressure. Journal of Physical and Chemical Reference Data, 20(6), 1201–1209.

Chapuis, R.P., and Légaré, P.P. 1992. A simple method for determining the surface area of fine aggregates and fillers in bituminous mixtures. Effects of aggregates and mineral filler on asphalt mixture performance, ASTM STP 1147, pp. 177-186

Cravotta III, C. A. (2008). Dissolved metals and associated constituents in abandoned coal-mine discharges , Pennsylvania , USA . Part 2 : Geochemical controls on constituent concentrations. Applied Geochemistry, 23(2), 203–226. http://doi.org/10.1016/j.apgeochem.2007.10.003

Éthier, M.-P., Bussière, B., Benzaazoua, M., Garneau, P. (2012). Effect of temperature on the weathering of various waste rock types from the Raglan Mine.

Sustainable Infrastructure Development in a Changing Cold Environment conference, Québec, Canada, pp. 800–810

Etschmann, B., Pring, A., Putnis, A., Grguric, B. A., & Studer, A. (2004). A kinetic study of the exsolution of pentlandite (Ni, Fe)$_9$S$_8$ from the monosulfide solid solution (Fe, Ni) S. American Mineralogist, 89(1), 39-50.

Frostadt, S., & Lawrence, R. W. (2005). Determining the weathering charaeteristics of a waste dump with field tests, 19(2), 132–144.

Gras, A., Beaudoin, G., Molson, J.W.H., Plante, B., Lemieux, J.M., Kandji, E. H. B. (2015). Evidence for passive mineral carbonation from carbon isotope geochemistry ofinterstitial air in mine wastes from the Dumont Nickel Project (Abitibi,Quebec). In AGU Fall Meeting, American Geophysical Union. Washington DC, United States.

Hakkou, R., Benzaazoua, M., & Bussière, B. (2008). Acid mine drainage at the abandoned kettara mine (Morocco): 2. mine waste geochemical behavior. Mine Water and the Environment, 27(3), 160–170. http://doi.org/10.1007/s10230-008-0035-7

Hitch, M., Ballantyne, S. M., & Hindle, S. R. (2010). Revaluing mine waste rock for carbon capture and storage. International Journal of Mining, Reclamation and Environment, 24(1), 64–79. http://doi.org/10.1080/17480930902843102

Kandji, E.H.B., Plante, B., Bussière, B., Beaudoin, G., Dupont, P. P. (2017a). Kinetic testing to evaluate the mineral carbonation and metal leaching potential of ultramafic tailings: case study of the Dumont Nickel Project, Amos, Québec. To be published

Kandji, E.H.B., Plante, B., Bussière, B., Beaudoin, G., & Dupont, P. P. (2017b). Geochemical behavior of ultramafic waste rocks with carbon sequestration potential:

a case study of the Dumont Nickel Project, Amos, Québec. Environmental Science and Pollution Research, 1-18.

Langmuir, D. (1965). Stability of Carbonates in the System. The Journal of Geology, 73(5), 730–754.

Lawrence, R. W., & Scheske, M. (1997). A method to calculate the neutralization potential of mining wastes. Environmental Geology, 32(September), 100–106. http://doi.org/10.1007/s002540050198

Malmström, M. E., Destouni, G., Banwart, S. A., & Strömberg, B. H. (2000). Resolving the scale-dependence of mineral weathering rates. Environmental science & technology, 34(7), 1375-1378.

MEND. (2009). MEND report 1.20.1. Prediction manual for drainage chemistry from sulphidic geologie materials. By Priee, W.A. CANMET, Natural resources Canada, Canada

Merkus, H. (2009). Particle size measurements: fundamentals, practice, quality. Particle Technology Series, 17(Springer), 519. http://doi.org/ISBN 978-1-4020-9016-5

Morin, K., Hutt, N., & Ferguson, K. (1995). Measured rates of sulfide oxidation and acid neutralization in kinetic test - Statistical lessons from the database. Conference on Mining and the Environment

Nicholson, R.V., Gillham, R.W., Reardon, E.J. (1988). Pyrite oxidation in carbonate-buffered solution: 1. Experimental kinetics. Geochim. Cosmochim. Acta 52, 1077–1085

Nordstrom, D. K., Blowes, D. W., & Ptacek, C. J. (2015). Hydrogeochemistry and microbiology of mine drainage: An update. Applied Geochemistry, 57, 3-16.

Nordstrom, D. K., & Alpers, C. N. (1999). Negative pH, efflorescent mineralogy, and consequences for environmental restoration at the Iron Mountain Superfund site, California. In Proceedings of the National Academy of Sciences (Vol. 96, pp. 3455–3462)

Oskierski, H. C., Dlugogorski, B. Z., & Jacobsen, G. (2013). Sequestration of atmospheric CO2 in chrysotile mine tailings of the Woodsreef Asbestos Mine, Australia: Quantitative mineralogy, isotopic fingerprinting and carbonation rates. Chemical Geology, 358, 156–169. http://doi.org/10.1016/j.chemgeo.2013.09.001

Plante, B., Benzaazoua, M., & Bussie, B. (2011). Predicting Geochemical Behaviour of Waste Rock with Low Acid Generating Potential Using Laboratory Kinetic Tests, 2–21. http://doi.org/10.1007/s10230-010-0127-z

Plante, B., Bussière, B., & Benzaazoua, M. (2014). Lab to field scale effects on contaminated neutral drainage prediction from the Tio mine waste rocks. Journal of Geochemical Exploration, 137, 37–47. http://doi.org/10.1016/j.gexplo.2013.11.004

Price, W, Morin, K, Hutt, N. (1997). Guidelines for the prediction of acid rock drainage and metal leaching for mines in british columbia: Part II. Recommended procedures for static and kinetic tesing. In Fourth International Conference on Acid Rock Drainage (p. 16). Vancouver, B.C. Canada.

Pronost, J., Beaudoin, G., Lemieux, J. M., Hébert, R., Constantin, M., Marcouiller, S., … Maldague, X. (2012). CO2-depleted warm air venting from chrysotile milling waste (Thetford Mines, Canada): Evidence for in-situ carbon capture from the atmosphere. Geology, 40(3), 275–278. http://doi.org/10.1130/G32583.1

Pronost, J., Beaudoin, G., Tremblay, J., Larachi, F., Duchesne, J., Hébert, R., & Constantin, M. (2011). Carbon sequestration kinetic and storage capacity of

ultramafic mining waste. Environmental Science & Technology, 45(21), 9413–20. http://doi.org/10.1021/es203063a

Rietveld HM, (1993). The Rietveld method. Oxford University Press, (Oxford, UK).

RNC, (2013). Technical Report on the Dumont Ni Project , Launay and Trécesson Townships , Quebec , Canada

Sapsford, D. J., Bowell, R. J., Dey, M., & Williams, K. P. (2009). Humidity cell tests for the prediction of acid rock drainage. Minerals Engineering, 22(1), 25-36.

SRK, (1989). Draft Acid Rock Drainage Technical Guide, Vancouver, Canada.

Villeneuve, M., Bussière, B., Benzaazoua, M., & Aubertin, M. (2009). Assessment of interpretation methods for kinetic tests performed on tailings having a low acid generating potential. 8th International Conference on Acid Rock Drainage, 8th Intern, 1–11.

White, A. F., & Brantley, S. L. (1995). Chemical weathering ates of silicate minerals: an overview. Chemical Weathering Rates of Silicate Minerals, 31, 1–22.

Wilson, S. a., Harrison, A. L., Dipple, G. M., Power, I. M., Barker, S. L. L., Ulrich Mayer, K., … Southam, G. (2014). Offsetting of CO2 emissions by air capture in mine tailings at the Mount Keith Nickel Mine, Western Australia: Rates, controls and prospects for carbon neutral mining. International Journal of Greenhouse Gas Control, 25, 121–140. http://doi.org/10.1016/j.ijggc.2014.04.002

Wilson, S. A., Dipple, G. M., Power, I. M., Barker, S. L. L., Fallon, S. J., & Southam, G. (2011). Subarctic weathering of mineral wastes provides a sink for atmospheric CO2. Environmental Science and Technology, 45(18), 7727–7736. http://doi.org/10.1021/es202112y

Wilson, S. a., Dipple, G. M., Power, I. M., Thom, J. M., Anderson, R. G., Raudsepp, M., … Southam, G. (2009a). Carbon dioxide fixation within mine wastes of ultramafic-hosted ore deposits: Examples from the Clinton Creek and Cassiar Chrysotile deposits, Canada. Economic Geology, 104(1), 95–112. http://doi.org/10.2113/gsecongeo.104.1.95

Wilson, S. a., Raudsepp, M., & Dipple, G. M. (2009b). Quantifying carbon fixation in trace minerals from processed kimberlite: A comparative study of quantitative methods using X-ray powder diffraction data with applications to the Diavik Diamond Mine, Northwest Territories, Canada. Applied Geochemistry, 24(12), 2312–2331. http://doi.org/10.1016/j.apgeochem.2009.09.018

Wilson, S. A., Raudsepp, M., & Dipple, G. M. (2006). Verifying and quantifying carbon fixation in minerals from serpertine-rich mine tailings using the Rietveld method with X-ray powder diffraction data. American Mineralogist, 91(8–9), 1331–1341. http://doi.org/10.2138/am.2006.2058

Xia, F., Pring, A., & Brugger, J. (2012). Understanding the mechanism and kinetics of pentlandite oxidation in extractive pyrometallurgy of nickel. Minerals Engineering, 27, 11-19.

Zarandi, A.E., Beaudoin, G., Plante, B., & Sciortino, M. (2016). Multivariate study of the dynamics of CO2 reaction with brucite-rich ultramafic mine tailings. International Journal of Greenhouse Gas Control, 52, 110–119. http://doi.org/10.1016/j.ijggc.2016.06.022

CHAPITRE V

DISCUSSION

Dans ce chapitre, l'influence de la carbonatation des rejets de concentrateur de Dumont sur son potentiel de neutralisation (PN) sera discutée. Dans la deuxième section de ce chapitre, une approche d'entreposage des matériaux de Dumont est proposée afin de promouvoir la séquestration passive du carbone des matériaux de Dumont. L'approche proposée ici est basée sur les résultats de cette thèse et sur les connaissances acquises ces dernières années sur la carbonatation passive des rejets ultramafiques.

5.1 Carbonatation des rejets de concentrateur de Dumont : Implications sur le potentiel de neutralisation (PN)

5.1.1 Introduction

Lors des premières étapes d'un projet minier en développement, le potentiel de génération d'acide des rejets est généralement évalué en faisant le bilan acide-base (Aubertin *et al.* 2002). Cette évaluation est réalisée sur des échantillons frais (non altérés) obtenus lors des essais métallurgiques sur des carottes de forage et sur des échantillons en vrac. Les tests statiques sont de ce point de vue très importants et il est alors primordial de déterminer le plus précisément possible le potentiel de génération d'acide des rejets. Cependant, ces rejets sont amenés à s'altérer et à changer dans le temps. L'oxydation des sulfures et la dissolution des minéraux neutralisants induisent alors une variation du potentiel d'acidité (PA) et du potentiel de neutralisation (PN), ce qui peut modifier le bilan acide-base. De ce point de vue, il

est important de bien connaitre les rejets étudiés et leurs propriétés afin de s'assurer que les réponses des essais statiques aillent dans le sens prédit initialement.

Les rejets miniers subissent une diminution de leur potentiel de neutralisation lors de leur altération. L'amplitude de cette diminution dépend de l'ampleur de l'altération des rejets. En effet, l'acidité générée par l'oxydation des sulfures consomme les minéraux neutralisants. Cependant, l'altération des rejets riches en minéraux séquestreurs de carbone conduit à la précipitation de carbonates secondaires (Wilson *et al.* 2014, 2009a, b; Beaudoin *et al.* 2008; Beinlich et Austrheim, 2012; Oskierski *et al.* 2013). Ainsi, on peut faire l'hypothèse que le PN de rejets miniers ultramafiques peut augmenter au fur et à mesure de la séquestration de CO_2. L'objectif est de cette section est de comparer les PN de résidus de Dumont, initial et post-essais en colonne afin de mieux comprendre son évolution.

5.1.2 Matériel et Méthodes

Pour simplifier, seul le cas des rejets de concentrateur de Dumont est traité ici et non des matériaux grossiers (stériles et lithologies). La méthode d'échantillonnage, les essais de caractérisation, la description des essais cinétiques et tous les résultats sont déjà présentés dans le chapitre II sur le comportement géochimique des rejets de concentrateur de Dumont.

Les méthodes de détermination du PN considérées dans cette section sont le potentiel de neutralisation des carbonates (PNC; Frostad *et al.* 2003), celle de Sobek modifié (Lawrence et Wang, 1997), ainsi que les méthodes dites « minéralogiques » de Lawrence et Scheske (1997) et de Paktunc, (1999). Une brève description de ces méthodes de détermination du PN est présentée dans les paragraphes suivantes.

Méthode du PNC :

La méthode du pouvoir de neutralisation des carbonates (PNC; Lawrence *et al.* 1989; Frostad *et al.* 2003) est basée sur les résultats de l'analyse de carbone et est exprimée en équivalent de $CaCO_3$/t. Cependant, cette méthode ne tient en compte que le potentiel de neutralisation des carbonates (e.g. calcite, dolomite, magnésite, sidérite) et pas du potentiel de neutralisation des silicates ou des hydroxydes. De ce point de vue, cette méthode peut sous-estimer le PN des rejets ultramafiques. Le PNC est calculé selon l'Équation 5.1.

$$PNC = 83{,}3 \times \%\, C \qquad (5.1)$$

Méthode PN de Sobek modifié (Lawrence et Wang, 1997):

La méthode de Sobek originale (1978) était abondamment utilisée pour évaluer le potentiel de génération d'acide des rejets miniers. Cette méthode consiste à ajouter un excès d'acide (HCl) sur un échantillon du rejet en suspension avec quelques ml d'eau distillée et portée à ébullition. Par la suite, un titrage en retour est réalisé avec du NaOH pour neutraliser l'excès d'acide. Le pH de fin de titrage pour cette méthode est de 7. La méthode modifiée par Lawrence et Wang (1997) ramène le pH de fin de titrage de 7 à 8,3 et supprime l'étape de chauffage de la suspension afin de ne pas exagérer la réaction de certains minéraux (Lapakko 1994; Frostad et al. 2003). La méthode modifiée propose aussi un ajout en trois étapes de l'acide et en plus faibles quantités.

PN minéralogiques de Lawrence et Scheske, (1997) et de Paktunc, (1999)

Les essais de détermination du PN par des méthodes chimiques ont souvent des limites liées au fait qu'ils ne tiennent pas compte de la minéralogie des rejets ainsi que des cinétiques de réactions des minéraux présents dans un rejet. Ainsi afin de mieux statuer sur le potentiel de génération d'acide des rejets miniers, l'utilisation de

la minéralogie a alors été suggérée afin d'évaluer la contribution sur le PN ou le PA de chaque phase minérale prise individuellement. Une revue des différentes méthodes est présentée dans Bouzahzah (2013).

Deux méthodes de PN minéralogiques seront considérées dans cette étude : celle de Lawrence et Scheske (1997) et de celle de Paktunc (1999). Lawrence et Scheske (1997) utilisent les réactivités relatives des minéraux proposées par Kwong (1993) pour calculer les PN alors que la méthode de Paktunc (1999) utilise le nombre de moles de chaque minéral neutralisant nécessaire pour neutraliser une mole d'H_2SO_4. La fiabilité des méthodes de détermination des PN minéralogiques dépend fortement de la précision de la détermination de la composition minéralogique. Les équations qui permettent de calculer le PN selon les méthodes de Lawrence et Scheske (1997) et de Paktunc sont données dans les Équations 5.2 et 5.3, respectivement.

$$PN = \frac{1000kg}{t} \times M_{CaCO3} \cdot \sum_{i=1}^{n} \frac{C_{Mi}}{M_{Mi}} R_i \tag{5.2}$$

Où M_{CaCO3} est la masse molaire de la calcite, M_{Mi} est la masse molaire du minéral i (g/mol), C_{Mi} est la concentration du minéral i (% massique) et R_i est le facteur de réactivité du minéral i.

$$PN = \sum_{i=1}^{k} \frac{10X_i\omega_a}{\omega_i n_{Mi}} \tag{5.3}$$

Dans l'équation 5.3, ω_a et ω_i représentent les masses molaires de l'acide sulfurique et du minéral i, respectivement. *Xi* est le pourcentage massique du minéral i dans le rejet et n_{Mi} est un facteur stœchiométrique (nombre de moles du minéral i requise pour neutraliser une mole de H_2SO_4). Les résultats du PN par la méthode de Paktunc sont généralement exprimés en kg de H_2SO_4/t mais pour faciliter la comparaison, le PN a été converti en kg de $CaCO_3$ par tonne de rejets. De plus, seules les contributions de

la brucite et des carbonates ont été considérées, puisque la contribution des silicates est surestimée avec cette méthode (Plante *et al.* 2012).

Pour les besoins du calcul des PN minéralogiques, le % de carbone des rejets est converti en hydromagnésite. En posant l'hypothèse que le Mg de l'hydromagnésite provient exclusivement de la dissolution de la brucite, la quantité de Mg dans l'hydromagnésite est retranchée de la brucite initiale dans les rejets afin d'estimer la quantité de brucite résiduelle dans les échantillons altérés. Pour la minéralogie complète des résidus de Dumont, se référer au chapitre II.

Le lecteur intéressé pourra apprendre davantage sur les principes, les limites et avantages des principaux essais statiques dans Plante (2004), Bouzahzah (2013) et Parbhakar-Fox et Lottermoser (2015).

5.1.3 Résultats et discussion

Le Tableau 5.1 regroupe les résultats des PN des résidus de Dumont frais et altérés (issus du démantèlement de la colonne de résidus). Le PNC, qui est fonction de la quantité de carbone total dans les rejets, augmente avec le degré d'altération des rejets. Le PNC du matériel altéré est de 2 à 6 fois supérieure à la valeur initiale. D'après cette méthode de calcul du PN, plus les rejets de Dumont sont altérés, plus son potentiel de neutralisation augmente. Cependant, comme indiqué plutôt, ce PN ne prend pas en compte le potentiel de neutralisation des silicates et surtout celui de la brucite, qui est aussi réactive que les carbonates. Le PN obtenu par la méthode de Sobek modifiée par Lawrence et Wang (1997) indique une diminution du PN d'environ 20 % dans les deux premiers cm de la colonne, alors qu'en profondeur, le PN a tendance à revenir à la valeur initiale (191 kg $CaCO_3$/t) avec des différences de 3 % seulement. Les PN de Lawrence and Scheske (1997) et de Paktunc (1999) qui sont basés sur la minéralogie, suivent la même tendance que pour la méthode de Sobek modifiée, mais avec des écarts plus prononcés (environ 20 à 40 % de différence).

Les faibles valeurs du PNC s'expliquent par le fait que la méthode ne tient en compte que le potentiel de neutralisation des carbonates alors que les rejets de Dumont contiennent majoritairement de la serpentine et de la brucite. Au contraire, les contributions de ces minéraux sont prises en compte avec la méthode minéralogique de Lawrence et Scheske, (1997), qui donne donc des résultats supérieurs au PNC. La contribution des silicates ayant été exclue du calcul du PN par la méthode de Paktunc, (1999) car irréaliste, le PN par cette méthode est donc plus faible que celui de Lawrence et Scheske, (1997). La principale limite de la méthode de Sobek modifiée par Lawrence et Wang, (1997) est le fait que la durée de l'essai est trop courte pour permettre à la serpentine et aux carbonates de magnésium hydratés de réagir complètement. Cependant, après l'altération des rejets, le PN de Sobek modifié devient supérieur aux PN calculés avec les méthodes minéralogiques.

Tableau 5.1 Compilation du Pouvoir de neutralisation (PN) des résidus de Dumont frais et des rejets issus du démantèlement de la colonne

	% C	PNC (kg de $CaCO_3$/t)	PN de Sobek modifié par Lawrence et Wang, 1997 (kg de $CaCO_3$/t)	PN minéralogique de Lawrence et Scheske, 1997 (kg de $CaCO_3$/t)	PN minéralogique de Paktunc, 1999 (kg de $CaCO_3$/t)
Résidus de Dumont frais	0,15	12	191	211	205
Résidus altérés (0 – 2 cm)	0,83	69	147	129	123
Résidus altérés (2 – 4 cm)	0,46	39	175	160	154
Résidus altérés (4 – 6 cm)	0,36	30	189	169	162
Résidus altérés (6 – 8 cm)	0,36	30	190	169	162
Résidus altérés (8 – 10 cm)	0,37	31	188	167	161
Résidus altérés (10 – 17 cm)	0,31	26	186	173	167
Résidus altérés (17 – 24 cm	0,32	26	188	172	166

La tendance générale indique que le potentiel de neutralisation des résidus de Dumont diminue avec le degré d'altération des résidus, malgré la présence des carbonates secondaires (l'altération étant plus importante en surface qu'en profondeur). Cette diminution s'explique par le fait que les carbonates remplacent principalement la brucite et, dans une moindre mesure, la serpentine. Or, la brucite est aussi réactive, sinon plus que les carbonates (Lawrence et Scheske, 1997), tel que montré à la Figure 5.1. La contribution de la brucite est donc importante à considérer dans le PN des rejets de Dumont. La consommation de la brucite dans les rejets devrait donc induire une diminution du PN dans les rejets de Dumont. De même, les carbonates formés peuvent normalement contribuer au PN au même titre que les carbonates primaires fréquemment rencontrés comme la calcite, la dolomite et la magnésite.

Cependant, Wilson *et al.* (2009b) ont suggéré, dans leur étude sur les rejets ultramafiques de Diavik, une augmentation du PN de 1 à 2 % attribuable à la formation des carbonates secondaires dont la nesquehonite (estimation du PN basée sur la méthode de Lawrence et Scheske, 1997). Il faut cependant préciser que les rejets de la mine Diavik ne contenaient pas de brucite. Les minéraux responsables de la précipitation des carbonates étaient la serpentine et la forstérite, qui sont moins réactives que les carbonates (Figure 5.1). On peut alors suggérer que lorsque c'est la serpentine qui s'altère pour former des carbonates, on peut s'attendre à avoir une augmentation du PN équivalent à la quantité de carbonate formée. Par contre, il semble que la présence de la brucite dans les rejets ultramafiques ne permettrait pas d'avoir une augmentation nette du PN, puisque la brucite est consommée pour former les carbonates.

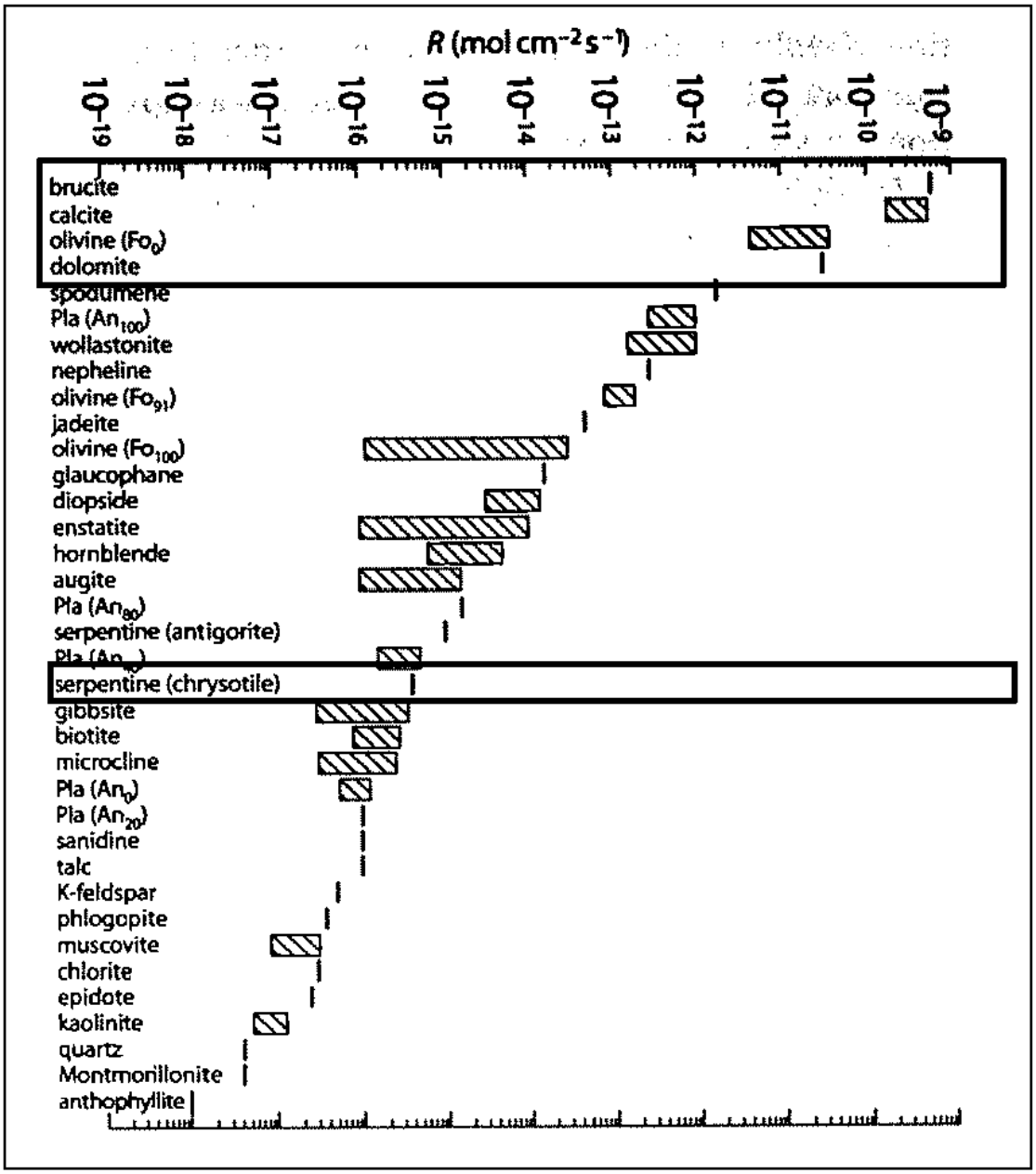

Figure 5.1 Vitesses de dissolution à pH 5 de différents minéraux (Tirée de Paktunc, 1999)

Une méthode de détermination du PN qui aurait pu permettre d'évaluer le PN des rejets de Dumont de la manière la plus précise et qui permettrait la réaction complète

des silicates et des carbonates néoformés est la méthode proposée par Bouzahzah *et al.* (2015). Cette méthode consiste en une addition séquentielle d'acide chlorhydrique jusqu'à stabilisation du pH à une valeur de 2.0. Avant de faire un titrage en retour, un ajout de H_2O_2 est réalisé afin de favoriser l'oxydation et l'hydrolyse du fer. Cette méthode possède l'avantage de permettre la dissolution complète des carbonates et des silicates, ainsi que l'oxydation et l'hydrolyse du fer, ce qui permet d'avoir une estimation plus réaliste du PN des rejets miniers. Cette méthode a été utilisée pour déterminer un PN des résidus de Dumont. Cependant, après plus de deux mois d'ajouts de HCl, le pH ne s'était pas stabilisé et l'essai a finalement été abandonné. Il serait pertinent de le reprendre mais cette fois sous une atmosphère exempte de CO_2 afin de limiter l'influence de la dissolution du CO_2 lors de l'essai.

5.2 Suggestions afin de favoriser la carbonatation des matériaux de Dumont

5.2.1 Quelques rappels sur les acquis de la carbonatation des rejets ultramafiques

Les résultats des essais en mini-cellules présentés au chapitre 2 suggèrent que la carbonatation des rejets de concentrateur de Dumont plafonne à environ 1 % de carbone lorsque la fraction disponible de brucite est consommée en surface des résidus. Ces résultats suggèrent que la brucite est le principal minéral impliqué dans la carbonatation des matériaux de Dumont et que la contribution de la serpentine est faible, voire négligeable. Dans les conditions des essais en mini-cellules, la brucite disponible est consommée et remplacée par l'hydromagnesite entre 28 et 59 jours. Ce résultat corrobore les conclusions de Pronost *et al.* (2011), Assima *et al.* (2014c), de Wilson *et al.* (2014) et de Zarandi *et al.* (2016). D'ailleurs, l'approche proposée par Wilson *et al.* (2014) pour augmenter le potentiel de carbonatation des rejets de Mount Keith (Australie) repose sur cette observation.

L'importance du degré de saturation en eau dans la vitesse de carbonatation des matériaux de Dumont a été précisée par Awoh *et al.* (2013) et par Assima *et al.* (2013a; 2012) via des protocoles différents. Ces résultats démontrent qu'une

saturation complète entrave la diffusion du CO_2, alors que l'absence d'eau ne permettrait pas la dissolution de la serpentine et de la brucite. Une saturation partielle des rejets ainsi qu'un arrosage périodique augmenteraient les taux de carbonatation passive (Assima *et al.* 2012). Les auteurs suggèrent aussi que la fréquence d'arrosage a un effet sur la passivation des surfaces des minéraux réactifs (Assima *et al.* 2012). Les travaux de Assima (2014c) ont également démontré que le rendement de la carbonatation dépendait à la fois de la taille des grains et de leur composition minéralogique. Les particules les plus fines se dissolvent très rapidement alors que pour les particules grossières, la carbonatation est limitée en surface. De même, la présence de fer dans le résidu minier induit une baisse de son potentiel de séquestration du CO_2 à cause de son oxydation et de sa précipitation sous forme d'hydroxyde qui peut inhiber la surface des minéraux réactifs. Tous ces facteurs sont à prendre en considération si on veut profiter du plein de potentiel de séquestration du CO_2 par les matériaux de Dumont et des rejets miniers ultramafiques en général.

A partir de ces considérations, Assima *et al.* (2014b) ont proposé un concept (Figure 5.2) de déposition qui permettrait de faciliter le drainage et la diffusion du CO_2. Ils préconisent aussi une récupération des eaux de drainage déjà riches en Mg et en CO_2 pour les recirculer sur les empilements, particulièrement durant les périodes sèches.

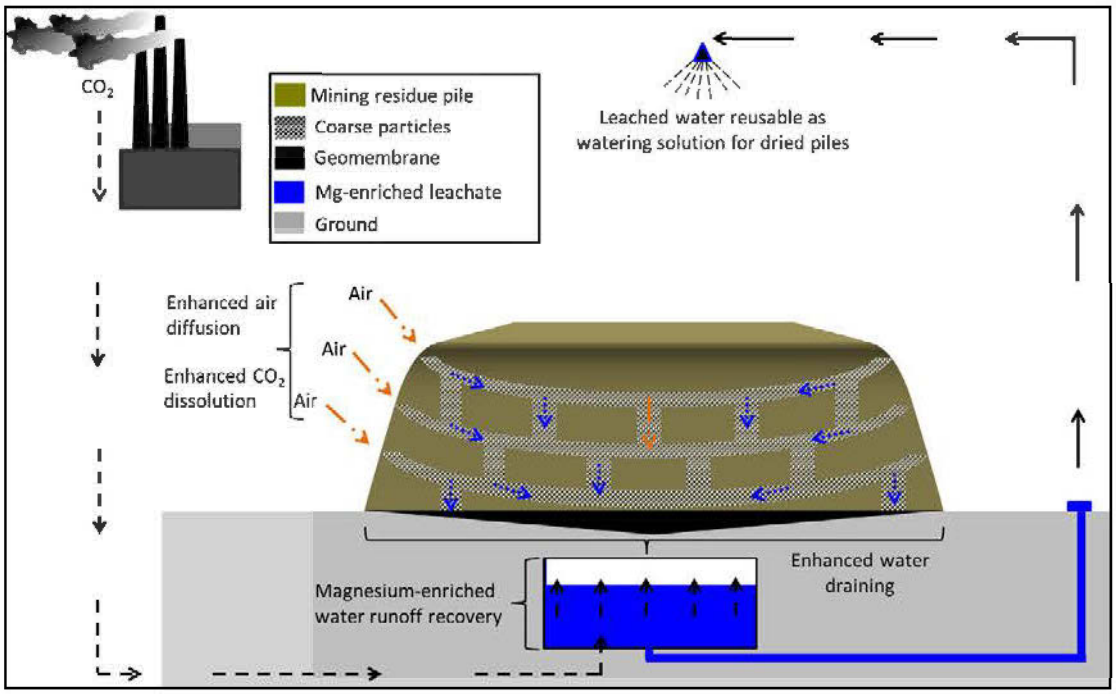

Figure 5.2 Schéma d'un tas de résidus miniers disposé afin d'améliorer la diffusion de l'air et la séquestration minérale du CO_2 (Assima *et al.* 2014c)

Pour augmenter le taux de carbonatation des rejets de Mount Keith, Wilson *et al.* (2014) ont suggéré une stratégie de déposition échelounée, avec pour objectif de maximiser le temps d'exposition des rejets afin de permettre la carbonatation de la brucite. La fréquence de déposition présentée la (Figure 5.3) est basée sur une estimation de la vitesse de carbonatation de la brucite dans les premiers deux cm de la pile de résidus. La carbonatation complète de la brucite des rejets de concentrateur de Mount Keith permettrait de compenser jusqu'à 60 % des émissions de gaz à effet serre de la mine (Wilson *et al.* 2014). La Figure 5.3 indique, par exemple, qu'avec une déposition des résidus de Mount Keith à une vitesse de 190 cm par aunée, plus de 80 % de la brucite ne sera pas convertie en carbonates, alors qu'une vitesse de déposition de 10 cm/aunée permettrait la carbonatation de la quasi-totalité de la brucite.

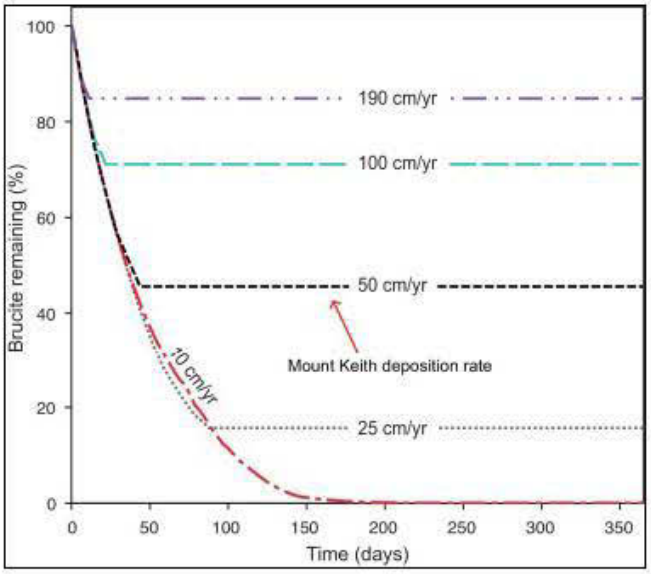

Figure 5.3 Quantité de brucite restante sur une épaisseur de 2 cm de résidus en fonction du temps, à différentes fréquences de déposition des résidus (Wilson *et al.* 2014)

5.2.2 Approche pour favoriser la carbonatation passive des rejets de Dumont

Les futurs rejets du projet Dumont ont un potentiel de séquestration de carbone important. Théoriquement, de par sa forte teneur en brucite (11 % dans les résidus et environ 6 % dans les stériles), les matériaux de Dumont possèdent un potentiel de séquestration de CO_2 beaucoup plus important que celui des autres mines mentionnées jusqu'ici. Par exemple, les rejets de Mount Keith ne contiennent que 2,5 % de brucite. L'exploitation du gisement de Dumont devrait produire un peu plus de 1 gigatonne de rejets de concentrateur, sur 33 ans. La carbonatation du dixième de la teneur en brucite des résidus (une carbonatation d'environ 1 % de brucite en absolu) permettrait de séquestrer plus de 6 millions de tonnes de CO_2, soit plus de 180 000 tCO_2/an, alors que la mine prévoit émettre, en moyenne, 127 700 tCO_2eq/an (communication personnelle). Il est alors possible de croire que la carbonatation des

rejets de Dumont pourrait compenser les émissions des activités de la mine sur les 33 ans. Cependant, pour profiter pleinement de ce potentiel de séquestration du CO_2 par les rejets de Dumont, il faudrait reconsidérer les méthodes de déposition des rejets miniers (stériles et résidus) conventionnellement utilisées afin de favoriser la carbonatation du 1 % de brucite considéré.

Avant de parler d'une approche de gestion des rejets qui pourrait favoriser leur carbonatation, il serait pertinent de rappeler quelques caractéristiques physiques des rejets miniers. Généralement, les rejets de concentrateur sont déchargés sous forme de pulpe et se retrouvent la plupart du temps saturés, voire même ennoyés. Ils sont composés de particules fines, avec une granulométrie comprise généralement entre 2 et 80 µm (Bussiere, 2007; Aubertin *et al.* 2002). Les rejets de concentrateur ont une faible porosité et une faible conductivité hydraulique saturée (*ksat*) qui se situe généralement entre 10^{-4} et 10^{-7} cm/s (Bussière, 2007). Ces conditions ne favorisent pas un drainage rapide et une diffusion importante des gaz. Par conséquent, la carbonatation de rejets de concentrateur ultramafiques sera très limitée dans ces conditions.

Les stériles sont, quant à eux, plus grossiers et entreposés en surface sous forme d'empilements (appelés haldes) de dimensions pouvant être considérables, surtout pour les opérations minières à ciel ouvert. Les caractéristiques de ces haldes (dimensions, distribution granulométrique, hétérogénéité) peuvent différer selon la méthode de déposition utilisée. Ces paramètres ont un effet sur le mouvement de l'eau et des gaz dans les haldes (Aubertin *et al.* 2002; Amos *et al.* 2015). Généralement, les méthodes de déposition génèrent une hétérogénéité au niveau de la répartition des stériles. De par leur granulométrie, les empilements de stériles ont une porosité importante et, par conséquent, une perméabilité qui induit un apport important de flux d'air, contrairement aux parcs à résidus. La principale limite qu'on peut déceler (par rapport à leur carbonatation) c'est que l'apport en eau dans les

haldes à stériles se fait au gré des précipitations (absence d'eau de procédés) et avec un drainage relativement rapide, ce qui fait que la teneur en eau des stériles est relativement faible par rapport à celle des rejets de concentrateur. Notons que le *ksat* dans les empilements de stériles varie généralement entre 10^{-1} à 10^{-4} cm/s (Bolduc, 2012; Bussière, 2007). Elle peut aussi diminuer avec la compaction.

Ces méthodes de déposition sont généralement adoptées pour satisfaire des besoins de stabilité physique (prévention des ruptures de digues) et géochimique (prévention de l'oxydation des sulfures) des rejets. Pour plus de détails sur les méthodes de déposition des résidus et des stériles, le lecteur intéressé trouvera une description détaillée dans Bussière (2007), Aubertin *et al.* (2002) et Vick (1990).

Les méthodes de stockage conventionnelles des résidus et des stériles ne permettent pas l'atteinte du plein potentiel de carbonatation des rejets ultramafiques de Dumont. Pour favoriser la carbonatation passive des rejets ultramafiques de Dumont, voici quelques caractéristiques qu'on devrait idéalement avoir pour le stockage des rejets :

- Des rejets ayant une granulométrie la plus fine possible;
- Des rejets partiellement saturés et maintenus proches de la saturation optimale de carbonatation (degré de saturation maintenu entre 20 et 60 %);
- Un apport en gaz (CO_2) important;
- Une surface d'exposition la plus importante possible et une faible épaisseur des couches de rejets;
- Une fréquence de déposition des rejets de concentrateur la plus faible possible;

- Un climat qui permet une alternance de cycles de séchage et de mouillage pour permettre les processus de dissolution et de précipitation des minéraux primaires et secondaires.

La méthode de déposition des résidus de Dumont devrait être réalisée de manière à favoriser un drainage des eaux de procédés, afin d'éviter l'ennoiement des résidus et de les maintenir dans une saturation idéale : pores partiellement saturés permettant la diffusion du CO_2, et présence d'eau pour permettre la dissolution des minéraux séquestreurs de carbone.

Ce qui est proposé ici est une combinaison des approches de Wilson *et al.* (2014) et de Assima *et al.* (2014b). De plus, ces deux approches peuvent être intégrées dans une configuration de co-disposition des deux types de rejets. La co-disposition est une approche qui a été suggérée ces dernières années surtout pour des aspects géotechniques (James *et al.* 2015; Ferdosi *et al.* 2015a, 2015b; James et Aubertin, 2012; Aubertin *et al.* 2002). Les stériles sont rigides et perméables, alors que c'est tout le contraire pour les résidus. Une combinaison des deux types de rejets permettrait alors d'utiliser les propriétés physiques favorables des stériles afin d'améliorer le drainage des résidus et par la même occasion, accroitre la résistance mécanique des ouvrages (James *et al.* 2015, 2013; Bolduc et Aubertin, 2014). Un exemple de parc à résidus avec des inclusions de stériles est illustré dans la Figure 5.4.

La méthode de co-disposition des résidus avec des inclusions de stériles ou même un mélange résidus-stériles semble être une approche qui permettrait de satisfaire certains critères cités plus haut. La carbonatation des résidus ultramafiques pourrait être favorisée dans une configuration de co-disposition. La technique consiste à placer d'abord une couche de stériles sur le fond et sur les côtés, avant de faire les premières dépositions de résidus. Par la suite, des inclusions sont réalisées de façon progressive afin de compartimenter les résidus (James *et al.* 2015). Les fréquences de

rehaussement et de déposition des résidus, ainsi que les dimensions du parc, peuvent être définies afin de favoriser un temps d'exposition suffisant pour carbonater le maximum de brucite.

Le concept de cette approche pourrait être optimisée davantage. En effet, le compartimentage des résidus peut offrir à la mine une certaine flexibilité au niveau des fréquences de déposition. Une utilisation par alternance des compartiments permettrait d'augmenter le temps d'exposition des résidus. Ainsi, certains compartiments seraient alimentés pendant que d'autres ne le seraient pas.

De plus, dans la méthode de co-disposition, les premières couches de stériles déposées au fond du parc seront moins exposées aux conditions atmosphériques. Dans cette situation, on peut privilégier l'utilisation des lithologies non réactives par rapport au CO_2, à savoir le gabbro et volcanique pour le projet Dumont, pour construire ces premières couches.

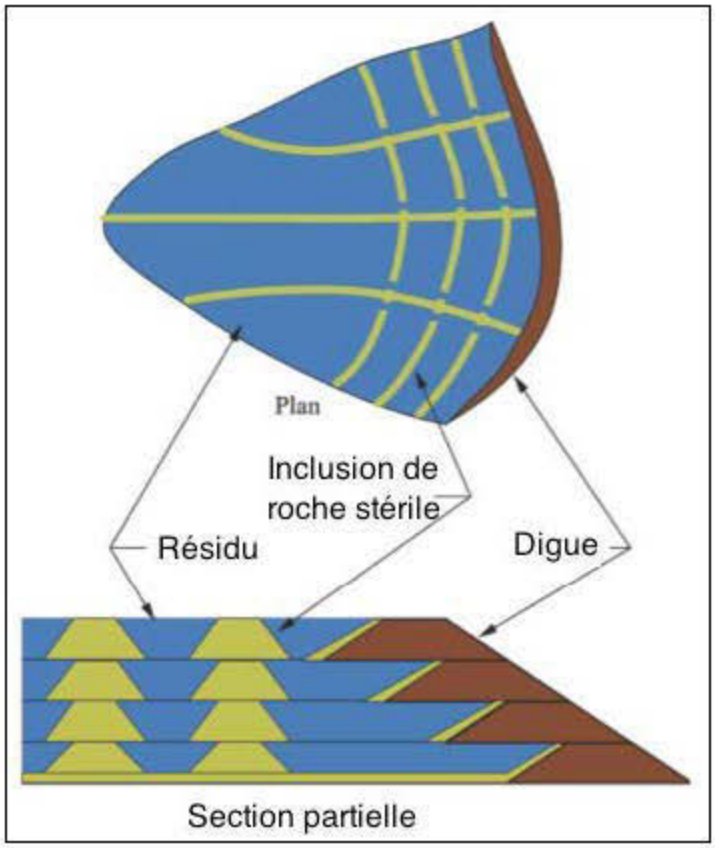

Figure 5.4 Illustration conceptuelle d'un bassin de résidus avec inclusions de roches stériles (tirée de Bolduc, 2012)

Afin de faciliter le drainage des rejets de concentrateur de Dumont dans l'approche proposée ici, les résidus peuvent être filtrés, ce qui permettrait de réduire considérablement les quantités d'eau présentent dans les résidus (avec un pourcentage solide de plus de 85 %) (Bussière, 2007). Cependant, pour les résidus de Dumont, un filtrage moins poussé permettrait de rehausser un peu plus la teneur en eau des résidus.

Une description des processus physiques et géochimiques impliqués est présentée de manière simplifiée à la Figure 5.5. Du fait de leur perméabilité supérieure aux rejets de concentrateur, les inclusions de stériles permettraient un meilleur accès au CO_2

ainsi qu'une alimentation en eau suffisante pour favoriser les processus de carbonatation des résidus et des stériles, comme le montre la Figure 5.6 proposée par Wilson *et al.* (2014). De plus, à cause du caractère exothermique des réactions de carbonatation, la production et les échanges de chaleurs permettront une alimentation supplémentaire en gaz par advection et convection grâce aux gradients de concentration et de pression.

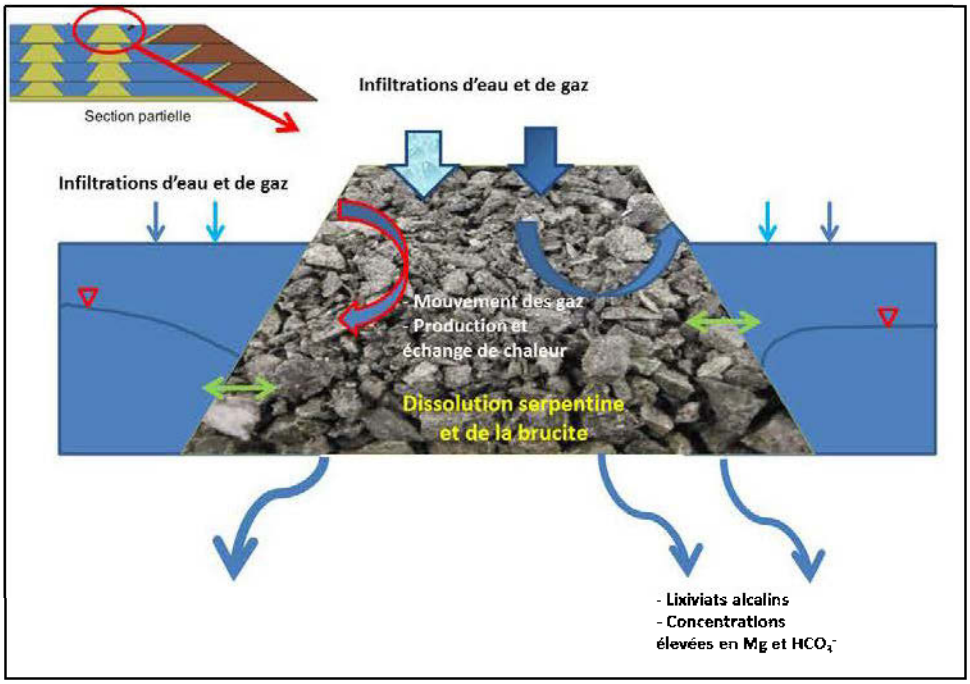

Figure 5.5 Processus physico-chimiques dans les piliers de stériles et aux interfaces stériles - résidus

Enfin, une meilleure stabilité physique des résidus est anticipée comparée à la méthode de déposition conventionnelle. La co-disposition permet une consolidation plus rapide des résidus (Jaouhar *et al.* 2011) et offre une résistance accrue aux séismes (Ferdosi *et al.* 2015a, 2015b; James et Aubertin, 2012; Pépin, 2010; James, 2009). De plus, la séparation des résidus en compartiments permet de limiter les quantités de rejets qui seront relâchés en cas de rupture de digue.

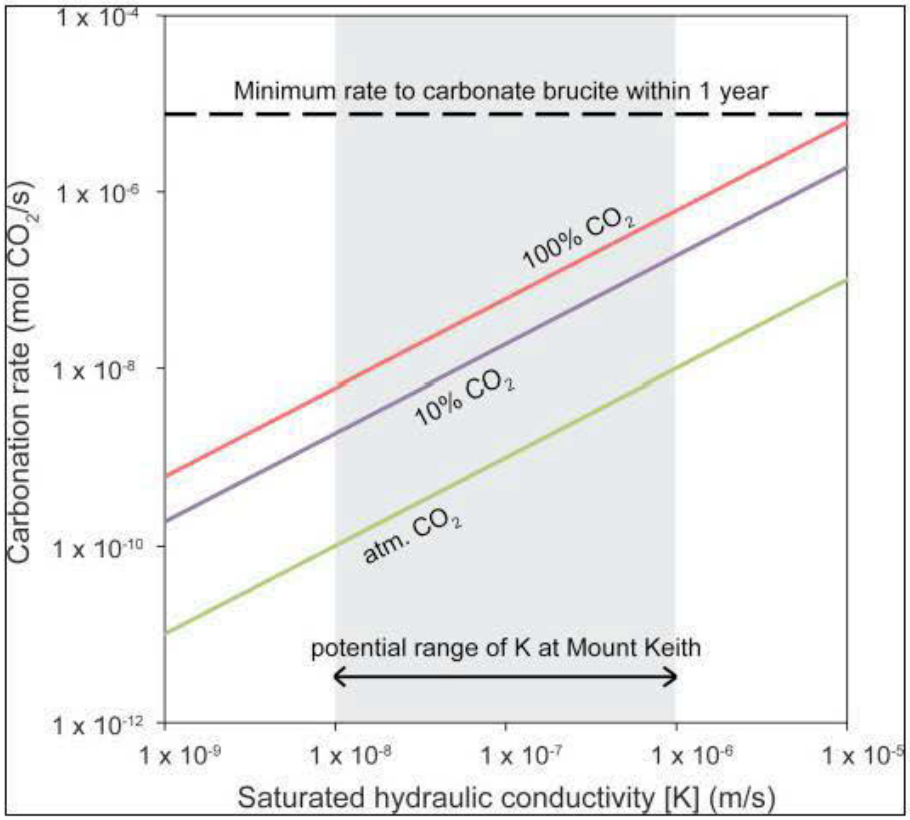

Figure 5.6 Vitesse de carbonatation de la brucite en fonction de la conductivité hydraulique. Les lignes continues représentent les vitesses de carbonatation à pression atmosphérique (ligne verte), atmosphère à 10 % de CO_2 (ligne violette) et à 100 % de CO_2 (ligne rouge). La ligne discontinue représente la vitesse minimale qu'il faudrait pour carbonater toute la brucite contenue dans les 50 cm de rejets (2,5 %), en une année. Les calculs sont basés sur une épaisseur de 50 cm de rejets de Mount Keith, ce qui représente une année de déposition pour la mine (Wilson *et al.* 2014)

Cependant, la faisabilité du concept proposé dans ce chapitre nécessitera une évaluation qui tient compte de certains aspects. En effet, le filtrage des rejets de concentrateur dans le but de réduire sa teneur en eau peut être coûteux et énergivore, ce qui peut augmenter l'empreinte carbone des activités de la mine. De plus, l'utilisation de large surface pour l'entreposage des rejets ultramafiques dans le but

d'augmenter son potentiel de carbonatation peut induire une forte emprise sur le sol. Tous ces facteurs font qu'une évaluation plus approfondie devrait etre réalisée afin de s'assurer de la viabilité technico-économique de ce concept.

CHAPITRE VI

CONCLUSION GÉNÉRALE ET RECOMMANDATIONS

6.1 Sommaire des principaux résultats

Une prédiction précise de la qualité des eaux de drainage des rejets miniers est une étape importante dans le développement d'une mine. Dans les rejets miniers composés de roches ultramafiques, certains minéraux comme la serpentine, la brucite et l'olivine peuvent réagir avec le CO_2 pour former des carbonates stables. Il est important de bien connaitre les effets des processus géochimiques ayant cours dans ce type de rejets sur la qualité des eaux interagissant avec ces minéraux (dissolution du CO_2, dissolution des minéraux primaires, précipitation des minéraux secondaires etc.). En plus d'améliorer la compréhension des aspects fondamentaux liés aux processus de carbonatation des rejets miniers, il est important de mieux connaitre les changements au niveau des eaux qui interagissent avec les rejets ultramafiques.

Le principal objectif de cette thèse était de comprendre le comportement géochimique de rejets miniers ayant un potentiel de séquestration de carbone et de comprendre aussi l'impact de ce potentiel sur la qualité des eaux de drainage. De plus, l'emphase a été mise sur les effets d'échelle au niveau des essais cinétiques sur les résultats obtenus afin d'identifier les principaux facteurs d'influence.

Dans les chapitres 2 et 3, il a été question d'évaluer le comportement géochimique des résidus de Dumont, des stériles et des principales lithologies rencontrées dans ce gisement. Aussi, le comportement géochimique des sulfures de nickel (pentlandite et

heazlewoodite) et de l'awaruite a été évalué via des essais en mini-cellules d'altération.

Les résultats en mini-cellules d'altération démontrent que les sulfures de nickel produisent du nickel et du fer dans les lixiviats. Ces sulfures, aussi présents en trace dans l'échantillon de concentré d'awaruite, sont responsables des faibles concentrations en métaux détectées dans les lixiviats. En effet, les résultats des essais cinétiques sur le concentré d'alliage fer-nickel suggèrent que celui-ci est stable dans ces conditions. Ainsi, la présence de l'awaruite dans les matériaux de Dumont ne devrait pas être problématique du point de vue de la qualité d'eau puisque celui-ci semble être stable dans les conditions d'exposition reproduites par les mini-cellules d'altération utilisées.

Les essais en colonnes et en mini-cellules sur les résidus de concentrateur libèrent de faibles quantités de nickel. Dans les lixiviats, le fer et le zinc sont pratiquement absents. Cependant, le pH des eaux de drainage montre des valeurs alcalines (9 – 10) qui, parfois, dépassent la limite permise par la Directive 019. Ce pH élevé diminue la mobilité des métaux, qui précipitent sous forme d'oxy-hydroxydes et demeurent dans la phase solide. Les qualités d'eau obtenues pour les stériles et les lithologies (l'upper péridotite, le footwall ultramafique et le low-grade dunite) sont pratiquement similaires à celles des résidus de concentrateur. Les pH sont aussi alcalins et les concentrations en métaux faibles, voire en deçà des limites de détection. Les lixiviats provenant des échantillons de gabbro et de volcanique ont, par contre, des pH variant entre 7 et 8 et montrant des concentrations en métaux faibles.

La composition minéralogique des matériaux explique cette différence au niveau de la géochimie des lixiviats. En effet, les résidus, les stériles et les lithologies upper péridotite, footwall ultramafique et low-grade dunite sont composés majoritairement de serpentine et de brucite (jusqu'à 90 %). Leur altération semble être contrôlée principalement par la dissolution du CO_2, plus que par l'oxydation des sulfures,

présents en faibles concentrations. Les résultats de ces interactions induisent des eaux de drainages alcalines dominées par le Mg et les ions carbonates et bicarbonates.

Les caractérisations post-démantèlement des matériaux altérés ont permis d'évaluer les changements au niveau des caractéristiques des matériaux de Dumont. Une augmentation importante de la quantité de carbone de plus de 100 % a été notée pour les rejets ultramafiques. Les calculs thermodynamiques, les caractérisations minéralogiques (MEB et DRX) ainsi que le DRIFT ont permis de confirmer la présence des carbonates secondaires de magnésium hydraté. La précipitation de ces carbonates induit une cimentation des grains et la formation d'une zone indurée qui, sur les sites miniers, pourrait diminuer les émanations de poussières par érosion éolienne. Ces résultats obtenus avec les essais cinétiques sont comparables à ceux obtenus avec les études *in situ* sur des sites miniers composés majoritairement de rejets ultramafiques.

Le taux de carbonatation a été estimé à partir des teneurs finales en carbone. Pour les résidus, les quantités de CO_2 séquestrées peuvent atteindre 2200 g $CO_2/m^2/an$. Ce taux est dans le même ordre de grandeur que pour les autres sites miniers où de la carbonatation passive a été rapportée. La brucite semble être le minéral principalement responsable de la séquestration du carbone. En effet, sa forte réactivité par rapport à la serpentine fait en sorte qu'elle est consommée dans les premiers centimètres des rejets. De plus, sa teneur initiale semble contrôler la capacité maximale de séquestration du carbone des rejets de Dumont dans les conditions testées. La teneur totale en carbone dans les résidus plafonne à environ 1 % dès que la brucite est consommée. Enfin, de la brucite résiduelle a été détectée au DRX dans les résidus alors que ceux-ci semblaient avoir atteint leur potentiel de carbonatation maximal. Il est possible que la précipitation des carbonates réduise la réactivité de la brucite. Cette observation a été confirmée par les travaux de Zarandi *et al.* (2016) sur les mêmes rejets de concentrateur de Dumont.

Le chapitre 4 présente une comparaison des résultats obtenus par des essais cinétiques sur différentes échelles au laboratoire (cellule humide, mini-cellule, colonne) et sur le terrain (cellule expérimentale) sur les résidus et les stériles. Malgré les différences au niveau des paramètres des différents essais, les résultats des qualités des eaux sont similaires pour les stériles et les résidus de Dumont. Par contre, les différences au niveau des taux de relargage de certains éléments peuvent atteindre jusqu'à 4 ordres de grandeur, surtout pour les éléments liés aux minéraux neutralisants comme le Mg, le Si, le Ca et l'Al. Les taux de relargage de nickel et de sulfate sont moins étalés, surtout après avoir appliqué des corrections liées aux différences de température entre les essais. Cependant, le paramètre qui semble causer le plus de différence au niveau des taux de libération est le rapport liquide-solide (RLS) de l'essai. En effet, les taux de libération augmentent généralement avec le RLS appliqué. Le type d'essai cinétique utilisé semble aussi avoir un effet sur la vitesse de séquestration du carbone, mais pas sur le potentiel total, puisque celui-ci semble stagner dès que la brucite est consommée.

Le chapitre 5 dresse quelques implications à tirer des résultats de cette thèse ainsi que des données récentes acquises sur les matériaux de Dumont. La comparaison du potentiel de neutralisation (PN) avant et après les essais cinétiques indique que la formation des carbonates secondaires n'implique pas forcément une augmentation du PN des rejets de concentrateur de Dumont. En effet, le remplacement de la brucite, aussi réactive que la calcite et la dolomite, induit une diminution du PN.

Une approche d'entreposage des rejets de Dumont a été proposée afin de maximiser le potentiel de séquestration passive du CO_2 par les rejets de Dumont. La méthode proposée préconise une co-déposition des résidus de concentrateur avec les stériles afin d'augmenter la perméabilité des rejets et de favoriser ainsi l'apport de CO_2 dans les rejets humides. Cette méthode de stockage permet aussi, par la même occasion, de garantir une meilleure stabilité physique des rejets. La co-déposition implique une

division de l'aire d'entreposage en compartiments. Ceci offrirait la possibilité d'allonger le temps d'exposition des rejets et, par conséquent, leur carbonatation, en alternant l'utilisation des compartiments. Une méthode de déposition efficace permettrait d'optimiser la séquestration de CO_2 des rejets Dumont.

6.2 Recommandations

Certains aspects soulevés dans cette thèse méritent des investigations supplémentaires. De ce fait, voici quelques recommandations proposées à la suite de nos travaux :

1) Afin de préciser la contribution de la serpentine dans la carbonatation des rejets de Dumont, il serait intéressant de réaliser des essais cinétiques et éventuellement des essais de carbonatation sur les rejets de Dumont exempts de brucite. Une méthode d'extraction ou de digestion sélective de la brucite pourrait être utilisée afin d'extraire la brucite dans les rejets de Dumont sans pour autant enlever la serpentine. Ces essais permettraient de clarifier la contribution de la serpentine dans la carbonatation et la neutralisation de l'acide.

2) Une fois la contribution de la serpentine clarifiée, le calcul du potentiel de neutralisation (PN) pourrait être amélioré et être applicable à tous les rejets miniers ultramafiques, une fois que leur composition minéralogique est bien connue.

3) Les essais en mini-cellules qui ont été réalisés sur les concentrés d'awaruite et de sulfures de nickel ont été arrêtés trop tôt pour observer la génération de pH acides. En effet, les essais ont été arrêtés au moment où le pH avait commencé à diminuer, alors que les minéraux neutralisants étaient sur le point de s'épuiser. Une reprise des essais cinétiques sur les concentrés est suggérée avec un délai plus long afin mieux comprendre le comportement géochimique de ces minéraux, surtout de l'awaruite.

4) Lors des essais cinétiques réalisés au laboratoire, l'hydromagnésite est le carbonate principal qui a été détecté, alors que dans tous les essais de carbonatation réalisés sur les mêmes rejets par l'équipe de l'Université Laval, la nesquehonite et/ou la dypingite sont les carbonates de magnésium hydratés qui ont été observés. Afin de mieux comprendre les facteurs qui déterminent la formation d'un type de carbonate plutôt qu'un autre, il serait intéressant de réaliser des essais de carbonatation, en faisant varier les conditions de réalisation des essais (température, pression partielle de CO_2, etc.) et surtout la durée des essais. Il est possible que la nesquehonite se forme en premier avant de se transformer progressivement en dypingite, puis en hydromagnésite. D'ailleurs, des travaux allant dans ce sens sont en cours à l'Université Laval (Zarandi *et al.* 2016).

5) Dans les conditions des essais cinétiques, la brucite a été consommée entre 28 et 59 jours. Il serait intéressant de déterminer ce délai dans les conditions *in situ* afin de définir une vitesse optimale de déposition des résidus dans les parcs et donc de maximiser la carbonatation des rejets de Dumont.

6) Une méthode de co-déposition des résidus et des stériles (par inclusion de stériles dans les parcs à résidus) a été suggérée afin de favoriser la carbonatation minérale passive des rejets de Dumont. Il serait important de passer du concept à la pratique en réalisant des cellules expérimentales de terrain instrumentées contenant différentes proportions de mélanges résidus-stériles et différents degrés de saturation des résidus. Un suivi hydrogéochimique combiné à des essais de consommation de CO_2 et des prélèvements de gaz interstitiels permettraient d'évaluer les performances de ces méthodes de co-déposition. Le comportement à long-terme de ces cellules pourrait être évalué en utilisant des modèles numériques de transport réactif comme MIN3P.

7) Seule l'option de la carbonatation passive des rejets de Dumont a été considérée dans cette thèse. Cependant, il serait intéressant d'évaluer la possibilité

d'une carbonatation accélérée. L'exploitation du gisement de Dumont devrait produire plus de 2 gigatonnes de rejets ultramafiques et, vu la quantité importante de brucite que contiennent ces rejets, la carbonatation par voie accélérée pourrait être une option viable du point de vue économique, environnementale et énergétique. En effet, l'extraction et la carbonatation de toute la brucite contenue dans les résidus et les stériles de Dumont dans des réacteurs, permettrait de compenser les émissions de la mine et même de vendre des crédits carbone. D'après Harrison *et al.* (2012), la carbonatation accélérée de la brucite contenue dans les rejets miniers ultramafiques pourrait fixer des millions de tonnes de CO_2 annuellement.

BIBLIOGRAPHIE GÉNÉRALE

Akcil, A. et Koldas.S. (2006). Acid Mine Drainage (AMD): Causes, Treatment and Case Studies. Journal of Cleaner Production 14 (12-13) (January): 1139–1145. doi:10.1016/j.jclepro.2004.09.006

Al, T., Martin, C. et Blowes, D. (2000). Carbonate-mineral/water interactions in sulfide-rich mine tailings. Geochimica et Cosmochimica Acta, 64(23), 3933–3948.

Allen, D.J. et Brent, G.F. (2010). Sequestering CO2 by Mineral Carbonation: Stability Against Acid Rain Exposure. Environmental Science & Technology 44 (7) (April 1): 2735–9. doi:10.1021/es903212j. http://www.ncbi.nlm.nih.gov/pubmed/20199068

Amos, R. T., Blowes, D. W., Bailey, B. L., Sego, D. C., Smith, L., & Ritchie, A. I. M. (2015). Waste-rock hydrogeology and geochemistry. Applied Geochemistry, 57, 140-156

Ardau, C., Blowes, D. W., Ptacek, C. J. (2009). Comparison of laboratory testing protocols to field observations of the weathering of sulfide-bearing mine tailings. Journal of Geochemical Exploration, 100(2-3), 182–191. doi:10.1016/j.gexplo.2008.06.005

Assima, G.P., Larachi, F., Beaudoin, G., Molson, J., (2014a). Impact of temperature and oxygen availability on the dynamics of ambient CO2 mineral sequestration by nickel mining residues. Chemical Engineering Journal, 240, pp.394–403

Assima, G.P., Larachi, F., Beaudoin, G., Molson, J. (2014b). Emulation of ambient carbon dioxide diffusion and carbonation within nickel mining residues. Minerals Engineering, 59, pp.39–44

Assima G. P., Larachi F., Molson J. and Beaudoin G. (2014c). Comparative study of five Quebec ultramafic mining residues for use in direct ambient carbon dioxide mineral sequestration. Chem. Eng. J. 245, 56–64

Assima, G.P., Larachi, F., Beaudoin, G., Molson, J. (2013a). Dynamics of carbon dioxide uptake in chrysotile mining residues – Effect of mineralogy and liquid saturation. International Journal of Greenhouse Gas Control, 12, pp.124–135

Assima, G.P., Larachi, F., Beaudoin, G., Molson, J. (2013b). Accurate and direct quantification of native brucite in serpentine ores New methodology and implications for CO2 sequestration by mining residues. Thermochimica Acta, 566, pp.281–291

Assima, G.P., Larachi, F., Beaudoin, G., Molson, J. (2012). CO2 Sequestration in Chrysotile Mining Residues: Implication of Watering and Passivation under Environmental Conditions. Industrial & Engineering Chemistry Research, pp.2–10

ASTM Standard D4892, 2014. Standard test method for density of solid pitch (Helium Pycnometer Method). West Conshohocken, PA, (www.astm.org)

ASTM Standard D6913-04. (2009). Standard test methods for particle-size distribution (gradation) of soils using sieve analysis. Annual Book of ASTM Standards vol. 0409

ASTM (2007). D5744-07. Standard Test Method for Accelerated Weathering of Solid Materials Using a Humidity Cell. Annual Book of ASTM Standards

ASTM. (1998). D5744-96. Standard Test Method for Accelerated Weathering of Solid Materials Using Modified Humidity Cell. Annual Book of ASTM Standards.11.04: 259-271

Aubertin, M., Bussière, B. & Berner, L., (2002). Environnement et gestion des résidus miniers. Les Presses Internationales Polytechnique, Montréal, Canada. Manuel sur Cédérom

Awoh, A.S., Plante, B., Bussière, B., Mbonimpa, M. (2013). CO2 consumption test for the quantification of the mineral carbonation potential of mine waste rock. Proceedings of the Canadian Geotechnical Conference, Montreal

Awoh, A.S., Plante, B., Bussière, B., Mbonimpa, M. (2014). Measurement and prediction of the CO2 effective diffusion coefficient in unsaturated media. Canada. Proceedings of the Canadian Geotechnical Conference, Regina, Canada

Baker, M.J., Blowes, D.W., Logsdon, M.J., and Jambor, J.L. (2003) Environmental geochemistry of kimberlite materials: Diavik Diamonds Project, Lac de Gras, Northwest Territories, Canada. Exploration and Mining Geology, 10, 155-163

Bales, R.C. et Morgan, J.J. (1985). Dissolution kinetics of chrysotile at pH 7 to 10. Geochimica et Cosmochimica Acta, 49(11), pp.2281–2288

Ballirano, P., De Vito, C., Ferrini, V., Mignardi, S. (2010). The thermal behaviour and structural stability of nesquehonite, MgCO3·3H2O, evaluated by in situ laboratory parallel-beam X-ray powder diffraction: new constraints on CO2 sequestration within minerals. J Hazard Mater 178, 522–528

Banks, D., Parnachev, V. P., Frengstad, B., Holden, W., Vedernikov, A. A., Karnachuk, O. V. (2002). Alkaline mine drainage from metal sulphide and coal mines: examples from Svalbard and Siberia. Geological Society, London, Special Publications, 198(1), 287-296

Bea, S.A., Wilson, S.A., Mayer, K.U., Dipple, G.M., Power, I.M., Gamazo, P. (2012). Reactive Transport Modeling of Natural Carbon Sequestration in Ultramafic Mine Tailings. Vadose Zone Journal, 11(2)

Beaudoin, G., Hébert, R. & Constantin, M. (2008). Spontaneous carbonation of serpentine in milling and mining waste, southern Québec and Italy. Proceedings of Accelerated Carbonation for Environmental and Materials Engineering (ACEME2008), pp.73–82

Beaupré, S. (2012). Des risques, des mines et des hommes : La perception du risque chez les mineurs de fond de l'Abitibi-Témiscamingue. Presses de l'université du Québec. D3554, ISBN 978-2-7605-3554-1. 144 p

Beinlich, A. et Austrheim, H. (2012). In situ sequestration of atmospheric CO2 at low temperature and surface cracking of serpentinized peridotite in mine shafts. Chemical Geology, 332-333, pp.32–44

Bénézeth, P., Saldi, G. D., Dandurand, J. L., & Schott, J. (2011). Experimental determination of the solubility product of magnesite at 50 to 200 C. Chemical Geology, 286(1), 21-31

Benzaazoua, M., Bussiere, B., Dagenais, AM., Archambault, M. (2004). Kinetic test comparison and interpretation for prediction of the Joutel tailings acid generation potential. Environmental Geology 46(8): 1086-1101

Benzaazoua, M., Bussiere, B., Dagenais, AM. (2001). Comparison of kinetic tests for sulfide mine tailings. In: Tailings and Mine Waste 01. Fort Collins, Colorado, January 2001. Balkema Ed., Rotterdam, pp.263-272

Bertos, M. F., Simons, S. J. R., Hills, C. D., Carey, P. J. (2004). A review of accelerated carbonation technology in the treatment of cement-based materials and sequestration of CO 2. Journal of hazardous materials, 112(3), 193-205

Blowes, D. W., Ptacek, C. J., Jambor, J. L., Weisener, C. G., Paktunc, D., Gould, W. D., Johnson, D. B. (2003). The Geochemistry of Acid Mine Drainage. Treatise on Geochemistry: Second Edition, 11, 131–190. http://doi.org/10.1016/B978-0-08-095975-7.00905-0

Blowes, D. W., Jambor, J. L., Hanton-Fong, C. J., Lortie, L., Gould, W. D. (1998). Geochemical, mineralogical and microbiological characterization of a sulphide-bearing carbonate-rich gold-mine tailings impoundment, Joutel, Québec. Applied Geochemistry, 13(6), 687-705

Blowes, D.W. et Ptacek, C.J. (1994). Acid-neutralization mechanisms in inactive mine tailings. Short Course Handbook on Environmental Geochemistry of Sulfide Mine-Waste, Jambor, J.L., Blowes, D.W. (eds). Mineralogical Association of Canada. Special Vol. 22, pp.272-292

Blowes, D.W. Reardon, E.J. Jambor, J.L. Cherry, J.A. (1991). The formation and potential importance of cemented layers in inactive sulfide mine tailings Geochim. Cosmochim. Acta, 55 (1991), pp. 965–978

Bobicki, E. R., Liu, Q., Xu, Z. (2015). Mineral carbon storage in pre-treated ultramafic ores. Minerals Engineering, 70, 43-54

Bobicki, E. R., Liu, Q., Xu, Z., Zeng, H. (2012). Carbon capture and storage using alkaline industrial wastes. Progress in Energy and Combustion Science, 38(2), 302-320

Bolduc, L.F., & Aubertin, M. (2014). Numerical investigation of the influence of waste rock inclusions on tailings consolidation. Canadian Geotechnical Journal, 51(9), 1021-1032

Bolduc, F. (2012). Une étude sur l'utilisation des roches stériles comme inclusions drainantes dans les résidus miniers. Master's thesis, Department of Civil, Geologic and Mining Engineering, École Polytechnique, Montréal, Québec

Botha, A. & Strydom, C. A., 2003. DTA and FT-IR analysis of the rehydration of basic magnesium carbonate. Journal of Thermal Analysis and Calorimetry, 71, pp.987–995

Botha, A., Strydom, C.A., (2001). Preparation of a magnesium hydroxy carbonate from magnesium hydroxide. Hydrometallurgy 62, 175–183

Bouzahzah, H., Benzaazoua, M., Plante, B., & Bussiere, B. (2015). A quantitative approach for the estimation of the "fizz rating" parameter in the acid-base accounting tests: a new adaptations of the Sobek test. Journal of Geochemical Exploration, 153, 53-65

Bouzahzah, H. (2013) Modification et amélioration des tests statiques et cinétiques pour une prédiction fiable du drainage minier acide. Thèse de doctorat inédite, Université du Québec en Abitibi-Témiscamingue (UQAT), Québec, Canada

Bradham, W., et Caruccio, F. (1990). A comparative study of tailings analysis using acid/base accounting, cells, columns and soxhlets. In 2nd International Conference on the Abatement of Acidic Drainage (pp. 157–173). Montréal, Québec

Brunauer, S., Emmett, P.H., Teller, E. (1938). Adsorption of gases in multimolecular layers. J. Am. Chem. Soc. 60 (2), 309–319. http://dx.doi.org/10.1021/ja01269a023

Bussiere, B. (2007a). Colloquium 2004: Hydrogeotechnical properties of hard rock tailings from metal mines and emerging geoenvironmental disposal approaches. Canadian Geotechnical Journal, 44(9), 1019-1052

Bussière, B., Aubertin, M., Mbonimpa, M., Molson, J. W., & Chapuis, R. P. (2007b). Field experimental cells to evaluate the hydrogeological behaviour of oxygen barriers made of silty materials. Canadian Geotechnical Journal, 44(3), 245-265

Bussière, B., Aubertin, M., Zagury, G.J., Potvin, P., Benzaazoua, M. (2005). Principaux défis et pistes de solution pour la restauration des aires d'entreposage de rejets miniers abandonnées. Symposium 2005 sur l'environnement et les mines. Rouyn-Noranda

Canterford, J.H., Tsambourakis, G., Lambert, B. (1984). Some observations on the properties of dypingite, $Mg_5(CO_3)_4(OH)_2 \cdot 5H_2O$, and related minerals. Miner Mag 48 (1984) 437–442

Carbone, C., Dinelli, E., Marescotti, P., Gasparotto, G., Lucchetti, G. (2013). The role of AMD secondary minerals in controlling environmental pollution: Indications from bulk leaching tests. Journal of Geochemical Exploration, 132, 188–200. doi:10.1016/j.gexplo.2013.07.001

Carroll, J. J., Slupsky, J. D., & Mather, A. E. (1991). The solubility of Carbon dioxide in water at low pressure. Journal of Physical and Chemical Reference Data, 20(6), 1201–1209

Chamley, H. (2002). Environnements géologiques et activités humaines. Vuibert. ISBN 2711752844. 512 p

Chapuis, R.P., and Légaré, P.P. (1992). A simple method for determining the surface area of fine aggregates and fillers in bituminous mixtures. Effects of aggregates and mineral filler on asphalt mixture performance, ASTM STP 1147, pp. 177-186

Cravotta, C. A. (2008). Dissolved metals and associated constituents in abandoned coal-mine discharges, Pennsylvania, USA. Part 1: constituent quantities and correlations. Applied Geochemistry, 23(2), 166-202

Cravotta III, C. A. 2008. Dissolved metals and associated constituents in abandoned coal-mine discharges, Pennsylvania, USA. Part 2: Geochemical controls on constituent concentrations. Applied Geochemistry 23(2): 203-226

Cruz, R., Bertrand, V., Monroy, M., González, I., 2001. Effect of sulfide impurities on the reactivity of pyrite and pyritic concentrates: A multi-tool approach. Applied Geochemistry 16:803–819

Daval, D., Hellmann, R., Martinez, I., Gangloff, S., Guyot, F. (2013). Lizardite serpentine dissolution kinetics as a function of pH and temperature, including effects of elevated pCO 2. Chemical geology, 351, 245-256

Davies P.J., Bubela, B., (1973). The transformation of nesquehonite into hydromagnesite. Chemical Geology, 12(4), 289-300

Demers, I., J. Molson, B. Bussière, and D. Laflamme. (2013). Numerical Modeling of Contaminated Neutral Drainage from a Waste-rock Field Test Cell. Applied Geochemistry (March). doi:10.1016/j.apgeochem.2013.02.025

Demers, I., Bussiere, B., Benzaazoua, M., Mbonimpa, M., Blier, A. (2008). Column test investigation on the performance of monolayer covers made of

desulphurized tailings to prevent acid mine drainage. Minerais Engineering 21, 317-329

Dold, B. (2010). Basic concepts in environmental geochemistry of sulfidic mine-waste management. INTECH Open Access Publisher

Dold, B., & Fontbote, L. (2002). A mineralogical and geochemical study of element mobility in sulfide mine tailings of Fe oxide Cu – Au deposits from the Punta del Cobre belt , northern Chile, 189, 135–163

Duncan, D.W. et Bruynesten, A. (1979). Determination of acid production potential of waste materials, Met. Soc. AIME, paper A79-29, 10p

Éthier, M.-P., Bussière, B., Benzaazoua, M., Garneau, P. (2012). Effect of temperature on the weathering of various waste rock types from the Raglan Mine. Sustainable Infrastructure Development in a Changing Cold Environment conference, Québec, Canada, pp. 800–810

Etschmann, B., Pring, A., Putnis, A., Grguric, B. A., & Studer, A. (2004). A kinetic study of the exsolution of pentlandite (Ni, Fe)9S8 from the monosulfide solid solution (Fe, Ni) S. American Mineralogist, 89(1), 39-50

Evangelou, V. P., & Zhang, Y. L. (1995). A review: pyrite oxidation mechanisms and acid mine drainage prevention. Critical Reviews in Environmental Science and Technology, 25(2), 141-199

Felmy A. R., Qafoku O., Arey B. W., Hu J. Z., Hu M., Schaef H. T., Ilton E. S., Hess N. J., Pearce C. I., Feng J. and Rosso K. M., 2012. Reaction of water-saturated supercritical CO2 with forsterite: evidence for magnesite formation at low temperatures. Geochim. Cosmochim. Acta 91, 271–282

Ferdosi, B., James, M., & Aubertin, M. (2015a). Effect of waste rock inclusions on the seismic stability of an upstream raised tailings impoundment: a numerical investigation. Canadian Geotechnical Journal, 52(12), 1930-1944

Ferdosi, B., James, M., & Aubertin, M. (2015b). Investigation of the Effect of Waste Rock Inclusions Configuration on the Seismic Performance of a Tailings Impoundment. Geotechnical and Geological Engineering, 33(6), 1519-1537

Ferrini, V., De Vito, C. & Mignardi, S., 2009. Synthesis of nesquehonite by reaction of gaseous CO2 with Mg chloride solution: its potential role in the

sequestration of carbon dioxide. Journal of Hazardous Materials, 168(2-3), pp.832–837

Frost, R.L. & Palmer, S.J., 2011. Infrared and infrared emission spectroscopy of nesquehonite Mg(OH)(HCO3)·2H2O-implications for the formula of nesquehonite. Spectrochimica acta. Part A, Molecular and biomolecular spectroscopy, 78(4), pp.1255–60

Frost, R.L., Bahfenne, S. & Graham, J., 2009. Infrared and infrared emission spectroscopic study of selected magnesium carbonate minerals: artinite and dypingite. Spectrochim. Acta, 71A, pp.1610–1616

Frostadt, S., & Lawrence, R. W. (2005). Determining the weathering charaeteristics of a waste dump with field tests, 19(2), 132–144

Frostad, S., Klein, B., Lawrence, R.W. (2002). Evaluation of Laboratory Kinetic Test Methods for Measuring Rates of Weathering. Mine Water and the Environment, vol21, p. 183-192

Furrer, G., Stumm, W. (1986). The coordination chemistry of weathering: I. Dissolution kinetics of δ-Al 2 O 3 and BeO. Geochimica et Cosmochimica Acta, 50(9), 1847-1860

Gautier, Q., Bénézeth, P., Mavromatis, V., Schott, J., 2014. Hydromagnesite solubility product and growth kinetics in aqueous solution from 25 to 75 °C. Geochimica et Cosmochimica Acta, 138, pp.1–20

Giere, N.V, Sidenko, E.V. Lazareva, E.V. (2003). The role of secondary minerals in controlling the migration of arsenic and metals from high-sulfide wastes (Berikul gold mine, Siberia) Appl. Geochem., 18 (2003), pp. 1347–1359

Gilbert, S. E., Cooke, D. R., & Hollings, P. (2003). The effects of hardpan layers on the water chemistry from the leaching of pyrrhotite-rich tailings material. Environmental Geology, 44(6), 687-697

Goff, F., et Lackner, K.S. (1998). Carbon dioxide sequestering using ultramafic rocks, Environmental Geosciences, 5, 89-101

Golightly, J.P. & Arancibia, O.N., 1979. The chemical composition and infrared spectrum of Nickel- and iron-substituted serpentine from a nickeliferous laterite profile, Sorobako Indonesia. Canadian Mineralogist 17, 719-728

Golubev, S.V, Pokrovsky, O.S. & Schott, J., 2005. Experimental determination of the effect of dissolved CO2 on the dissolution kinetics of Mg and Ca silicates at 25 °C. Chem. Geol., 217, pp.227–238

González, V., García, I., Del Moral, F., De Haro, S., Sánchez, J. A., Simón, M. (2012). Spreading of pollutants from alkaline mine drainage. Rodalquilar mining district (SE Spain). Journal of environmental management, 106, 69-74

Gras, A., Beaudoin, G., Molson, J.W.H., Plante, B., Bussière, B., Lemieux, J.M., Dupont, P.P., (2017). Isotopic evidence of passive mineral carbonation in mine wastes from the Dumont Nickel Project (Abitibi, Quebec). To be published

Gras, A., Beaudoin, G., Molson, J.W.H., Plante, B., Lemieux, J.M., Kandji, E. H. B. (2015). Evidence for passive mineral carbonation from carbon isotope geochemistry ofinterstitial air in mine wastes from the Dumont Nickel Project (Abitibi,Quebec). In AGU Fall Meeting, American Geophysical Union. Washington DC, United States

Gras, A. (2013). Séquestration du CO2 associée aux phénomènes de carbonatation dans les résidus miniers du projet Dumont Nickel (Abitibi): Caractérisation et modélisation. Projet de Recherche 2012/2015. Université Laval.

Gunsinger, M. R., Ptacek, C. J., Blowes, D. W., Jambor, J. L. (2006). Evaluation of long-term sulfide oxidation processes within pyrrhotite-rich tailings, Lynn Lake, Manitoba. Journal of contaminant hydrology, 83(3), 149-170

Gunsinger, R., Ptacek, J., Blowes, W., Jambor, L., & Moncur, C. (2006). Mechanisms controlling acid neutralization and metal mobility within a Ni-rich tailings impoundment. Applied Geochemistry, 21, 1301–1321. http://doi.org/10.1016/j.apgeochem.2006.06.006

Hageman, P., et Smith, K. (2005). Comparison of mine waste assessment methods at the Rattler Mine Site, Virginia Canyon, Colorado. In National Meeting of the American Society of Mining and Recclamation (pp. 470–486). Breckenridge CO

Hakkou, R., Benzaazoua, M. & Bussière, B., 2008. Acid mine drainage at the abandoned kettara mine (Morocco): 2. mine waste geochemical behavior. Mine Water and the Environment, 27(3), pp.160–170

Hamilton, J. L., Wilson, S. A., Morgan, B., Turvey, C. C., Paterson, D. J., MacRae, C., ... & Southam, G. (2016). Nesquehonite sequesters transition metals and CO 2 during accelerated carbon mineralisation. International Journal of Greenhouse Gas Control, 55, 73-81

Hänchen, M., Prigiobbe, V., Baciocchi, R., Mazzotti, M., 2008. Precipitation in the Mg-carbonate system-effects of temperature and CO2 pressure. Chemical Engineering Science, 63(4), pp.1012–1028

Harrison, A. L., Dipple, G. M., Power, I. M., & Mayer, K. U. (2016). The impact of evolving mineral–water–gas interfacial areas on mineral–fluid reaction rates in unsaturated porous media. Chemical Geology, 421, 65-80

Harrison, A.L., Dipple, G.M., Power, I.M., Mayer, U.K. (2015). Influence of surface passivation and water content on mineral reactions in unsaturated porous media: Implications for brucite carbonation and CO2 sequestration. Geochimica et Cosmochimica Acta, 148, pp.477–495

Harrison, A.L., Power, I.M., Dipple, G.M. (2012). Accelerated carbonation of brucite in mine tailings for carbon sequestration. Environmental science & technology, 47(1), 126-134

Harvey, O. R., Qafoku, N. P., Cantrell, K. J., Lee, G., Amonette, J. E., Brown, C. F. (2012). Geochemical implications of gas leakage associated with geologic CO2 storage□ A qualitative review. Environmental science & technology, 47(1), 23-36

Heikkinen, P., Räisänen, M., Johnson, R., 2009. Geochemical characterization of seepage and drainage water quality from two sulphide mine tailings impoundments: acid mine drainage vs. neutral mine drainage. Mine Water Environ 28:30–49

Heikkinen, P. M., et Räisänen, M. L. (2008). Mineralogical and geochemical alteration of Hitura sulphide mine tailings with emphasis on nickel mobility and retention. Journal of Geochemical Exploration, 97(1), 1-20

Hitch, M., Ballantyne, S.M., Hindle, S.R. (2010). Revaluing mine waste rock for carbon capture and storage. International Journal of Mining, Reclamation and Environment, 24(1), pp.64–79

Hopkinson, L., Rutt, K.. & Cressey, G., 2008. The transformation of nesquehonite to hydromagnesite in the system CaO-MgO-H2O-CO2: an experimental spectroscopic study. Journal of Geology, 116(4), pp.387–400

Huijgen, W. J. J., et Comans, R. N. J. (2003). Carbon dioxide sequestration by mineral carbonation. Literature Review (No. ECN-C--03-016). Energy research Centre of the Netherlands ECN

Huntzinger, D. N., Gierke, J. S., Sutter, L. L., Kawatra, S. K., & Eisele, T. C. (2009). Mineral carbonation for carbon sequestration in cement kiln dust from waste piles. Journal of hazardous materials, 168(1), 31-37

Huot, F., Beaudoin, G., Hebert, R., Constantin, M., Bonin, G., Dipple, G. (2003). Evaluation of Southern Québec asbestos residues for CO2 sequestration by mineral carbonation; preliminary results. Joint Annual Meeting of the Geological and Mineralogical Associations of Canada, Vancouver, Canada. May 25-28, 2003

IPCC, (2007). Climate Change 2007: The Physical Basis. Contribution of Working Group I to the Fourth Assessment Report of the Intergovernmental Panel on Climate Change. Solomon, S., Qin, D., Manning, M., Chen, Z., Marquis, M., Averyt, K.B., Tignor, M., and Miller, H.L., Eds. Cambridge University Press, Cambridge, UK and New York, NY, USA, 996 p

IPCC, (2005). IPCC Special Report on Carbon Dioxide Capture and Storage. Metz, B., Davidson, O., de Coninck, H.C., Loos, M., and Meyer, L.A., Eds. Cambridge University Press, Cambridge, UK and New York, NY, USA, 431 p

Jacobs, A.D. et Hitch, M. (2011). Experimental Mineral Carbonation Approaches to Accelerate CO2 Sequestration in Mine Waste Materials. International Journal of Mining, Reclamation and Environment. 25.4 (2011): 321-331

Jambor J.L., Dutrizac J.E. Raudsepp, M. (2007). Measured and computed neutralization potential from static tests of diverse rock types. Environmental Geology, 52:1173-1185

Jambor, J.L., Dutrizac, J.E., Raudsepp, M., Groat, L.A. (2003). Effect of Peroxide on Neutralization-Potential Values of Siderite and Other Carbonate Minerais. J. Environ. Qual. 32:2373-2378

Jambor, J.L., Dutrizac, J.E., Groat, L.A., Raudsepp, M., (2002). Static tests of neutralization potentials of silicates and aluminosilicaté minerals. Envirnomental Geology, 43: 1-17

James, M. (2015). Waste rock inclusions: A co-disposal method to improve the performance and reduce the risk of tailings impoundments. Proceedings of the symposium sur l'environnement et les mines 2015. Rouyn-Noranda, QC. Canada

James, M., Aubertin, M., & Bussière, B. (2013). On the use of waste rock inclusions to improve the performance of tailings impoundments. In Proceedings of the 18th International Conference on Soil Mechanics and Geotechnical Engineering, Paris, France (pp. 735-738)

James, M., & Aubertin, M. (2012). The use of waste rock inclusions to improve the seismic stability of tailings impoundments. Proceedings of GeoCongress, 4166-4175

James, M. (2009). The Use of Waste Rock Inclusions to Control the Effects of Liquefaction in Tailings Impoundments. Thèse de Doctorat, École Polytechnique de Montréal, Canada

Jaouhar, E. M., Aubertin, M., & James, M. (2011). Effect of mine waste rock inclusions on the consolidation of tailings. In Proceedings, Pan-Am CGS Geotechnical Conference, Toronto

Johnson, R. H., Blowes, D. W., Robertson, W. D., Jambor, J. L. (2000). The hydrogeochemistry of the Nickel Rim mine tailings impoundment, Sudbury, Ontario. Journal of Contaminant Hydrology, 41(1), 49-80

Jurjovec J. (2002). Acid Neutralisation Mechanisms in Mine Tailings. Thèse de doctorat inédite. University de Waterloo, Ontario, Cananda

Kandji, E.H.B., Plante, B., Bussière, B., Beaudoin, G., Dupont, P. P. (2017a). Kinetic testing to evaluate the mineral carbonation and metal leaching potential of ultramafic tailings: case study of the Dumont Nickel Project, Amos, Québec.To be published

Kandji, E.H.B., Plante, B., Bussière, B., Beaudoin, G., & Dupont, P. P. (2017b). Geochemical behavior of ultramafic waste rocks with carbon sequestration potential: a case study of the Dumont Nickel Project, Amos, Québec. Environmental Science and Pollution Research, 1-18.

Karam, N. B., Mineyama, H., Valix, M., & Abbas, A. (2011). Carbon dioxide sequestration by carbonation of mine tailings. Chemeca 2011: Engineering a Better World: Sydney Hilton Hotel, NSW, Australia, 18-21 September 2011, 2477

Keith, C.N., & Vaughan, D.J. (2000). Mechanisms and rates of sulphide oxidation in relation to the problmes of acid rock (mine) drainage. In Environmental Mineralogy , Microbial Interactions, Anthropogenic Influences, Contaminated Land and Waste Management. The Mineralogical Society Series, 9, 117-140

Kleinmann, R. L. P., Crerar, D. A., Pacelli, R. R. (1981). Biogeochemistry of acid mine drainage and a method to control acid formation. Min. Eng.(NY);(United States), 33(3)

Kling, George W., Clark, Michael A., Wagner, Glen N., et al. (1986). The 1986 lake nyos gas disaster in cameroon, west Africa. Science, 1987, vol. 236, no 4798, p. 169-175

Kloprogge, J.T., Martens, W.N., Nothdurft, L., Duong, L.V., Webb, G.E., 2003. Low temperature systhesis and characterization of nesquehonite. Journal of Materials Science Letters, 22(11), pp.27–32

Kodali, B., Rao, B.M., Narasu, L.M., Pogaku, R., 2004. Effect of biochemical reactions in enhancement of rate of leaching. Chemical Engineering Science, 59(22-23), pp.5069–5073

Kohfahl, C., Graupner, T., Fetzer, C., & Pekdeger, A. (2010). The impact of cemented layers and hardpans on oxygen diffusivity in mining waste heaps A field study of the Halsbrücke lead–zinc mine tailings (Germany). Science of the total environment, 408(23), 5932-5939

Königsberger, E., Königsberger, L. C., & Gamsjäger, H. (1999). Low-temperature thermodynamic model for the system Na 2 CO 3− MgCO 3− CaCO 3− H 2 O. Geochimica et Cosmochimica Acta, 63(19), 3105-3119

Krevor, S. et Lackner, K.S,(2011). Enhancing serpentine dissolution kinetics for mineral carbon dioxide sequestration. International Journal of Greenhouse Gas Control, 5(4), pp.1073–1080

Kwong, Y.T.J. et Ferguson, K.D. (1997). Mineralogical changes during NP determinations and their implications. In: Proc. 4th Int. Conf. on Acid Rock Drainage, Vancouver, BC, Canada. 31 May-6 June 1997. Vol. 1. Mine

Environment Neutral Drainage, Nat. Resour. Canada, Ottawa, ON. pp. 435-447

Lackner, K.S.,Wendt, C.H., Butt, D.P., Joyce, E.L., Sharp, D.H. (1995). Carbon dioxide disposal in carbonate minerals. Energy 20, 1153–1170

Langman, J.B., Blowes, D.W., Veeramani, H., Wilson, D., Smith, L., Sego, D.C., Paktunc, D., 2015. The mineral and aqueous phase evolution of sulfur and nickel with weathering of pyrrhotite in a low sulfide, granitic waste rock. Chemical Geology, 401, pp.169–179

Langmuir, D. (1965). Stability of Carbonates in the System MgO–CO2–H2O. The Journal of Geology, 730-754

Lapakko, K. (2002). Metal mine rock and waste characterization tools: an overview. Mining, Minerals and Sustainable Development, 67, 1-30

Lapakko, K. (1994). Evaluation of neutralization potential determination for metal waste and a proposed alternative. Proceedings of the International Land Reclamation and Mine Drainage Conference and 3rd International Conference on the Abatement of Acidic Drainage, Pittsburgh, 1 : 129-137

Larachi, F., Daldoul, I., & Beaudoin, G. (2010). Fixation of CO2 by chrysotile in low-pressure dry and moist carbonation: Ex-situ and in-situ characterizations. Geochimica et Cosmochimica Acta, 74(11), 3051-3075

Lawrence, R. W. et Scheske, M. (1997). A method to calculate the neutralization potential of mining wastes. Environmental Geology (Berlin) 32:100-106

Lawrence, R.W. et Wang, Y. (1997). Determination of neutralization potential in the prediction of acid rock drainage. p. 451-464. In Proc. 4th Int. Conf. on Acid Rock Drainage, Vancouver, BC, Canada. 31 May-6 June 1997. Vol. 1. pp.449-464, Mine Environment Neutral Drainage, Nat. Resour. Canada, Ottawa, ON

Lechat, K., Lemieux, J.M., Molson, J., Beaudoin, G., Hébert, R. (2016). Field evidence of CO2 sequestration by mineral carbonation in ultramafic milling wastes, Thetford Mines, Canada. Int. J. Greenhouse Gas Control, 47 (2016), pp. 110–121

Li, J., & Hitch, M. (2017). Structural and chemical changes in mine waste mechanically-activated in various milling environments. Powder Technology, 308, 13-19

Li, J., & Hitch, M. (2016a). Carbon dioxide adsorption isotherm study on mine waste for integrated CO 2 capture and sequestration processes. Powder Technology, 291, 408-413

Li, J., & Hitch, M. (2016b). Mechanical activation of ultramafic mine waste rock in dry condition for enhanced mineral carbonation. Minerals Engineering, 95, 1-4

Li, M. G. (2000). Acid Rock Drainage Prediction for Low-Sulphide, Low-Neutralisation Potential Mine Wastes. In Proceedings of the fifth international conference on acid rock drainage (ICARD 2000). Society for Mining, Metallurgy, and Exploration, Inc (pp. 567-580)

Lin, F.C. et Clemency, C. V. (1981). The dissolution kinetics of brucite, antigorite, talc, and phlogopite at room temperature and pressure. American Mineralogist, 66(7-8), pp.801–806

Lindsay, M.B.J., Moncur, M.C., Bain, J.G., Jambor, J.L., Ptacek, C.J., Blowes, D.W., et al. 2015. Geochemical and mineralogical aspects of sulfide mine tailings. Applied Geochemistry, 57, pp.157–177

Lindsay, M. B. J., Condon, P. D., Jambor, J. L., Lear, K. G., Blowes, D. W., Ptacek, C. J. (2009). Mineralogical, geochemical, and microbial investigation of a sulfide-rich tailings deposit characterized by neutral drainage. Applied Geochemistry, 24(12), 2212–2221. doi:10.1016/j.apgeochem.2009.09.012

Liu, K., Chen, Q., Hu, H., Yin, Z., 2010. Characterization and leaching behaviour of lizardite in Yuanjiang laterite ore. Applied Clay Science. 47. pp. 311–316

Lottermoser B.G. (2010). Mine Wastes: Characterization, Treatment and Environmental Impacts, 3rd Edition. Springer, Berlin, Heidelberg, 400 pp

Luce, R.W., Bartlett, R.W., Parks, G.A. (1972). Dissolution Kinetics of Magnesium Silicates. Geochimica Et Cosmochimica Acta, 36(1), p.35–50

Maest, A. et Kuipers, J. (2005). Predicting Water Quality at Hardrock Mines : Predicting Water Quality at Hardrock Mines Methods and models, uncertaintities, and state-of-the-art (p. 90). Washington, U.S.A

Malmström, M. E., Destouni, G., Banwart, S. A., & Strömberg, B. H. (2000). Resolving the scale-dependence of mineral weathering rates. Environmental science & technology, 34(7), 1375-1378

Matter, J. M., Stute, M., Snæbjörnsdottir, S. Ó., Oelkers, E. H., Gislason, S. R., Aradottir, E. S., ... & Axelsson, G. (2016). Rapid carbon mineralization for permanent disposal of anthropogenic carbon dioxide emissions. Science, 352(6291), 1312-1314

McGregor, R.G. et Blowes, D.W. (2002). The physical, chemical, and mineralogical properties of three cemented layers within sulfide-bearing mine tailings J. Geochem. Explor., 76 (2002), pp. 195–207

Mcgregor, R.G., Blowes, D.W., Jambor, J,L., Robertson, W.D., 1998. Mobilization and attenuation of heavy metals within a nickel mine tailings impoundment near Sudbury, Ontario, Canada. Environmental Geology, pp.305–319

MEND, (2009). MEND report 1.20.1. Prediction manual for drainage chemistry from sulphidic geologie materials. By Priee, W.A. CANMET, Natural resources Canada, Canada

MEND, (1995). Perkins, E.H., Nesbitt, H.W., Gunter, W.D., St-Arnaud, L.C. et Mycroft, J.R. (1995). Critical review of geochemical processes and geochemical models adaptable for prediction of acidic drainage from waste rock. Report 1.42.1, Mine Environment Neutral Drainage (MEND)

MEND, (1991). Acid Rock Drainage Prediction. Annual. MEND report 1.16.1b

Merkus, H., 2009. Particle size measurements: fundamentals, practice, quality. Particle Technology Series, 17(Springer), 519. http://doi.org/ISBN 978-1-4020-9016-5

Miller, S.D., Jeffery, J.J., Wong, J.W.C. (1991). Use and misuse of the acid base account for "AMD" prediction. Proc. of the Second International Conference on the Abatement of Acidic Drainage. Montreal, Canada. 3,489-506

Molson, J., Aubertin, M., Bussière, B., Benzaazoua. M. (2008). Geochemical Transport Modelling of Drainage from Experimental Mine Tailings Cells Covered by Capillary Barriers. Applied Geochemistry 23 (1) (January): 1–24. doi:10.1016/j.apgeochem.2007.08.004

Moon, Y., Song, Y., Moon, H.-S. (2007). The potential acid-producing capacity and factors controlling oxidation tailings in the Guryong mine, Korea. Environmental Geology, 53(8), 1787–1797. doi:10.1007/s00254-007-0784-9

Moncur, M. C., Jambor, J. L., Ptacek, C. J., Blowes, D. W. (2009). Mine drainage from the weathering of sulfide minerals and magnetite. Applied Geochemistry, 24(12), 2362–2373. doi:10.1016/j.apgeochem.2009.09.013

Moncur, M. C., Ptacek, C. J., Blowes, D. W., Jambor, J. L. (2005). Release, transport and attenuation of metals from an old tailings impoundment. Applied Geochemistry, 20(3), 639–659. doi:10.1016/j.apgeochem.2004.09.019

Morgan, B., Wilson, S.A., Madsen, I.C., Gozukara, Y.M., Habsuda, J., 2015. Increased thermal stability of nesquehonite (MgCO3·3H2O) in the presence of humidity and CO2: Implications for low-temperature CO2 storage. International Journal of Greenhouse Gas Control, 39, pp.366–376

Morin, K.A. et Hutt, N.M.(1998). Kinetic Tests and Risk Assessment for ARD. Paper presented at the Fifth Annual British Columbia Metal Leaching and ARD Workshop. December 9-10, 1998, Vancouver, British Columbia, Canada, B.C. Ministry ofEnergy and Mines and MEND 2000

Morin, K., Hutt, N., & Ferguson, K. (1995). Measured rates of sulfide oxidation and acid neutralization in kinetic test - Statistical lessons from the database. Conference on Mining and the Environment

Morin, KA. (2003). Problems with Acid Rock Drainage Predictions at the Ekati Diamond Mine, Northwest Territories, Canada … Sixth International Conference on Acid Rock Drainage (July): 12–18.

Morin, K.A. et Hutt, N.M. (1994). Observed Preferential Depletion of Neutralization Potential Over Sulfide Minerals in Kinetic Tests: Site-Specific Criteria for Safe NP/AP ratios, presented at the international and Land Reclamation and Mine Drainage Conference and the 3rd International Conference on the Abatement of Acidic Drainage, Pittsburg, USA. 148-156

Muriithi, G. N., Petrik, L. F., Fatoba, O., Gitari, W. M., Doucet, F. J., Nel, J., Chuks, P. E. (2013). Comparison of CO2 capture by ex-situ accelerated carbonation and in in-situ naturally weathered coal fly ash. Journal of environmental management, 127, 212-220

Mylona E., X. A., Paspaliaris I. (2000). Inhibition of acid generation from sulphidic wastes by the addition of small amounts of limestone. Minerais Engineerieng, Vol. 13, No. 10-1, pp. 1161-1175

Nduagu, E., Björklöf, T., Fagerlund, J., Wärnå, J., Geerlings, H., Zevenhoven, R. (2012a). Production of magnesium hydroxide from magnesium silicate for the purpose of CO2 mineralisation – Part 1: Application to Finnish serpentinite. Miner. Eng. 30, 75–86

Nduagu, E., Björklöf, T., Fagerlund, J., Mäkilä, E., Salonen, J., Geerlings, H., Zevenhoven, R. (2012b). Production of magnesium hydroxide from magnesium silicate for the purpose of CO2 mineralization – Part 2: Mg extraction modeling and application to different Mg silicate rocks. Miner. Eng. 30, 87–94

Nicholson, R.V. (2004). Overview of neutral pH drainage and its mitigation: results of a MEND study. Proceedings of the MEND Ontario workshop, Sudbury, 2003

Nicholson, R.V., Gillham, R.W., Reardon, E.J. (1988). Pyrite oxidation in carbonate-buffered solution: 1. Experimental kinetics. Geochim. Cosmochim. Acta 52, 1077–1085

Nordstrom, D. K., Blowes, D. W., & Ptacek, C. J. (2015). Hydrogeochemistry and microbiology of mine drainage: An update. Applied Geochemistry, 57, 3-16

Nordstrom, D. K., Blowes, D. W., & Ptacek, C. J. (2015). Hydrogeochemistry and microbiology of mine drainage: An update. Applied Geochemistry, 57, 3-16

Nordstrom, D. K., et Alpers, C. N. (1999). Negative pH, efflorescent mineralogy, and consequences for environmental restoration at the Iron Mountain Superfund site, California. In Proceedings of the National Academy of Sciences. Vol. 96, pp. 3455–346)

Nordstrom, D.K., et Southam, G. (1997). Geomicrobiology of sulfide mineral oxidation. In Geomicrobiology , Interactions between microbes and minerals. Rev. Mineral., 35, 361-385

Orlando, A., Borrini, D., & Marini, L. (2011). Dissolution and carbonation of a serpentinite: inferences from acid attack and high P–T experiments performed in aqueous solutions at variable salinity. Applied geochemistry, 26(8), 1569-1583

Oskierski, H.C., Dlugogorski, B.Z. & Jacobsen, G. (2013). Sequestration of atmospheric CO2 in chrysotile mine tailings of the Woodsreef Asbestos Mine, Australia: Quantitative mineralogy, isotopic fingerprinting and carbonation rates. Chemical Geology, 358, pp.156–169

Paktunc, A. D., et Davé, N. K. (2002). Formation of secondary pyrite and carbonate minerals in the Lower Williams Lake tailings basin, Elliot Lake, Ontario, Canada. American Mineralogist, 87(5-6), 593-602

Paktunc, A. D. (1999). Characterization of mine wastes for prediction of acid mine drainage. In Environmental impacts of mining activities (pp. 19-40). Springer Berlin Heidelberg

Park, A.H.A. & Fan, L.S., 2004. CO2 mineral sequestration: Physically activated dissolution of serpentine and pH swing process. Chemical Engineering Science, 59(22-23), pp.5241–5247

Pépin, N. (2010). Étude du Comportement Cyclique de Résiduss Miniers avec Inclusions Drainantes par des Essais sur Table Sismique. Mémoire de Maîtrise, École Polytechnique de Montréal, Canada

Plante, B., Benzaazoua, M., Bussière, B., Kandji, E.B., Chopard, A., Bouzahzah, H., 2015. Use of EDTA in modified kinetic testing for contaminated drainage prediction from waste rocks: case of the Lac Tio mine. Environmental Science and Pollution Research, pp.1–15

Plante, B., Bussière, B., Benzaazoua, M. (2014). Lab to field scale effects on contaminated neutral drainage prediction from the Tio mine waste rocks. J Geochem Explor 137:37–47

Plante B., Bussière B., Benzaazoua M. (2012). Static tests response on 5 Canadian hard rock mine tailings with low net acid-generating potentials. Journal of Geochemical Exploration, Volume 114, March 2012, Pages 57-69

Plante, B., Benzaazoua, M., Bussière, B. (2010a). Predicting Geochemical Behaviour of Waste Rock with Low Acid Generating Potential Using Laboratory Kinetic Tests. Mine Water and the Environment, 30(1), 2–21. doi:10.1007/s10230-010-0127-z

Plante, B., Benzaazoua, M., Bussière, B. (2010b). Kinetic Testing and Sorption Studies by Modified Weathering Cells to Characterize the Potential to

Generate Contaminated Neutral Drainage. Mine Water and the Environment, 30(1), 22–37. doi:10.1007/s10230-010-0131-3

Plante B (2010c) Prédiction du drainage neutre contaminé en Ni: cas de la mine Tio. Ph.D. thesis, Université du Québec en Abitibi-Témiscamingue (UQAT), Québec, Canada

Plante, B. (2004). Comparaison des essais statiques et évaluation de l'effet de l'altération pour des rejets de concentrateur à faible potentiel de génération d'acide. Mémoire de maîtrise inédit en sciences appliquées (Génie minéral) Département des génies civil, géologique et des mines. Université de Montréal, Québec, Canada

Pokrovsky, O. S., et Schott, J. (2004). Experimental study of brucite dissolution and precipitation in aqueous solutions: surface speciation and chemical affinity control. Geochimica et Cosmochimica Acta, 68(1), 31-45

Pokrovsky, O. S., & Schott, J. (2000). Kinetics and mechanism of forsterite dissolution at 25 C and pH from 1 to 12. Geochimica et Cosmochimica Acta, 64(19), 3313-3325

Power, I. M., McCutcheon J., Harrison A. L., Wilson S. A., Dipple G. M., Kelly S., Southam C., Southam G. (2014). Strategizing carbon-neutral mines: A case for pilot projects. Minerals 4, 399–436

Power, IM, Wilson, S.A, Dipple, G.M. (2013). "Serpentinite Carbonation for CO2 Sequestration." Elements. http://171.66.125.216/content/9/2/115.short

Power, I., Harrison, A.L., Dipple, G.M., Wilson, S.A., Kelemen, P.B., Hitch, M., Southam, G. (2013). Carbon mineralization: From natural analogues to engineered systems. Reviews in Mineralogy & Geochemistry, Mineralogical Society of America, Vol. 77, pp. 305-360

Power, I. M., Dipple, G. M., & Southam, G. (2009). Bioleaching of ultramafic tailings by Acidithiobacillus spp. for CO2 sequestration. Environmental science & technology, 44(1), 456-462

Price, W. A., Morin K. et Hutt, N. (1997). Guidelines for the Prediction of Acid Rock Drainage and Metal Leaching for Mines in British-Columbia: Part II - Recommended Procedures for Static and Kinetic Testing. 4th International Conference on Acid Rock Drainage (ICARD), Vancouver, BC

Pronost, J., Beaudoin, G., Lemieux, J.-M., Hébert, R., Constantin, M., Marcouiller, S., Klein, M., Duchesne, J., Molson, J.W., Larachi, F., Maldague, X. (2012). CO2-depleted warm air venting from chrysotile milling waste (Thetford Mines, Québec, Canada): evidence for in situ carbon capture from the atmosphere. Geology 40, 275–278

Pronost, J., Beaudoin, G., Tremblay, J., Larachi, F., Hébert, R., Constantin, M., Duchesne, J. (2011). Carbon sequestration kinetics and storage capacity of ultramafic mining waste. Environmental Science & Technology 45, 9413–9420

Raade G. (1970). Dypingite, a new hydrous basic carbonate of magnesium from Norway. American Mineralogist, 55: 1457-1465

RFI, (2013. "La Hausse Du CO2 Fait Suffoquer La Planète." Radio France Internationale. http://www.rfi.fr/science/20130507-hausse-co2-planete-ges-mauna-loa-courbe-keeling?ns_campaign=editorial&ns_source=FB&ns_mchannel=reseaux_sociaux&ns_fee=0&ns_linkname=20130507_hausse_co2_planete_ges_mauna_loa.

Rietveld HM, 1993. The Rietveld method. Oxford University Press, (Oxford, UK).

RNC, 2013. Technical Report on the Dumont Ni Project , Launay and Trécesson Townships , Quebec , Canada

Robie, R. A., & Hemingway, B. S. (1995). Thermodynamic properties of minerals and related substances at 298.15 K and 1 bar (10^ 5 Pascals) pressure and at higher temperatures (No. 2131). USGPO; For sale by US Geological Survey, Information Services

Rollo, H.A. et Jamieson, H.E. (2006). Interaction of diamond mine waste and surface water in the Canadian Arctic. Applied Geochemistry, 21(9), pp.1522–1538

Rose, A.W. et Cravotta III, C.A. (1998). Geochemistry of coal-mine drainage. In: Brady, K.B.C., Smith, M.W., Schueck., J. (Eds.), Coal Mine Drainage Prediction and Pollution Prevention in Pennsylvania. Harrisburg, PA, Pennsylvania Department of Environmental Protection, 5600-BK-DEP2256, 1.1–1.22

Rousseau, P. (2012). A critical review of static geochemical test methods applied to mining wastes, including their applicability to field conditions. imwa.info, 499–504

Sáinz, A., Grande, J. A., de la Torre, M. L., Sánchez-Rodas, D. (2002). Characterisation of sequential leachate discharges of mining waste rock dumps in the Tinto and Odiel rivers. Journal of Environmental Management, 64(4), 345–353. doi:10.1006/jema.2001.0497

Saldi G. D., Jordan G., Schott J., Oelkers E. H., 2009. Magnesite growth rates as a function of temperature and saturation state. Geochim. Cosmochim. Acta 73, 5646–5657

Santos, R., Bodor, M., Van Bouwel, J., Kriskova, L., Elsen, J., Vlad, M., Van Gerven, T. (2012). Mineralogical effects on the intensified mineral carbonation of steel slags: kinetics, conversion, basicity and products

Sapsford, D.J., Bowell, R.J., Dey, M., Williams, K.P. (2009). Humidity cell tests for the prediction of acid rock drainage. Minerais Engineering, Volume 22, Issue 1, Pages 25-36

Sapsford, D., et Williams, K. (2005). Predominant chemical kinetics in laboratory prediction of ARD. Proceedings of the 9th International Mine Water Congress, Oviedo, Spain. Vol. 5. 2005

Schaef, H. T., Windisch, C. F., McGrail, B. P., Martin, P. F., Rosso, K. M. (2011). Brucite [Mg (OH 2)] carbonation in wet supercritical CO 2: An in situ high pressure X-ray diffraction study. Geochimica et cosmochimica acta, 75(23), 7458-7471

Scharer, J. M., Pettit, C. M., Kirkaldy, J. L., Bolduc, L., Halbert, B. E., & Chambers, D. B. (2000). Leaching of metals from sulphide mine wastes at neutral pH. In Proceedings of the 5th International Conference on Acid Rock Drainage (ICARD 2000). Denver, Colorado (pp. 21-24)

Scharer, J.M., Garg, V., Smith, R., Halbert, B.E. (1991). Use of steady state models for assessing acid generation in pyritic mine tailings. Proceedings, 2nd ICARD, Montreal CANMET, Ottawa, Vol 2, pp 211–229

Schott J., Berner, R.A., Sjoberg, E.L. (1981). Mechanism of pyroxene and amphibole weathering–I experimental studies of iron-free minerals. Geochim Cosmochim Acta 45:2123–2135

Sciortino, M., Mungall, J.E. & Muinonen, J.(2015). Generation of High-Ni Sulfide and Alloy Phases During Serpentinization of Dunite in the Dumont Sill, Quebec. Economic Geology, 110, pp.733–761

Seifritz, W. (1990). CO2 disposal by means of silicates. Nature, 345, 486

Sherlock, E. J., Lawrence, R. W., & Poulin, R. (1995). On the neutralization of acid rock drainage by carbonate and silicate minerals. Environmental Geology, 25(1), 43-54

Skousen, J., Renton, J., Brown, H., Evans, P., Leavitt, B., Brady, K., Cohen, L., Ziemkiewicz, P., (1997). Neutralization potential of overburden samples containing siderite. J. Environ. Quai. 26: 673-681

Smith, L.J.D., Bailey, B.L., Blowes, D.W., Jambor, J.L., Smith, L., Sego, D.C., 2013. The Diavik Waste Rock Project: initial geochemical response from a low sulfide waste rock pile. Applied Geochemistry. 36, 210–221

Sobek, A.A., Schuller, W.A., Freeman, J.R., Smith, R.M. (1978). Field and laboratory methods applicable to overburdens and minesoils. EPA-600/2-78-054. U.S. Gov. Print. Office, Washington, DC

SRK, 1989. Draft acid rock drainage technical guide. Prepared by Steffen, Robertson and Kirsten (BC) Inc. in association with Norecol Environmental Consultants and Gormely Process Engineering. Technical Guide, Vancouver, Canada

Staples, L.P., Bowen, J.M., Bernier, S.B., Warren, D.A., Scott, C.C., Duncan, J.F., Murphy, B.A., Bertrand, V.J., Scott, K.C., and Latulippe, S. (2013). Technical report on the Dumont Ni Project, Launay and Trécesson Townships, Quebec, Canada, 432 p., downloaded from http://www.royalnickel.com/pr-dumont-project.php

Stillings, L.L., Foster, A.L., Koski, R.A., Munk, L., Shanks, W.C. (2008). Temporal variation and the effect of rainfall on metals flux from the historic Beatson mine, Prince William Sound, Alaska, USA. Applied Geochemistry, 23(2), 255–278. doi:10.1016/j.apgeochem.2007.10.013

Taylor, B. E., Wheeler, M. C., Nordstrom, D. K. (1984). Stable isotope geochemistry of acid mine drainage: Experimental oxidation of pyrite.Geochimica et Cosmochimica Acta, 48(12), 2669-2678

Teir, S., Elanova, S., Fogelholm, C.J., Zevenhoven, R. (2009). Fixation of carbon dioxide by producing hydromagnesite from serpentinite. Applied Energy, 86(2), pp.214–218

Teir, S., Kuusik, R., Fogelholm, C.J., Zevenhoven, R. (2007). Production of magnesium carbonates from serpentinite for long-term storage of CO2. International Journal of Mineral Processing, 85(1-3), pp.1–15

Teir, S., Elanova, S., Fogelholm, C.J., Zevenhoven, R. (2006). Stability of calcium carbonate and magnesium carbonate in rainwater and nitric acid solutions. Energy Conversion and Management, 47(18-19), pp.3059–3068

The New York Times. 2013. "Heat-Trapping Gas Passes Milestone, Raising Fears." The New York Times. http://www.nytimes.com/2013/05/11/science/earth/carbon-dioxide-level-passes-long-feared-milestone.html?hp&_r=2&

Thom, J. G., Dipple, G. M., Power, I. M., & Harrison, A. L. (2013). Chrysotile dissolution rates: Implications for carbon sequestration. Applied geochemistry, 35, 244-254

Tomsich, C. S., Hanks, C. L., Stone, D. B., Newberry, R. J., & Coakley, B. J. (2015). Ultramafic and Mafic Rock Distributions in Central Alaska and Implications for CO2 Sequestration. Natural Resources Research, 24(3), 349-368

USEPA. (2006). MINTEQA2, Metal speciation equilibrium model for surface and ground water, version 3.1 Available at: https://vminteq.lwr.kth.se/

US EPA, 1999. MINTEQA2, Metal speciation equilibrium model for surface and ground water, version 4.0. Available at: http://epa.gov/ceampubl/

US EPA, 1994. Technical Document Acid Mine Drainage Prediction. Environmental Protection, (December), p.52. Available at: U.S. Environnmental Protection Agency

Vick, S. G. (1990). Planning, design, and analysis of tailings dams. BiTech Publishers Ltd. Vancouver, B.C

Villeneuve, M. (2004). Evaluation du comportement géochimique à long terme de rejets miniers à faible potentiel de génération d'acide à l'aide d'essais cinétiques. Mémoire de maîtrise inédit en sciences appliquées (Génie minéral), Département des génies civil, géologique et des mines. Université de Montréal, Québec, Canada

Villeneuve, M., Bussière, B., Benzaazoua, M., Aubertin,M., Monroy, M., 2003. The Influence of Kinetic Test Type on the Geochemical Response of Low Acid

Generating Potential Tailings, Tailings and Mine Waste '03. Sweets & Zeitlinger, Vail, CO., USA 269–279

Vogeli, J., Reid, D.L., Becker, M., Broadhurst, J., Franzidis, J.-P. (2011). Investigation of the potential for mineral carbonation of PGM tailings in South Africa. Minerals Engineering, 24(12), pp.1348–1356

Walker, S.R., J. Millard, J. Andrina and S. Sibbick (2012) Predicting ML/ARD from Low Sulfide and Low Neutralization Potential Waste Rock; Baffinland Iron Mines Mary River Project, Nunavut, Canada, Proc. Of the 9th International Conference on Acid Rock Drainage, May 20-26, 2012, Ottawa, Canada

White, A.F. (2003). Natural weathering rates of silicate minerals In: Holland, HD, Turekian, KK (Ex Eds), Treatise on Geochemistry vol 5 Drever, JI (Ed) Surface and Ground Water, Weathering, and Soils, Elsevier, New York, 133–168

White, A.F., et Brantley, S.L. (2003). The effect of time on the weathering of silicate minerals: why do weathering rates differ in the laboratory and field?" Chemical Geology 202, 479-506

White, A.F., Brantley, S.L. (1995). Chemical Weathering Rates of Silicate Minerals. Rev Mineral, Mineralogical Society of America, vol. 31

White, W.B., 1971. Infrared characterization of water and hydroxyl ion in the basic magnesium carbonate. The American Mineralogist, 56(100), pp.46–53

Wilkin, R.T. (2008). Contaminant Attenuation Processes at Mine Sites. Mine Water and the Environment, 27(4), 251–258. doi:10.1007/s10230-008-0049-1

Wilson, S. A., Harrisson, A.L., Dipple, G.M., Power, I.M., Barker, S.L.L., Mayer, K.U., Fallon, S.J., Raudsepp, M., Southam, G. (2014). Offsetting of CO2 emissions by air capture in mine tailings at the Mount Keith Nickel Mine, Western Australia: Rates, controls and prospects for carbon neutral mining. International Journal of Greenhouse Gas Control, 25, pp.121–140

Wilson, S.A., Dipple, G.M., Power, I.M., Barker, S.L.L., Fallon, S.J., Southam, G. (2011). Subarctic weathering of mineral wastes provides a sink for atmospheric CO2. Environmental Science and Technology, 45(18), pp.7727–7736

Wilson, S. A., Dipple, G.M., Power, I.M., Thom, J.M., Anderson, R.G., Raudsepp, M., Gabites, J.E., Southam, G. (2009a). Carbon dioxide fixation within mine wastes of ultramafic-hosted ore deposits: Examples from the Clinton Creek and Cassiar Chrysotile deposits, Canada. Economic Geology, 104(1), pp.95–112

Wilson, S. A., Raudsepp, M., Dipple, G.M. (2009b). Quantifying carbon fixation in trace minerals from processed kimberlite: A comparative study of quantitative methods using X-ray powder diffraction data with applications to the Diavik Diamond Mine, Northwest Territories, Canada. Applied Geochemistry, 24(12), pp.2312–2331

Wilson, S.A., Raudsepp, M. & Dipple, G.M. (2006). Verifying and quantifying carbon fixation in minerals from serpertine-rich mine tailings using the Rietveld method with X-ray powder diffraction data. American Mineralogist, 91(8-9), pp.1331–1341

Xia, F., Pring, A., & Brugger, J. (2012). Understanding the mechanism and kinetics of pentlandite oxidation in extractive pyrometallurgy of nickel. Minerals Engineering, 27, 11-19

Zarandi, A. E., Larachi, F., Beaudoin, G., Plante, B., & Sciortino, M. (2017). Nesquehonite as a carbon sink in ambient mineral carbonation of ultramafic mining wastes. Chemical Engineering Journal, 314, 160-168

Zarandi, A. E., Larachi, F., Beaudoin, G., Plante, B., Sciortino, M. (2016). Multivariate study of the dynamics of CO 2 reaction with brucite-rich ultramafic mine tailings. International Journal of Greenhouse Gas Control, 52, 110-119

Zhang, J., Zhang, R., Geerlings, H., Bi, J. I. C. H. E. N. G. (2012). Mg-Silicate Carbonation Based on an HCl-and NH3-Recyclable Process: Effect of Carbonation Temperature. Chemical Engineering & Technology, 35(3), 525-531

Zhang, Z., Zheng, Y., Ni, Y., Liu, Z., Chen, J., Liang, X., 2006. Temperature- And pH-dependent morphology and FT-IR analysis of magnesium carbonate hydrates. Journal of Physical Chemistry B, 110(26), pp.12969–12973

Zingaretti, D., Costa, G., Baciocchi, R. (2013). Assessment of the energy requirements for CO 2 storage by carbonation of industrial residues. Part 1: definition of the process layout. Energy Procedia, 37, 5850-5857

ANNEXE A

SCHEMAS DES CELLULES EXPÉRIMENTALES DE TERRAIN

Les figures A.1 et A.2 montrent les schémas et photos des parcelles expérimentales de stériles et de résidus de concentrateur qui ont été construites sur le site du projet Dumont.

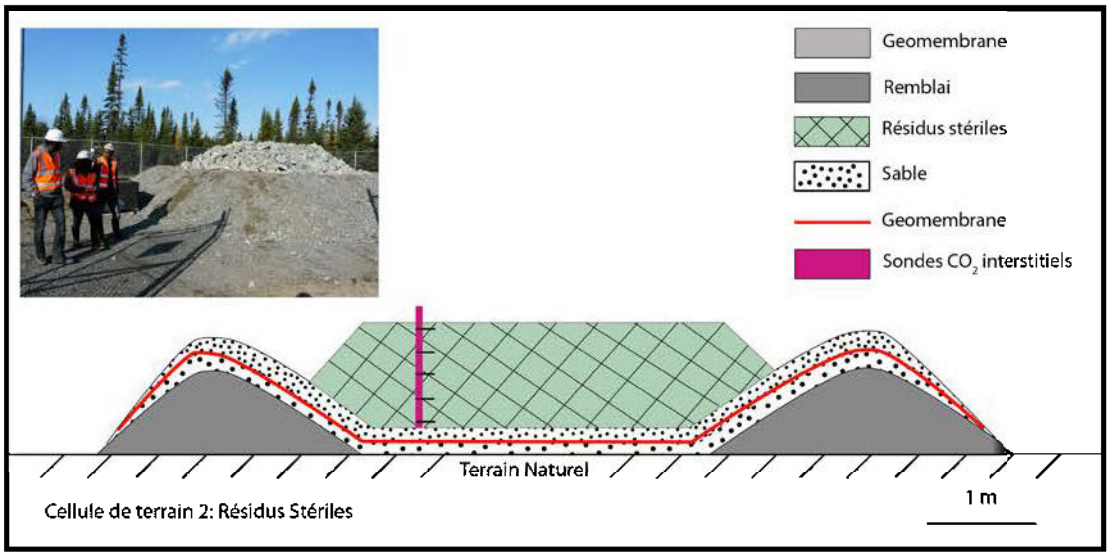

Figure A.1 Cellule expérimentale de stériles (échelle verticale non respectée; Gras, 2013)

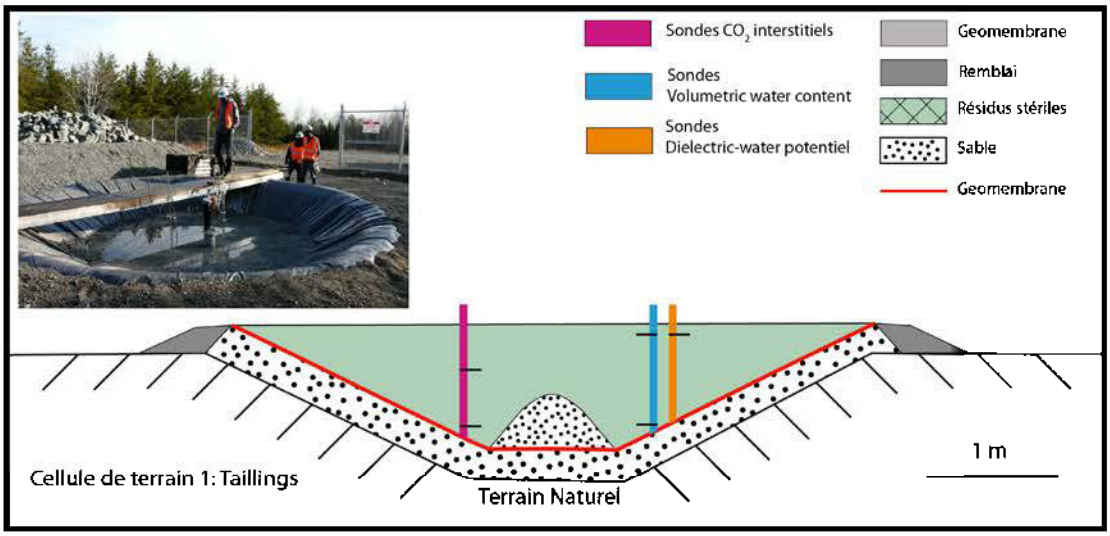

Figure A.2 Cellule expérimentale de résidus (échelle verticale non respectée; Gras, 2013)

ANNEXE B

RÉSULTATS DES ESSAIS EN COLONNE SUR LES TAILINGS ET STÉRILES
(CD-ROM)

ANNEXE C

RÉSULTATS DU DRIFT (CD-ROM)

ANNEXE D

COMPARAISON DE LA GÉOCHIMIE ENTRE LES ÉCHELLES - CALCUL DES TAUX DE RÉACTION ET DES SSA (CD-ROM)

ANNEXE E

RÉSUMÉ DES OBSERVATIONS MO ET MEB-AWARUITE ET CONCENTRÉS DE SULFURES DE NICKEL (CD-ROM)

ANNEXE F

RÉSULTATS DU SUIVI GÉOCHIMIQUE DES CELLULES EXPÉRIMENTALES DE TERRAIN (CD-ROM)

ANNEXE G

RÉSULTATS DES CALCULS THERMODYNAMIQUES AVEC VMINTEQ POUR LES TAILINGS, LES STÉRILES ET LES LITHOLOGIES (CD-ROM)

ANNEXE H

RÉSULTATS DES ESSAIS EN MINI-CELLULES SUR LES RÉSIDUS ET LES STÉRILES (CD-ROM)

ANNEXE I

RÉSULTATS DES ESSAIS EN MINI-CELLULE SUR LES CONCENTRÉS DE SULFURES ET D'AWARUITE (CD-ROM)

ANNEXE J

RÉSUMÉ DES OBSERVATIONS MEB SUR LES TAILINGS ET STÉRILES (CD-ROM)

ANNEXE K

DIFFRACTOGRAMMES DES CONCENTRÉS DE SULFURES ET D'AWARUITE (CD-ROM)

ANNEXE L

DIFFRACTOGRAMMES DES TAILINGS, DES STÉRILES ET DES LITHOLOGIES (CD-ROM)